Life history inferences in extant and extinct Equus from the histological analysis of bone and enamel tissues

Carmen Nacarino Meneses

PhD Thesis
Universitat Autònoma de Barcelona
Doctorate in Biodiversity
2018

Life history inferences in extant and extinct *Equuus* from the histological analysis of bone and enamel tissues

Carmen Nacarino Meneses

Universitat Autònoma de Barcelona

Supervisors

Meike Köhler
Xavier Jordana

Institut Català de Paleontologia
Miquel Crusafont

Universitat Autònoma de Barcelona
Department de Biologia Animal, Biologia Vegetal i d'Ecologia

Institut Català de Paleontologia
Miquel Crusafont

PhD Thesis – 2018

Life history inferences in extant and extinct *Equus* from the histological analysis of bone and enamel tissues

Carmen Nacarino Meneses

Dissertation presented by Carmen Nacarino Meneses in fulfillment of the requirements for the degree of Doctor in the Universitat Autònoma de Barcelona, doctorate program in Biodiversity of the Department de Biologia Animal, Biologia Vegetal i d'Ecologia. Under the supervision of:

- Dra. Meike Köhler, ICREA at Institut Català de Paleontologia Miquel Crusafont and teacher of the Departament de Biologia Animal, Biologia Vegetal i d'Ecologia at Universitat Autònoma de Barcelona.

- Dr. Xavier Jordana, teacher of the Departament de Biologia Animal, Biologia Vegetal i d'Ecologia at Universitat Autònoma de Barcelona.

Doctoral candidate

Carmen Nacarino Meneses

Supervisors

Dra. Meike Köhler **Dr. Xavier Jordana**

All the work (text, tables, figures and design) comprised in this PhD thesis is the result of research and tasks carried out by the author. When information has been derived from another sources, it is accurately indicated in the text.

Carmen Nacarino Meneses
Barcelona, June 2018

Abstract

The study of life histories provides valuable insights into many aspects of a species' biology and ecology, including the ecological conditions of its ecosystem, its biodiversity, its demography and its vulnerability to extinction. Life histories of extant and extinct vertebrates can be reconstructed from bone and dental microstructure. However, histological research in key mammalian groups for paleontology and ecology, such as equids, is still little explored. The present PhD thesis aims to analyze bone and dental histology in extant and extinct *Equus* to obtain information about their most important life history and biological traits. The extant sample of the present dissertation comprises bones and teeth of Asiatic wild ass, plains zebra and Grevy's zebra. Their detailed histological study has provided a solid framework for the subsequent analysis of fossil *Equus* species, which has been limited here to Middle and Late Pleistocene taxa. Results obtained from bone histology in living equids show that bone tissue types vary through ontogeny, recording individual growth. This dissertation also indicates that changes in bone tissue types are related to certain life history characteristics. Thus, for instance, results of this thesis reveal that the transition from fibrolamellar to lamellar bone (i.e. external fundamental system) in equid femora is associated with the onset of reproductive maturity. Key life history events, such as the moment of birth, are also registered in the bone tissue of equids. For the first time in mammals, the present dissertation describes a non-cyclical bone growth mark in the limb bones of equids whose timing of deposition agrees with a period of growth arrest/decline during birth in foals (neonatal line). This discovery is of high importance for the histological reconstruction of life histories in extant and extinct mammals. Bone skeletochronology in extant *Equus* further reveals that the femur is the best bone to obtain life history data in equids, and that bone growth curves yield information about skeletal maturity. On the other hand, the counting of incremental markings of daily periodicity in equid enamel yields new estimates of daily secretion rates for these mammals that invalidate previous inaccurate studies. The detailed study of dental enamel in first lower molars of extant *Equus* also shows that the development of this tooth involves three different stages. Each of them presents a specific rate and pattern of growth, and is related to ontogenetic and structural modifications of the tooth. The histological analysis performed here further indicates that enamel extends beyond the molar's cervix in equids, hampering measurements of the crown height from the external appearance of the tooth. Results of this thesis also reveals that the time of first lower molar crown formation in the Asiatic wild ass doubles that of the African zebras, probably due to differences in habitat and longevity among these species. Dental histology further yields information about rates of wear in equids, indicating much higher wear rates for the first lower molar early in ontogeny than commonly thought. In a first attempt to reconstruct the life history of extinct *Equus*, bone histology was analyzed in the Middle Pleistocene species *E. steinheimensis* and *E. mosbachensis* and dental enamel was studied in the Late Pleistocene taxa *E. ferus* and *E. hydruntinus*. The preliminary findings obtained from these investigations allowed the first analysis of the body size trend towards dwarfing in European Pleistocene *Equus* under a life history perspective. First results indicate that larger Middle Pleistocene equids grew at higher rates than smaller Late Pleistocene and extant species. This finding agrees with published paleoenvironmental reconstructions and conforms to life history models that propose resource availability as one of the main selection pressures influencing adult body size.

Resumen

El estudio de *life histories* proporciona información sobre la biología y ecología de las especies, incluyendo las condiciones ecológicas de su ecosistema, su biodiversidad, su demografía y su vulnerabilidad. La *life history* de vertebrados actuales y extintos puede ser reconstruida a partir de la microestructura ósea y dental. Sin embargo, el estudio de mamíferos clave en paleontología y ecología, como los équidos, es aún escaso. La presente tesis doctoral tiene como objetivo analizar la histología ósea y dental de *Equus* actuales y extintos para inferir sus características biológicas y de *life history* más importantes. La muestra actual se compone de huesos y dientes de asno salvaje asiático, cebra común y cebra de Grevy. Su estudio ha proporcionado un marco sólido para el análisis de *Equus* fósiles, limitado en esta tesis a especies del Pleistoceno Medio y Superior. Los resultados obtenidos de histología ósea en équidos actuales muestran que el tipo de tejido varía a lo largo de la ontogenia, registrando el crecimiento del individuo. Los cambios de tejido óseo también se han relacionado con ciertas características de *life history*. Así, el cambio de hueso *fibrolamellar* a *lamellar* (*external fundamental system*) en fémures de équidos se ha visto asociado a la madurez reproductiva. Eventos clave del ciclo vital, como el nacimiento, quedan igualmente registrados en el tejido óseo de los équidos. Por primera vez en mamíferos, esta tesis doctoral describe una marca de crecimiento no cíclica en huesos apendiculares, cuya deposición está relacionada con una reducción/parada del crecimiento en los potros durante el nacimiento (línea neonatal). Este descubrimiento es de gran importancia para la reconstrucción histológica de *life histories* en mamíferos actuales y extintos. El estudio esqueletocronológico en *Equus* actuales ha revelado, además, que el fémur es el mejor hueso para obtener datos de *life history* y que las curvas de crecimiento reflejan la madurez esquelética. Por otro lado, el contaje de marcas diarias en el esmalte de équidos actuales ha proporcionado nuevas tasas de secreción que invalidan estudios incorrectos previos. El estudio del esmalte dental realizado en primeros molares inferiores de *Equus* indica, además, que el desarrollo de este diente consta de tres fases. Cada una de ellas presenta un patrón y una tasa de crecimiento específica, y está relacionada con modificaciones ontogenéticas y estructurales del diente. Asimismo, el análisis histológico muestra que el esmalte se extiende más allá del cérvix, dificultando la toma de medidas de la altura de la corona a partir de la apariencia externa del diente. Los resultados obtenidos indican, también, que el desgaste del primer molar es mucho más pronunciado en etapas tempranas de la ontogenia, y que la corona de este diente tarda en formarse el doble de tiempo en el asno asiático que en las cebras africanas debido, probablemente, a diferencias en hábitat y longevidad entre especies. Además, se ha analizado la histología ósea de las especies del Pleistoceno Medio *E. steinheimensis* y *E. mosbachensis* y el esmalte dental de las del Pleistoceno Superior *E. ferus* y *E. hydruntinus*, en un primer intento por reconstruir la *life history* de *Equus* fósiles. Esto, a su vez, ha permitido analizar los cambios evolutivos de tamaño corporal descritos en *Equus* durante el Pleistoceno europeo bajo una perspectiva de *life history*. Los resultados preliminares obtenidos en esta tesis indican que los équidos más grandes del Pleistoceno Medio crecían a tasas más elevadas que las especies del Pleistoceno Superior y actuales, más pequeñas. Este resultado se corresponde con reconstrucciones paleoambientales y con modelos teóricos de *life history* que proponen la disponibilidad de recursos como una de las presiones de selección más importantes en la determinación del tamaño corporal.

Contents

Prologue 5
Abbreviations 7

Chapter 1. Introduction 11
1.1. Life history theory: a framework to study evolution 11
1.2. The histological analysis of bones and teeth: a tool to reconstruct life histories in extant and extinct vertebrates 13
1.2.1. Bones as recording structures 15
1.2.2. Teeth as recording structures 17
1.3. The genus *Equus*: A paradigm of evolution 19
1.3.1. Evolutionary history of the genus *Equus* 20
1.3.2. Biology and ecology of extant *Equus* 22

Chapter 2. Aims & Objectives 29

Chapter 3. Material & Methods 35
3.1. Material 35
3.1.1. Extant sample 36
3.1.2. Fossil sample 36
3.2. Methods: histological thin sections of bones and teeth 37
3.2.1. Preparation of histological thin sections 37
3.2.2. Analysis of histological thin sections 39
3.2.2.1. Microscopy 39
3.2.2.2. Histological features of bone 40
Bone tissue types *40*
Bone growth marks *43*
Vascularization: quantitative and qualitative measurements *45*
3.2.2.3. Enamel histological features 46
Enamel growth parameters *46*
Assessment of the daily periodicity of enamel laminations in equids *48*
3.3. Methods: body size inferences in extinct taxa 48
3.1. Inferring adult body mass in extinct *Equus* 49
3.2. Estimating size at birth in extinct *Equus* 49

Chapter 4. First approach to bone histology and skeletochronology of *Equus hemionus* 53
Abstract 53
Keywords 53
Introduction 54
Material and methods 54

Results 56
Discussion 60
Conclusions 61
Acknowledgements 61
References 62

Chapter 5. Histological variability in the limb bones of the Asiatic wild ass and its significance for life history inferences..... 67
Abstract 67
Keywords 67
Introduction 67
Material and methods 69
Results 71
Discussion 79
Conclusions 83
Acknowledgements 84
References 85

Chapter 6. Limb bone histology records birth in mammals..... 93
Abstract 93
Keywords 93
Introduction 94
Material and methods 95
Results 99
Discussion 105
Conclusions 108
Acknowledgements 108
References 109
Supporting Information 113

Chapter 7. The life history of European Middle Pleistocene equids: First insights from bone histology..... 117
Abstract 117
Keywords 117
Introduction 118
Material and methods 119
Results 122
Discussion 126
Conclusions 130
Acknowledgements 131
References 131

Chapter 8. Reconstructing molar growth from enamel histology in extant and extinct *Equus*..... 139
Abstract 139
Introduction 139
Results 140

Discussion 143
Methods 147
References 148
Acknowledgements 150
Supplementary information 151

CHAPTER 9. DISCUSSION **157**
9.1. Bone and dental histology of extant *Equus*: Setting the basis for life history inferences **157**
9.1.1. Bone histology of extant *Equus* 157
9.1.1.1. The bone tissue of extant *Equus*: ontogenetic changes in bone matrix and vascularization 158
9.1.1.2. Non-cyclical and cyclical BGMs: bone skeletochronology and the inference of biological and LH traits in extant *Equus* 160
9.1.2. Enamel histology of extant *Equus* 163
9.1.2.1. Daily incremental markings in the enamel of extant *Equus*: the assessment of enamel secretion rate in equids 164
9.1.2.2. Growth and ontogeny of equid molar crowns: histological findings and LH implications 164
9.2. The life history of extinct *Equus*: Insights from bone and dental histology **167**
9.2.1. The LH of Middle Pleistocene *Equus*: inferences from bone histology 168
9.2.2. The LH of Late Pleistocene *Equus*: inferences from enamel histology 170
9.2.3. Evolutionary changes in body size of the genus *Equus*: preliminary analysis from a LH perspective 171

CHAPTER 10. CONCLUSIONS **177**

CHAPTER 11. REFERENCES **183**

CHAPTER 12. ACKNOWLEDGEMENTS **205**

Prologue

Bone and dental histology are powerful tools for reconstructing the life history (LH) of extant and extinct vertebrates. At their microscopic level, bones and teeth present specific features known as growth marks that are deposited following a certain periodicity, and therefore recording individual growth and development. In bones, these structures record annual cycles of growth, which provide valuable insights into the key LH characteristics age at maturity, growth rate and age at death. In dental enamel, however, most incremental markings register daily growth. Their analysis allows the reconstruction of rates, timings and patterns of tooth formation, which, in turn, provides information about essential mammalian LH traits such as age at weaning. Nonetheless, studies in bone histology are commonly biased towards reptiles, birds and dinosaurs, while dental histology has traditionally focused on hominoids. As a result, bone and dental histology is still relatively unexplored in most mammalians groups. This is the case, for instance, of the genus *Equus*, despite horses, zebras and asses being key taxa in many ecological communities and paleoecological death assemblages. In point of fact, LH data obtained from the histological study of equid bones and teeth would provide valuable information that is of interest to many different scientific areas, including Ecology and Paleontology. On the one hand, the histological assessment of LH traits in extant *Equus* is expected to be useful in demographic studies and in developing and improving conservation plans for the group. Such studies are urgently needed, as most living equids are highly threatened in the wild and classical monitoring in the field to obtain such data is time intensive and expensive. On the other hand, the histological study of extant species is indispensable to set a well-founded basis for the analysis of fossil taxa. Histological studies of fossil *Equus*, indeed, are highly relevant in Paleontology, as they aid the understanding of characteristic evolutionary trends of and within the group, such as the tendency during the European Pleistocene towards a smaller body size.

The present PhD thesis attempts to reconstruct the LH strategy (i.e. the combination of LH traits that maximize reproductive success in a given environment) of extant and extinct *Equus* species from the histological analysis of bone and enamel tissues, to shed light on their (paleo-)biology and (paleo-)ecology. This dissertation is the result of the studies carried out at the Evolutionary Paleobiology department of the *Institut Català de Paleontologia Miquel Crusafont* (Bellaterra, Spain), during the years 2014 – 2018. It is structured in two different sections. Thus, the aim of the first part of the thesis is to provide a well-founded basis for the interpretation of bone and dental histology in the genus *Equus*. Here, a fundamental piece is the description of bone tissue microstructure over ontogeny, and the identification of the most reliable long bone for skeletochronological studies in

equids. Amongst the most outstanding results are the first finding of a non-cyclical growth mark in the limb bones of mammals related to the moment of birth (the neonatal line) and the identification of key LH traits, such as the age at reproductive maturity, from bone tissue types. On the other hand, enamel histology allowed the establishment of three different developmental stages for the equid first lower molar crown, characterized by different rates and patterns of growth and related to ontogenetic and structural changes of the tooth. The recalculation of daily rates of enamel secretion in *Equus* disproved already published data based on erroneous identifications of enamel incremental markings. Enamel histology further revealed differences in crown formation time between extant *Equus* species, which are likely related to differences in habitat and longevity. Finally, wear rates calculated from enamel microstructure indicated much higher wear rates early in ontogeny than usually reported. The second part of the thesis is dedicated to the analysis of fossil *Equus* species. It is a first attempt to reconstruct the pace of life of several European fossil horses applying analytical tools and knowledge acquired in the first part of this dissertation. The aim is to test whether changes in body size are associated with changes in LH traits, as predicted from LH theory. First results indeed indicate differences in growth rate between larger Middle Pleistocene equids and smaller Late Pleistocene and extant *Equus*. At this preliminary stage, published data of climate and paleoenvironment for the fossil sites analyzed support LH models that suggest resource availability to be an important selection pressure behind changes in body size.

The present PhD dissertation is structured according to the standards for compendium of publications of the *Departament de Biologia Animal, Biologia Vegetal i Ecologia* of the *Universitat Autònoma de Barcelona* (Bellaterra, Spain), doctorate program in Biodiversity. The *Introduction* (Chapter 1) provides an overview and an essay of the state-of-the-art of the central issues to be covered in this PhD thesis. It is divided into several sections. The first one describes the main postulates of the LH theory, a central tenet in this research. In the second section, the histological features of bones and teeth that allow inferences of mammalian LH traits are explained, as they constitute the main tool used in the present dissertation. Finally, a third section provides a thorough review of the evolution, biology and ecology of the genus *Equus*, which is the mammalian group studied in this thesis. *Aims & Objectives* (Chapter 2) justifies the research performed and details the hypotheses and goals to be tested in the dissertation. *Material & Methods* (Chapter 3) describes the extant and fossil samples studied, and explains the procedure of preparation and analysis of bone and dental histological thin sections. This chapter also details the methodology used for the estimation of adult and neonatal body sizes in fossil species. The main results of the dissertation (Chapters 4 to 8) are presented as either published articles in SCI rated journals or still unpublished manuscripts. All of them present the classical structure of a scientific article, which includes an introduction, material and methods, results, discussion and conclusion sections. The *Discussion* (Chapter 9) collects the main results of the thesis and provides an integrated and general discussion. Finally, the *Conclusions* (Chapter 10) summarize the main conclusions of this PhD dissertation.

Abbreviations

BGM – Bone growth mark
CFT – Crown formation time
CGM – Cyclical growth mark
DSR – Daily secretion rate
EB – Endosteal bone
EDJ – Enamel dentine junction
EER – Enamel extension rate
EFF – Enamel formation front
EFFa – Enamel formation front angle
EFS – External fundamental system
FLC – Fibrolamellar complex
LAG – Line of arrested growth
LH – Life history
LHT – Life history theory
LB – Laminar bone
LLB – Lamellar bone
NL – Neonatal line
PFB – Parallel-fibered bone
PO – Primary osteon
RI – Repeat interval
VCs – Vascular canals
WFB – Woven bone or woven-fibered bone

- Chapter 1 -

Introduction

Introduction

1.1. Life history theory: A framework to study evolution

Life histories (LHs) describe how organisms live their life cycles in a given environmental context. They explain, for instance, how long an individual lives, when it matures or how fast it grows under certain ecological conditions (Stearns 1992; Roff 2002; Ricklefs 2008). These scheduled events that conform life cycles, along with other biological characteristics, are the so-called LH traits (Stearns 1992; Braendle et al. 2011). Generally, all life history components that affect the survival and reproduction of the individual are considered LH traits (Stearns 1992; Braendle et al. 2011). Some of the most important LH traits are also demographic characters (e.g. growth rate, longevity, age at maturity) (Stearns 1992). Other biological attributes that correlate and co-vary with these features, such as adult body size or size at birth, are also studied as LH traits (Stearns 1992; Braendle et al. 2011). LH traits combine to determine individual fitness (reproductive success) (Stearns 1992; Roff 2002) and, as fitness components (Braendle et al. 2011), they are sensitive to the action of natural selection (Stearns 1992).

Life history theory (LHT) provides an explanation of how evolutionary forces (i.e. natural selection) shape LHs optimizing reproductive success under the prevailing ecological conditions (Roff 1992; Stearns 1992; Stearns 2000). The adaptive response of the organism to the action of natural selection is, however, not unrestricted but subject to constraints intrinsic to the organism (Stearns 2000). Genetic factors, developmental characteristics and phylogeny limit the expression and combination of LH traits (Roff 1992; Braendle et al. 2011). Evolution is also restricted by LH trade-offs (Roff 1992; Stearns 1992; Roff 2002; Braendle et al. 2011), a key concept in LHT intimately linked to the problem of resource allocation (Stearns 1989; Roff 2002; Ricklefs 2008). According to LHT, organisms dispose of limited energy, time and nutrients that must be distributed among different vital tasks including growth, reproduction, survival and maintenance (Ricklefs 2008; Braendle et al. 2011). Because the energy assigned to one function cannot be invested in another function at the same time (van Noordwijk and de Jong 1986; Roff 2002; Begon et al. 2006), a compromise (trade-off) must be reached among alternative and complementary time and energy drains (Cody 1966). In terms of LHT, trade-offs thus occur when an increase in one fitness component is coupled with a reduction in another fitness component (Roff 1992; Stearns 1992; Braendle et al. 2011). Trade-offs are analyzed at the phenotypic, genotypic and physiological level (Stearns 1989; Ricklefs and Wilkelski 2002; Roff 2002). Among the numerous trade-offs encountered in nature (Stearns 1989), the one between future and current reproduction is especially noteworthy (Roff 1992;

Stearns 1992; Ricklefs 2008). It illustrates how individuals must optimally allocate resources between growth (future reproduction) and reproduction (current reproduction) (van Noordwijk and de Jong 1986), which forces them to wait until attaining a minimum age and size for which fitness is optimal and a maximum of resources can be devoted to reproduction (Ricklefs 2008).

Energy distribution (timing and rates of the different LH traits) is mainly determined by extrinsic ecological factors that influence survival and reproduction (Stearns and Koella 1986; Stearns 2000; Ricklefs 2008). LHT predicts age-specific extrinsic mortality (i.e. predation) to be the main selective pressure acting upon LH traits and controlling resource allocation decisions (Roff 1992; Stearns 1992). In environments with high extrinsic mortality, theory suggests that organisms mature earlier (Stearns 1992) by principally devoting resources to LHs traits related to reproduction (Ricklefs 2008). An earlier maturation increases their probability of survival until adulthood by decreasing their period of exposure to juvenile mortality before the first breeding (Stearns 2000). An advanced reproduction has additional benefits at the demographic level such as reduction in generation time (Stearns 2000). Low extrinsic mortality, instead, favors a delay in the age at maturity (Stearns 1992) that allows individuals to increase their fecundity by achieving larger sizes and behavioral maturity (experience), and to give birth to higher-quality offspring (Stearns 2000). In late-maturing organisms, most resources are thus channeled to growth, maintenance and survival at the expense of reproduction (Ricklefs 2008). The variation in LH traits observed in nature between individuals, populations and species has led to the description of a continuum of values denominated "fast-slow continuum" (Stearns 1983; Read and Harvey 1989; Promislow and Harvey 1990). At the "slow" end of the continuum, organisms (populations or species) are characterized by long life-span, slow development, delayed maturity, long generation times and high parental investment (Ricklefs 2008). At the other extreme of the continuum, the "fast" end, individuals (populations or species) present the opposite trends (Ricklefs 2008). The combination of LH traits for maximizing fitness in a specific environment, which determines the position of the individual (population or species) along the fast-slow continuum, is termed LH strategy (Stearns 1992).

Although trade-offs (the central issue of LHT) in nature were already described by Goethe, Saint-Hilaire and Darwin in the 18th and 19th century (Zawojska and Siudek 2016), it was not until the middle of the 20th century when the publication of the seminal works of Lack (1954) and Cole (1954) initiated the comprehensive study of LH evolution (Reznick et al. 2002). Few years later, MacArthur and Wilson (1967) presented their theory of *r*- and *K*-selection. It suggests the degree of density-dependent mortality (i.e. resource limitation) to be the main selective pressure driving evolution, providing a first framework to analyze the evolution of LHs (Pianka 1970). The *r*/*K* theory proposes two different kinds of selection (*r* and *K*) depending on how populations grow and how they are regulated (MacArthur and Wilson 1967). On the one hand, populations exposed to extreme environmental fluctuations experience density-independent mortality followed by episodes of fast population growth (Reznick et al. 2002). In this case, selection favors LH

traits that increase population size and maximize *r* (intrinsic rate of population growth), such as an earlier and single (semelparity) reproduction, a fast development, a short lifespan and a small body size (Pianka 1970). *r*-strategists (Pianka 2000), hence, mainly invest energy and resources in reproductive tasks (Begon et al. 2006). In predictable and constant environments, on the other hand, populations approach their carrying capacity (*K*) and are subject to density-dependent mortality and to intraspecific competition (Reznick et al. 2002). In these scenarios, traits that favor the persistence of individuals, such as delayed and repeated (iteroparity) reproduction, large body size, long lifespan and slow development will be selected (Pianka 1970). Therefore, species following a *K*-strategy (Pianka 2000) devote more resources to growth and survival than to reproduction (Begon et al. 2006). Although the *r*/*K* theory became extremely popular during the late 1960s and the 1970s (Reznick et al. 2002), ecologists and evolutionary biologists soon criticized its simplicity and the general lack of empirical support (Stearns 1992; Reznick et al. 2002). This led to the first studies in the framework of LHT (Gadgil and Bossert 1970; Schaffer 1974; Stearns 1976; Stearns 1977; Charlesworth 1980; Stearns 1983; Stearns 1989; Roff 1992; Stearns 1992), which emphasizes the use of demographic models for explaining life history evolution and proposes extrinsic mortality as the major agent of selection (Reznick et al. 2002).

Nowadays, LHT is placed in the core of evolutionary ecology (Stearns 2000) and the study of LHs is a central issue even in related scientific areas such as Conservation Biology or Paleontology (Begon et al. 2006; Köhler 2010). The LH of a species is analyzed, for instance, before developing habitat restoration projects or when dealing with invasive species (Begon et al. 2006). LHs are also examined in detail to achieve a successful management and conservation of endangered species (Begon et al. 2006), as vulnerability to extinction is known to increase in those species that present a concrete set of LH traits (McKinney 1997; Purvis et al. 2000; González-Suárez and Revilla 2013). Furthermore, LHT is gaining popularity in Paleontology. Studies aimed at reconstructing the LH strategy of fossil organisms are considerably increasing, allowing interpretation of evolutionary trends and the reconstruction of past environments. Hitherto, most of these studies focused on islands (Bromage et al. 2002; Palkovacs 2003; Raia et al. 2003; Raia and Meiri 2006; Köhler and Moyà-Solà 2009; Köhler 2010; Jordana and Köhler 2011; Marín-Moratalla et al. 2011; Moncunill-Solé et al. 2016; Orlandi-Oliveras et al. 2016).

1.2. The histological analysis of bones and teeth: A tool to reconstruct life histories in extant and extinct vertebrates

Bones and teeth are the major components of the vertebrate skeleton (Francillon-Vieillot et al. 1990). They grow incrementally, leaving marks in bone and dental tissues that record the growth and development of the organism (Castanet et al. 1993; Klevezal 1996; Chinsamy-Turan 2005; Smith 2006). The detailed histological study of these features, along with other characteristics in the case of bone tissue (i.e. bone matrix typology, bone

vascularization, etc.), set the basis for the inference of LH traits in past and modern taxa (Castanet et al. 1993; Klevezal 1996; Chinsamy-Turan 2005; Castanet 2006; Smith 2008; Woodward et al. 2013).

Histology (i.e. the microscopic study of tissues) was founded as a scientific discipline in the 18th century after the invention of the microscope (Turner-Walker and Mays 2008). Since then, first descriptions of vertebrate bone tissue are documented from the last half of the 19th and the beginning of the 20th century (Padian 2011; de Ricqlès 2011). Systematic studies on bone histology, however, only date back to the middle of the 20th century, when the extensive descriptive work on extant and extinct species by Enlow and Brown (Enlow and Brown 1956; Enlow and Brown 1957; Enlow and Brown 1958) was published (de Ricqlès 2007; Padian 2011; de Ricqlès 2011). Few years later, between 1968 and 1981, de Ricqlès presented a series of papers under the title "*Recherches paléohistologiques sur les os longs des tétrapodes*" (Padian 2011; Padian 2013). This pioneering research shortly became a basic reference for the forthcoming histological and paleohistological studies on vertebrates (Padian 2011; Padian 2013). Research on bone microstructure continued during the next decades with investigations mainly focused on dinosaurs, birds, reptiles and amphibians (Chinsamy et al. 1994; Horner et al. 1999; Botha and Chinsamy 2000; Horner et al. 2000; Sander 2000; Padian et al. 2001; de Margerie et al. 2002; de Margerie et al. 2004; Padian et al. 2004; Ray et al. 2004; Botha and Chinsamy 2005; Chinsamy-Turan 2005; Sander et al. 2006; Botha-Brink and Angielczyk 2010; Chinsamy-Turan 2012; Botha-Brink et al. 2016), while mammalian histology received only little attention (Klevezal 1996). Over the last years, however, interest in bone histology as a tool to decipher the biology and life history of extant and fossil mammals has importantly increased (Castanet et al. 2004; Castanet 2006; Chinsamy and Hurum 2006; Sander and Andrássy 2006; Köhler and Moyà-Solà 2009; Köhler 2010; García-Martínez et al. 2011; Marín-Moratalla et al. 2011; Hurum and Chinsamy-Turan 2012; Köhler et al. 2012; Marín-Moratalla et al. 2013; Marín-Moratalla et al. 2014; Martínez-Maza et al. 2014; Amson et al. 2015; Kolb et al. 2015a; Kolb et al. 2015b; Moncunill-Solé et al. 2016; Orlandi-Oliveras et al. 2016; Montoya-Sanhueza and Chinsamy 2017).

First comprehensive studies on dental microanatomy also date back to the middle of the 19th and the beginning of the 20th century (Schour and Hoffman 1939a; Boyde 1964; Foster 2017). At that time, scientists such as Andersen, Retzius, or Von Ebner described the incremental features on enamel and dentine tissues that have been named after them (Schour and Hoffman 1939a). During the 1930s and 1940s, researchers mainly focused on testing the rhythmicity of these structures (Bromage 1991; FitzGerald 1998; FitzGerald and Rose 2008). Some of the most remarkable studies of these years are those developed by Schour and colleagues (Schour and Hoffman 1939a; Schour and Hoffman 1939b; Schour and Massler 1940) and their Japanese contemporaneous scholars (Mimura 1939; Okada 1943). About two decades later, Boyde presented his dissertation (Boyde 1964), which is considered essential for our understanding of growth, development and microscopic structure of enamel tissue (Smith 2004). However, it was not until the end of the 20th and the beginning of the 21st century when incremental markings in enamel

and dentine were regularly analyzed to study the life history of extant and extinct species, mainly primates (Bromage and Dean 1985; Dean 1987; Bromage 1991; Dirks 1998; Dean et al. 2001; Dirks et al. 2002; Dean and Leakey 2004; Smith 2004; Dirks and Bowman 2007; Hogg and Walker 2011, among others; see Smith 2008 for a review). During the last years, dental histology has also been applied in other mammalian groups such as bovids (Macho and Williamson 2002; Jordana and Köhler 2011; Kierdorf et al. 2012; Kierdorf et al. 2013; Jordana et al. 2014; Kahle et al. 2017), suids (Kierdorf et al. 2014), proboscideans (Dirks et al. 2012; Metcalfe and Longstaffe 2012), cervids (Iinuma et al. 2004a; Iinuma et al. 2004b) and rhinoceros (Tafforeau et al. 2007). Although to a lesser extent, dental incremental markings have also been analyzed in crocodiles and dinosaurs (Erickson 1996; Erickson et al. 2017).

1.2.1. Bones as recording structures

At the histological level, bones present several characteristics that allow the estimation of three main life history traits: the age at death, the age at maturity and the growth rate. Inferences on the rate of growth are mostly based on the qualitative and quantitative analysis of different features of the bone tissue (Amprino 1947; de Margerie et al. 2002; Chinsamy-Turan 2005; Huttenlocker et al. 2013), while estimations about the age at death and the age at maturity rely on the counting of bone growth marks (BGMs) by means of a methodology known as skeletochronology (Castanet et al. 1993; Woodward et al. 2013).

According to the number and density of bone cells, the distribution of collagen fibers within the bone matrix and the quantity of vascular canals, bone tissues are classified under several typologies that differ in the rate of bone formation (Amprino's rule) (Amprino 1947; Francillon-Vieillot et al. 1990; de Margerie et al. 2002; Chinsamy-Turan 2005; Huttenlocker et al. 2013). On the one hand, bone tissue can be highly vascularized (many vascular canals) with many osteocytes (i.e. bone cells) and with the collagen fibers of the bone matrix loosely and randomly organized. This kind of bone tissue, named *woven bone* (WFB), is deposited at very fast rates (Francillon-Vieillot et al. 1990; Currey 2002; Chinsamy-Turan 2005; Huttenlocker et al. 2013). On the other hand, bone tissue can be poorly vascularized, with few osteocytes and with the collagen fibers of the bone matrix closely and highly organized. This type of bone tissue, which is formed at very low rates, is known as *lamellar bone* (LLB) (Francillon-Vieillot et al. 1990; Currey 2002; Chinsamy-Turan 2005; Huttenlocker et al. 2013). Other types of bone tissue such as *parallel-fibered* (PFB) or *fibrolamellar bone* (also called *fibrolamellar complex* – FLC), present intermediate characteristics and rates of formation (See Chapter 3 for further information) (Francillon-Vieillot et al. 1990; Currey 2002; Chinsamy-Turan 2005; Huttenlocker et al. 2013). Due to the close relationship between bone tissue types and their respective rate of formation, bone typologies have been widely used as a proxy of the rate of growth in extant and extinct taxa (Köhler and Moyà-Solà 2009; Cubo et al. 2012; Marín-Moratalla et al. 2014; Orlandi-Oliveras et al. 2016). Interestingly, bone tissue types not only vary among species but also during ontogeny, recording individual growth and development. For instance,

mammals deposit a fast-growing bone (either FLC or PFB) during the first stages of ontogeny and a slow-growing LLB when growth rate decreases as the animal approaches adult body size (Currey 2002; Chinsamy-Turan 2005; Huttenlocker et al. 2013). FLC (or PFB), hence, makes up most part of the bone cross-section (Fig 1.1), while LLB is usually restricted to the most external (periosteal) part of the bone cortex (Fig. 1.1) constituting the external fundamental system (EFS) (Huttenlocker et al. 2013). The transition from the FLC (or PFB) to the EFS in a bone cortex is considered to mark the attainment of maturity, although it is still under debate whether this refers to skeletal maturity (Cormack 1987; Chinsamy-Turan 2005; Woodward et al. 2013; Martínez-Maza et al. 2014; Amson et al. 2015; Kolb et al. 2015a; Kolb et al. 2015b) or to sexual/reproductive maturity (Chinsamy and Valenzuela 2008; Marín-Moratalla et al. 2013; Jordana et al. 2016).

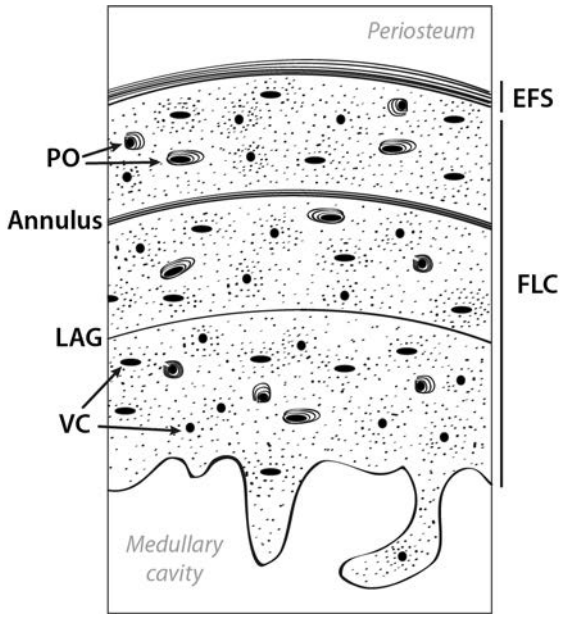

Figure 1.1. Schematic drawing of a hypothetical mammalian bone cortex. It is shown a fast-growing bone tissue (FLC) interrupted by bone growth marks (Annulus, LAG) occupying most part of the bone cortex. The slow-growing bone tissue (EFS) deposited after growth rate decrease makes up the most external cortex. EFS = external fundamental system; FLC = fibrolamellar complex; LAG = line of arrested growth; PO = primary osteon; VC = vascular canal.

Bones present other histological structures that also record individual growth and development. These are the *bone growth marks* (BGMs), histological features that record changes and interruptions in the rate of bone formation (Castanet et al. 1993; Huttenlocker et al. 2013). They are classified as *annuli* if they consist of a low-vascularized LLB or PFB (Fig. 1.1), or as *lines of arrested growth* (LAGs) if they occur as thin black lines within the bone cortex (Fig. 1.1) (Francillon-Vieillot et al. 1990; Castanet et al. 1993; Chinsamy-Turan 2005). *Annuli* register a drop in the rate of bone growth, while LAGs represent a pause in bone deposition (Francillon-Vieillot et al. 1990; Castanet et al. 1993; Chinsamy-Turan 2005; Huttenlocker et al. 2013). Nowadays, it is widely accepted that the vast majority of the BGMs found in vertebrates register annual cycles of growth (cyclical growth marks – CGMs) in response to physiological cycles (Köhler et al. 2012) that reflect environmental variations (Castanet et al. 1993; Chinsamy-Turan 2005). This assumption constitutes the basis for skeletochronological studies and thus for inferences of the individual timing of LH events. Therefore, the age at death of an individual can be estimated by counting the total number of CGMs within a bone cross-section (Castanet et al. 1993; Castanet et al. 2004; Castanet 2006; Woodward et al. 2013) while age at maturity can be calculated by counting the number of CGMs before deposition of the EFS (Chinsamy-Turan 2005; Chinsamy

and Valenzuela 2008; Marín-Moratalla et al. 2013; Woodward et al. 2013; Jordana et al. 2016). In mammals, the estimation of the age at death always yields a minimum individual age (Castanet et al. 2004; Castanet 2006), due to the characteristic asymptotic growth of this group of animals (Lee et al. 2013) and to the difficulty in differentiating CGMs from the lamellae of the EFS (Horner et al. 1999). CGMs can further provide insights into the growth rate of an individual. The pattern and rate of growth can also be reconstructed from the study of these features by measuring the distance between consecutive CGMs (Bybee et al. 2006; Woodward et al. 2013).

Non-cyclical BGMs can also be found in the bone cortices of vertebrates (Castanet et al. 1993; Castanet 2006; Woodward et al. 2013). Although they are less studied than CGMs, the identification of non-cyclical BGMs is critical for LH reconstructions made from bone histology. On the one hand, estimations of important LH traits such as age at death or age at maturity are inaccurate if a non-cyclical BGM is incorrectly counted as a cyclical one. Furthermore, non-cyclical BGMs have been associated to key LH events, such as hatching (Castanet and Baéz 1991; Bruce and Castanet 2006; Hugi and Sánchez-Villagra 2012), metamorphosis (Hemelaar 1985; Sinsch 2015) or weaning (Morris 1970; Castanet et al. 2004; Castanet 2006). Thus, their identification can provide valuable insights for LH reconstructions made from bone histology.

1.2.2. Teeth as recording structures

Teeth consist of three dental tissues: enamel, dentine and cementum (Fig. 1.2) (Carlson 1990; Hillson 2005). All of them present incremental markings in their microstructure, consequence of periodical variations on the particular secretion rhythm of each tissue (Carlson 1990; Klevezal 1996; Hillson 2005; FitzGerald and Rose 2008). Cementum deposition, for instance, leaves incremental marks following a yearly periodicity (Lieberman 1993; Klevezal 1996; Ungar 2010). The counting of these features, hence, yields information about LH variables such as the age and/or the season of death in extant and extinct mammals (Morris 1972; Spinage 1973; Fancy 1980; Penzhorn 1982; Burke and Castanet 1995; Klevezal 1996; Azorit et al. 2004; Jordana et al. 2012; Lkhagvasuren et al. 2013; Kolb et al. 2015b). Enamel and dentine, on the other hand, are formed at higher rates than cementum and thus record secretory pulses of shorter periodicity (Dean 1987). Therefore, enamel and dentine tissues present incremental markings of daily, supra-daily and sub-daily periodicity (Bromage 1991; Dean and Scandrett 1996; Dean 2000; Hillson 2005; Smith 2006; FitzGerald and Rose 2008; Smith 2008). Daily and supra-daily features in these tissues have been widely analyzed to calculate timings and rates of tooth formation in different mammalian species (Dean 1987; Dirks 1998; Tafforeau et al. 2007; Dirks et al. 2009; Jordana and Köhler 2011; Dirks et al. 2012; Metcalfe and Longstaffe 2012). This information is important for reconstructing the LH strategy of present and past animals (Bromage et al. 2002; Dirks et al. 2009; Jordana and Köhler 2011; Dirks et al. 2012; Jordana et al. 2014), as several stages of mammalian dental development, such as the eruption of the first or the third permanent molar, are tightly linked to key LH events (Smith 1989; Smith 2000; Dean 2006).

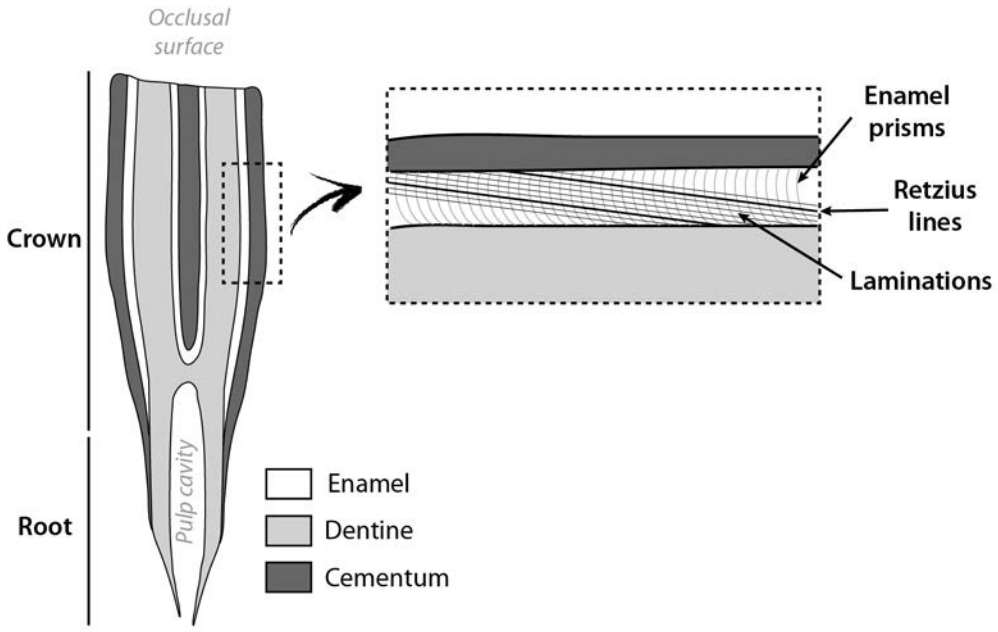

Figure 1.2. Schematic drawing of a hypothetical longitudinal cut on a hypsodont tooth. It shows the different tissues and structures that conforms a tooth. Figure also presents a magnification of dental enamel (dashed rectangle), where incremental markings (laminations, Retzius lines) and enamel prisms are displayed.

Among dental tissues, most researches have focused on dental enamel because it is simpler and less prone to diagenetic alterations than dentine (FitzGerald and Rose 2008). Enamel is formed from the tooth cusp to the root during amelogenesis, a biological process that is divided into two different stages (Boyde 1964; Hillson 2005; Ungar 2010). During a first phase of enamel development, the enamel-forming cells (i.e. ameloblasts) secrete thin hydroxyapatite-like crystals and an organic matrix rich in enamel-specific proteins (mainly amelogenin, ameloblastin and enamelin) (Hillson 2005; Lacruz et al. 2017). This stage is known as the matrix production phase of amelogenesis (Boyde 1964; Hillson 2005; Ungar 2010). It is followed by the maturation stage (Boyde 1964; Hillson 2005; Ungar 2010), during which enamel crystals grow in thickness and width while proteins and water of the previously deposited matrix are removed (Smith 1998; Hillson 2005; Ungar 2010; Lacruz et al. 2017). Enamel crystallites are arranged into bundles named *enamel prisms* (Fig. 1.2) (Hillson 2005), configuring the structural fundamental units of dental enamel (Smith 2006).

During matrix production, the secretory activity of the ameloblasts undergoes rhythmic fluctuations that lead to the formation of enamel incremental markings (Fig. 1.2) (Boyde 1964; Hillson 2005; Smith 2006; Smith and Tafforeau 2008; Lacruz et al. 2012). These are classified as short- or long-period marks according to their daily or supra-daily periodicity (FitzGerald and Rose 2008; Smith 2008). The most studied short-period marks are the so-called *cross-striations*. Under polarized or transmitted light, they appear as transversal bright and dark bands that cross the enamel prisms (Hillson 2005; FitzGerald and Rose 2008). Cross-striations have been mainly described in primates,

including humans (Smith 2008). Several studies using vital labelling have demonstrated that these features register circadian cycles of enamel formation (Bromage 1991; Smith 2006) that are regulated by the biological clock (Lacruz et al. 2012). *Laminations* (Fig. 1.2) are a second type of daily incremental marks found in mammalian enamel. Thus, they are temporally equivalent to cross-striations (Smith 2006). Although they may appear in primates (Smith 2006; Smith and Tafforeau 2008), laminations are the most important incremental features identified in the enamel of hypsodont animals (Iinuma et al. 2004a; Jordana and Köhler 2011; Kierdorf et al. 2013; Jordana et al. 2014). They run parallel to the enamel formation front, presenting a more oblique orientation than cross-striations (Smith and Tafforeau 2008). Finally, enamel long-periods marks comprise those incremental lines denominated *Retzius lines* (Fig. 1.2) (FitzGerald and Rose 2008; Smith 2008). They appear parallel to enamel laminations but more marked than daily lines (Smith and Tafforeau 2008), registering the position of the enamel-forming front at consecutive points in time (Smith 2006). Their periodicity, which has been one of the most studied topics in dental microanatomy (FitzGerald 1998), varies considerably across species: from few days in small primates to several weeks in proboscideans (Bromage et al. 2009).

Based on the distance and regularity of deposition of both short- and long-period enamel incremental markings, several parameters can be estimated that reflect enamel growth (Smith 2008). These are (i) the enamel *daily secretion rate* (DSR) or the amount of enamel formed by ameloblasts every 24 hours, (ii) the *enamel extension rate* (EER) or the number of ameloblasts activated at the same time, and (iii) the *repeat interval* (RI) or the periodicity of Retzius lines (See Chapter 3 for the methodology of calculation of each enamel growth parameter) (Smith 2008; Bromage et al. 2009; Hogg and Walker 2011). DSR and EER determine tooth growth in height and thickness (Smith 2008; Hogg and Walker 2011), so they are frequently used to estimate another variable: (iv) the *crown formation time* (CFT) or total period of crown formation (Smith et al. 2006; Smith 2008) (See Chapter 3 for the methodology of calculation of the CFT). The assessment of all these parameters sets the basis for obtaining information about the LH of extant and extinct species (Smith 2008). For instance, CFT estimations in the fossil bovid *Myotragus balearicus* provided evidence of an extended period of dental development that has been related, among others, to a slow pace of life based on bone histology (Köhler 2010; Jordana and Köhler 2011). EER and RI, on the other hand, have been correlated with several LH variables, such as the age at first reproduction or the adult body mass respectively (Bromage et al. 2009; Bromage et al. 2012; Jordana et al. 2014).

1.3. The genus *Equus*: A paradigm of evolution

The genus *Equus* comprises extant wild horses (*E. ferus*), zebras (*E. quagga* – formerly *E. burchelli*, *E. zebra*, *E. grevyi*) and asses (*E. africanus*, *E. hemionus*, *E. kiang*) (Moehlman 2002), as well as several extinct forms of Pliocene and Pleistocene equids (Azzaroli 1990). The domestic horse (*E. caballus*), the donkey (*E. africanus asinus*) and their respective

crossbreeds (the mule and the hinny) are also grouped in this clade (Cucchi et al. 2017). *Equus* is included in the family Equidae, which along with Tapiridae and Rinocerontidae comprises the order Perissodactyla (Steiner and Ryder 2011). The genus is characterized by different anatomical features of the cranium, teeth and limb bones (Alberdi and Cerdeño 2003; Garrido 2008), among which the reduction in the number of digits and the extremely hypsodont high-crowned teeth are outstanding (MacFadden 1992). The enamel pattern of the lower cheek teeth is used to classified extant and fossil *Equus* in two distinct groups, the "caballoids" (after *Equus caballus*) and the "stenonoids" (after *Equus stenonis*) (Hopwood 1936; Forsten 1988; Alberdi et al. 1998). Specifically, caballoid horses present a U-shaped linguaflexid between the metaconid and the metastylid, while stenonoids show and V-shaped linguaflexid (Hopwood 1936). Stenonoids comprise the extant species of zebras and asses (Forsten 1988) and the most primitive fossil *Equus* found in Pliocene and Pleistocene paleontological sites of the Old World (Forsten 1988; Alberdi et al. 1998). Extant feral and domestic horses, as well as several extinct species of Middle/Upper Pleistocene and Holocene equids, belong to caballoid horses (Forsten 1988; Cucchi et al. 2017).

Equid evolution is considered iconic in Paleontology (MacFadden 1992; Janis 2007). The great amount of well-preserved equid remains in the fossil record has allowed researchers to exhaustively track the most important evolutionary tendencies of the group, from their first appearance in the Eocene to the most recent *Equus* species (MacFadden 1992; Alberdi and Cerdeño 2003; Janis 2007; Orlando 2015). As a result, the evolution of horses has been widely used to exemplify macroevolution, and is an indispensable topic in student text-books (MacFadden 2005). Equids are considered of extreme importance in both extant and fossil ecological communities (Janis 1976; Odadi et al. 2011) due to their position as tope grazer consumers (Forsten 1989). Despite their high diversity in the past, extant equids are now only represented by the genus *Equus* (MacFadden 2005; Orlando 2015) and most of their representatives are seriously threatened according to the International Union for Conservation of Nature and Natural Resources (IUCN) (Orlando 2015; IUCN 2018). From the seven wild living species that comprises the genus, *E. kiang* is catalogued as "least concerned", *E. quagga* and *E. hemionus* as "near threatened", *E. zebra* as "vulnerable", *E. ferus* and *E. grevyi* as "endangered" and *E. africanus* as "critically endangered" (IUCN 2018).

1.3.1. Evolutionary history of the genus *Equus*

Family Equidae is thought to originate around 55 Ma ago from the "Hyracothere clade" (previously known as *Hyracotherium* or "Eohippus") (MacFadden 1992; Froehlich 2002; MacFadden 2005; Prothero 2009). Hyracotherine fossils have been found in the Eocene of North America and Europe (Forsten 1989; Janis 2007). They were dog-sized hoofed mammals with low-crowned teeth adapted for browsing, four toes on the front feet and only three toes on the hind feet (MacFadden 1992; Eisenmann 1993; Janis 2007; Orlando 2015). In this group initiated a general evolutionary trend within Equidae towards an increase in molar height, a diminution in the number of digits and an increase

in body size (MacFadden 1992; Eisenmann 1993; Alberdi and Cerdeño 2003). Because *Equus* present very high-crowned teeth and only one toe in both the fore and hind feet (MacFadden 1992), first evolutionary studies on equids proposed a linearly evolution from the Eocene ancestries to these more derived horses (MacFadden 1992; MacFadden 2005; Janis 2007; Prothero 2009). This view, however, rapidly changed during the 20th century when a huge number of new equid genera and species were described, and it is now well-known that there are many different evolutionary branches within Equidae (Simpson 1953; MacFadden 1992; MacFadden 2005; Janis 2007).

Equus is believed to have emerged 4.0 – 4.5 Ma ago (Orlando et al. 2013) in North America (Azzaroli 1990; Forstén 1992), where they survived, underwent radiation and dispersed to other continents until becoming extinct at the end of the Pleistocene due to climatic changes and human hunting (Azzaroli 1992; Guthrie 2003; MacFadden 2005; Janis 2007; Lorenzen et al. 2011). Taxonomic and phylogenetic relationships among species of Pleistocene North American *Equus* are still not well resolved. Researchers have usually classified them in two different groups: the stout-legged and the stilt-legged horses (Heintzman et al. 2017). While the first ones are widely accepted to be closer linked to other Pleistocene caballine equids (Weinstock et al. 2005), stilt-legged horses have been related either to Asiatic wild asses based on morphological similarities (Eisenmann et al. 2008) or to other caballine forms based on genetic studies (Weinstock et al. 2005; Vilstrup et al. 2013). Recently, these slender equids have even been grouped under a new genus named *Haringtonhippus* (Heintzman et al. 2017). During the Pliocene and the Pleistocene, *Equus* dispersed from North America into the Old World and South America (Azzaroli 1992; Eisenmann 1992; MacFadden 1992; Janis 2007; Orlando 2015). They are thought to have arrived in South America through the Panamanian Isthmus during the Great American Biotic Interchange 1 Ma ago (MacFadden 2013; Prado and Alberdi 2017). There, they coexisted with *Hippidion* (Prado and Alberdi 2017), another clade of Plio-Pleistocene American equids (Prado and Alberdi 1996; Der Sarkissian et al. 2015). Like North American horses and many other groups of big mammals, both groups of South American equids did not survive the megafaunal extinction that took place 10,000 years ago on this continent (Azzaroli 1992; MacFadden 2005; Barnosky and Lindsey 2010).

Regarding the Old World, *Equus* reached Eurasia in two different migration waves (Alberdi and Bonadonna 1988; Forsten 1988; Azzaroli 1992; Alberdi and Cerdeño 2003; Orlando 2015). A first dispersal event took place 3.0 – 2.5 Ma ago (Lindsay et al. 1980; Azzaroli 1983), when an episode of climate cooling allowed stenonoid horses to reach this continent (Alberdi and Bonadonna 1988; Alberdi et al. 1998) through the Bering Strait (Orlando 2015). During the Pliocene and the Early and Middle Pleistocene, stenonoids quickly flourished and dispersed through Eurasia (Orlando 2015), becoming important elements of the faunal complexes of these epochs (Forsten 1988; Alberdi et al. 1998). From there, stenonoids entered Africa in at least two different events (Orlando 2015). Caballine *Equus* arrived at Eurasia from the New World during a second migration that took place in the Middle Pleistocene (1 – 0.8 Ma) (Alberdi and Bonadonna 1988; Forsten 1988; Orlando 2015). They rapidly replaced stenonoid forms, which became confined to Africa (Forsten

1988), probably as a consequence of the climatic changes that occurred during the Early/Middle Pleistocene boundary (Alberdi and Bonadonna 1988; Forsten 1988; Alberdi et al. 1995). One of the most striking evolutionary tendencies of *Equus* in the Old World is its reduction in body size, which has been observed in both the stenonoid and the caballoid lineages (Forsten 1991; Alberdi et al. 1995; Alberdi et al. 1998). During the Pleistocene and Holocene of Europe and Africa, stenonoid and caballoid equids exhibit a dwarfing trend (Forsten 1991; Alberdi et al. 1995; Alberdi et al. 1998) that has usually been explained as an adaptation to climatic and resources variations during these time periods (Forsten 1991; Alberdi et al. 1995; Alberdi et al. 1998; Cantalapiedra et al. 2017).

Over the last decades, multiple molecular analyses have been performed to address the phylogenetic relationships and the divergence times between extant *Equus* species (George and Ryder 1986; Steiner and Ryder 2011; Steiner et al. 2012; Vilstrup et al. 2013; Jónsson et al. 2014; Rosenbom et al. 2015). A recent phylogeny based on the analysis of complete equid genomes, for instance, suggests that caballoid (*E. ferus* and *E. caballus*) and non-caballoid (zebras and asses) *Equus* diverged around 2 Ma ago (Jónsson et al. 2014). Among non-caballine groups, zebra species form a monophyletic clade that started to diversify 1.6 Ma ago (Jónsson et al. 2014), with mountain zebra (*E. zebra*) diverging from Grevy's (*E. grevyi*) and plains zebra (*E. quagga*), which are sister species (Steiner et al. 2012; Vilstrup et al. 2013; Jónsson et al. 2014). African (*E. africanus*) and Asiatic wild asses (*E. hemionus* and *E. kiang*) are grouped in a second clade within non-caballine horses (Steiner et al. 2012; Vilstrup et al. 2013; Jónsson et al. 2014) that is estimated to have split approximately 1.7 Ma ago (Jónsson et al. 2014). Both Asiatic wild asses, the hemione (*E. hemionus*) and the kiang (*E. kiang*), diverged sometime later around 600 Ky ago (Jónsson et al. 2014).

1.3.2. Biology and ecology of extant *Equus*

Extant wild *Equus* are spread across different environments of Africa and Asia. In Asia, *E. ferus* is found in small patches in semi-desert habitats of China and Mongolia, where it was reintroduced in the 1990s after being almost extinct in the wild (King et al. 2015). *E. hemionus* also inhabits semi-desert and desert Asiatic plains (Nowak 1999; Kaczensky et al. 2015). It is mainly distributed across the Gobi Desert (southern Mongolia and China), though small populations have also been found in Iran and India (Kaczensky et al. 2015). On the contrary, *E. kiang* dwells in broad valleys, alpine meadows and hills where grass-like plants are abundant (Nowak 1999; Shah et al. 2015). Its distribution is restricted to the Tibetan Plateau (China, Pakistan, India and Nepal) at elevations up to 5,400 m (Shah et al. 2015). The wild ass of the African continent, *E. africanus*, lives in stony arid bushlands and grasslands of Eritrea and Ethiopia (Moehlman et al. 2015). Nowadays, it is the most threatened *Equus* species (IUCN 2018) with a distribution of only 23,000 km^2 (Moehlman et al. 2015). Grévy's zebra inhabits arid and semi-arid grasslands and shrublands too, but its habitat is limited to the horn of Africa, specifically to Ethiopia and Kenya (Rubenstein et al. 2016). *E. zebra*, on the other hand, occurs in escarpment mountainous areas up to 2,000 m in Namibia and South Africa (Eastern, Northern and Western Cape Province)

where there is a high diversity of grasses (Novellie 2008). Finally, the plains zebra shows the widest range of distribution among all extant *Equus* (IUCN 2018). It can be found in open savanna or open woodland with abundance of grass, ranging from southern Angola, northern Namibia and northern South Africa to South Sudan and southern Ethiopia (King and Moehlman 2016).

All living equids are considered grazers because they mainly feed on grass (Nowak 1999). Several species, however, do also browse to some degree (Nowak 1999). Unlike artiodactyls, *Equus* are hind-gut fermenters, which means that most of their microbial digestion takes place in the caecum (Janis 1976). This digestive strategy allows them to feed on low-quality forage with a high content in cellulose, such as stems instead of leaves (Janis 1976). Dietary traits of extant equids are quite diverse (Schulz and Kaiser 2013), consequence of the different environments that these animals inhabit. For instance, *E. hemionus* and *E. africanus* incorporate a high percentage of browse in their diets (Nowak 1999; Grinder et al. 2006; Schulz and Kaiser 2013; Kaczensky et al. 2015). As they live in very arid environments, they must browse or graze on any available forage (Grinder et al. 2006; Kaczensky et al. 2015). Conversely, plains and mountain zebras have plenty access to grass-like plants (Novellie 2008; King and Moehlman 2016) and thus grazing comprises most of their diet (Grubb 1981; Penzhorn 1988; Nowak 1999; Schulz and Kaiser 2013). They only browse if forced to do so, which only happens in dry periods (Grubb 1981; Novellie 2008; King and Moehlman 2016). Water is a very limiting factor in populations of extant wild equids (Saltz 2002). It restricts the distribution of several taxa, such as *E. grevyi* or *E. zebra*, which inhabit areas where permanent water can be found (Novellie 2008; Rubenstein et al. 2016). Other equids present certain behaviors that facilitate their access to hydric resources. *E. hemionus* is known to walk very long distances looking for water and even to dig deep holes for obtaining it from subterranean aquifers (Kaczensky et al. 2015), while *E. kiang* covers most of its water requirements with water stored in snow and plants (St-Louis and Côté 2009).

Extant wild equids exhibit two different types of social organization (Klingel 1974). On the one hand, species inhabiting temperate environments live in permanent family groups comprising several mares with their foals and one leading stallion (Klingel 1974; St-Louis and Côté 2009). Males also organized in stallion groups once they leave the family group due to illness or old age (Klingel 1974). Sick and old mares, however, use to stay in the same family group for all their life (Klingel 1974). The species showing this kind of social organization are considered non-territorial (Klingel 1974), as they share their home range with other associations of the same species. The non-territorial behavior has been documented in the Przewalski's horse (Nowak 1999; King et al. 2015) and in the plains (Grubb 1981; King and Moehlman 2016) and mountain zebra (Penzhorn 1988). Equids adapted to arid environments, on the other hand, present a complete different social arrangement (St-Louis and Côté 2009) that is characterized by the lack of stable bonds between animals, with the exception of that between a mare and her foals (Klingel 1974). These species can be found either in solitary or conforming mixed herds, stallion groups, mare groups or mares-foals groups, but bands are always temporary (Klingel

1974). Solitary males under this social organization exhibit a marked territorial behavior (Klingel 1974). Territoriality is known to occur in the African species *E. grevyi* (Churcher 1993; Nowak 1999) and *E. africanus* (Grinder et al. 2006; Moehlman et al. 2015) and in both Asiatic wild asses (Klingel 1998; Nowak 1999; St-Louis and Côté 2009; Shah et al. 2015). Although most extant equids mate, mark, look after their foals and fight in a similar way, the kind of social arrangement strongly influences other social behaviors such as dominance (Klingel 1974). For instance, non-territorial species show a marked hierarchy within their family groups, while no dominance ranks are observed in territorial equids (Klingel 1974; Nowak 1999). Furthermore, most wild *Equus* inhabit areas that are subject to extreme seasonal variations on resources and water supply, which force them to migrate repeatedly (Klingel 1974). This migratory behavior is closely linked to the type of social organization. In non-territorial species, population migrates as a whole, which facilitates breeding at any time during the entire year (Klingel 1974). This is the case, for instance, of *E. quagga*, whose migrations across the Serengeti are considered one of the most massive among ungulates (King and Moehlman 2016). On the contrary, only mares of territorial species migrate during the dry season, as the alpha-stallion always remains to defend its territory (Klingel 1974). In these species, mating is limited therefore to the rainy season (Churcher 1993; Nowak 1999; Grinder et al. 2006).

The most important LH traits of extant wild *Equus* are summarized in Table 1.1. Adult body mass of living equids ranges from 200 to 400 kg, being *E. hemionus* the lightest species with only 230 kg (Nowak 1999; Ernest 2003). By contrast, Grevy's zebra (384 kg, Ernest 2003) and kiang males (350 – 400 kg, St-Louis and Côté 2009) show the highest weight among extant wild taxa (Table 1.1). The domestic species *E. africanus* is reported to live up to 47 years (Ernest 2003), but they usually live only half of this time span in the wild (Table 1.1). Interestingly, the Asiatic wild ass has a longer life span than expected from its body mass (Table 1.1), as it is documented to live up to almost 30 years in the wild (Lkhagvasuren et al. 2018) being the smallest living *Equus* species (Ernest 2003). Stallions of all species attain sexual maturity between their third and fourth year of life (Grubb 1981; Churcher 1993; Monfort et al. 1994; Nowak 1999; Tacutu et al. 2013), with the exception of the African wild ass that is sexually mature at the age of two (Grinder et al. 2006) (Table 1.1). Female *Equus* mature a bit earlier than males, usually when they are two or three years old (Monfort et al. 1994; Nowak 1999; Tacutu et al. 2013) (Table 1.1). Again, *E. africanus* mares deviate from this pattern by maturing between their first and second year of life (Grinder et al. 2006). Plains zebra mares are reported to attain sexual maturity at the same range of age (1 – 2 years, Grubb 1981), while some Grévy's zebras may delay the onset of maturity up to the age of four (Nowak 1999). Like many other ungulates (Vanpé et al. 2009), both male and female equids show a decoupling between their physiological maturity and the time of their first breeding (Table 1.1). Generally, stallions reproduce for the first time at the age of five (Penzhorn 1988; Monfort et al. 1994; Kaczensky et al. 2015) although males of *E. quagga* and *E. grevyi* may reproduce at 4.5 and 6 years respectively (Grubb 1981; Nowak 1999). In females, age at first mating varies considerably among species (Table 1.1). Mares of African wild ass and plains zebra show the earliest age at first reproduction (2 – 3 years, Grubb 1981; Grinder et al. 2006), followed by the Asiatic wild

	E. ferus	*E. hemionus*	*E. kiang*	*E. africanus*	*E. quagga*	*E. grevyi*	*E. zebra*
Adult weight (kg)	200 – 300 [a]	230 [b]	250 – 300 ♀, 350 – 400 ♂ [c]	250 [b]	257 [b]	384 [b]	296 [b]
Longevity (y)	38 * [a]	29 [d]	20 [c]	47 * [b]	21 [e]	18 [f]	29 * [b]
Age at sexual maturity (y)	2.5 – 3 ♂ [g]	3 ♂ [a]	–	2 ♂ [h]	4 ♂ [i]	4 ♂ [f]	3.5 ♂ [j]
	2 ♀ [g]	2 ♀ [a]	–	1.5 ♀ [h]	1 – 2 ♀ [i]	3 – 4 ♀ [a]	2.8 ♀ [j]
Age at first reproduction (y)	5 ♂ [g]	5 ♂ [k]	–	–	4.5 ♂ [i]	6 ♂ [a]	5 ♂ [m]
	4 ♀ [g]	3 ♀ [k]	3 – 4 ♀ [c]	2 – 3 ♀ [h]	2.5 ♀ [i]	3 – 6 ♀ [f]	5 ♀ [m]
Weaning age (mo)	24 [a]	12 – 18 [a]	–	12 – 14 [h]	7 – 11 [a]	9 [f]	10 [a]
Gestation length (d)	322 – 420 [g]	330 [a]	355 [l]	365 [a]	371 [i]	390 [f]	364 [m]
Weight at birth (kg)	25 – 30 [a]	–	≤ 36 [c]	29 [a]	32 [a]	40 [f]	25 [m]

Table 1.1. Main life history traits of extant wild equids. The star (*) indicates data from captive animals. Kg = kilograms; y = years; mo = months; d = days. Information has been compiled from the following sources: [a]Nowak 1999; [b]Ernest 2003; [c]St-Louis and Côté 2009; [d]Lkhagvasuren et al. 2018; [e]Smuts 1974, [f]Churcher 1993; [g]Monfort et al. 1994; [h]Grinder et al. 2006; [i]Grubb 1981; [j]Tacutu et al. 2013; [k]Kaczensky et al. 2015; [l]Shah et al. 2015; [m]Penzhorn 1988.

ass (3 years, Kaczensky et al. 2015), the kiang (3 – 4 years, St-Louis and Côté 2009), the wild horse (4 years, Monfort et al. 1994) and the mountain zebra (5 years, Penzhorn 1988). Females of *E. grevyi* breed for the first time over a wider range of age, from their third to their sixth year of life (Churcher 1993). Age at weaning also varies widely among extant *Equus* (Table 1.1). African zebras show the earliest age at weaning amongst equids: *E. zebra* at their tenth month (Nowak 1999), *E. grevyi* at their ninth month (Churcher 1993) and *E. quagga* between their seventh and eleventh month of live (Nowak 1999). Foal wild asses, on the other hand, stop suckling some time later: between their twelfth and their fourteenth or between their twelfth and their eighteenth month in *E. africanus* and *E. hemionus* respectively (Nowak 1999; Grinder et al. 2006). Przewalski's horses are weaned at the age of two (Nowak 1999). In all living equids, gestation length is approximately one year (Grubb 1981; Penzhorn 1988; Churcher 1993; Monfort et al. 1994; Nowak 1999; Shah et al. 2015) (Table 1.1). Equid foals weight between 25 and 40 kg when born (Penzhorn 1988; Churcher 1993; Nowak 1999; St-Louis and Côté 2009) (Table 1.1). Grévyi's zebra has the largest neonates (40 kg, Churcher 1993), while *E. zebra* neonates are the smallest with only 25 kg (Penzhorn 1988).

- Chapter 2 -

Aims & Objectives

Aims & Objectives

The histological analyses of bones and teeth aimed at reconstructing the biology and LH of vertebrates is an active area of research. The vast majority of bone histological studies focus on amphibians and reptiles (Castanet et al. 1993) due to the traditional belief that endotherm organisms grow continuously (Chinsamy-Turan 2005). Recent research, however, has shown that bones of these animals also record cyclical periods of growth that are synchronized with seasonal physiology (Köhler et al. 2012). Since then, the number of studies that analyze bone histology in living (Marín-Moratalla et al. 2013; Marín-Moratalla et al. 2014; Jordana et al. 2016) and fossil (Martínez-Maza et al. 2014; Amson et al. 2015; Kolb et al. 2015a; Kolb et al. 2015b; Moncunill-Solé et al. 2016; Orlandi-Oliveras et al. 2016) mammals have significantly increased, though many mammalian groups still remain poorly studied. Furthermore, the biological significance of several histological features, such as the deposition of non-cyclical BGMs or the appearance of EFS, are not well known yet. Thus, studies on living taxa are still necessary to completely understand the biological signals recorded in bone tissue (Martínez-Maza et al. 2014; Woodward et al. 2014; Cambra-Moo et al. 2015; Kolb et al. 2015a; Jordana et al. 2016). The study of extant species is also indispensable for creating a solid framework that allows the comparison and analysis of fossil forms (de Ricqlès 2011).

Regarding dental histology, enamel microstructure of low-crowned primates is broadly studied in comparison to other mammalian groups, as most histological research has traditionally focused on these animals (Smith 2008). In hypsodont species, however, enamel histology is still relatively unexplored. Only a few studies have extensively analyzed this dental tissue in several groups of bovids and cervids (Macho and Williamson 2002; Iinuma et al. 2004a; Jordana and Köhler 2011; Kierdorf et al. 2013; Jordana et al. 2014), while previous descriptions of enamel incremental lines and their periodicity in equids (Hoppe et al. 2004) have recently been challenged by several authors (Kierdorf et al. 2013; Kierdorf et al. 2014). Hence, exhaustive histological studies that investigate the enamel tissue of high-crowned vertebrates are absolutely needed.

Among mammals, equids are an essential group of study in several scientific disciplines including Ecology, Zoology and Paleontology. The ecological and zoological interest in *Equus* mainly centers on the development of conservation plans for the clade (Moehlman 2002), as most wild equid species are under threat of extinction (IUCN 2018). In this regard, bone and dental histology could serve as powerful tool for obtaining information about their main LH and demographic traits (Chinsamy and Valenzuela 2008; García-Martínez et al. 2011; Marín-Moratalla et al. 2013), which would help in turn

to improve their conservation strategies. In Paleontology, Equidae is an emblematic clade (MacFadden 2005). Nonetheless, paleohistological studies in these mammals are still scarce (Enlow and Brown 1958; Sander and Andrássy 2006), the study of Martínez-Maza et al. (2014) being hitherto the only one that provides LH data for a fossil equid (*Hipparion concudense*) from the histological analysis of their bones. In fact, the microscopic study of bones and teeth in *Equus* is expected to provide key information about LH traits that tightly correlate with body size (Köhler 2010), which is one of the most interesting features of equid evolution (MacFadden 1992). During the evolutionary history of *Equus* in the Old World, for instance, a trend towards dwarfed forms in both the stenonoid and caballoid lineages has been described (Forsten 1991; Alberdi et al. 1995; Alberdi et al. 1998). However, despite body size being one of the most important LH trait of an animal (Peters 1983; Calder 1984), these body size variations have never been investigated from a LH perspective. Instead, the size decrease observed in European fossil horses has been related to changes in resources and climatic conditions because of the tight relationship between body size and environment (Forsten 1991; Alberdi et al. 1995; Cantalapiedra et al. 2017).

Therefore, the main aim of the present PhD dissertation is to thoroughly analyze bone and dental histology of extant and extinct *Equus* to reconstruct their most important LH traits and to shed light on their LH strategies. On the one hand, the study of extant species will contribute to the knowledge about mammalian bone and dental histology and, at the same time, it will provide a firm basis for the subsequent paleohistological analysis on fossil taxa. In extinct equids, bone and dental paleohistology provides the opportunity to study the size variation reported for Pleistocene forms within a LH framework. In this regard, the hypothesis to be tested in this PhD dissertation is that different-sized equids differ in their LH strategies, due to the coupling between body size and LH (Blueweiss et al. 1978; Calder 1984).

The present PhD thesis addresses the following specific goals:

I. To reconstruct the histological development of bones and teeth in ontogenetic series of different extant *Equus* species

II. To correlate the histological features found in bones and teeth of living *Equus* with different LH traits of the species and with key biological events.

III. To reconstruct the most important LH traits and the LH strategy of different-sized extinct *Equus* from the histological analysis of their bones and teeth.

IV. To shed light on the body size trends observed in *Equus* from a LH perspective.

Table 2.1 explains how the different chapters, the specific objectives and the publications that conform the present dissertation are related.

PhD Chapter	Goal achieved	Publication
Chapter 4. First approach to bone histology and skeletochronology of *Equus hemionus*	**I, II**	**Nacarino-Meneses C., Jordana X. & Köhler M. (2016)** *Comptes Rendus Palevol* 15: 267-277 Q2 (Paleontology); IF (2016): 1.376
Chapter 5. Histological variability in the limb bones of the Asiatic wild ass and its significance for life history inferences	**I, II**	**Nacarino-Meneses C., Jordana X. & Köhler M. (2016)** *PeerJ* 4: e2580 Q2 (Multidisciplinary sciences); IF (2016): 2.177
Chapter 6. Limb bone histology records birth in mammals	**I, II**	**Nacarino-Meneses C. & Köhler M.** (Accepted) *PLoS ONE* Q1 (Multidisciplinary sciences); IF (2016): 2.806
Chapter 7. The life history of European Middle Pleistocene equids: first insights from bone histology	**III, IV**	**Nacarino-Meneses C. & Orlandi-Oliveras G.** (To be submitted)
Chapter 8. Reconstructing molar growth from enamel histology in extant and extinct *Equus*	**I, II, III, IV**	**Nacarino-Meneses C., Jordana X., Orlandi-Oliveras G. & Köhler M. (2017)** *Scientific Reports* 7: 15965 Q1 (Multidisciplinary sciences); IF (2016): 4.259

Table 2.1. Overview of the chapters included in the present PhD dissertation. For each chapter (number and title), it is the objective achieved and the publication (authors, year, journal, number, pages, quartile, discipline and impact factor) to which it refers.

- Chapter 3 -

Material & Methods

Material & Methods

3.1. Material

The sample studied in the present PhD dissertation comprises 81 bone and dental thin sections from a minimum number of 35 individuals belonging to different species of extant and extinct *Equus* (Table 3.1). 70 histological thin sections from different limb bones (femora, tibiae, metacarpi and metatarsi) and first lower molars were analyzed in 27 specimens of living equids (see Chapters 4 to 8 for further information) (Table 3.1). In extinct *Equus*, 7 metapodia and 4 first lower molars from a minimum number of 8 individuals were studied (see Chapters 7 and 8 for further information) (Table 3.1). All material came from museum collections from which permission to prepare histological thin sections was obtained.

EXTANT SPECIES

	Individuals	Bone thin sections		Dental thin sections	
		n	Chapter	n	Chapter
Equus hemionus	12	36	4 to 7	5	8
Equus quagga	11	14	6	3	8
Equus grevyi	4	10	6 and 7	2	8
Total extant *Equus*	**27**	**60**	**4 to 7**	**10**	**8**

EXTINCT SPECIES

	Individuals	Bone thin sections		Dental thin sections	
		n	Chapter	n	Chapter
Equus ferus	2	-	-	2	8
Equus hydruntinus	2	-	-	2	8
Equus steinheimensis	2*	4	7	-	-
Equus mosbachensis	2*	3	7	-	-
Total extinct *Equus*	**8***	**7**	**7**	**4**	**8**

	Individuals	Bone thin sections		Dental thin sections	
		n	Chapter	n	Chapter
TOTAL PhD	**35***	**67**	**4 to 7**	**14**	**8**

Table 3.1. Summary of the sample analyzed in the present PhD thesis. See the specific chapter for further details on the sample. n = number of bone/dental thin sections. The star (*) indicates minimum number of individuals.

3.1.1. Extant sample

Ontogenetic series of limb bones and teeth from Asiatic wild ass (*E. hemionus*), plains zebra (*E. quagga*) and Grevy's zebra (*E. grevyi*) comprise the extant sample of this PhD thesis (Table 3.1). These three equids differ greatly in ecology and life history, covering almost all the biological variability reported for living wild *Equus* (Nowak 1999; Ernest 2003; Kaczensky et al. 2015; King and Moehlman 2016; Rubenstein et al. 2016; see also Table 1.1 in Chapter 1). Therefore, they were considered the most appropriate taxa to histologically exemplify the growth and development of the whole clade.

The extant *Equus* sample includes captive, semi-captive and wild individuals. Most specimens of *E. hemionus*, *E. quagga* and *E. grevyi* were born and lived captive at the Hagenbeck Zoo (Hamburg, Germany). They currently belong to the scientific collections of the Zoological Institute of Hamburg University (Germany) (See Chapters 4 to 8 for further information). Some of them had associated sex information, but all lacked age data. Thus, each captive individual was aged according to the wear and eruption patterns described for the species (Silver 1963; Smuts 1974; Penzhorn 1982; Lkhagvasuren et al. 2013). Additionally, annual cementum layers were counted in the first lower incisor of captive adult specimens to obtain a more accurate estimation of their age at death (Lkhagvasuren et al. 2013; see also Chapter 8 for further information). The exhaustive analysis of dental enamel performed in Chapter 8 also provided a more precise age assessment for some captive subadult individuals of *E. hemionus*, *E. grevyi* and *E. quagga*. Several plains and Grevy's zebras of the sample lived semi-captive in the African Reserve of Sigean (Sigean, France) (see Chapter 6 for further information). At present, they are part of the Natural History collection of the Catalan Institute of Paleontology (Barcelona, Spain), where they are also housed. Key biological information of semi-captive zebras, such as their sex, their date of birth or their date of death, was provided by veterinarians of the African Reserve of Sigean (B. Lamglait, pers. comm.). Finally, bone samples of adult *E. hemionus* came from the collections of the Museum of Domesticated Animals of the Martin-Luther-University Halle-Wittenberg (Halle, Germany) (see Chapters 4 to 7 for further information). They belonged to animals that lived wild in the Gobi Desert before being killed by poachers (Schöpke et al. 2012). Curator of the museum provided sex data and age estimations for these specimens of *E. hemionus* (R. Schafberg, pers. comm.).

3.1.2. Fossil sample

The fossil sample of this PhD dissertation is comprised of bones and teeth of different European species of Pleistocene *Equus* (Table 3.1). Metapodial bones were histologically studied in the Middle Pleistocene species *Equus steinheimensis* and *Equus mosbachensis* (Table 3.1), whereas thin sections from first lower molars were prepared from the Late Pleistocene *Equus ferus* and *Equus hydruntinus* (Table 3.1).

Fossil bones of Middle Pleistocene equids belong to the collections of the Staatliches Museum für Naturkunde (Stuttgart, Germany) (See Chapter 7 for further information).

Specifically, metapodia of *E. steinheimensis* were recovered from Steinheim an der Murr site (Germany) (Adam 1954), a late Middle Pleistocene locality dated as the Holsteinian Interglacial (MIS 11) (Van Asperen 2013). Material of *E. mosbachensis* comes from the early Middle Pleistocene site of Mosbach Sands (Wiesbaden, Germany) (Koenigswald et al. 2007), which is generally correlated with the Cromerian Interglacial (MIS 13, 15) (Maul et al. 2000; Kahlke et al. 2011).

Fossil teeth of *E. ferus* and *E. hydruntinus* were found in La Carihuela cave (Piñar, Spain) (See Chapter 8 for further information). This fossil locality is dated as Late Pleistocene, between 82,500 and 11,200 years BP (Carrión 1992; Fernández et al. 2007; Samper Carro 2010). Specifically, fossil teeth studied in the present PhD thesis were recovered along with material belonging to other species of macro- (*Cervus elaphus*, *Bos primigenium*) and micromammals (*Chionomys nivalis*, *Allocricetus bursae*) typical of cold climates (Ruiz Bustos and García Sánchez 1977; Fernández et al. 2007).

3.2. METHODS: Histological thin sections of bones and teeth

3.2.1. Preparation of histological thin sections

The preparation of histological thin sections is a destructive process (Chinsamy and Raath 1992; Lamm 2013) that usually involves the subtraction of a bone portion (Fig. 3.1A). In some cases (e.g. small samples, teeth), not only a part but the whole element (Fig. 3.1B) may be partially or totally damaged (Lamm 2013). Hence, it is of extreme importance to document and collect as much information as possible from the original bone/tooth before beginning the sectioning process (Lamm 2013). In this PhD thesis, all material was exhaustively measured and photographed before starting the preparation of the histological slices. This information, together with any other relevant associated data (e.g. sex, age, degree of bone epiphyseal fusion, degree of tooth wear) was annotated and incorporated into the histological database of the Evolutionary Paleobiology department of the Catalan Institute of Paleontology (ICP, Barcelona). In the case of fossil specimens, only fragmentary bones/teeth were used to avoid any possible damage to more valuable samples.

The procedure followed to obtain histological slices from extant and fossil bones began with the extraction of a 3-cm block from its mid-diaphysis (1.5 cm above and 1.5 cm below the exact mid-diaphysis of the bone) (Fig. 3.1A). This bone chunk was then embedded into an epoxy resin (Araldite 2020), which prevents its fracture during the following steps of the process (Chinsamy and Raath 1992). Afterwards, this embedded block was divided into two halves (Fig. 3.1C) with a low speed diamond saw (IsoMet, Buehler) (Fig. 3.1D), each exposing the mid-shaft surface of the bone (Fig. 3.1C). One of these surfaces was later polished either in a grinder-polisher machine (Metaserv®250, Buehler) (Fig. 3.1E) or with carborundum powder of decreasing particle size (350, 800

and 1000 grit) (Fig. 3.1F). Then, it was fixed to frosted glass that was previously polished too (Fig. 3.1F). The sample and the glass were joined using Loctite 358, a glue that must be exposed to ultraviolet light for 30 minutes to completely harden (Fig. 3.1G). The thin section was finally obtained from the fixed bone block using PetroThin (Buehler) (Fig. 3.1H), a specific machine that cuts slices of »400 µm thick and then grounds them up into several microns. With this device, histological thin sections of ≈150 µm thick were obtained. However, these samples were still too thick to be observed under the microscope (Bromage and Werning 2013). Thus, they were polished again in the Metaserv®250 or with carborundum powder to obtain a final thickness of 100 – 120 µm. Histological thin sections were finished by covering and mounting them using different products that enhance viewing under the microscope. Histological slices obtained from extant samples were covered with a mix of oils (Lamm 2013) before being protected with a cover slip. Thin sections prepared from fossil bones, on the other hand, were mounted using DPX medium (Scharlau). This latter procedure requires the dehydration of the histological slice

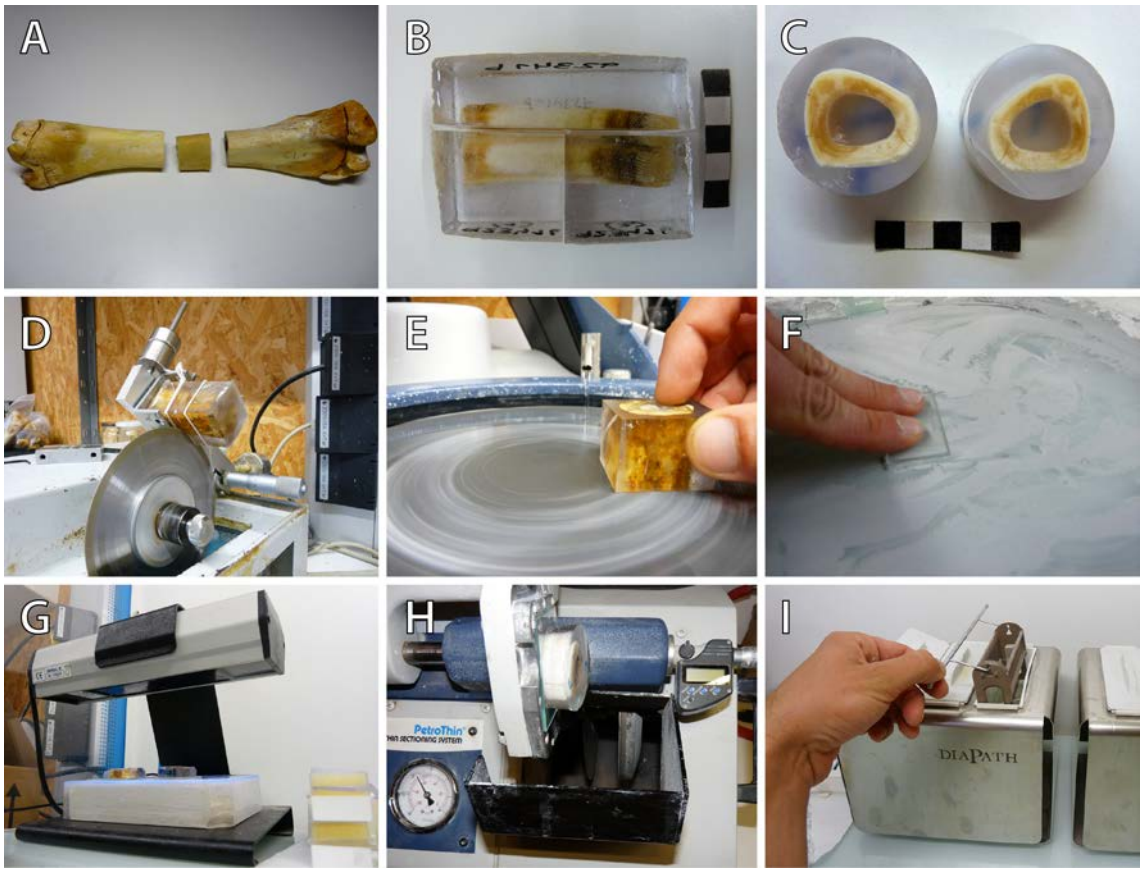

Figure 3.1. Preparation of histological thin sections from bones and teeth. (A) A 3-cm-portion is extracted from the mid-diaphysis of long bones. **(B)** Teeth, on the other hand, are completely embedded and cut through the protoconid. Due to the high height of the crown, they are also transversally divided into different parts to be mounted in two different slides. **(C)** Embedded bone blocks are cut into two halves to expose the mid-shaft surface of the bone. **(D)** This cut is performed using a low speed diamond saw. **(E)** The surface of interest of each bone/tooth block is polished using a grinder-polisher machine. **(F)** Glasses are also polished with caborundum powder to obtain frosted glasses. **(G)** The bone/tooth block is glued to the frosted glass with an UV-curing glue. **(H)** The thin section is performed with Petrothin (Buehler), a specific machine that presents two different saws that cut and ground the sample respectively. **(I)** Histological thin sections obtained from fossil bones and from extant and fossil teeth are bathed in alcohol and in Histo-Clear II before their mounting with DPX medium.

in increasing concentrations of alcohol and its submersion in a histological clearing agent (Histo-Clear II) (Fig. 3.1I) before applying the DPX medium.

Histological thin sections from extant and fossil teeth are prepared following a similar procedure as that already described for bone samples. In extant species, first lower molars were first extracted from the mandible and dehydrated in different concentrations of alcohol (70, 96 and 100%), where they remained for 72 hours (24 h in each concentration). Unlike bones, both extant and fossil teeth were completely embedded in epoxy resin (Araldite 2020) (Fig 3.1B). This hardened block was then longitudinally cut through the dental protoconid in the buco-lingual plane using a low-speed diamond saw (IsoMet, Buehler) (Fig 3.1B). The next steps of grinding and polishing followed the procedure specified for bone samples and, similar to fossil bones, dental thin sections were also finished by mounting with DPX medium (Scharlau). Because equid tooth crowns are extremely high, most dental thin sections had to be prepared on two different slides. When two thin sections were obtained from one tooth (Fig. 3.1B), the course of enamel incremental markings were used to determine that both slides were cut from the same plane following Dirks et al. (2012).

3.2.2. Analysis of histological thin sections

3.2.2.1. Microscopy

Histological thin sections of bones and teeth are commonly analyzed under polarized light microscopy (Smith 2004; Bromage and Werning 2013), as it provides information about their structure and composition that is not available with other techniques (Bromage et al. 2003). Polarized light microscopes have two different polarizing filters that isolate light vibration in only one direction (Bromage and Werning 2013). The first polarizing filter, the polarizer, is positioned between the light source and the sample. It allows light to pass in only one vibration direction. The analyzer is the second filter of the microscope and it is placed between the sample and the observer. Its vibration direction is at 90º to that of the polarizer, blocking the light that exits from this first filter when no sample or an isotropic material is observed on the microscope. In these circumstances, therefore, no image is displayed (Bromage et al. 2003). If a birefringent (i.e. two refraction indexes) material is placed between the two filters (the polarizer and the analyzer), it interacts with the light that radiates from the polarizer and changes its vibrational direction to that of the analyzer (Bromage et al. 2003). In this case, light may pass through the analyzer and the sample is observed (Fig 3.2A, C). Besides these polarizing filters, a quarter lambda plate (1/4 λ) can also be added to the microscope (Turner-Walker and Mays 2008). This crystal filter retards the wavelength of the light and colors the sample (Fig. 3.2B), facilitating the identification of histological features in bone cross-sections (Turner-Walker and Mays 2008).

The collagen fibers of the bone tissue (Bromage et al. 2003) and the crystalline structure of enamel (Smith 2004) are birefringent when viewed under polarized light.

Collagen fibers appear brighter or darker depending on their orientation when observed under polarized light microscopes (Fig. 3.2A) (Bromage et al. 2003). This allows the classification of bone tissue into different typologies (e.g. lamellar bone vs. woven bone) (Turner-Walker and Mays 2008). In dental thin sections, polarized light helps to identify enamel incremental features (Smith 2004), as it displays alternating bands crossing enamel prims that correspond to enamel laminations (Fig. 3.2C).

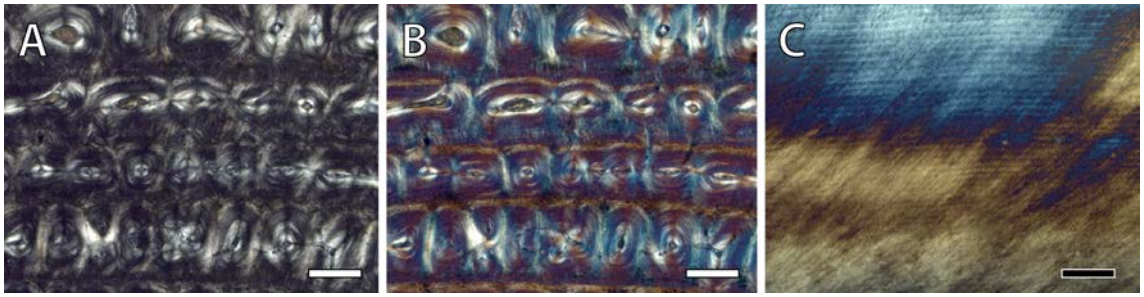

Figure 3.2. Bone (A – B) and enamel (C) tissues observed under polarized light microscopy. (A) Metatarsal cortex of *E. grevyi* IPS84964 under polarized light. **(B)** Metatarsal cortex of *E. grevyi* IPS84964 under polarized light with 1/4λ filter. Note that panel B shows the same area of the bone cortex than panel A. **(C)** Enamel tissue of *E. quagga* IPS92342 under polarized light. White scale bars = 200 µm; black scale bar = 100 µm.

All histological samples of this PhD dissertation were observed using the polarized light microscopes Zeiss Scope.A1 and Leica DM 2500P. Micrographs of bone and dental tissues were captured with the cameras mounted on them (AxioCam ICc5 in the Zeiss Scope.A1 microscope and Leica DFC490 in the Leica DM 2500P microscope).

3.2.2.2. Histological features of bone

Bones from extant and extinct *Equus* species were histologically analyzed to infer essential LH traits. Specifically, bone tissue types, bone growth marks (BGMs) and bone vascularization were qualitatively and quantitatively studied in this PhD thesis.

Bone tissue types

Bone tissue is classified as primary or secondary regarding its origin. Primary bone is the first tissue formed in ontogeny, while secondary bone is deposited in areas where primary bone has been previously resorbed (Francillon-Vieillot et al. 1990; Currey 2002). *Secondary bone* (Fig. 3.3) results from the joint action of the osteoclasts (i.e. bone-resorbing cells) and the osteoblasts (i.e. bone-forming cells) during a process known as bone remodeling (Currey 2002). It takes place over the whole life of an individual, repairing the tissue damaged by biomechanical stress and coping with physiological demands in the organism (Francillon-Vieillot et al. 1990). The newly formed secondary bone may appear as *secondary osteons* (also name Haversian canals) occupying different parts of the bone cortex (Fig. 3.3A), or as *endosteal bone* (EB) bordering the medullary cavity (Fig. 3.3B) (Chinsamy-Turan 2005).

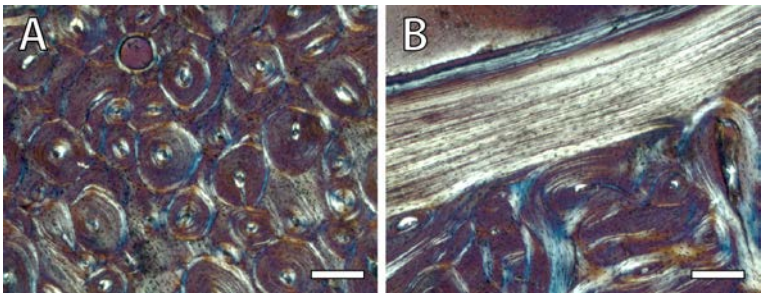

Figure 3.3. Secondary bone tissue types. (A) Secondary osteons (Haversian systems) in the metatarsal cortex of *E. hemionus* IPS83155. **(B)** Endosteal bone in the metatarsal cortex of *E. hemionus* IPS83155. All images show bone cross-sections observed under polarized light with 1/4λ filter. Scale bars = 200 µm.

Primary bone is categorized based on the arrangement of the collagen fibers within the bone matrix and its pattern and quantity of vascularization (de Ricqlès 1975; Francillon-Vieillot et al. 1990; de Margerie et al. 2002; Huttenlocker et al. 2013). The general typologies are lamellar (Fig 3.4A), parallel-fibered (Fig 3.4B) and woven bone (WFB, Fig 3.4C), according to the order of the collagen fibers (Francillon-Vieillot et al. 1990; Huttenlocker et al. 2013). Within each primary tissue type, several sub-classifications are described regarding the amount and arrangement of the vascular canals (VCs) (Francillon-Vieillot et al. 1990; de Margerie et al. 2002; Huttenlocker et al. 2013). Interestingly, each primary bone tissue is associated with functional and physiological characteristics, among which the pattern and rate of bone deposition are noteworthy (Huttenlocker et al. 2013).

Among primary bone tissue types, *lamellar bone* (LLB) (Fig 3.4A) presents the highest level of organization, with its closely-packaged collagen fibers arranged into layers known as lamellae (Francillon-Vieillot et al. 1990; Currey 2002; Huttenlocker et al. 2013). In each lamella, collagen fibers are parallel to each other, and their direction only changes from one lamella to the next (Francillon-Vieillot et al. 1990; Huttenlocker et al. 2013). This arranfement displays a characteristic alternating dark and light pattern when observed under a polarized light microscope (Francillon-Vieillot et al. 1990; Huttenlocker et al. 2013). LLB usually presents few bone cells, which are mostly flattened in shape and arranged in rows (Francillon-Vieillot et al. 1990). Simple VC may be embedded in the LLB

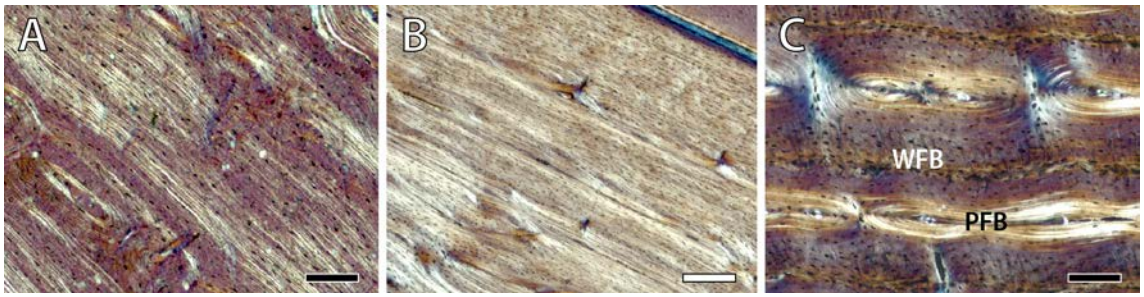

Figure 3.4. Primary bone tissue types. (A) Lamellar bone (LLB) in the tibial cortex of *E. grevyi* IPS84963. **(B)** Parallel-fibered bone (PFB) in the femoral cortex of *E. hemionus* IPS83155. **(C)** Fibrolamellar complex (FLC) in the femoral cortex of *E. quagga* IPS92342. WFB = woven bone, PFB = parallel-fibered bone. All images show bone cross-sections observed under polarized light with 1/4λ filter. White scale bar = 200 µm; black scale bars = 100 µm.

bone matrix, forming the tissue known as *lamellar bone with simple vascular canals* (LSV) (de Margerie et al. 2002). Primary osteons (i.e. vascular canals encircled by concentric bone lamellae; Francillon-Vieillot et al. 1990) might also be found in LLB. In this case, it is classified as *lamellar bone with primary osteons* (LPO) (de Margerie et al. 2002). Whether showing simple VC or primary osteons, LLB is generally low-vascularized (Francillon-Vieillot et al. 1990). No VC may even be present at all, in which case it is classified as *lamellar non vascular bone* (LNV) (de Margerie et al. 2002). The scarcity of vascularization, along with the extreme order of the collagen fibers, are indicative of the very low rates of formation of the LLB (Currey 2002; de Margerie et al. 2002). This bone tissue type is usually found in the bone cortex of crocodilians, turtles and reptiles (Huttenlocker et al. 2013).

Parallel-fibered bone (PFB) (Fig 3.4B) (also named *pseudo-lamellar bone*) consists of closely-packaged collagen fibers oriented in the same direction, each running parallel to each other (Francillon-Vieillot et al. 1990; Huttenlocker et al. 2013). It is highly anisotropic when observed under polarized light. Therefore, it appears homogeneously dark or bright (according to the preferred orientation of the collagen fibers) under this kind of microscopy (Francillon-Vieillot et al. 1990; Huttenlocker et al. 2013). Bone cells of PFB are also flattened in shape, but randomly distributed (Francillon-Vieillot et al. 1990). Similarly to LLB, PFB is classified as *non-vascular parallel-fibered bone*, *parallel-fibered bone with simple vascular canals* or *parallel-fibered bone with primary osteons* according to the absence of VCs, the presence of simple VCs, or the presence of primary osteons respectively (de Margerie et al. 2002). PFB is deposited at very low rates (Huttenlocker et al. 2013), but not as slowly as LLB (Currey 2002). Besides reptiles, turtles and crocodilians, this primary bone tissue type is also found in mammals, mainly in small-sized ones (Huttenlocker et al. 2013).

Finally, *woven bone* or *woven-fibered bone* (WFB) (WFB, Fig 3.4C) is composed of loosely-packaged collagen fibers distributed without any specific spatial arrangement (Francillon-Vieillot et al. 1990; Huttenlocker et al. 2013). This lack of order makes WFB to appear highly isotropic (relatively dark) under polarized light (Francillon-Vieillot et al. 1990; Huttenlocker et al. 2013). WFB present multiple and huge vascular spaces, as well as numerous rounded or star-shaped bone cells (Francillon-Vieillot et al. 1990). This bone tissue is laid down at very high rates (Francillon-Vieillot et al. 1990; Currey 2002; de Margerie et al. 2002; Huttenlocker et al. 2013) and thus it is typically found in embryonic bones (Francillon-Vieillot et al. 1990; Currey 2002). During postnatal growth, vascular spaces of WFB are filled with PFB (PFB, Fig 3.4C) (Francillon-Vieillot et al. 1990; Currey 2002), resulting in a bone tissue that presents many primary osteons surrounded by a WFB matrix (de Margerie et al. 2002). This tissue, which combines WFB and PFB (Prondvai et al. 2014), is named either *fibrolamellar bone* or *fibrolamellar complex* (FLC) (Fig 3.4C) (Francillon-Vieillot et al. 1990; Huttenlocker et al. 2013). It is the main primary bone tissue found in large mammals (Currey 2002; Huttenlocker et al. 2013). VCs embedded in the FLC may present multiple orientations, including radial (orthogonal to the bone edge), longitudinal (parallel to the bone diaphysis), oblique (between orthogonal and parallel to

the bone margin) and circular (parallel to the bone periphery) (Francillon-Vieillot et al. 1990). This leads to a classification of the FLC under different sub-typologies, which are the *radial* FLC (mainly composed of radial VCs), the *laminar* FLC (mainly composed of circular VCs), the *plexiform* FLC (mainly composed of circular VCs connected by oblique and radial VCs), the *longitudinal* FLC (mainly composed of longitudinal VCs) and the *reticular* FLC (mainly composed of anastomosed oblique VCs) (Francillon-Vieillot et al. 1990).

In this PhD thesis, primary bone tissues were qualitatively studied to analyze differences in the rate of bone formation between limb bones, ontogenetic stages and *Equus* species (Chapters 4 to 7). The presence of secondary bone was also reported, although it was not exhaustively analyzed because it does not provide any relevant information for the reconstruction of the LH in mammals.

Bone growth marks

BGMs are histological features that register changes in the rate of bone deposition (Castanet et al. 1993; Huttenlocker et al. 2013). They may take the form of either LAGs or *annuli* (Francillon-Vieillot et al. 1990; Castanet et al. 1993; Chinsamy-Turan 2005; Huttenlocker et al. 2013). In adult individuals, BGMs may be erased and obscured due to the action of bone remodeling (Woodward et al. 2013). The ontogenetic increase in area of the medullary cavity (Hall 2005) might also delete previously deposited BGMs (Woodward et al. 2013). Bone superimposition (Fig. 3.5) provides a good solution to reconstruct incomplete growth records by retrocalculating lost BGMs (Woodward et al. 2013). This methodology, which requires the use of ontogenetic series, is based on the hypothesis that

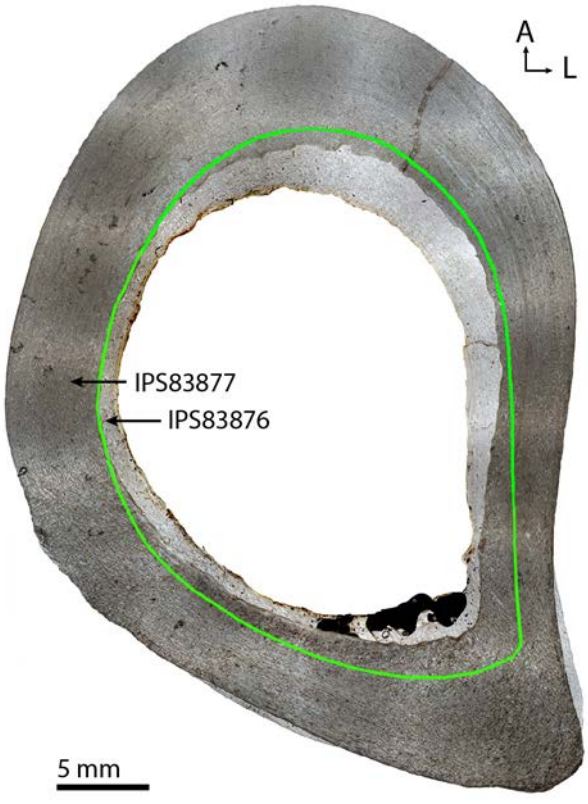

Fig. 3.5. Retrocalculation of BGMs in the femora of adult Asiatic wild asses (IPS83877, IPS83876). Superimposition shows that one BGM has been lost (green line) in the femur of IPS83877 due to secondary remodeling and the expansion of the medullary cavity. All images show bone cross-sections observed under polarized light. A = anterior; L = lateral. Modified from Nacarino-Meneses et al. (2016a).

the dimensions (e.g. perimeter) of a particular BGM (e.g. the CGM corresponding to the first winter) is similar in a given bone of individuals of the same species (Woodward et al. 2013). Superimposition of individual bone sections was applied in the present dissertation to identify, among other characteristics, lost BGMs in the bone tissue of equids (Fig. 3.5).

BGMs are classified as cyclical (CGMs) or non-cyclical features regarding their periodicity (Castanet et al. 1993; Woodward et al. 2013). Periodicity cannot be assessed from BGM morphology (Woodward et al. 2013), but from comparing individual age with the position and number of BGMs within a bone cross-section (Chapters 5 and 6). CGMs are deposited when physiological and metabolic changes occur in the organisms during the unfavorable season (i.e. winter in north-hemisphere dwelling species) (Köhler et al. 2012). Therefore, only a BGM located in the outermost cortex of a 6-month-old specimen born in summer should be considered as CGM. Following the same line of reasoning, any internal mark in this individual should be classified as a non-cyclical feature. When more BGMs than expected from individual age are found in a bone cross-section (e.g. two BGMs in a specimen aged 1 year), some might be recording non-cyclical growth. The specific location of the BGM within the cortex (inner, medium or outer cortex) in relation to the age of the specimen will provide the clue for determining which BGM should be considered as a non-cyclical feature in this case. Superimposition of individuals (Woodward et al. 2013) may also help in identifying and differentiating between non-cyclical and cyclical BGMs. Those BGMs that do not match known CGMs by superimposition can be considered as non-cyclical BGMs. The study of CGMs and non-cyclical BGMs performed in this PhD thesis allowed the inference of mammalian key LH traits from bone histology (Chapters 4 to 7). Age at maturity and age at death, on the one hand, were calculated by counting GCMs in equid cross-sections (total number of CGM for age at death calculation, number of CGM before the presence of EFS for age at maturity calculation) (Castanet et al. 2004; Chinsamy and Valenzuela 2008; Marín-Moratalla et al. 2013; Jordana et al. 2016). On the other hand, non-cyclical BGMs were thoroughly analyzed to determine their relationship to a specific life history event: the moment of birth. Such correlation was assessed by superimposing ontogenetic series of different limb bones on the species *E. hemionus*, with the aim of finding a match between the perimeter of the perinatal individual and that of the non-cyclical BGM identified in later ontogenetic stages.

BGMs were also quantitatively analyzed in this dissertation to obtain information about the pace and the rate of growth of the different limb bones and the species studied. Bone growth curves were obtained by measuring either the distance between CGMs or the perimeter of each BGM (Bybee et al. 2006; Woodward et al. 2013) (Chapter 4, 5 and 7). All measurements were performed using Image J software, after tracing the BGMs' contour on Adobe Photoshop CS3. Non-cyclical BGMs were considered as time zero on growth plots because of the tight association between these features and the moment of birth found in Chapter 6. The rate of growth, represented as the difference in BGM perimeters between consecutive annual cycles of growth, was assessed in different limb bones for the extant species *E. hemionus* (Chapter 5). Bone growth reconstructions performed in Chapter 5 revealed that bone growth curves provide useful information about the timing

of the epiphyseal fusion of limb bones in *Equus*. According to these findings, this biological event was estimated from growth plots for the fossil bones studied in the extinct Middle Pleistocene *Equus* of the sample (Chapter 7).

Vascularization: quantitative and qualitative measurements

Bone growth rate is closely related to several aspects of bone vascularization (Lee et al. 2013). Avascular bone, for instance, is formed at slower rates than well-vascularized bone tissue (de Margerie et al. 2002). Among vascularized bone tissues, those composed of primary osteons grow faster than those showing simple vascular canals (de Margerie et al. 2002). Furthermore, the size of primary osteons and vascular cavities influences the rate of bone growth; the higher the rates of bone formation the larger are these histological structures (de Margerie et al. 2002). The specific orientation of the VCs within a bone cross-section also provides information about the relative rate of bone growth (Lee et al. 2013). For a particular long bone, radial bone (FLC with radial VCs) is deposited at higher rates than laminar bone (FLC with circular VCs), while longitudinal (FLC with longitudinal VCs) and reticular (FLC with anastomosed oblique VCs) bone present intermediate rates

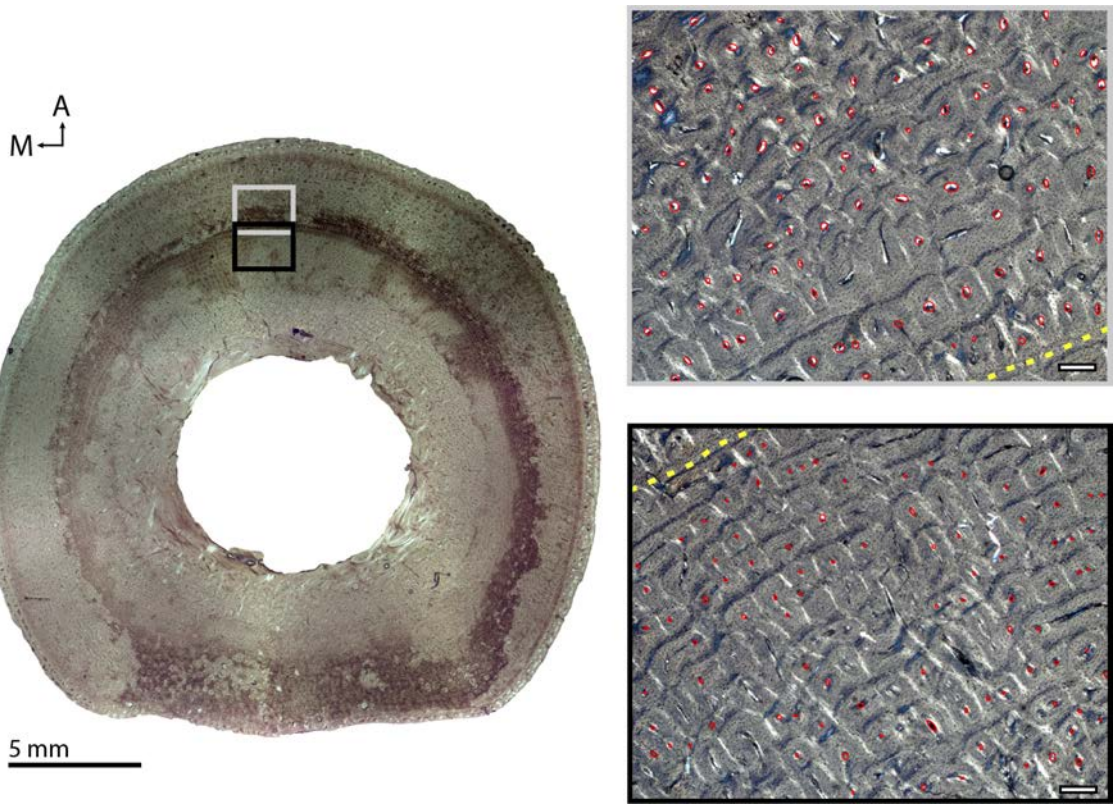

Figure 3.6. Quantification of the area of the longitudinal vascular canals (VCs) formed before (black framed micrograph) and after (grey framed micrograph) the presence of the neonatal line (NL). The area of the longitudinal VCs is measured in the antero-medial region (grey and black rectangles, left image) of each bone cross-section (left image: metatarsal cortex of *E. hemionus* IPS83149). For each VC, an ellipse (red circles) is adjusted to the edges of this biological structure. The area of this geometric form is then measured with ImageJ software. Yellow dashed line indicates the NL. Note that black and grey framed micrographs are magnifications of the areas highlighted with a black and grey rectangle respectively in the left image. All images show bone cross-sections observed under polarized light. White scale bar = 200 µm. Modified from Nacarino-Meneses and Köhler (accepted).

of growth (de Margerie et al. 2004).

In the present PhD dissertation, bone vascularization was qualitatively and quantitatively studied. On the one hand, the arrangement of the vascular canals (e.g. longitudinal, radial, circular) was described following classical bibliography (Francillon-Vieillot et al. 1990; de Margerie et al. 2002) (Chapters 4, 5 and 7). On the other hand, vascular density was qualitatively assessed in fossil samples and compared with extant ones with the aim to shed light on the rate of growth of extinct *Equus* species (Chapter 7). Finally, the area of the longitudinal VCs after and before deposition of the non-cyclical BGM (neonatal line, NL) was quantitatively analyzed in extant *Equus* (Chapter 6). Measurements were performed using Image J software by adjusting an ellipse to the borders of the longitudinal VCs and then measuring its area (Fig. 3.6). Regions of 2.6 x 2.2 mm (5.7 mm^2) were sampled at both sides of the non-cyclical BGM, in the antero-medial cortex of each bone (Figure 3.6). Results obtained from the quantification of the area of the longitudinal VCs were then statistically analyzed with Java Gui for R version 1.7-16 (Fellows 2012). Specifically, Mann-Whitney *U* test was performed to analyze differences between groups and a *p*-value of $p<0.05$ was considered to be statistically significant.

3.2.2.3. Enamel histological features

In this PhD thesis, enamel incremental markings were exhaustively analyzed to reconstruct the pattern of growth and development of the first lower molar in extant and extinct *Equus* (Chapter 8). Specifically, measurements and counts of daily and supra-daily marks were performed along the buccal cusp of each tooth to calculate the most relevant enamel growth parameters. Measurements were taken with Image J software on micrographs obtained from the cameras incorporated on the polarized light microscope (AxioCam ICc5 in the Zeiss Scope.A1 microscope).

Enamel growth parameters

Daily secretion rate (DSR), crown formation time (CFT), enamel extension rate (EER) and the repeat interval (RI) were the enamel growth parameters estimated in the present dissertation (Fig. 3.7).

Daily secretion rate (DSR) represents the quantity of enamel deposited by enamel-forming cells over the period of 24 hours (Smith 2008). Its calculation relies on the tested hypothesis that daily incremental marks (i.e. cross-striations and laminations) are formed during that period of time (Bromage 1991; Smith 2006; Kierdorf et al. 2013). DSR is thus assessed by measuring the distance between a series of consecutive daily marks and then dividing this value by the time they took to be formed (Smith 2008). For instance, the distance between a sequence of 5 laminations was measured in the enamel of *E. hemionus* IPS83151 and then divided by 4 (the number of days that they needed to be formed) to obtain the DSR of the species (Fig. 3.7A). Several studies indicate that DSR is not constant throughout the crown but that it varies from the inner to the outer enamel and

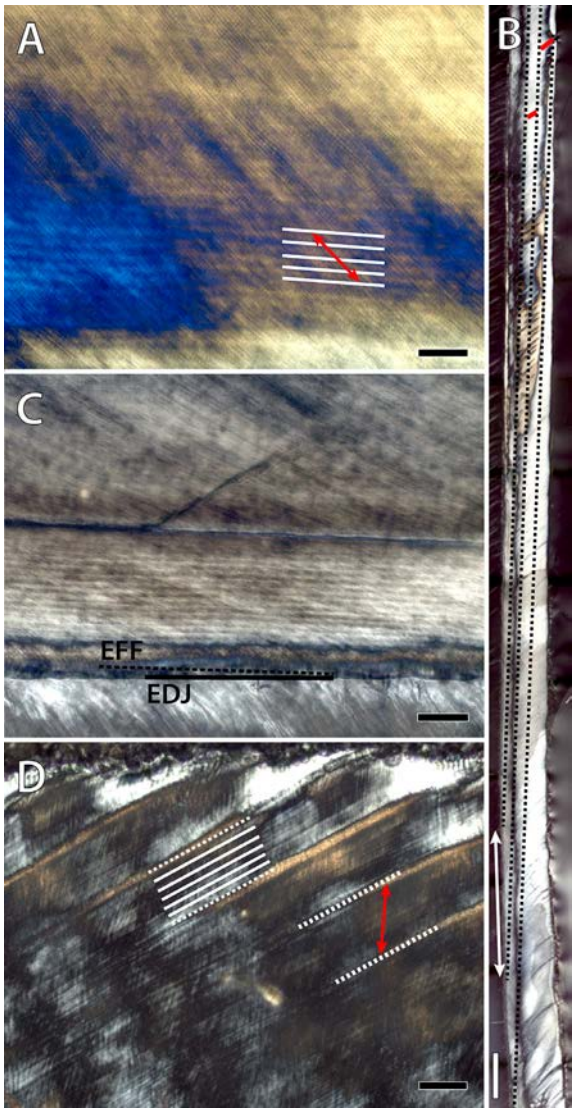

Figure 3.7. Quantification of enamel growth parameters. (A) To estimate the enamel daily secretion rate (DSR) in *E. hemionus* IPS83151, the distance (red doubled arrow) between a series of consecutive laminations (white lines) is measured and divided by the number of days that they take to be formed. **(B)** Crown formation time (CFT) is estimated in IPS92342 (*E. quagga*) by measuring the distance (red lines) between incremental lines (black dashed lines) and then dividing this value by the DSR. As a result, the time required to form a specific portion of the EDJ (white doubled arrow) is obtained. **(C)** The enamel formation front angle (EFFa) is calculated in IPS84964 (*E. grevyi*) by measuring the angle between the enamel formation front (EFF, black dashed line) and the enamel dentine junction (EDJ, black line). **(D)** The number of laminations (white lines) between consecutive Retzius lines (white dotted lines) is counted to quantify the repeat interval (RI) in the enamel of IPS92346 (*E. quagga*). If laminations are not well preserved, the distance (red doubled arrow) between consecutive Retzius lines is measured and divided by the DSR. All images show enamel tissue observed under polarized light microscopy. White scale bar = 1mm; black scale bars = 50 µm.

from the tooth cusp to the cervix (Smith 2008; Kierdorf et al. 2013; Kierdorf et al. 2014). Consequently, measurements of DSR were performed randomly in different areas of the enamel and the tooth crown to obtain representative values for this parameter.

Crown formation time (CFT), or the amount of time required for the tooth crown to be completely developed (Smith 2008), was calculated following the methodology described in Jordana and Köhler (2011). The course of enamel laminations was first outlined from the enamel-dentine junction (EDJ) to the enamel surface on each tooth (Fig. 3.7B). Afterwards, the distance between these incremental markings was measured (Fig. 3.7B) and divided by the DSR to obtain the number of days needed to form a particular segment of the EDJ (Fig. 3.7B). CFT of first lower molars was finally estimated as the sum of the days calculated along the EDJ.

Enamel extension rate (EER) defines the tooth growth in height (Smith 2008; Hogg and Walker 2011) and represents the rate of growth of the enamel along the EDJ (Smith 2008). It was quantified by dividing the length of a determinate portion of the EDJ by the time that it needs to be formed. The enamel formation front angle (EFFa), which is the

angle formed between the enamel formation front (EEF) and the EDJ, is related to the EER too (Hogg and Walker 2011; Jordana et al. 2014). Thus, it was also measured in all equid teeth studied (Fig. 3.7C).

Finally, the *repeat interval* (RI) concerns the periodicity of supra-daily lines (Smith 2008). It was determined by counting the number of daily enamel laminations between Retzius lines (Fig. 3.7D). Additionally, RI was calculated from the quotient between the distance of successive supra-daily lines and the DSR of the species (Fig. 3.7D). This latter methodology was applied when laminations between Retzius lines were not clearly identified.

Several enamel growth parameters, such as DSR and EER, were statistically studied to test for differences between species, developmental stages and enamel/tooth areas. All these analyses were performed with Java Gui for R version 1.7-16 (Fellows 2012). Specifically, Kruskal-Wallis and Mann-Whitney *U* tests were applied to analyze the differences between groups. A *p*-value of $p<0.05$ was considered statistically significant after applying Bonferroni correction.

Assessment of the daily periodicity of enamel laminations in equids

The periodicity of enamel laminations in equids has recently been a matter of debate within the specialized scientific community (Kierdorf et al. 2013; Kierdorf et al. 2014). Kierdorf et al. (2013, 2014) considered that Hoppe et al. (2004) misidentified sub-daily and daily incremental markings in their enamel analysis of the domestic species *E. caballus*, leading to incorrect estimations of DSR for this taxon. Ideally, the interval of deposition of incremental markings should be established from experimental studies that involve vital labelling (Bromage 1991; Smith 2006; Kierdorf et al. 2013). However, this kind of investigations are usually expensive and time-consuming. Moreover, it requires the approval of an ethic commission in the country where the experiment will be performed. As an alternative, the daily periodicity of enamel laminations can be assessed by comparing the CFT of unworn teeth and the estimated age of the specimen to which they belong. This methodology was employed in the present dissertation to test for the daily periodicity of enamel laminations in several extant *Equus* species.

3.3. METHODS: Body size inferences in extinct taxa

Adult body size and size at birth are key LH traits of mammals (Stearns 1992) that co-vary with other LH characteristics that can be inferred from bone and dental histology (Köhler 2010). In order to analyze the LH strategy of extinct *Equus* in the context of their body size (See Chapter 2 for further information), adult and neonatal size of the Middle Pleistocene species *E. steinheimensis* and *E. mosbachensis* were calculated in this PhD dissertation (Chapter 7). Adult weight of Late Pleistocene species (*E. ferus* and *E. hydruntinus*) was compiled from literature (Cantalapiedra et al. 2017) (Chapter 8), but no

information about their size at birth could be obtained neither from previous studies nor from the methodology developed in this thesis.

3.3.1. Inferring adult body mass in extinct *Equus*

Body size is frequently represented by its proxy, body mass (Damuth and MacFadden 1990). Body mass (weight) cannot be directly inferred from fossil remains, though it can be estimated from allometric models that relate bone dimensions to body mass (Damuth and MacFadden 1990). These models are represented by the power function $y = ax^b$ (Damuth and MacFadden 1990), which can be log transformed to obtain a linear relationship $\ln y = \ln a + b \ln x$ (Peters 1983). In both equations, y is the dependent variable (i.e. body mass), x is the independent variable (i.e. measurement taken on the bone), a is a constant and b is the allometric coefficient (Alberdi et al. 1995). In the present PhD thesis, adult body mass of *E. steinheimensis* and *E. mosbachensis* was assessed from different measurements on the metacarpi and phalanges of adult (fused epiphyses) specimens. Specifically, the proximal depth of the first phalanx and the distal minimal depth of the lateral condyle of the third metacarpus were measured (Fig. 3.8) (Eisenmann et al. 1988) using a digital electronic precision caliper (0.05 mm error). Measurements were then applied to the equations of Alberdi et al. (1995) to predict the adult weight of these Middle Pleistocene species.

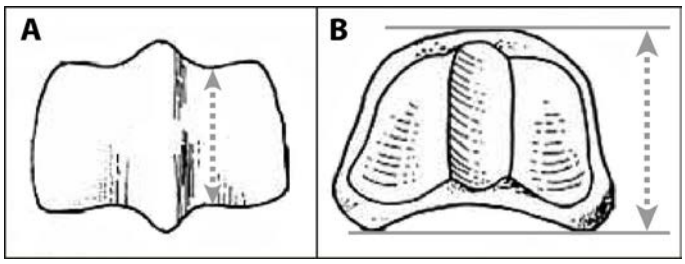

Figure 3.8. Measurements taken (grey dotted arrows) on the distal metacarpus (A) and the proximal phalanx (B) of Middle Pleistocene *Equus* for weight estimation. Modified from Eisenmann et al. (1998).

3.3.2. Estimating size at birth in extinct *Equus*

Size at birth of Middle Pleistocene equids could not be represented on terms of body mass. On the one hand, equations of Alberdi et al. (1995) to estimate body weight from skeletal measurements are derived from adult specimens. Hence, they provide inaccurate results if applied at earlier ontogenetic stages (Köhler 2010). Furthermore, measurements performed at the mid-diaphysis of metacarpi and metatarsi on extant *Equus* do not significantly correlate with body mass (Alberdi et al. 1995). As thin sections were prepared at this point of the metapodial diaphysis, dimensions of BGMs (including the NL) are not useful to infer body weight. Therefore, neonatal body mass of fossil specimens was not calculated and just the perimeter of the NL was used as a proxy of the size at birth for these extinct equid species.

- Chapter 4 -

First approach to bone histology and skeletochronology of *Equus hemionus*

Reproduced from:

Nacarino-Meneses C., Jordana X. & Köhler M. (2016) *Comptes Rendus Palevol* 15: 267-277. DOI: 10.1016/j.crpv.2015.02.005

Nacarino-Meneses, C., Jordana, X. & Köhler, M. (2016) First approach to bone histology and skeletochronology of *Equus hemionus*. Comptes Rendus Palevol 15: 277 – 287

Available at: https://doi.org/10.1016/j.crpv.2015.02.005

- Chapter 5 -

Histological variability in the limb bones of the Asiatic wild ass and its significance for life history inferences

Reproduced from:

Nacarino-Meneses C., Jordana X. & Köhler M. (2016)
PeerJ 4: e2580. DOI: 10.7717/peerj.2580

PeerJ

Histological variability in the limb bones of the Asiatic wild ass and its significance for life history inferences

Carmen Nacarino-Meneses[1], Xavier Jordana[1] and Meike Köhler[1,2,3]

[1] Department of Evolutionary Biology, Institut Català de Paleontologia Miquel Crusafont (ICP), Campus de la Universitat Autònoma de Barcelona, Bellaterra, Barcelona, Spain

[2] Institut Català de Recerca i Estudis Avançats (ICREA), Barcelona, Spain

[3] Department of Animal Biology, Plant Biology and Ecology (BABVE), Universitat Autònoma de Barcelona, Bellaterra, Barcelona, Spain

ABSTRACT

The study of bone growth marks (BGMs) and other histological traits of bone tissue provides insights into the life history of present and past organisms. Important life history traits like longevity or age at maturity, which could be inferred from the analysis of these features, form the basis for estimations of demographic parameters that are essential in ecological and evolutionary studies of vertebrates. Here, we study the intraskeletal histological variability in an ontogenetic series of Asiatic wild ass (*Equus hemionus*) in order to assess the suitability of several skeletal elements to reconstruct the life history strategy of the species. Bone tissue types, vascular canal orientation and BGMs have been analyzed in 35 cross-sections of femur, tibia and metapodial bones of 9 individuals of different sexes, ages and habitats. Our results show that the number of BGMs recorded by the different limb bones varies within the same specimen. Our study supports that the femur is the most reliable bone for skeletochronology, as already suggested. Our findings also challenge traditional beliefs with regard to the meaning of deposition of the external fundamental system (EFS). In the Asiatic wild ass, this bone tissue is deposited some time after skeletal maturity and, in the case of the femora, coinciding with the reproductive maturity of the species. The results obtained from this research are not only relevant for future studies in fossil *Equus*, but could also contribute to improve the conservation strategies of threatened equid species.

Submitted 5 July 2016
Accepted 18 September 2016
Published 13 October 2016

Corresponding author
Carmen Nacarino-Meneses,
carmen.nacarino@icp.cat

Academic editor
William Jungers

Additional Information and Declarations can be found on page 18

DOI **10.7717/peerj.2580**

Subjects Biodiversity, Conservation Biology, Paleontology, Zoology, Histology

Keywords *Equus hemionus*, Bone histology, External fundamental system, Bone growth marks, Life history, Skeletochronology, Intraskeletal histological variability, Longevity, Reproductive maturity, Limb bones

INTRODUCTION

The study of bone growth marks (BGMs) is nowadays the focus of many investigations due to its potential to reconstruct many aspects of the life history of present and past vertebrates (*Amson et al., 2015*; *Kolb et al., 2015a*; *Woodward et al., 2015*; *Jordana et al., 2016*; *Moncunill-Solé et al., 2016*; *Nacarino-Meneses, Jordana & Köhler, 2016*; *Orlandi-Oliveras et al., 2016*). These histological features, which record cyclic variation in bone growth rate, can take the form of "lines of arrested growth" (LAGs) or of "annuli" within the

How to cite this article Nacarino-Meneses et al. (2016), Histological variability in the limb bones of the Asiatic wild ass and its significance for life history inferences. **PeerJ 4:e2580; DOI 10.7717/peerj.2580**

cortical bone (*Castanet et al., 1993*). LAGs appear as thin dark lines in bone cross-sections and are considered to represent moments of cessation of growth (*Francillon-Vieillot et al., 1990*; *Chinsamy-Turan, 2005*). Annuli, on the other hand, are poorly vascularized rings of lamellar or parallel-fibered bone within the bone cortex (*Francillon-Vieillot et al., 1990*; *Chinsamy-Turan, 2005*) that indicate periods of growth rate decrease. From *Peabody (1961)* to the present, it has repeatedly been demonstrated that most of the BGMs found in the bone tissue record annual cycles of growth (cyclical growth marks—CGMs) reflecting physiological cycles (*Köhler et al., 2012*) that match environmental cycles (*Castanet et al., 1993*; *Chinsamy-Turan, 2005*). Nevertheless, BGMs are also suggested to register biological events that entail moments of physiological stress in the organism (*Woodward, Padian & Lee, 2013*) instead of periodical growth (*Castanet, 2006*).

From dinosaurs to mammals, the annual periodicity of the CGMs is the basis for inferences of life history strategies in many groups of fossil organisms (e.g., *Klevezal, 1996*; *Horner, De Ricqlès & Padian, 2000*; *Köhler & Moyà-Solà, 2009*). The number of CGMs within a bone cortex allows researchers to calculate important life history traits such as longevity (*Castanet et al., 2004*; *Köhler & Moyà-Solà, 2009*; *Köhler, 2010*) or age at maturity (*Chinsamy & Valenzuela, 2008*; *Horner, De Ricqlès & Padian, 2000*; *Köhler & Moyà-Solà, 2009*; *Köhler, 2010*; *Marín-Moratalla, Jordana & Köhler, 2013*; *Jordana et al., 2016*) by means of a technique called skeletochronology (*Castanet et al., 1993*). This method also provides information about other biological aspects of the animals such as their growth strategy or physiology (*Horner, De Ricqlès & Padian, 2000*; *Padian, De Ricqlès & Horner, 2001*; *Köhler et al., 2012*; *Woodward et al., 2015*). However, skeletochronology has some limitations that are particularly important when dealing with mammals. Firstly, the remodelling process (haversian systems) and the expansion of the medullary cavity that accompany the increase in age can hide the presence of previous CGMs and, thus, give an underestimated individual age (*Woodward, Padian & Lee, 2013*). The inference of this important trait could also be altered if non-cyclical BGMs are erroneously counted as cyclical ones. On the other hand, CGMs are difficult to identify if they are located in the lamellar and avascular bone tissue deposited in the outermost cortex of adult individuals (external fundamental system—EFS) (*Woodward, Padian & Lee, 2013*), because of the structural similarity between LAGs and the lamellae of this tissue (*Horner, De Ricqlès & Padian, 1999*). Such misidentification of CGMs within the EFS, along with the fact that mammals present asymptotic growth (*Lee et al., 2013*), also reduces the accuracy of longevity estimates when old specimens are analyzed (*Castanet et al., 2004*; *Woodward, Padian & Lee, 2013*). Finally, several authors had reported a variable number of CGMs depending on the bone analyzed within an individual (*García-Martínez et al., 2011*; *Woodward, Horner & Farlow, 2014*). Thus, it is important to select the most appropriate bone for skeletochronological studies in each taxon before making general assessments about the life history of the species (*Horner, De Ricqlès & Padian, 1999*).

The histological analysis of bones for this kind of research in mammals is still little explored in comparison with other vertebrate groups (*Castanet et al., 2004*; *Kolb et al., 2015a*; *Jordana et al., 2016*). However, since the study of *Köhler et al. (2012)* that demonstrated the correlation between cyclical bone growth and seasonal

physiology in a wide sample of ruminants, the number of histological works in extant (*Marín-Moratalla, Jordana & Köhler, 2013*; *Marín-Moratalla et al., 2014*; *Jordana et al., 2016*; *Nacarino-Meneses, Jordana & Köhler, 2016*) and extinct mammals (*Martínez-Maza et al., 2014*; *Kolb et al., 2015b*; *Amson et al., 2015*; *Moncunill-Solé et al., 2016*; *Orlandi-Oliveras et al., 2016*) has considerably increased. Among all mammalian clades, members of the family Equidae play a key role in extant and fossil ecosystems (*MacFadden, 1992*; *Downer, 2014*). Besides, they are a classical group of research in Paleontology due to their characteristic evolution (*MacFadden, 2005*). Nevertheless, histological studies in equids are scarce and only a few aimed to infer the life history strategies of some fossil (*Sander & Andrássy, 2006*; *Martínez-Maza et al., 2014*) or extant representatives (*Nacarino-Meneses, Jordana & Köhler, 2016*) of the group.

For the reasons set out above, the main objective of the present work is to study the histological variability (BGMs, pattern of vascularization, bone tissue types) between different limb bones of the same individual in the Asiatic wild ass (*Equus hemionus* Pallas, 1775). With this study, we aim to find out what life history information can be inferred from the histological study of equids and to try to determine which is the best skeletal element to develop skeletochronological studies in this mammal. The kulan or Asiatic wild ass, a mammal endemic to the Gobi desert, is one of the eight extant species of the family Equidae (*Steiner & Ryder, 2011*) and presents nowadays a delicate conservation status (*Kaczensky et al., 2015*). Because previous studies pointed out the potential of histological analyses in conservation management of wild populations (*Chinsamy & Valenzuela, 2008*; *García-Martínez et al., 2011*; *Marín-Moratalla, Jordana & Köhler, 2013*), we have considered this species as the most appropriate to conduct this study. Moreover, its extant habitat—the steppe and semi-desert plains of Mongolia, Iran, Turmekistan, India and China (*Feh et al., 2001*; *Reading et al., 2001*; *Kaczensky et al., 2015*)—make this extant taxon the most similar to fossil stenoid horses (*Forstén, 1992*) extending the importance of our research form Conservation Biology to Palaeontology.

MATERIAL AND METHODS

Thin sections from femur, tibia, metatarsus and metacarpus were analyzed in an ontogenetic series of 9 specimens of *E. hemionus* (Table 1). Only specimen IPS83154 lacks metacarpal bone, totaling 35 the cross-sections studied. As shown in Table 1, the sample includes individuals from different habitats, sex and ages. Sex data were provided by curators while age at death was estimated according to dental eruption pattern of the species (*Lkhagvasuren et al., 2013*) and corroborated with the analysis of cementum layers in adult individuals (R Schafberg, pers. comm., 2014). Wild specimens (IPS83876–IPS83877) were collected during the Mongolian-German Biological Expeditions in the Gobi desert (*Schöpke et al., 2012*) and are housed at the Natural History Collections of the Martin-Luther-University Halle-Wittenberg (Halle, Germany). Captive individuals (IPS83149–IPS83155) lived in the Hagenbeck Zoo (Hamburg, Germany) and belong to the collections of the Zoological Institute of Hamburg University (Hamburg, Germany).

From the mid-shaft of each bone, we prepared histological slices following standard procedures in our laboratory (*Nacarino-Meneses, Jordana & Köhler, 2016*). After measuring

Table 1 Sample studied.

Individual	Estimated age	Age group	Habitat	Sex	Bones studied	Collection
IPS83152	<3 weeks	Perinatal	Hagenbeck Zoo	–	Fe, Ti, Mc, Mt	Zoological Institute of Hamburg University (Hamburg, Germany)
IPS83153	0.5 years	Foal	Hagenbeck Zoo	M	Fe, Ti, Mc, Mt	Zoological Institute of Hamburg University (Hamburg, Germany)
IPS83154	0.5 years	Foal	Hagenbeck Zoo	M	Fe, Ti, Mc	Zoological Institute of Hamburg University (Hamburg, Germany)
IPS83149	1 year	Yearling	Hagenbeck Zoo	–	Fe, Ti, Mc, Mt	Zoological Institute of Hamburg University (Hamburg, Germany)
IPS83150	1 year	Yearling	Hagenbeck Zoo	–	Fe, Ti, Mc, Mt	Zoological Institute of Hamburg University (Hamburg, Germany)
IPS83151	1 year	Yearling	Hagenbeck Zoo	–	Fe, Ti, Mc, Mt	Zoological Institute of Hamburg University (Hamburg, Germany)
IPS83155	2 years	Juvenile	Hagenbeck Zoo	F	Fe, Ti, Mc, Mt	Zoological Institute of Hamburg University (Hamburg, Germany)
IPS83876	4.5 years	Adult	Gobi desert	F	Fe, Ti, Mc, Mt	Museum of Domesticated Animals (Halle, Germany)
IPS83877	8 years	Adult	Gobi desert	M	Fe, Ti, Mc, Mt	Museum of Domesticated Animals (Halle, Germany)

Notes.
M, male; F, female; Fe, femur; Ti, tibia; Mc, metacarpus; Mt, metatarsus.

and photographing each bone, three centimeters of its mid-shaft were cut and embedded in an epoxy resin (Araldite 2020). This block was later cut into two halves (ISO Met, Biometa) and the exposed surface was polished with carborundum powder to be fixed to a frosted glass with an UV curing glue (Loctite 358). Afterwards, it was cut with a diamond saw (Petrothin, Buehler) up to a thickness of 100–120 microns and polished again with carborundum powder. Finally, a mix of oils (*Lamm, 2013*) was spread over the slice before being sheltered with a cover slip. Longitudinal sections were also prepared from several blocks to corroborate that the identification of bone tissue types does not rely on the orientation of the cutting plane (*Stein & Prondvai, 2014*). All thin-sections were observed in a Leica DM 2500P microscope under polarized light with a 1/4λ filter and photographed with the camera incorporated in the microscope. The use of a retardation filter that colors the cross-section, which is not mandatory in this kind of studies, was used to improve the visualization of BGMs and to facilitate the description of bone histology and skeletochronology (*Turner-Walker & Mays, 2008*).

To analyze the histological variability between skeletal elements, bone tissue types and BGMs were studied. The histological descriptions follow the classification of *Francillon-Vieillot et al. (1990)* and *De Margerie, Cubo & Castanet (2002)*. The terminology proposed by *Prondvai et al. (2014)* was employed to describe the different components of the fibrolamellar complex (FLC) (a special case of woven-parallel complex for this authors): "fibrous" or woven bone (WB) and "lamellar" or parallel-fibered bone (PFB). Because the femoral bone histology of the Asiatic wild ass has previously been described in detail (*Nacarino-Meneses, Jordana & Köhler, 2016*), only descriptions of the bone tissue of tibiae,

metacarpi and metatarsi will be detailed in the present work. Regarding growth marks, we have generally used the term "bone growth mark—BGM," interchangeably for LAGs or annuli, instead of "cyclical growth mark—CGM" because not all the marks identified in the samples have proved to be periodical. Double LAGs or LAGs that split were considered as a single event. BGMs were traced along the cross-sections and superimposition of individuals was performed to identify growth marks that have been erased by the remodeling process or the expansion of the medullary cavity (*Woodward, Padian & Lee, 2013*). Each BGM circumference was measured with ImageJ® software to estimate the bones' perimeter at different times during ontogeny and the results were plotted to obtain growth curves for each sample (*Bybee, Lee & Lamm, 2006*). The perimeter of the cross-section was also calculated with ImageJ® software in those animals that are still growing (subadult individuals) to estimate its bone perimeter at the time of death. The perimeter of adult individuals was not determined and only the length of the BGMs identified within the EFS is shown. Because it is generally considered that the presence of EFS indicates the cessation of radial growth in long bones (*Huttenlocker, Woodward & Hall, 2013*), the length of the BGMs located in this bone tissue and the perimeter of the cross-section are almost the same value. Thus, the estimation of the cross-section's perimeter in adult specimens does not provide relevant information about the growth of the animal. Furthermore, we calculated the size variation per year of each bone in yearling and adult specimens as the difference of BGMs' perimeters of consecutive annual growth cycles and interpreted it as a proxy of growth rate. Finally, several life history traits were calculated in each bone from the study of CGMs. Age at death of the specimens was determined as the total number of CGMs present in the bone cortex (*Castanet et al., 2004*) and compared with the age estimated from teeth. Age at maturity was calculated by counting the CGMs before the deposition of the EFS (*Chinsamy & Valenzuela, 2008*; *Marín-Moratalla, Jordana & Köhler, 2013*) and contrasted with literature data.

RESULTS

Bone tissue types

All bones of *E. hemionus* present a well-vascularized FLC that is progressively remodeled during ontogeny. However, the arrangement of the vascular canals embedded in the FLC varies among the bones sampled and in the course of ontogeny. An ontogenetic change in the proportion of the different components of the bone matrix (WB and PFB) has also been noted in some of the limb bones studied, regardless of the orientation of the cutting plane (transversal or longitudinal preparations).

The histology of kulan's femora was previously described in *Nacarino-Meneses, Jordana & Köhler (2016)*. It consists of a highly vascularized FLC that presents an ontogenetic change in the orientation of the vascular canals to a predominantly circumferential arrangement, along with a decrease in the proportion of the WB of the matrix. The EFS was only indentified in adult stages and remodeling was associated to the course of ontogeny and to mechanical loading.

Tibial cortices consist of laminar bone (Fig. 1A) and remodeling begins early in ontogeny, as the high number of secondary osteons (SO) identified in yearling specimens (Fig. 1B)

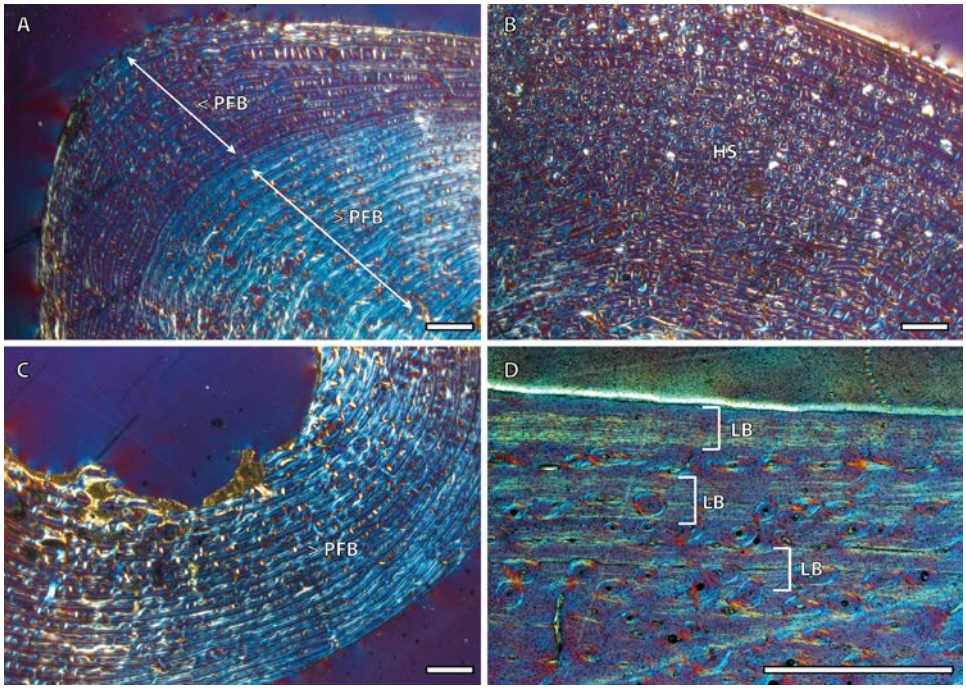

Figure 1 Tibial bone histology of the Asiatic wild ass. (A) Detail of the lateral cortex of the foal IPS83153, showing two areas that differ in the proportions of the parallel-fibered component (PFB) of the bone matrix. (B) Haversian systems in the anterior cortex of the yearling IPS83150. (C) Anterior cortex of the newborn individual (IPS83152) with a high proportion of parallel-fibered component (PFB) in its bone matrix. (D) Packages of lamellar bone within the fibrolamellar complex in the anterior cortex of the wild male (IPS83877). HS, haversian systems; LB, lamellar bone; PFB, parallel-fibered bone. Scale bars: 1 millimeter. All images were obtained under polarized light with a 1/4λ filter.

suggests. Regarding primary bone tissue, the cortical bone of the perinatal individual presents FLC with a high proportion of PFB in the bone matrix (Fig. 1C). The cortex of foals, as well as those of yearling and juvenile individuals, is divided into two well-defined areas that differ in the proportion of this bone matrix component. In these specimens, the laminar bone of the internal cortex presents a higher proportion of PFB than the outer one (Fig. 1A). The EFS is not identified in any of the tibiae analyzed. Instead, several packages of a poorly vascularized lamellar bone that interrupt the FLC matrix, can be recognized in the mid-outer cortex of adult specimens (Fig. 1D). This bone tissue differs from the real EFS (*Huttenlocker, Woodward & Hall, 2013*) because it is not restricted to the outermost cortex.

Bone tissue and vascular arrangement is very similar in metatarsi and metacarpi. In both skeletal elements, the bone cortex is mainly composed of a FLC with primary osteons (POs) oriented in circular rows (Fig. 2A). The vascular canals of these POs present a larger diameter in the outer half of the cortex than in the inner half (Fig. 2A). Some radial canals are situated in the proximity of the medullary cavity in metacarpal bones (Fig. 2B) whereas metatarsi present several areas with laminar bone (Fig. 2C). Haversian bone is restricted

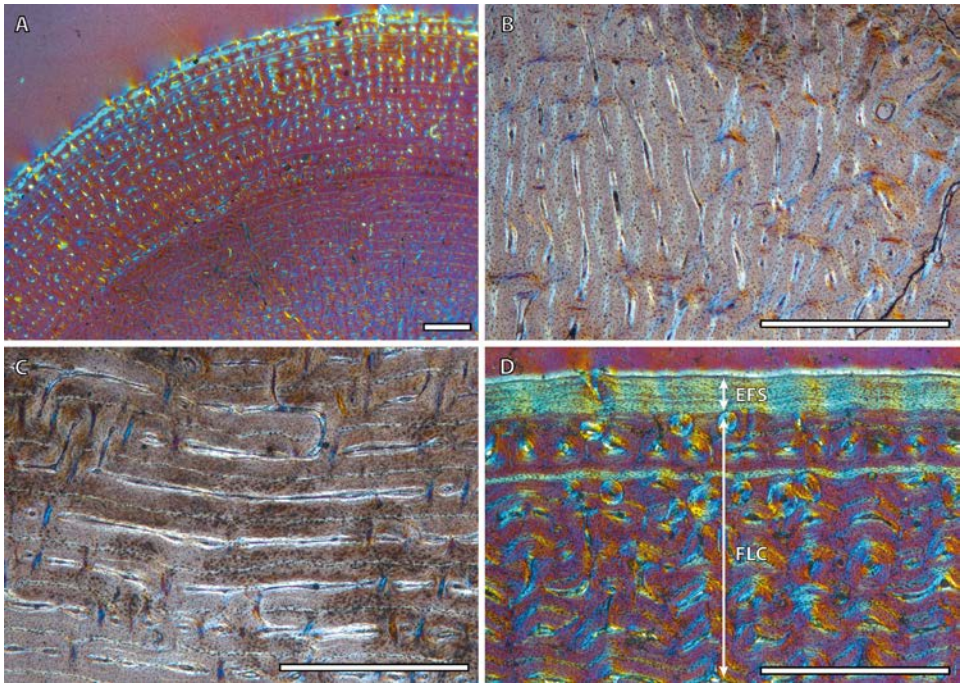

Figure 2 Metapodial bone histology of the Asiatic wild ass. (A) Anterior metatarsal cortex of the yearling IPS83149, showing a fibrolamellar complex with primary osteons oriented in circular rows. (B) Radial canals in the metacarpus of the yearling IPS83150. (C) Circular canals in the metatarsus of the foal IPS83153. (D) Detail of the external fundamental system in the metatarsus of the wild female IPS83876. EFS, external fundamental system; FLC, fibrolamellar complex. Scale bars: 1 millimeter. All images were obtained under polarized light with a 1/4λ filter.

to the posterior side of the cortex in immature kulans but it is more generalized in adult ones. The EFS is identified in the outermost cortex of adult individuals (Fig. 2D).

Bone growth marks

Table 2 shows the number of BGMs identified in the different bones of each individual. From foals to adults, all samples present these features, although its number varies among skeletal elements of the same individual and between individuals of the same age category.

The presence of a BGM in the middle cortex of tibia, metacarpus and metatarsus (Fig. 3, Table 2) of foals (IPS83153 and IPS83154) is surprising. LAGs and annuli are known to be annual and deposited during the unfavorable season (i.e., winter for *E. hemionus*) in mammals (*Köhler et al., 2012*). Because kulans tend to give birth in summer (*Zuckerman, 1952*; *Nowak, 1999*; *Feh et al., 2001*; *Feh et al., 2002*) and our foals are around six months old (Table 1), the CGM corresponding to the first winter should be observed in the outermost cortex, not in the mid-cortex (Fig. 3). Therefore, this feature is interpreted as a non-cyclical growth mark and will not be taken into account for age estimation.

Yearling specimens (IPS83149, IPS83150 and IPS83151) present a variable number of LAGs. As it is shown in Table 2, one BGM is identified in all skeletal elements of IPS83151, while IPS83149 and IPS83150 present two (Fig. 4). Such variability might be explained by

PeerJ

Table 2 Number of bone growth marks (BGMs) identified in each cross-section.

Individual	Estimated age	Age group	Sex	Femur			Tibia			Metacarpus			Metatarsus		
				FLC	EFS	Total	FLC	EFS	Total	FLC	EFS	Total	FLC	EFS	Total
IPS83152	<3 weeks	Perinatal	–	0	–	**0**	0	–	**0**	0	–	**0**	0	–	**0**
IPS83153	0.5 years	Foal	M	0	–	**0**	1	–	**1***	1		**1***	1	–	**1***
IPS83154	0.5 years	Foal	M	0	–	**0**	1	–	**1***	1	–	**1***	–	–	–
IPS83149	1 year	Yearling	–	2	–	**2***	2	–	**2***	2	–	**2***	2	–	**2***
IPS83150	1 year	Yearling	–	2	–	**2***	2	–	**2***	2	–	**2***	2	–	**2***
IPS83151	1 year	Yearling	–	1	–	**1***	1	–	**1***	1	–	**1***	1	–	**1***
IPS83155	2 years	Juvenile	F	1	–	**1**	2	–	**2***	1	–	**1**	2	–	**2***
IPS83876	4.5 years	Adult	F	4	1	**5**	4	–	**4**	3	2	**5***	3	2	**5***
IPS83877	8 years	Adult	M	4	2	**6**	5	–	**5**	4	2	**6***	4	2	**6***

Notes.
M, male; F, female; FLC, number of BGMs identified within the fibrolamellar complex; EFS, number of BGMs identified within the external fundamental system.
*Indicates that the most internal BGM has been considered as a non-cyclical BGM.

the fact that the first permanent molar is totally unworn in IPS38151 but presents initial wear in IPS83149 and IPS83150. Thus, the former might be somewhat younger than the others. Because these specimens are aged as one year, we interpret the most external BGM identified in all bones of IPS83149 and IPS83150 (Figs. 4B and 4D) as CGM deposited during the first year of life. However, we consider the internal BGM observed in these individuals (Figs. 4B and 4D), as well as the single BGM identified in the mid-cortex of all bones of IPS83151 (Figs. 4A and 4C), as a non-cyclical growth mark.

Two BGMs are identified in the tibia and the metatarsus of the juvenile individual (IPS83155) while the femur and the metacarpus present only one (Table 2, Fig. 5). In these latter bones, the growth mark appears in the outer cortex (Figs. 5A and 5C). Because this individual is aged around two years, we consider that this external BGM is representing the winter growth arrest during its second year of life. The second BGM in the tibia and metatarsus is also found in the external part of the cortex (Figs. 5B and 5D), so we interpret it as the CGM corresponding to the second winter. On the other hand, superimposition of individuals reveals that the first BGM of these bones (Figs. 5B and 5D) does not correspond to the CGM identified in yearlings, as it appears more internally within the cortex. This fact suggests that the first winter has not been recorded in this animal and that such internal BGM could be considered as non-cyclical.

Wild adult individuals (IPS83876 and IPS83877) also present differences in the number of BGMs between limb bones (Table 2, Fig. 6). Femur, metatarsus and metacarpus of the

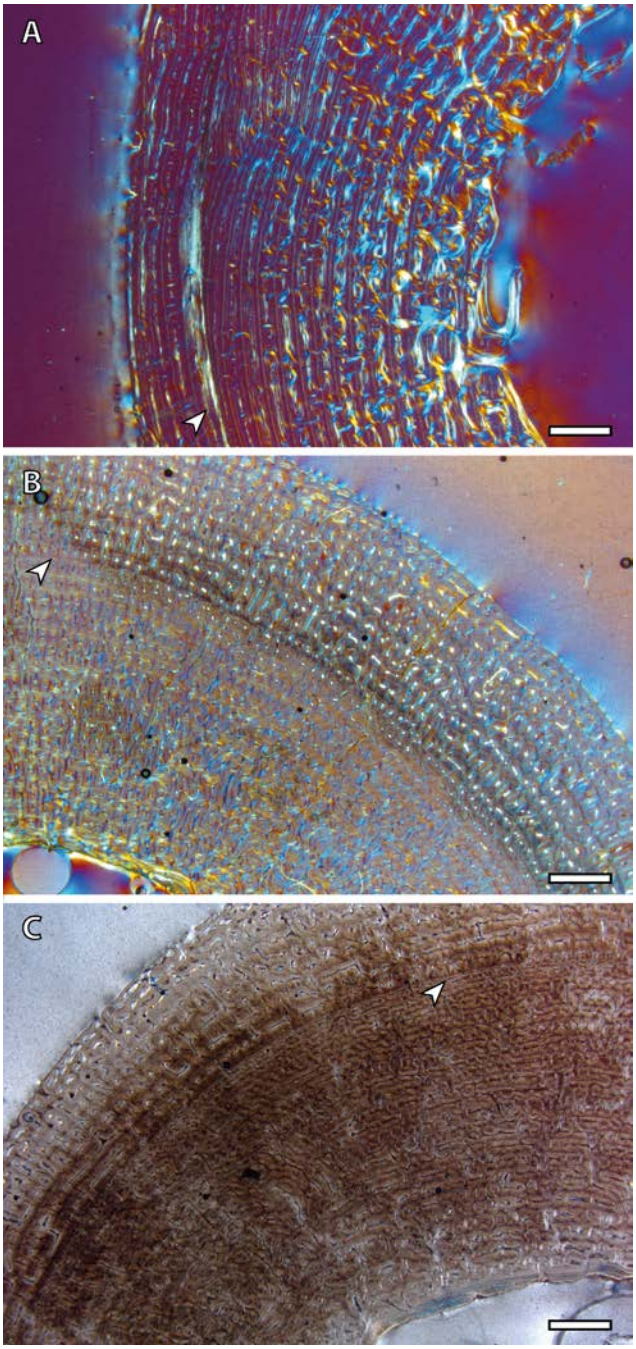

Figure 3 Bone growth marks in foal kulans. (A) BGM in the lateral side of the tibia (IPS83154). (B) BGM in the anterior cortex of the metacarpus (IPS83153). (C) BGM in the anterior side of the metatarsus (IPS83153). White arrows indicate bone growth marks. Scale bar: 1 millimeter. All images were obtained under polarized light with a 1/4λ filter.

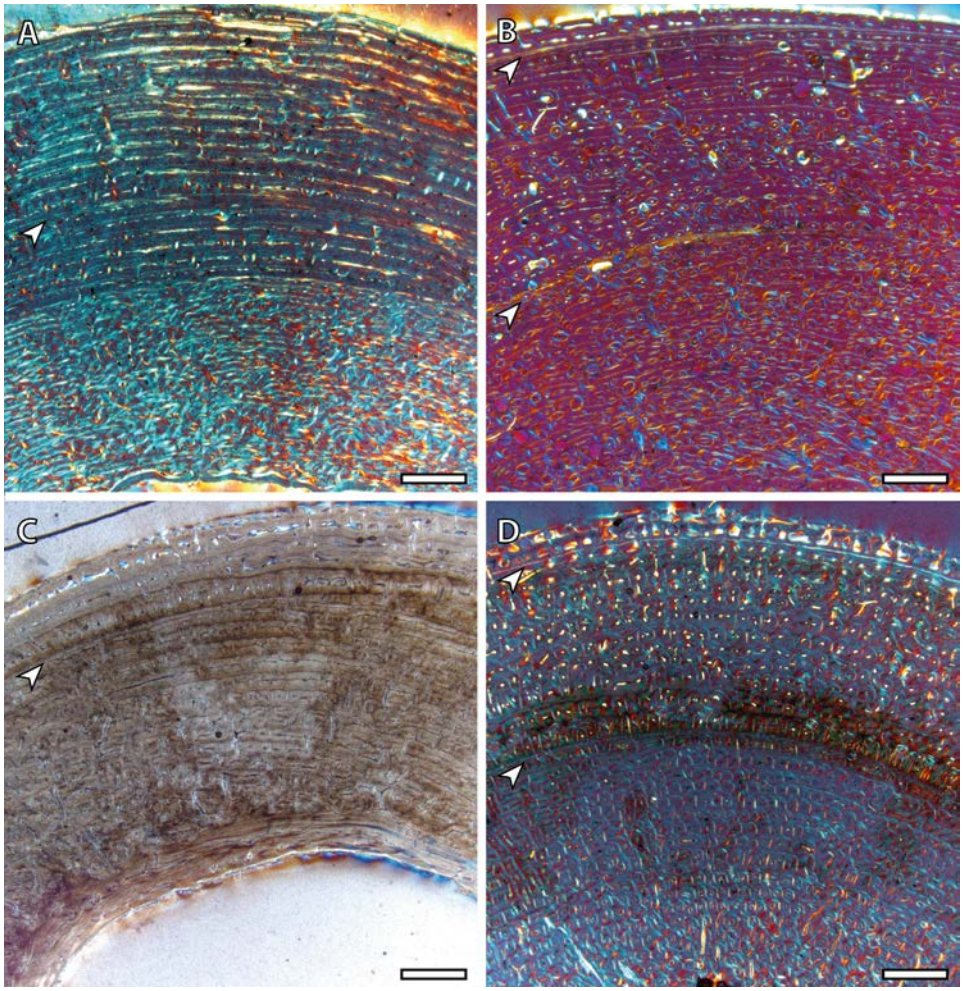

Figure 4 Bone growth marks in yearling kulans. (A) Femoral bone cortex of IPS83151 showing one BGM in its anterior side. (B) Tibial bone cortex of IPS83150 showing two BGMs in its lateral side. (C) Metacarpal bone cortex of IPS83151 showing one BGM in its lateral side. (D) Metatarsal bone cortex of IPS83149 showing two BGMs in its anterior side. White arrows indicate bone growth marks. Scale bar: 1 millimeter. All images were obtained under polarized light with a 1/4λ filter.

wild female (IPS83876) show five BGMs while only four BGMs are identified in its tibia (Table 2, Figs. 6A, 6B, 6E and 6F). In the femur, four BGMs lie within the FLC and one within the avascular and highly organized lamellar tissue deposited in the periphery of the bone (EFS) (Table 2, Figs. 6A and 6B). Metapodial bones, however, present three BGMs within the FLC and two BGMs in the EFS (Table 2, Figs. 6E and 6F). The four BGMs found in the tibia are within the FLC, as an EFS is not identified in this bone. On the other hand, the wild male (IPS83877) presents six BGMs in its femur and metapodial bones, whereas five BGMs are found in the tibia (Table 2, Figs. 6C, 6D, 6G and 6H). Superimposition of both adult individuals reveals that one BGM has been lost in the femur of the wild male due to bone remodeling (*Nacarino-Meneses, Jordana & Köhler, 2016*). This process, however,

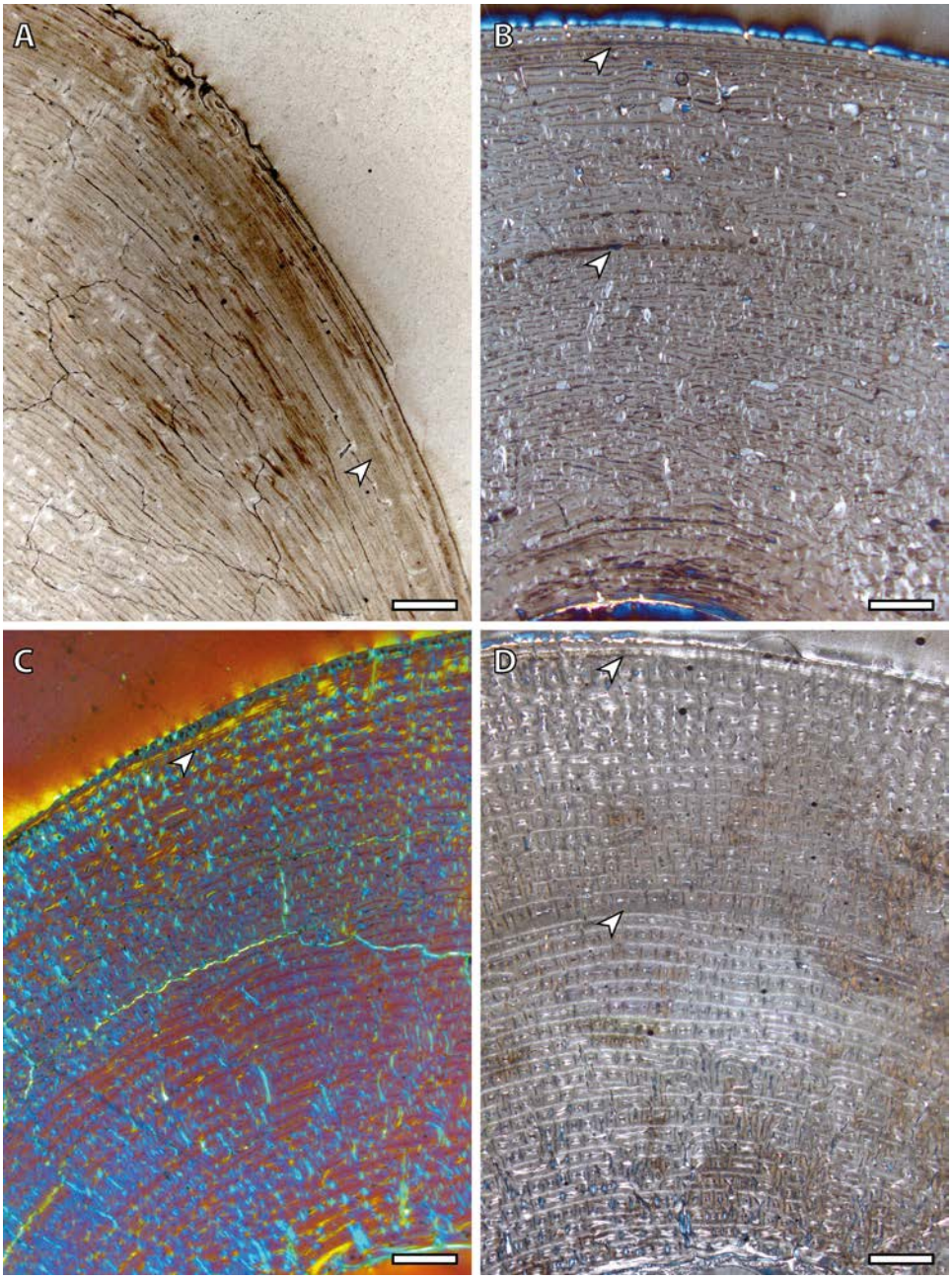

Figure 5 Bone growth marks in the juvenile kulan (IPS83155). (A) Femoral bone cortex showing one BGM in its anterior side. (B) Tibial bone cortex showing two BGMs in its lateral side. (C) Metacarpal bone cortex showing one BGM in its anterior side. (D) Metatarsal bone cortex showing two BGMs in its anterior side. White arrows indicate bone growth marks. Scale bar: 1 millimeter. All images were obtained under polarized light with a 1/4λ filter.

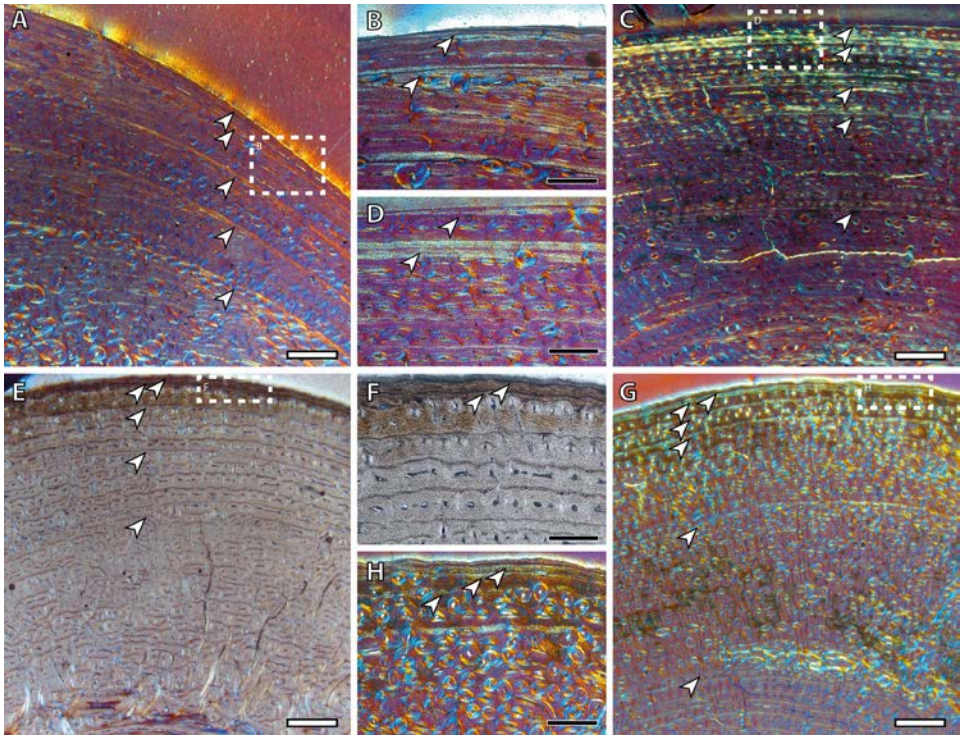

Figure 6 Bone growth marks in adult kulans. (A) Femoral bone cortex of the wild female (IPS83876) showing five BGMs in its anterior side. (B) Detail of the most external BGMs identified in the femur of IPS83876. Fifth BGM is located within the external fundamental system. (C) Tibial bone cortex of the wild male (IPS83877) showing five BGMs in its lateral side. (D) Detail of the most external BGMs identified in the tibia of IPS83877. (E) Metacarpal bone cortex of the wild female (IPS83876) showing five BGMs in its anterior side. (F) Detail of the most external BGMs identified in the metacarpus of IPS83876. Fourth and fifth BGMs are located within the external fundamental system. (G) Metatarsal bone cortex of the wild male (IPS83877) showing six BGMs in its anterior side. (H) Detail of the most external BGMs identified in the metacarpus of IPS83877. Fifth and sixth BGMs are located within the external fundamental system. White dashed rectangles indicate areas of image magnifications. White arrows indicate bone growth marks. White scale bar: 1 millimeter; black scale bar: 500 microns. All images were obtained under polarized light with a 1/4λ filter.

has not erased the presence of any BGM in the other limb bones studied. Thus, a total of seven BGMs should be counted in the femur of the wild male: five in the FLC (one hidden by secondary osteons) and two in the EFS. Five BGMs, all located in the FLC, are identified in the tibia of this wild male (IPS83877; Table 2, Figs. 6C and 6D). Finally, four BGMs are found in the FLC and two in the EFS of its metatarsus and metacarpus (Table 2, Figs. 6G and 6H). The correspondence between the age of both adults and the number of BGMs identified in their limb bones indicates that all these features could be considered as CGMs. However, superimposition suggests that the most internal BGM observed in metapodial bones of wild adults might be a non-cyclical feature, as they are deposited previously to the CGM identified in yearlings.

Growth curves

Based on the ontogenetic time schedule obtained from the study of the BGMs, we represented the growth curve for the different bones of each specimen (Figs. 7A–7D). In these graphs, the perimeter of the bone (outline of the BGM) at different years is plotted against the estimated age. Because the non-cyclical BGM identified in several bones is deposited sometime before the six months of life (Table 2, Fig. 3), it has been considered as time "zero" in the growth curves. The amount of growth in successive years, calculated as a proxy of growth rate, is also represented for yearlings and adult kulans (Figs. 7E–7H).

In adult individuals, the growth curves, as well as the plots of growth rate estimations, indicate a change in the pace of growth during ontogeny. Figure 7A shows that in both adults, growth of the femur slows down at the fourth year of life and from this time onwards growth is minimal (Fig. 7E). However, this decrease in growth rate takes place at the age of two in tibia, metatarsus and metacarpus (Figs. 7B–7D), followed by only minimal growth (Figs. 7F–7H). Figure 7 also reveals differences in growth between captive and wild kulans. The results obtained from the analysis of bone growth cycles of the femur indicate two different growth tendencies with wild specimens growing more slowly than captives (Fig. 7A). While this difference is not perceived in the growth curves of the other limb bones studied (Figs. 7B–7D), growth rates of captive individuals are always higher than those of wild kulans in the first year of life (Figs. 7E–7H).

DISCUSSION

In the present research, we analyzed the histological variability between limb bones in the extant species *Equus hemionus* for the first time. Previous studies have addressed this issue in isolated bones of fossil vertebrate species (*Horner, De Ricqlès & Padian, 2000*; *Sander & Andrássy, 2006*; *Cullen et al., 2014*; *Martínez-Maza et al., 2014*), but only a few have studied the histological variation of bone tissue within the same individual (*Horner, De Ricqlès & Padian, 1999*; *García-Martínez et al., 2011*; *Woodward, Horner & Farlow, 2014*; *Cambra-Moo et al., 2015*). Our analysis of kulan's bone histology contributes to the knowledge of intraskeletal variability in mammals, providing new and important results that are of interest in different scientific areas. The applicability of histological studies to describe the life history of past animals and their evolutionary trends is well known (*Köhler & Moyà-Solà, 2009*; *Marín-Moratalla et al., 2011*; *Martínez-Maza et al., 2014*; *Woodward et al., 2015*). However, many researchers claim that more studies in living taxa are needed to truly understand the correlation between bone histology and the life history strategy of past organisms (*Martínez-Maza et al., 2014*; *Woodward, Horner & Farlow, 2014*; *Cambra-Moo et al., 2015*; *Kolb et al., 2015a*; *Jordana et al., 2016*). The results obtained from the present research will serve as a basis for the inference of life history parameters from the histology of extinct mammal species. Even more, skeletochronological studies of extant species are also of interest in related biological disciplines like Conservation Biology (*Chinsamy & Valenzuela, 2008*; *García-Martínez et al., 2011*; *Marín-Moratalla, Jordana & Köhler, 2013*). Nowadays, most of the wild species of the genus *Equus* are threatened and conservation policies are usually focus on genetic studies of captive individuals (*Orlando, 2015*). By

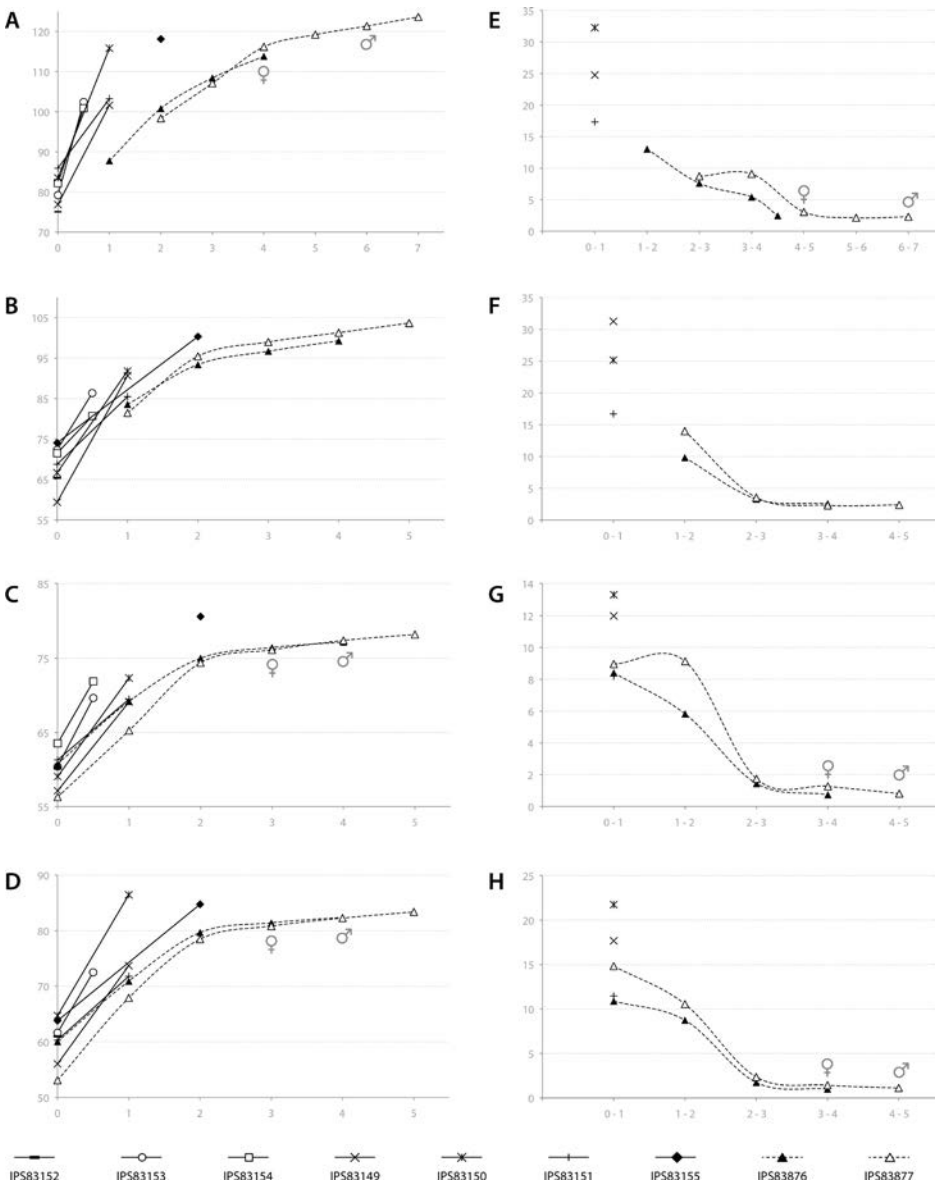

Figure 7 **Bone growth of the Asiatic wild ass.** From (A–D), bone perimeter (mm, ordinate axis) is plotted against estimated age (years, abscissa axis) to obtain growth curves. From (E–F), variation of bone perimeter (mm, ordinate axis) is plotted against estimated age (years, abscissa axis) as a proxy of growth rate. (A) Growth curves obtained from the femora. (B) Growth curves obtained from the tibiae. (C) Growth curves obtained from the metacarpi. (D) Growth curves obtained from the metatarsi. (E) Femoral growth rate. (F) Tibial growth rate. (G) Metacarpal growth rate. (H) Metatarsal growth rate. Legend is shown in the bottom of the figure. In the graphs, filled characters represent females, unfilled ones correspond to males and linear ones indicate animals with unknown sex. Dashed lines indicate wild animals while continuous lines represent captive ones. Male and female symbols indicate the time of deposition of the external fundamental system (EFS) in each wild adult respectively. It could be noted that this moment does not match with the decline in periosteal growth rate.

means of skeletochronology, however, key life history traits such as longevity or age at sexual maturity can be inferred from the bone tissue of wild specimens (*Castanet et al., 2004*; *Marín-Moratalla, Jordana & Köhler, 2013*; *Jordana et al., 2016*). This information can be later used to calculate demographic parameters (e.g., life expectancy, generation time) that are essential to improve the conservation status of the species in the wild (*Feh et al., 2001*).

The detailed analysis of LAGs and annuli performed in the present research reveals that the number of BGMs recorded by the different limb bones varies within the same specimen (Table 2), a fact that has previously been reported for other vertebrate groups (*Horner, De Ricqlès & Padian, 1999*; *García-Martínez et al., 2011*; *Cullen et al., 2014*; *Woodward, Horner & Farlow, 2014*). Our results show that the femur registers the highest total number of BGMs, as well as the highest number of these features within the FLC (Table 2). This observation, which has previously been observed in mammals (*García-Martínez et al., 2011*), is likely related with the fact that the femur is the bone that more tightly correlates with the final size of the individual because it fuses its epiphyses late in ontogeny (*Silver, 1969*). Furthermore, the total number of CGMs identified in this bone agrees fairly well with the estimated age of the specimens (Table 2), even in the oldest one, which is aged 8 years and present 7 CGMs (one obscured by haversian systems) in the cross-section. This result provides reliability to the estimation of longevity in wild populations of Asiatic wild ass that are known to live around nine years in the wild (*Kaczensky et al., 2015*). *Horner, De Ricqlès & Padian (1999)*, in their study of *Hypacrosaurus stebingeri*, suggested that also the tibia is suitable for skeletochronology. However, the presence of many haversian systems in the tibial cortices of hemionus yearlings (Fig. 1B) indicates that it does not provide accurate skeletochronological results in the Asiatic wild ass. The use of metapodial bones in skeletochronology is still a controversial issue. While *Horner, De Ricqlès & Padian (1999)* do not recommend it, for perissodactyls, *Martínez-Maza et al. (2014)* obtained acceptable results in their histological analysis of the fossil species *Hipparion concudense*. In artiodactyls, however, it does not work because of the ontogenetically late fusion of metatarsus III and IV that deletes growth structures (M Köhler, pers. obs., 2006). Our results show that these bones record a similar total number of BGMs as the femur (Table 2), although the first BGM identified in these skeletal elements seems to be a non-cyclical BGM (Table 2, Figs. 3–6), a fact that must be taken into account when calculating individual age. This information is especially important for studies that comprise a single individual, to not overestimate the results. Moreover, adult metacarpi and metatarsi show a lower number of BGMs than femora within the FLC (Table 2, Fig. 6), which contrasts with the results obtained by *Martínez-Maza et al. (2014)*. The presence of BGMs in the fibrolamellar tissue provides important information about the growth and the timing of key life history traits of the species. Because it is deposited during growth (*Huttenlocker, Woodward & Hall, 2013*) distance between BGMs has been used to estimate growth rates in extant and extinct mammals (*Marín-Moratalla, Jordana & Köhler, 2013*; *Kolb et al., 2015b*). On the other hand, the number of BGMs within the FLC seems to correlate with the time of sexual maturity in artiodactyls (*Marín-Moratalla, Jordana & Köhler, 2013*; *Jordana et al., 2016*). Therefore, the results obtained from metapodial bones should be used with caution.

Despite these drawbacks, the skeletochronological study of metacarpi and metatarsi still provide valuable individual age estimates because they present a similar total number of BGMs as femora (Table 2). This result is especially interesting for the inference of longevity in fossil species, as these bones are the most abundant remains of equids in paleontological sites.

Regarding bone tissue types, our results show that femora and tibiae present laminar bone (Fig. 1A) while the cortices of metapodial bones are mainly composed of longitudinal POs arranged in circular rows (Fig. 2A) (*Francillon-Vieillot et al., 1990*). This histological variability, which agrees with previous descriptions of the bone tissue of extant (*Enlow & Brown, 1958*; *Stover et al., 1992*) and fossil (*Sander & Andrássy, 2006*; *Martínez-Maza et al., 2014*) equid species, is likely related with the specific growth rate and biomechanics of each bone (*Horner, De Ricqlès & Padian, 1999*; *De Margerie, Cubo & Castanet, 2002*; *De Margerie et al., 2004*). On the one hand, the kind of bone matrix is associated with different growth rates (*Amprino, 1947*; *Huttenlocker, Woodward & Hall, 2013*) while the arrangement of the vascular canals is commonly related to mechanical forces (*De Margerie, Cubo & Castanet, 2002*; *De Margerie, Cubo & Castanet, 2002*). Furthermore, ontogenetic histological changes regarding bone matrix have been noticed in the different limb bones studied. Our study shows a marked change in the proportion of PFB (Fig. 1A) within the FLC matrix in tibiae of subadult kulans. Bone matrix change, along with a modification of the orientation of the vascular canals, has also been observed in femora of *E. hemionus* (*Nacarino-Meneses, Jordana & Köhler, 2016*). These histological modifications are likely related to both the changes in loadings (*Firth, 2006*) and in growth rate (*Peters, 1983*) that foals experience at the moment of birth.

Amongst all bone tissue types, the occurrence of EFS in vertebrates is a controversial issue. Traditionally, its deposition has been interpreted as the attainment of skeletal maturity (*Cormack, 1987*; *Chinsamy-Turan, 2005*; *Woodward, Padian & Lee, 2013*; *Martínez-Maza et al., 2014*; *Amson et al., 2015*; *Kolb et al., 2015b*) but recent studies have shown that, at least in mammals, it might also be related with the onset of sexual maturity of the species (*Klevezal, 1996*; *Marín-Moratalla, Jordana & Köhler, 2013*; *Jordana et al., 2016*). Growth studies have been shown to provide good estimations of these traits in fossil species (*Lee et al., 2013*). Our results indicate that the EFS is deposited after epiphyseal fusion in all bones and at a later time in the male than in the female (Table 3, Fig. 7). Actually, in most of the bones analyzed, the time of fusion of both epiphyses agrees with an important drop in the rate of radial growth (inflection point in the growth curves, Fig. 7) and does not match the time of deposition of the EFS. Concretely in the femur, which epiphyses are fused at the age of three (*Silver, 1969*), the EFS of the wild female is deposited in the fourth year of life while in the wild male it appears at the age of six (Table 3, Fig. 7). In metapodials, the EFS appears after the third year in the female and after the fourth year in the male (Table 3, Fig. 7). These skeletal elements are completely fused at the age of two (*Silver, 1969*). The correspondence between the pronounced decrease in periosteal growth rate and the age of epiphyseal fusion (*Silver, 1969*) (Table 3) suggests the decrease in periosteal growth rate to be a good indicator of the end of longitudinal growth in the respective bone. However, the deposition of the EFS some time after growth decline (Fig. 7)

Table 3 Age of deposition of the external fundamental system (EFS) in the limb bones of adult kulans and time of several biological traits in equids obtained from the literature. Age of epiphyseal fusion (*Silver, 1969*) is indicated for the closely related species *Equus caballus* while age at sexual maturity (*Nowak, 1999*) and age at first reproduction (*Kaczensky et al., 2015*) is reported for *Equus hemionus*. All data are expressed in years.

	EFS				Epiphyseal fusion					
	F	T	Mc	Mt	F	T	Mc	Mt	Sexual maturity	Age at first reproduction
Female	4	–	3	3	3–3.5	3–3.5	1.25–1.5	1.3–1.6	2	3
Male	6	–	4	4	3–3.5	3–3.5	1.25–1.5	1.3–1.6	3	5

Notes.
F, femur; T, tibia; Mc, metacarpus; Mt, metatarsus.

indicates that the bone shaft continues growing at minimal rates over some time until full radial growth is achieved (*Huttenlocker, Woodward & Hall, 2013*). This decoupling between longitudinal and radial growth suggests that inferences of skeletal maturity from the time of deposition of the EFS in equids might be incorrect. However, the presence of the EFS in femora agrees fairly well with the age at first reproduction reported for *E. hemionus* (Table 3; *Kaczensky et al., 2015*). In general terms, the femur in mammals presents the longest time of development with the latest epiphyseal fusion (*Silver, 1969*). Thus, its histological structure should provide the best record of life history events. It is known that although kulans are sexually mature at their second or third year of life (*Nowak, 1999*), they delay some years its first mating (*Kaczensky et al., 2015*). Hence, our results provide histological evidence for this well-known behavior in equids (*Fielding, 1988*; *Monfort, Arthur & Wildt, 1994*).

Finally, the growth analysis has also revealed a high inter-individual variability in size (Fig. 7) that should be taken into account when retrocalculating lost CGMs. Our results, although obtained from a relatively small sample size, show different femoral growth tendencies between wild and captive individuals (Fig. 7A) and a higher growth rate in captive exemplars than in wild ones during the first year of life (Figs. 7E–7H). These differences, that reflect the influence of the habitat in the life history of the species, have previously been reported for mammals (*Marín-Moratalla, Jordana & Köhler, 2013*) and alligators (*Woodward, Horner & Farlow, 2014*) and are related with the constant food supply and care that captive animals experience during their life (*Asa, 2010*). To obtain the most accurate data, we propose to study wild animals when possible to avoid overestimation of growth rates for the species under study.

CONCLUSIONS

Our study analyzes the histological variation between different limb bones of the Asiatic wild ass. Our research provides evidence that the femur is the most reliable bone for skeletochronological studies in equids, although metapodial bones also provide good individual age estimations. The use of tibiae, however, is not recommended for this group due to the high presence of secondary osteons observed in early ontogenetic stages. Furthermore, all bones present histological changes regarding the proportions of bone matrix components and / or the arrangement of vascular canals in the course of ontogeny. Finally, the presence of an EFS in the outermost cortex of adult femora is likely related

to the reproductive maturity of the species (first reproduction) than to skeletal maturity. Skeletal maturity, however, is recorded in growth curves as a significant drop in periosteal growth rate.

ACKNOWLEDGEMENTS

We are grateful to Thomas Kaiser for loans of the collection of the Zoological Institute of Hamburg University (Hamburg, Germany) and to Renate Schafberg for permission to cut the adult kulan bones from the collections housed at Museum of Domesticated Animals of the Martin-Luther-University Halle-Wittenberg (Halle, Saale, Germany). We are indebt to Gemma Prats-Muñoz and Luis Gordon for preparing the thin sections of the study. Finally, we acknowledge William Jungers for handling the article as editor of PeerJ and Clara Stefen, Jorge Cubo and Tim Bromage for their useful reviews, which greatly improve an earlier version of the manuscript.

ADDITIONAL INFORMATION AND DECLARATIONS

Funding

This work is supported by the Spanish Ministry of Economy and Competitiveness (MINECO) (PI: M.K. & X.J., CGL2015-63777) and by the Government of Catalonia (2014-SGR-1207). C.N.-M. holds a grant from the MINECO (BES-2013-066335). The funders had no role in study design, data collection and analysis, decision to publish, or preparation of the manuscript.

Grant Disclosures

The following grant information was disclosed by the authors:
Spanish Ministry of Economy and Competitiveness (MINECO): CGL2015-63777.
The Government of Catalonia: 2014-SGR-1207.
MINECO: BES-2013-066335.

Competing Interests

The authors declare there are no competing interests.

Author Contributions

- Carmen Nacarino-Meneses conceived and designed the experiments, performed the experiments, analyzed the data, wrote the paper, prepared figures and/or tables, reviewed drafts of the paper.
- Xavier Jordana analyzed the data, reviewed drafts of the paper.
- Meike Köhler conceived and designed the experiments, analyzed the data, contributed reagents/materials/analysis tools, reviewed drafts of the paper.

Data Availability

The following information was supplied regarding data availability:
The raw data is included in the results.

REFERENCES

Amprino R. 1947. La structure du tissu osseux envisagée comme expression de différences dans la vitesse de l'accroissement. *Archives of Biology* **58**:315–330.

Amson E, Kolb C, Scheyer TM, Sánchez-Villagra MR. 2015. Growth and life history of Middle Miocene deer (Mammalia, Cervidae) based on bone histology. *Comptes Rendus Palevol* **14**:637–645 DOI 10.1016/j.crpv.2015.07.001.

Asa CS. 2010. Reproductive physiology. In: Kleiman DG, Thompson KV, Kirk-Baer C, eds. *Wild Mammals in Captivity*. Chicago: The University of Chicago Press, 219–252.

Bybee PJ, Lee AH, Lamm ET. 2006. Sizing the Jurassic theropod dinosaur *Allosaurus*: assessing growth strategy and evolution of ontogenetic scaling limbs. *Journal of Morphology* **267**:347–359 DOI 10.1002/jmor.10406.

Cambra-Moo O, Nacarino-Meneses C, Díaz-Güemes I, Enciso S, García Gil O, Llorente Rodríguez L, Rodríguez Barbero MA, De Aza AH, González Martín A. 2015. Multidisciplinary characterization of the long-bone cortex growth patterns through sheep's ontogeny. *Journal of Structural Biology* **191**:1–9 DOI 10.1016/j.jsb.2015.06.013.

Castanet J. 2006. Time recording in bone microstructures of endothermic animals; functional relationships. *Comptes Rendus Palevol* **5**:629–636 DOI 10.1016/j.crpv.2005.10.006.

Castanet J, Croci S, Aujard F, Perret M, Cubo J, De Margerie E. 2004. Lines of arrested growth in bone and age estimation in a small primate: *Microcebus murinus*. *Journal of Zoology* **263**:31–39 DOI 10.1017/S0952836904004844.

Castanet J, Francillon-Vieillot H, Meunier FJ, De Ricqlès A. 1993. Bone and individual aging. In: Hall BK, ed. *Bone, vol. 7*. Boca Raton: CRC Press, 245–283.

Chinsamy A, Valenzuela N. 2008. Skeletochronology of the endangered side-neck turtle, *Podocnemis expansa*. *South African Journal of Science* **104**:311–314.

Chinsamy-Turan A. 2005. *The microstructure of dinosaur bone*. Baltimore: The Johns Hopkins University Press.

Cormack D. 1987. *Ham's Histology*. Philadelphia: JC Lippincott Williams and Wilkins.

Cullen TM, Evans DC, Ryan MJ, Currie PJ, Kobayashi Y. 2014. Osteohistological variation in growth marks and osteocyte lacunar density in a theropod dinosaur (Coelurosauria: Ornithomimidae). *BMC Evolutionary Biology* **14**:231 DOI 10.1186/s12862-014-0231-y.

De Margerie E, Cubo J, Castanet J. 2002. Bone typology and growth rate: testing and quantifying "Amprino's rule" in the mallard (*Anas platyrhynchos*). *Comptes Rendus Biologies* **325**:221–230 DOI 10.1016/S1631-0691(02)01429-4.

De Margerie E, Robin JP, Verrier D, Cubo J, Groscolas R, Castanet J. 2004. Assessing a relationship between bone microstructure and growth rate: a fluorescent labeling study in the king penguin chick (*Aptenodytes patagonicus*). *Journal of Experimental Biology* **207**:869–879 DOI 10.1242/jeb.00841.

Downer CC. 2014. The horse and burro as positively contributing returned natives in North America. *American Journal of Life Sciences* **2**:5–23 DOI 10.11648/j.ajls.20140201.12.

Enlow DH, Brown SO. 1958. A comparative histological study of fossil and recent bone tissue. Part III. *Texas Journal of Science* **10**:187–230.

Feh C, Munkhtuya B, Enkhbold S, Sukhbaatar T. 2001. Ecology and social structure of the Gobi khulan *Equus hemionus* subsp. in the Gobi B National Park, Mongolia. *Biological Conservation* **10**:51–61 DOI 10.1016/S0006-3207(01)00051-9.

Feh C, Shah N, Rowen M, Reading R, Goyal SP. 2002. Status and action plan for the Asiatic wild Ass (*Equus hemionus*). In: Mohelman PD, ed. *Zebras, Asses and Horses. Status Survey and Conservation Action Plan*. Gland and Cambridge: IUCN/SS Equid Specialist Group, 62–71.

Fielding D. 1988. Reproductive characteristics of the jenny donkey-*Equus asinus*: a review. *Tropical Animal Health and Production* **20**:161–166 DOI 10.1007/BF02240085.

Firth EC. 2006. The response of bone, articular cartilage and tendon to exercise in the horse. *Journal of Anatomy* **208**:513–526 DOI 10.1111/j.1469-7580.2006.00547.x.

Forstén A. 1992. Mitochondrial-DNA time-table and the evolution of *Equus*: comparison of molecular and paleontological evidence. *Annales Zoologici Fennici* **28**:301–309.

Francillon-Vieillot H, De Buffrénil V, Castanet J, Géraudie J, Meunier FJ, Sire JY, Zylberberg L, de Ricqlès A. 1990. Microstructure and mineralization of vertebrate skeletal tissues. In: Carter JG, ed. *Skeletal biomineralization: patterns, processes and evolutionary trends*. New York: Van Nostrand Reinhold, 471–530.

García-Martínez R, Marín-Moratalla N, Jordana X, Köhler M. 2011. The ontogeny of bone growth in two species of dormice: Reconstructing life history traits. *Comptes Rendus Palevol* **10**:489–498 DOI 10.1016/j.crpv.2011.03.011.

Horner JR, De Ricqlès A, Padian K. 1999. Variation in dinosaur skeletochronology indicators: implications for age assessment and physiology. *Paleobiology* **25**:295–304 DOI 10.1017/S0094837300021308.

Horner JR, De Ricqlès A, Padian K. 2000. Long bone histology of the hadrosaurid dinosaur *Maiasaura peeblesorum*: growth dynamics and physiology based on an ontogenetic series of skeletal elements. *Journal of Vertebrate Paleontology* **20**:115–129 DOI 10.1671/0272-4634(2000)020[0115:LBHOTH]2.0.CO;2.

Huttenlocker AK, Woodward HN, Hall BK. 2013. The biology of Bone. In: Padian K, Lamm ET, eds. *Bone histology of fossil tetrapods*. Berkeley: University of California Press, 13–34.

Jordana X, Marín-Moratalla N, Moncunill-Solé B, Nacarino-Meneses C, Köhler M. 2016. Ontogenetic changes in the histological features of zonal bone tissue of ruminants: a quantitative approach. *Comptes Rendus Palevol* **15**:265–276.

Kaczensky P, Lkhagvasuren B, Pereladova O, Hemami M, Bouskila A. 2015. *Equus hemionus. The IUCN Red List of Threatened Species* **2015**:e.T7951A45171204 DOI 10.2305/IUCN.UK.2015-4.RLTS.T7951A45171204.en.

Klevezal GA. 1996. *Recording structures of mammals: determination of age and reconstruction of life history*. Rotterdam: AA Balkema.

Köhler M. 2010. Fast or slow? The evolution of life history traits associated with insular dwarfing. In: Pérez-Mellado V, Ramon MM, eds. *Islands and evolution*. Maó: Institut Menorquí d'Estudis, Recerca 19, 261–279.

Köhler M, Marín-Moratalla N, Jordana X, Aanes R. 2012. Seasonal bone growth and physiology in endotherms shed light on dinosaur physiology. *Nature* **487**:358–361 DOI 10.1038/nature11264.

Köhler M, Moyà-Solà S. 2009. Physiological and life history strategies of a fossil large mammal in a resource-limited environment. *Proceedings of the National Academy of Sciences of the United States of America* **106**:20354–20358 DOI 10.1073/pnas.0813385106.

Kolb C, Scheyer TM, Lister AM, Azorit C, De Vos J, Schlingemann MAJ, Rössner GE, Monaghan NT, Sánchez-Villagra MR. 2015b. Growth in fossil and extant deer and implications for body size and life history evolution. *BMC Evolutionary Biology* **15**:1–15 DOI 10.1186/s12862-015-0295-3.

Kolb C, Scheyer TM, Veitschegger K, Forasiepi AM, Amson E, Van der Geer AAE, Van den Hoek Ostende LW, Hayashi S, Sánchez-Villagra MR. 2015a. Mammalian bone paleohistology: a survey and new data with emphasis on island forms. *PeerJ* **3**:e1358 DOI 10.7717/peerj.1358.

Lamm ET. 2013. Preparation and sectioning of specimens. In: Padian K, Lamm ET, eds. *Bone histology of fossil tetrapods*. Berkeley: University of California Press, 55–160.

Lee AH, Huttenlocker AK, Padian K, Woodward HN. 2013. Padian K, Lamm ET, eds. *Bone histology of fossil tetrapods*. Berkeley: University of California Press, 217–251.

Lkhagvasuren D, Ansorge H, Samiya R, Schafberg R, Stubbe A, Stubbe M. 2013. Age determination of the Mongolian wild ass (*Equus hemionus*, Pallas 1775) by the dentition patterns and annual lines in the tooth cementum. *Journal of Species Research* **2**:85–90 DOI 10.12651/JSR.2013.2.1.085.

MacFadden BJ. 1992. *Fossil horses. Systematics, Paleobiology, and Evolution of the Family Equidae*. Cambridge: Cambridge University Press.

MacFadden BJ. 2005. Fossil Horses –Evidence of evolution. *Science* **307**:1728–1730 DOI 10.1126/science.1105458.

Marín-Moratalla N, Cubo J, Jordana X, Moncunill-Solé B, Köhler M. 2014. Correlation of quantitative bone histology data with life history and climate: a phylogenetic approach. *Biological Journal of the Linnean Society* **112**:678–687 DOI 10.1111/bij.12302.

Marín-Moratalla N, Jordana X, García-Martínez R, Köhler M. 2011. Tracing the evolution of fitness components in fossil bovids under different selective regimes. *Comptes Rendus Palevol* **10**:469–478 DOI 10.1016/j.crpv.2011.03.007.

Marín-Moratalla N, Jordana X, Köhler M. 2013. Bone histology as an approach to providing data on certain key life history traits in mammals: implications for conservation biology. *Mammalian Biology* **78**:422–429 DOI 10.1016/j.mambio.2013.07.079.

Martínez-Maza C, Alberdi MT, Nieto-Diaz M, Prado JL. 2014. Life-history traits of the miocene *Hipparion concudense* (Spain) inferred from bone histological structure. *PLoS ONE* **9**:e103708 DOI 10.1371/journal.pone.0103708.

Moncunill-Solé B, Orlandi-Oliveras G, Jordana X, Rook L, Köhler M. 2016. First approach of the life history of *Prolagus apricenicus* (Ochotonidae, Lagomorpha) from Terre Rosse sites (Gargano, Italy) using body mass estimation and paleohistological analysis. *Comptes Rendus Palevol* **15**:235–245 DOI 10.1016/j.crpv.2015.04.004.

Monfort SL, Arthur NP, Wildt DE. 1994. Reproduction in the Przewalski's horse. In: Boyde L, Houpt KA, eds. *Przewalski's horse. The history and biology of an endangered species*. Albany: State University of New York Press, 173–194.

Nacarino-Meneses C, Jordana X, Köhler M. 2016. First approach to bone histology and skeletochronology of *Equus hemionus*. *Comptes Rendus Palevol* **15**:277–287 DOI 10.1016/j.crpv.2015.02.005.

Nowak RM. 1999. *Walker's Mammals of the World, 6th ed*. Baltimore and London: The Johns Hopkins University Press.

Orlandi-Oliveras G, Jordana X, Moncunill-Solé B, Köhler M. 2016. Bone histology of the giant fossil dormouse *Hypnomys onicensis* (Gliridae, Rodentia) from Balearic Islands. *Comptes Rendus Palevol* **15**:247–253 DOI 10.1016/j.crpv.2015.05.001.

Orlando L. 2015. Equids. *Current Biology* **25**:R973–R978 DOI 10.1016/j.cub.2015.09.005.

Padian K, De Ricqlès A, Horner JR. 2001. Dinosaurian growth rates and bird origins. *Nature* **412**:405–408 DOI 10.1038/35086500.

Peabody FE. 1961. Annual growth zones in living and fossil vertebrates. *Journal of Morphology* **108**:11–62 DOI 10.1002/jmor.1051080103.

Peters RH. 1983. *The ecological implications of body size*. Cambridge: Cambridge University Press.

Prondvai E, Stein KHW, De Ricqlès A, Cubo J. 2014. Development-based revision of bone tissue classification: the importance of semantics for science. *Biological Journal of the Linnean Society* **112**:799–816 DOI 10.1111/bij.12323.

Reading RP, Mix HM, Lhagvasuren B, Feh C, Kane DP, Dulamtseren S, Enkhbold S. 2001. Status and distribution of khulan (*Equus hemionus*) in Mongolia. *Journal of Zoology* **254**:381–389 DOI 10.1017/S0952836901000887.

Sander PM, Andrássy P. 2006. Lines of arrested growth and long bone histology in Pleistocene large mammals from Germany: what do they tell us about dinosaur physiology? *Palaeontographica Abteilung A* **277**:143–159.

Schöpke K, Stubbe A, Stubbe M, Batsaikhan N, Schafberg R. 2012. Morphology and variation of the Asiatic wild ass. *Erforschung biologischer Ressourcen der Mongolei* **12**:77–84.

Silver IA. 1969. The ageing of domestic mammals. In: Brothwell D, Higgs E, eds. *Science in Archaeology*. New York: Basic Books, 250–268.

Stein K, Prondvai E. 2014. Rethinking the nature of fibrolamellar bone: an integrative biological revision of sauropod plexiform bone formation. *Biological Reviews* **89**:24–47 DOI 10.1111/brv.12041.

Steiner CC, Ryder OA. 2011. Molecular phylogeny and evolution of the Perissodactyla. *Zoological Journal of the Linnean Society* **163**:1289–1303 DOI 10.1111/j.1096-3642.2011.00752.x.

Stover SM, Pool RR, Martin RB, Morgan P. 1992. Histological features of the dorsal cortex of the third metacarpal bone mid-diaphysis during postnatal growth in thoroughbred horses. *Journal of Anatomy* **181**:455–469.

Turner-Walker G, Mays S. 2008. Histological studies on ancient bone. In: Pinhasi R, Mays S, eds. *Advances in human palaeopathology*. Chichester: John Wiley & Sons, Ltd, 121–146.

Woodward HN, Freedman Fowler EA, Farlow JO, Horner JR. 2015. *Maiasaura*, a model organism for extinct vertebrate population biology: a large sample statistical assessment of growth dynamics and survivorship. *Paleobiology* **41**:503–527 DOI 10.1017/pab.2015.19.

Woodward HN, Horner JR, Farlow JO. 2014. Quantification of intraskeletal histovariability in *Alligator mississippiensis* and implications for vertebrate osteohistology. *PeerJ* **2**:e422 DOI 10.7717/peerj.422.

Woodward HN, Padian K, Lee AH. 2013. Skeletochronology. In: Padian K, Lamm ET, eds. *Bone histology of fossil tetrapods*. Berkeley: University of California Press, 195–216.

Zuckerman S. 1952. The breeding season of mammals in captivity. *Proceedings of the Zoological Society of London* **122**:827–950 DOI 10.1111/j.1096-3642.1952.tb00251.x.

- Chapter 6 -

LIMB BONE HISTOLOGY RECORDS BIRTH IN MAMMALS

Reproduced from:

Nacarino-Meneses C. & Köhler M. (Accepted) *PLoS ONE*

Limb bone histology records birth in mammals

Carmen Nacarino-Meneses[1]* & Meike Köhler[1,2]

[1] Institut Català de Paleontologia Miquel Crusafont (ICP), Campus de la Universitat Autònoma de Barcelona, 08193 Bellaterra, Barcelona, Spain.

[2] ICREA, Pg. Lluís Companys 23, 08010 Barcelona, Spain.

Correspondence (*): Carmen Nacarino-Meneses, Institut Català de Paleontologia Miquel Crusafont (ICP), C/ de les Columnes s/n, Edifici Z, Campus UAB, 08193 Bellaterra, Barcelona, Spain. Phone number: +34 93 586 86 19. E-mail: carmen.nacarino@icp.cat

Abstract

The annual cyclicality of cortical bone growth marks (BGMs) allows reconstruction of some important life history traits, such as longevity, growth rate or age at maturity. Little attention has been paid, however, to non-cyclical BGMs, though some record key life history events such as hatching (egg-laying vertebrates), metamorphosis (amphibians), or weaning (suggested for *Microcebus* and the hedgehog). Here, we investigate the relationship between non-cyclical BGMs and a stressful biological event in mammals: the moment of birth. In the present study, we histologically examine ontogenetic series of femora, tibiae and metapodia in several extant representatives of the genus *Equus* (*E. hemionus*, *E. quagga* and *E. grevyi*). Our analysis reveals the presence of a non-cyclical growth mark that is deposited around the moment of birth, analogous to the neonatal line described for teeth. We therefore refer to it as neonatal line. The presence of this feature within the bone cross-section agrees with a period of growth arrest in newborn foals regulated by the endocrine system. The neonatal line is accompanied by modifications in bone tissue type and vascularization, and has been identified in all bones studied and at different ontogenetic ages. Our discovery of a non-cyclical BGM related to the moment of birth in mammals is an important step towards the histological reconstruction of life histories in extant and fossil equids.

Keywords

Neonatal line, birth, non-cyclical bone growth marks, skeletochronology, bone histology

Introduction

The study of bone microstructure provides key insights into the life history strategy of extant and extinct vertebrates. Bones present distinctive histological features that allow inference of important life history traits of species, such as growth rate (Padian et al. 2001; de Margerie et al. 2002; Cubo et al. 2012; Lee et al. 2013), longevity (Castanet et al. 2004; Köhler and Moyà-Solà 2009; Woodward et al. 2015; Nacarino-Meneses et al. 2016a) or age at maturity (Chinsamy and Valenzuela 2008; Köhler 2010; Marín-Moratalla et al. 2013; Jordana et al. 2016; Nacarino-Meneses et al. 2016b). The arrangement of collagen fibers within the bone matrix, its vascularization and the density and number of bone cells are directly related to the rate of bone deposition (Amprino 1947; Castanet et al. 2000; de Margerie et al. 2002; Chinsamy-Turan 2005; Huttenlocker et al. 2013; Lee et al. 2013). Analysis of these histological characteristics, hence, allows estimation of growth rate in extant and extinct taxa (Padian et al. 2001; Köhler and Moyà-Solà 2009; Cubo et al. 2012; Marín-Moratalla et al. 2013; Marín-Moratalla et al. 2014; Orlandi-Oliveras et al. 2016). Inferences of longevity and age at maturity, on the other hand, are based on the study of bone growth marks (BGMs) by means of skeletochronology (Köhler and Moyà-Solà 2009; Köhler 2010; Marín-Moratalla et al. 2013; Woodward et al. 2013; Jordana et al. 2016; Moncunill-Solé et al. 2016; Nacarino-Meneses et al. 2016b). This sort of studies relies on the annual periodicity of cyclical growth marks (CGMs), which record hormonal and physiological cycles (Köhler et al. 2012) that are synchronized with seasonal photoperiod and resource availability (Castanet et al. 1993; Chinsamy-Turan 2005).

However, not all BGMs reflect periodical growth (Castanet et al. 1993; Castanet 2006; Woodward et al. 2013). Although the ultimate causes of deposition of non-cyclical BGMs are poorly understood, they are supposed to record stressful biological events that affect the organism (Castanet 2006) and thereby periosteal bone growth (Woodward et al. 2013). During their growth, long bones increase in diameter and change in shape to cope with biomechanical loads (Martin et al. 1998; Currey 2002). Microscopically, these diaphyseal changes involve the simultaneous deposition of bone at the periosteal (external) surface and its resorption at the endosteal (internal) margin of the bone shaft (Martin et al. 1998; Chinsamy-Turan 2005; Woodward et al. 2013). This process, named cortical drift (Martin et al. 1998; Chinsamy-Turan 2005), may leave non-cyclical resorption lines within the bone cross-section (Woodward et al. 2013). These consist of incomplete circles that are limited to the affected bone area (Woodward et al. 2013). Other non-cyclical BGMs have been related to specific biological events that represent moments of physiological stress in the individual (Castanet et al. 1993; Castanet 2006). These BGMs do not result from resorption but they are deposited along the whole growth front of the bone, thus forming complete circles within the bone cross-section at the time of deposition (Castanet et al. 1993). Several authors have described non-cyclical BGMs that record hatching in amphibians and reptiles (Castanet and Baéz 1991; Bruce and Castanet 2006; Chinsamy and Hurum 2006; Hugi and Sánchez-Villagra 2012), metamorphosis in amphibians (Hemelaar 1985; Esteban et al. 1999; Khonsue et al. 2001; Ento and Matsui 2002; Esteban et al. 2002; Jakob et al. 2002; Olgun et al. 2005; Sinsch 2015) and weaning in mammals

(Morris 1970; Castanet et al. 2004; Castanet 2006).

In a previous study of limb bone histology of the Asiatic wild ass (*Equus hemionus*), we identified a non-cyclical BGM in most of the bone cortices analyzed (Nacarino-Meneses et al. 2016b). On that basis, we develop the present research, which primary objective is to thoroughly explore the causes that led to the deposition of this feature in *Equus*, and to increase our understanding of the appearance of non-cyclical BGMs of physiological origin in mammals in general. Thus, we aim to investigate the non-cyclical BGM previously found in *E. hemionus* and to explore its presence in other *Equus* species at different ontogenetic stages from perinates to adults. We will further examine if this non-cyclical BGM appears associated to other histological changes. When deposited as a consequence of a physiologically stressful event, such as hatching, these structures have been described to be associated with changes in bone tissue type and vascularization (Bruce and Castanet 2006; Chinsamy and Hurum 2006; Hugi and Sánchez-Villagra 2012).

Material and methods

Thin sections of femur, tibia, metacarpus and metatarsus were prepared from ontogenetic series (perinates to adults) of *E. hemionus*, *E. quagga* (Plains zebra) and *E. grevyi* (Grevy's zebra) (Table 1). We selected these *Equus* species because they cover almost all habitats and life histories of the genus (Nowak 1999; Ernest 2003; Kaczensky et al. 2015; King and Moehlman 2016; Rubenstein et al. 2016). We studied 9 individuals of *E. hemionus*, 11 of *E. quagga* and 4 of *E. grevyi* (Table 1). The sample comprises 35 thin sections of *E. hemionus*, 14 of *E. quagga* and 10 of *E. grevyi*, totaling 59 the thin sections of the study (Table 1). As shown in Table 1, specimens differ in habitat, age and sex. Most specimens of this study lived captive in the Hagenbeck Zoo (Hamburg, Germany) and are stored at the Zoological Institute of Hamburg University (Germany). Several zebra specimens (Table 1) lived semi-captive in the African Reserve of Sigean (Sigean, France) and belong to the collections of the Catalan Institute of Paleontology (Barcelona, Spain). Finally, adult individuals of Asiatic wild ass lived wild in the Gobi Desert (Table 1). Found killed by poachers, they were collected during the Mongolian-German Biological Expeditions (2001 – 2006) (Schöpke et al. 2012) and are currently housed at the Museum of Domesticated Animals (Halle, Germany). Curators and veterinarians of the different institutions provided information of the sex (R. Schafberg and B. Lamglait, pers. comm.). Additionally, B. Lamglait of the African Reserve of Sigean (France) facilitated the exact age at death of the animals that lived in their institution (B. Lamglait, pers. comm.) and R. Schafberg provided an estimated age for adult kulans (R. Schafberg, pers. comm.). The rest of specimens belonging to museum collections were aged according to the eruption and wear pattern of the species (Silver 1963; Smuts 1974; Penzhorn 1982; Lkhagvasuren et al. 2013; Nacarino-Meneses et al. 2017). In adult individuals, these estimations were validated by the number of annual cementum layers present in the first lower incisor (Lkhagvasuren et al. 2013; Nacarino-Meneses et al. 2017). In several subadult specimens, age calculation was also corroborated by crown formation time inferred from the study of enamel laminations (Nacarino-Meneses et al. 2017). We grouped our specimens into

the classical life stages proposed for equids (Table 1): foals (less than 1 year), yearlings (between 1 and 2 years), juveniles (between 2 and 4 years) and adults (more than 4 years). We further considered an additional age category for the youngest animals of our sample: the perinatal stage. Perinatal specimens were aged by the species-specific tooth eruption sequence, which starts between the first (in *E. quagga*; (Smuts 1974)) and the third week of life (in *E. hemionus*; (Lkhagvasuren et al. 2013)). Tooth eruption in our animals indicates that they were younger than 1 and 3 weeks respectively, but we cannot assess from this methodology whether they died during birth, just after birth or few days before birth. Therefore, we preferred to use the term "perinate" to designate this age group, instead of "newborn", "fetus" or similar.

Species	Code	Collection code	Age	Age group	Sex	Habitat	Bones studied	Collection
E. hemionus	IPS83152	UH 6970	< 3 w.	Perinate	-	HZ	Fe, Ti, Mc, Mt	ZIHU
	IPS83153	UH 7009	5 mo.	Foal	M	HZ	Fe, Ti, Mc, Mt	ZIHU
	IPS83154	UH 7016	5 mo.	Foal	M	HZ	Fe, Ti, Mc	ZIHU
	IPS83151	UH 5929	6 mo.	Foal	-	HZ	Fe, Ti, Mc, Mt	ZIHU
	IPS83150	UH 5547	6 - 12 mo.	Yearling	-	HZ	Fe, Ti, Mc, Mt	ZIHU
	IPS83149	UH 5546	6 - 12 mo.	Yearling	-	HZ	Fe, Ti, Mc, Mt	ZIHU
	IPS83155	UH 7528	1 - 2 y.	Juvenile	F	HZ	Fe, Ti, Mc, Mt	ZIHU
	IPS83876	225	4.5 y.	Adult	F	GD	Fe, Ti, Mc, Mt	MDA
	IPS83877	381	8 y.	Adult	M	GD	Fe, Ti, Mc, Mt	MDA
E. quagga	IPS92343	UH 903	< 1 w.	Perinate	-	HZ	Fe	ZIHU
	IPS92344	UH 6189	< 1 w.	Perinate	-	HZ	Fe	ZIHU
	IPS101798	A15/007	4 mo.	Foal	F	ARS	Fe, Ti	ICP
	IPS92345	UH 7467	4 mo.	Foal	-	HZ	Fe	ZIHU
	IPS92342	UH 7529	5 mo.	Foal	F	HZ	Fe	ZIHU
	IPS104356	A16/085	9 mo.	Foal	F	ARS	Ti, Mc, Mt	ICP
	IPS92341	UH 800	1 y.	Yearling	-	HZ	Fe	ZIHU
	IPS104357	A15/013	1 y.	Yearling	F	ARS	Ti	ICP
	IPS101800	A14/330	1 y. + 2mo.	Yearling	M	ARS	Fe	ICP
	IPS101801	A15/049	1 y. + 2mo.	Yearling	F	ARS	Ti	ICP
	IPS92346	UH 397	5 y.	Adult	-	HZ	Fe	ZIHU
E. grevyi	IPS101802	A15/020	1 mo.	Foal	M	ARS	Fe, Ti	ICP
	IPS84964	UH 8255	4 mo.	Foal	F	HZ	Fe, Ti, Mt	ZIHU
	IPS101804	A15/120	2 y.	Juvenile	M	ARS	Fe, Ti	ICP
	IPS84963	UH 7111	5 y.	Adult	F	HZ	Fe, Ti, Mt	ZIHU

Table 1. Sample studied. w.: weeks; mo.: months; y.: years; M: male; F: female; Fe: femur; Ti: tibia; Mc: metacarpus; Mt: metatarsus; GD: Gobi Desert (Mongolia, Asia); HZ: Hagenbeck Zoo (Hamburg, Germany); ARS: African Reserve of Sigean (Sigean, France); ICP: Catalan Institute of Paleontology (Barcelona, Spain); MDA: Museum of Domesticated Animals (Halle, Germany); ZIHU: Zoological Institute of Hamburg University (Hamburg, Germany).

Histological slices were prepared following standard methods in our laboratory (Nacarino-Meneses et al. 2016a; Nacarino-Meneses et al. 2016b). From the mid-shaft of

each bone, we extracted a block of 3 cm that was then embedded in epoxy resin (Araldite 2020). This block was later cut into two halves using a low speed diamond saw (IsoMet, Buehler). The cut surfaces were then polished with carborundum powder or with a MetaServ 250 (Buehler) and fixed to a frosted glass with Loctite 358, an ultraviolet-curing adhesive. Samples were then cut and grounded with a diamond saw (PetroThin, Buehler) and polished again either with carborundum powder or with a grinder-polisher (MetaServ 250, Buehler) to obtain a final thickness of approximately 100 – 120 μm. Finally, thin sections were covered with a mix of oils (Lamm 2013) to improve the visualization of the histological features under the microscope. All thin sections obtained in the present research belong to the collections of the Catalan Institute of Paleontology (ICP, Barcelona, Spain) and are available to researchers. Histological thin sections were observed using polarized light under a Leica DM 2500P microscope and under a Zeiss Scope.A1 microscope. Micrographs were taken with the incorporated cameras (Leica DFC490 and AxioCam ICc5). Several samples were also analyzed under polarized light with a ¼ λ filter to facilitate the identification of the bone tissue types and the visualization of the BGMs (Turner-Walker and Mays 2008).

We recorded the presence or absence of non-cyclical BGMs in all species, bones and ontogenetic stages under study. The classification of BGMs as cyclical or non-cyclical was made considering the position of the BGM within the bone cross-section in relation to the age of the individual. For instance, a BGM identified in the mid-cortex of a kulan foal aged 5 months (e.g. IPS83153, Table 1) was considered as non-cyclical (Nacarino-Meneses et al. 2016b). As *E. hemionus* tends to give birth in summer (Zuckerman 1952; Nowak 1999), the CGM that records the growth arrest during the unfavorable season (i.e. winter for this species) (Köhler et al. 2012) is expected to be found in its outermost cortex. Accordingly, any BGM deposited in the internal part of the cross-section at this ontogenetic stage should be considered as non-cyclical. In yearlings, the identification of non-cyclical BGMs and its differentiation from cyclical ones was made following a similar procedure as in foals, that is, considering the age of the individual and the location of the BGM within the bone cortex. In yearlings, we identified an additional BGM to that expected from age (2 BGMs in total) (Nacarino-Meneses et al. 2016b). Because CGMs are known to be deposited annually (Köhler et al. 2012) and these specimens are aged around one year (Table 1), we considered the most external BGM as a CGM and the most internal BGM as a non-cyclical one (Nacarino-Meneses et al. 2016b). In juveniles and adults, we did not always find an extra BGM in relation to their age, but non-cyclical features were recognized by performing superimposition of individuals (Woodward et al. 2013). In these age categories, those BGMs were considered as non-cyclical whether they were deposited earlier than the CGM found in yearlings (Nacarino-Meneses et al. 2016b). Superimposition (Woodward et al. 2013) was also applied to identify non-cyclical BGMs that have been erased by resorption of the medullary cavity. Likewise, this technique was employed to evaluate the correspondence between the perimeter of the non-cyclical BGM identified in different ontogenetic stages and the perimeter of the perinatal individual, with the objective to find a correlation between this non-cyclical feature and a specific key life history event such as the moment of birth. In our sample, we have a complete set of

all limb bones (femur, tibia, metacarpus and metatarsus) of the perinatal stage only from *E. hemionus* (IPS83152, Table 1). Therefore, we used superimposition in this equid to establish the relationship between the non-cyclical BGM and birth. Since this non-cyclical feature shares several characteristics between species (position, associated histological changes), we considered this structure analogous in all equids analyzed. This allowed us to extrapolate this life history trait to the other species under study.

We further analyzed bone tissue types and vascularization in the proximity of the non-cyclical BGM to identify any histological changes related to the deposition of this line. Bone tissue types were classified following Francillon-Vieillot et al. (1990) and de Margerie et al. (2002), while the description of the different components of the fibrolamellar complex (FLC) follows Prondvai et al. (2014). These authors indicate that the FLC is composed of a mix of "fibrous" or woven bone (WB) and "lamellar" or parallel-fibered bone (PFB) (Prondvai et al. 2014). The pattern of vascularization was also classified following classical bibliography (Francillon-Vieillot et al. 1990; de Margerie et al. 2002). In all limb bones studied, we quantitatively analyzed the area of the longitudinal vascular canals (VCs) before and after the presence of the non-cyclical BGM. We restricted the measurements to longitudinal VCs and we did not consider other VC orientations because we have previously noted a difference in size of VCs with this specific arrangement regarding its location in the inner or in the outer cortex of *E. hemionus*' foals (Nacarino-Meneses et al. 2016b). VCs with blurred contours were not drawn or measured (S1 Fig) to reduce error. Secondary osteons (Haversian canals) were also excluded from the analysis (S1 Fig), as the present research is only focused on primary bone. Measurements were taken with Image J software on areas of 2.6 x 2.2 mm (5.7 mm^2) in the antero-medial region of each bone, at both sides of the non-cyclical BGM (S1 Fig). For each longitudinal VC, we used the circle tool provided by this computer program to manually adjust an ellipse to the edges of this biological structure (S1 Fig). Afterwards, the area of such ellipse was calculated with the "Measure" action integrated in the "Analyze" panel of Image J. Statistical analyses were carried out with Java Gui for R version 1.7-16 (Fellows 2012). For each bone and *Equus* species, we first calculated the main descriptive statistics (*n*, mean, standard deviation) for the variable "area of the longitudinal VCs" regarding the position of the VC before or after deposition of the non-cyclical BGM (Table 2). Afterwards, we tested the variable for normality within each group (before the non-cyclical BGM and after the non-cyclical BGM) on the different bones (femur, tibia, metacarpus and metatarsus) and species studied (*E. hemionus*, *E. quagga* and *E. grevyi*) using Shapiro-Wilk normality test (Dytham 2011). Because several data did not follow a normal distribution (p-value<0.05), we performed a non-parametric test (Dytham 2011) to statistically evaluate the differences in area of the longitudinal VCs at both sides of the non-cyclical BGM within each bone and species under study. Specifically, Mann-Whitney *U* test (also named Mann-Whitney-Wilcoxon, Wilcoxon rank-sum test or Wilcoxon-Mann-Whitney test) was applied (Dytham 2011) and a p-value of $p<0.05$ was considered to be statistically significant.

Results

Non-cyclical BGMs are recognized in the bone cortices of all equid species under study, although the identification of these features varies between bones and ontogenetic stages (Fig 1). Only one non-cyclical BGM, which always appears as the first BGM

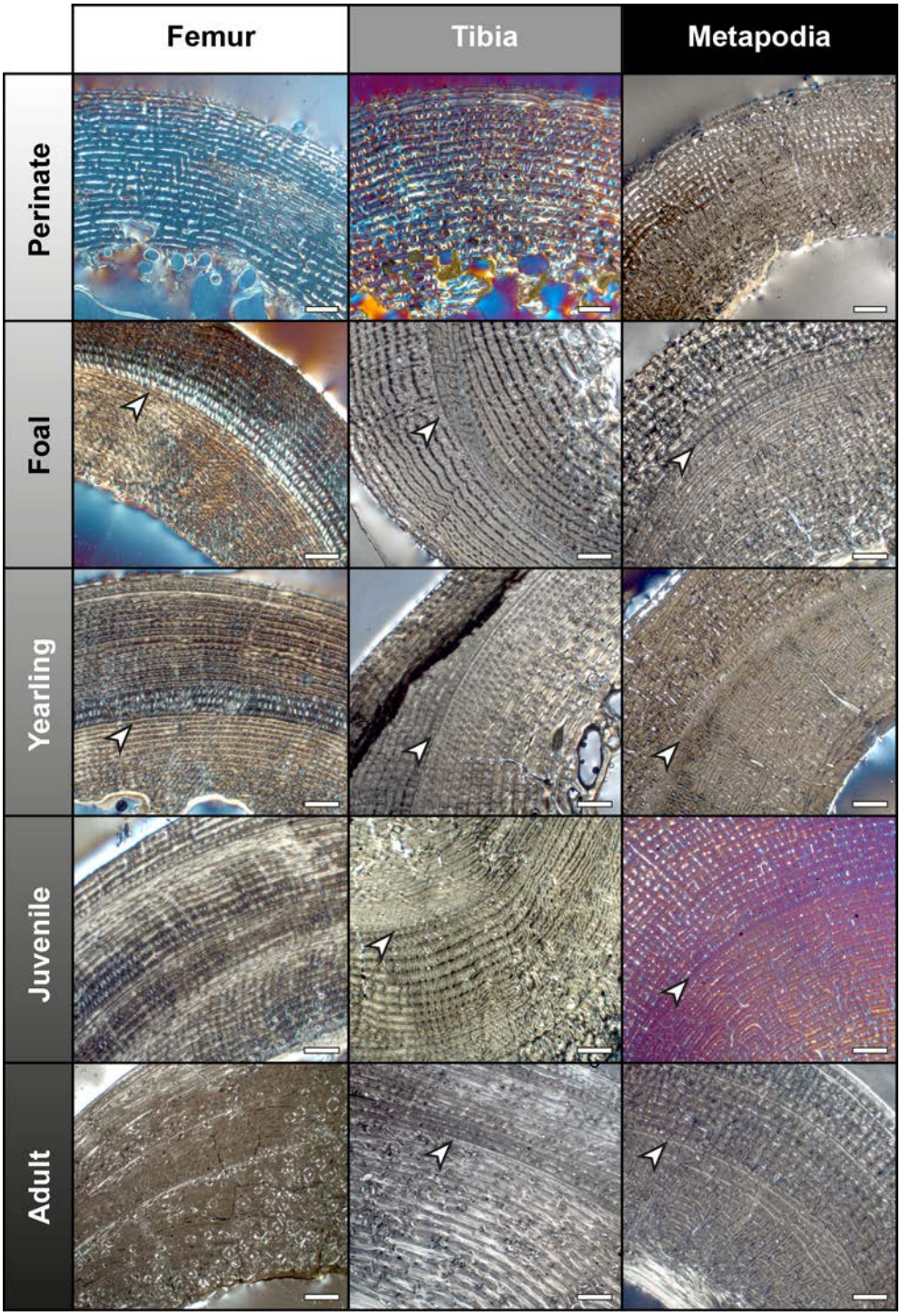

Figure 1. Presence and absence of the neonatal line (NL) in the limb bones of extant *Equus*. From up to down: Femur – IPS92343 (*E. quagga*), IPS101798 (*E. quagga*), IPS101800 (*E. quagga*), IPS101804 (*E. grevyi*), IPS83876 (*E. hemionus*); Tibia – IPS83152 (*E. hemionus*), IPS101798 (*E. quagga*), IPS101801 (*E. quagga*), IPS101804 (*E. grevyi*), IPS84963 (*E. grevyi*); Metapodials – IPS83152 (Mc, *E. hemionus*), IPS84964 (Mt, *E. grevyi*), IPS83150 (Mt, *E. hemionus*), IPS83155 (Mc, *E. hemionus*), IPS83876 (Mt, *E. grevyi*). Mc = metacarpus; Mt = metatarsus. White arrows indicate the NL. Scale bars = 1 mm.

deposited (i.e. the most internal BGM), is found in bone cross-sections (Fig 1). Changes in vascularity and bone matrix typology are also identified associated to the presence of this non-cyclical feature in the different limb bones analyzed.

Femur

In all species analyzed, we identify a non-cyclical BGM in the femoral cortex of foals (IPS83153, IPS83154, IPS83151, IPS101798, IPS92345, IPS92342, IPS101802, IPS84964) and yearlings (IPS83149, IPS83150, IPS92341, IPS101800) (Fig 1). In the youngest animal of our sample, a 1-month-old Grevy's zebra (IPS101802, Table 1), this feature is situated in the outermost cortex (Fig 2A and 2B). We do not find any non-cyclical BGM, however, in

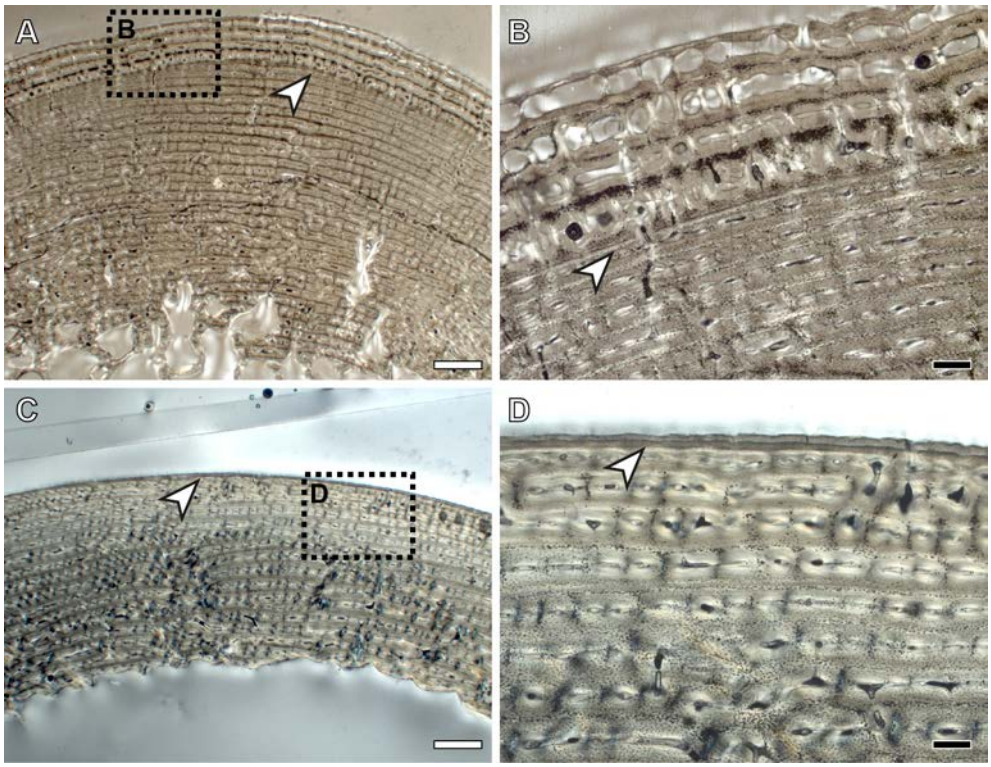

Figure 2. Neonatal line (NL) identified in the femoral and tibial external cortex of a 1-month-old Grevy's zebra. (A) Femoral cortex of IPS101802. **(B)** Detail of the NL identified in the femur of IPS101802. **(C)** Tibial cortex of IPS101802. **(D)** Detail of the NL identified in the tibia of IPS101802. White arrows indicate NL. White dashed rectangles indicate areas of image magnification. White scale bars = 1mm; black scale bars = 200 µm.

the femur of perinates (IPS83152, IPS92343, IPS92344), juveniles (IPS83155, IPS101804) or adults (IPS83876, IPS83877, IPS92346, IPS84963) (Fig 1). Superimposition performed in this bone shows that the bone tissue formed during the earliest ontogenetic stages (perinatal, foal) is lost in juvenile individuals through resorption of the medullary cavity (Fig 3), which erased any early non-cyclical BGM in the femora of juvenile and/or adult specimens. Interestingly, superimposition performed in the Asiatic wild ass reveals that the cortical perimeter of the perinatal individual almost matches the non-cyclical BGM found in the femora of foals and yearlings (Table 2 and Fig 4A). As shown in Table 2, the perimeter of the perinatal femur is 75.08 mm while the perimeter of the non-cyclical BGM varies between 76.89 mm and 85.93 mm in this bone. For this reason, we consider

this BGM as a stress line related to the birth event of the animal and, henceforward, we will refer to it as neonatal line (NL).

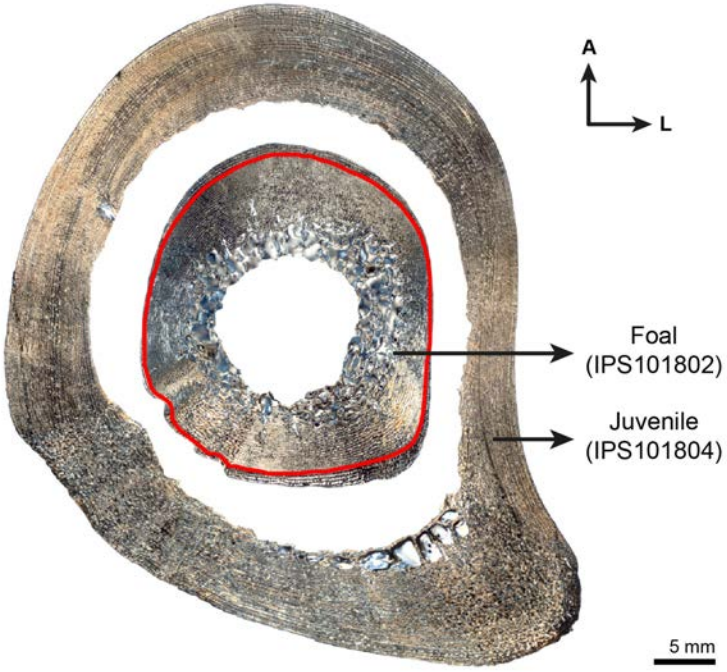

Figure 3. Superimposition of foal's (IPS101802) and juvenile's (IPS101804) femur of *E. grevyi*. Figure shows a high resorption of the medullary cavity in the juvenile femur that has erased the neonatal line (NL) identified in the foal (red line). A = anterior, L = lateral.

We recognize several histological changes related to bone tissue type and to the arrangement of the VCs in the surroundings of the NL (Fig 5A – C). In femora of *E. hemionus*, the NL divides the bone cortex in two areas: an internal one composed of FLC with longitudinal VCs and an external ring of laminar bone (Fig 5A). In *E. quagga* and *E. grevyi*, however, the NL is associated with a change in the components of the FLC, as femora of both zebras shows a higher proportion of PFB before the deposition of this non-cyclical BGM (Fig 5B and 5C). In all species studied, we observe significant differences in the area of the longitudinal VCs before and after the NL (*E. hemionus*, W=14004.5 and $p<0.001$; *E. quagga*, W=9408.5 and $p<0.001$; *E. grevyi*, W=3208 and $p<0.001$). VCs identified before this mark are smaller than those found after this feature in equid femoral cortices (Fig 6A and 7A, E). Specifically, longitudinal VCs formed before deposition of the NL present a mean area of ≈250 μm², ≈350 μm² and ≈170 μm² in the Asiatic wild ass, the Plains zebra and the Grevy's zebra respectively (Table 3 and Fig 6A). On the contrary, the mean area of the VCs found after the NL is ≈370 μm² in *E. hemionus*, ≈500 μm² in *E. quagga* and ≈290 μm² in *E. grevyi* (Table 3 and Fig 6A).

Tibia

From foals to adults, we find a non-cyclical BGM in the tibiae of all species under study (IPS83153, IPS83154, IPS83151, IPS83150, IPS83149, IPS83155, IPS83876, IPS83877, IPS101798, IPS104356, IPS104357, IPS101801, IPS101802, IPS84964, IPS101804, IPS84963) (Fig 1). The same as in the femur, this mark is identified in the tibial cortex of IPS101802 (Fig 2C and 2D), the youngest specimen of *E. grevyi* aged one month old (Table 1). Only the perinatal tibia of *E. hemionus* (IPS93152) does not show a non-cyclical BGM in its cortex (Fig 1). Superimposition of individuals performed with the tibiae of *E.*

hemionus indicates a correspondence between the perimeter of the non-cyclical BGM and that of the perinatal individual (Fig 4B), as the perimeter of the NL measures between ≈66 mm and ≈74 mm and the perimeter of IPS83152 measures 65.4 mm (Table 2). This also indicates that the non-cyclical feature is recording the moment of birth in this bone.

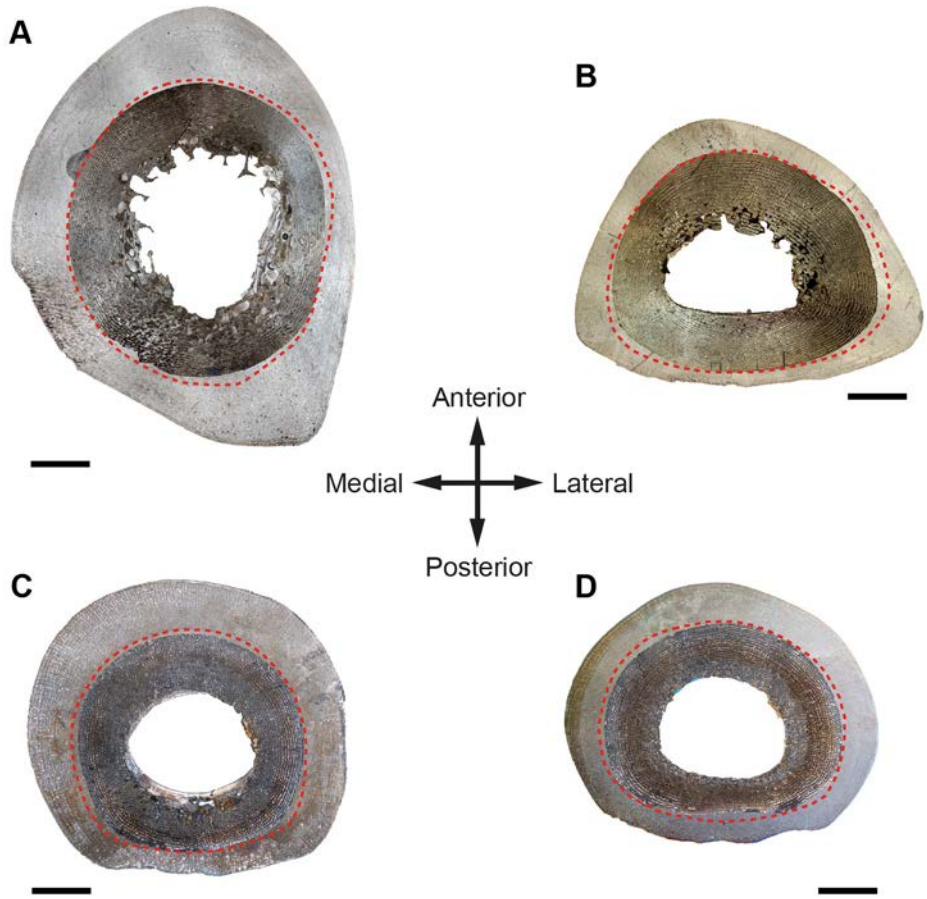

Figure 4. Correspondence between the perimeter of the perinatal Asiatic wild ass (dark images, IPS83152) and the neonatal line (NL) (red dashed line) identified in different limb bones and ontogenetic stages of *E. hemionus* (light images). (A) Superimposition of newborn's and yearling's (IPS83149) femora. **(B)** Superimposition of newborn's and foal's (IPS83154) tibiae. **(C)** Superimposition of newborn's and juvenile's (IPS83155) metatarsi. **(D)** Superimposition of newborn's and adult's (IPS83876) metacarpi. Scale bars = 5 mm.

Code	Age	Age group	Femur	Tibia	Metacarpus	Metatarsus
IPS83152	< 3 w.	Perinate	75.08	65.4	60.15	61
IPS83153	5 mo.	Foal	79.21	72.31	60.40	61.65
IPS83154	5 mo.	Foal	82.21	71.47	63.53	-
IPS83151	6 mo.	Foal	85.93	66.64	61.29	60.34
IPS83150	6 - 12 mo.	Yearling	85.53	68.75	59.05	64.72
IPS83149	6 - 12 mo.	Yearling	76.89	59.38	57.13	56.04
IPS83155	1 - 2 y.	Juvenile	-	74.04	-	63.81
IPS83876	4.5 y.	Adult	-	-	60.77	60.04
IPS83877	8 y.	Adult	-	-	56.29	53.09

Table 2. Perimeter of *E. hemionus*' perinatal bones and perimeter of the neonatal line (NL) identified in other ontogenetic stages of the same species. w.: weeks; mo.: months; y.: years. All measurements are expressed in mm.

Regarding bone tissue, tibial cortices of *E. hemionus*, *E. quagga* and *E. grevyi* show a change in the proportions of the FLC components associated to the deposition of the neonatal line (Fig 5D – F). In all samples, we notice that the FLC formed before the deposition of the NL presents a higher proportion of PFB than the FLC deposited after the presence of the NL (Fig 5D – F). The area of the longitudinal VCs also varies significantly at both sides of the NL in all species under study (*E. hemionus*, W=21609.5 and $p<0.001$; *E. quagga*, W=19060 and $p<0.001$; *E. grevyi*, W=7903.5 and $p<0.001$). The VCs identified before this feature are smaller than those deposited after the NL (Fig 6B and 7B, F). The mean area of the longitudinal VCs found earlier than the presence of the NL is ≈240 μm² in *E. hemionus*, ≈350 μm² in *E. quagga* and ≈170 μm² in *E. grevyi* (Table 3 and Fig 6B). After this feature, longitudinal VCs present a mean area of ≈440 μm², ≈820 μm² and ≈460 μm² respectively (Table 3 and Fig 6B).

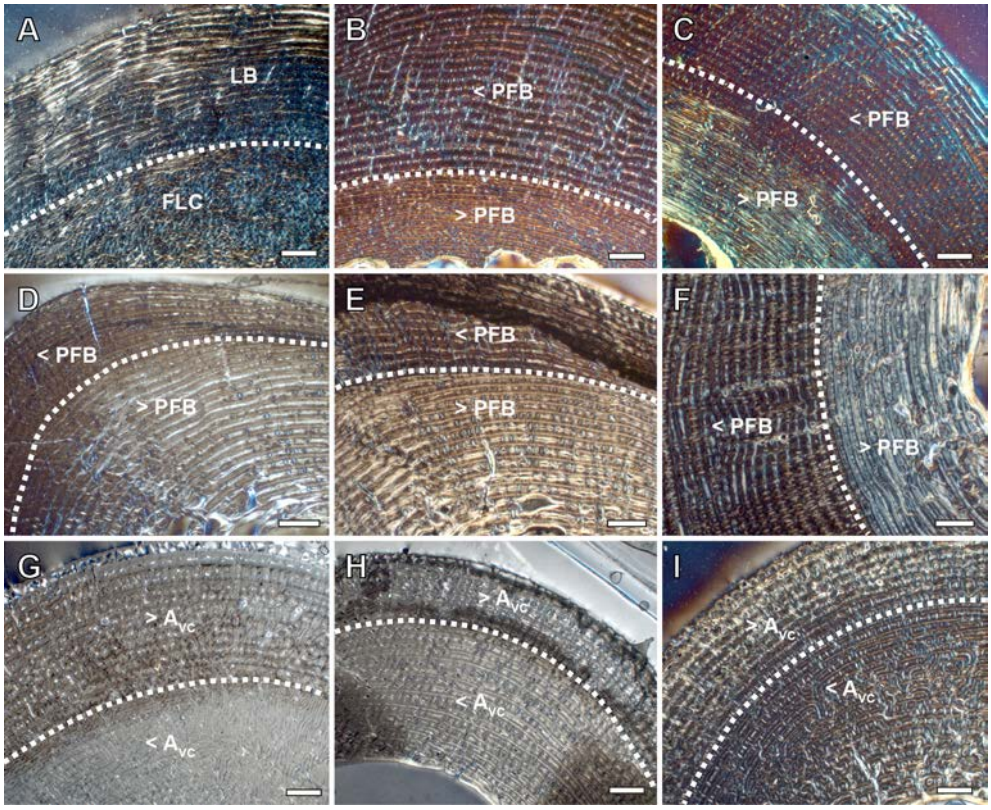

Figure 5. Histological changes associated to the presence of the neonatal line in extant *Equus*. (A) Femoral cortex of *E. hemionus* IPS83153. **(B)** Femoral cortex of *E. quagga* IPS92345. **(C)** Femoral cortex of *E. grevyi* IPS84964. **(D)** Tibial cortex of *E. hemionus* IPS83154. **(E)** Tibial cortex of *E. quagga* IPS101801. **(F)** Tibial cortex of *E. grevyi* IPS101804. **(G)** Metacarpal cortex of *E. hemionus* IPS83150. **(H)** Metatarsal cortex of *E. quagga* IPS104356. **(I)** Metatarsal cortex of *E. grevyi* IPS84964. White dotted line indicates the neonatal line. AVC = area of the longitudinal VCs; FLC = fibrolamellar complex; LB = laminar bone; PFB = parallel-fibered bone. Scale bars = 1 mm.

Metapodial bones

We recognize a non-cyclical BGM in metacarpus and metatarsus of foals (IPS83153, IPS83154, IPS83151, IPS104356, IPS84964), yearlings (IPS83150, IPS83149), juvenile (IPS83155) and adults (IPS83876, IPS83877, IPS84963) of all *Equus* species examined (Fig 1). Thus, the only ontogenetic stage that does not record this mark is the perinatal period

(IPS83152) (Fig 1). The youngest individual of our sample that presents this non-cyclical BGM is a 4-month-old Grevyi's zebra (IPS84964, Table 1). In this specimen, this mark is identified in the middle cortex of the metatarsus (Fig 1). Superimposition of individuals in the Asiatic wild ass shows that the perimeter of the non-cyclical BGM identified in both metapodials is almost the same as the perimeter of the perinatal kulan (Fig 4C and 4D), which supports the hypothesis that this mark is deposited around birth. The perimeter of *E. hemionus*' perinatal metapodia measures ≈60 mm, while the perimeter of the non-cyclical BGM identified in older ontogenetic stages is ≈53 – 64 mm in these bones (Table 2).

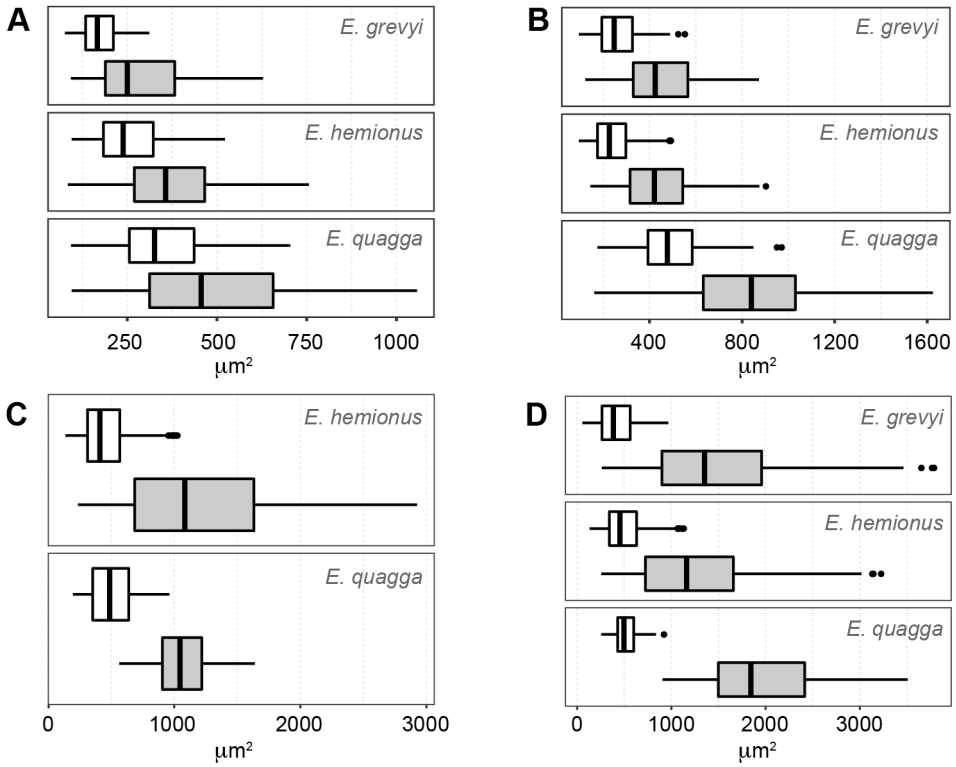

Figure 6. Boxplot of the area of the vascular canals (VCs) at both sides of the neonatal line (NL) in the limb bones of *Equus*. (A) Femora. **(B)** Tibiae. **(C)** Metacarpi. **(D)** Metatarsi. White boxplot = Area of the VCs located before the deposition of the NL; grey boxplot = Area of the VCs located after the deposition of the NL.

We do not find differences in bone tissue type or in the arrangement of VCs associated to the presence of the NL, although we also observe a variation in the size of the longitudinal VCs at both sides of this feature in metacarpi and metatarsi of the different *Equus* species studied (Fig 5G – I). In our equid metapodial sample, VCs found earlier than the deposition of the NL are significantly smaller than those identified after the mark (Metacarpi: *E. hemionus*, W=181501 and $p<0.001$; *E. quagga*, W=2017 and $p<0.001$; Metatarsi: *E. hemionus*, W=196227 and $p<0.001$; *E. quagga*, W=1767 and $p<0.001$; *E. grevyi*, W=6677 and $p<0.001$) (Table 3 and Fig 6C – D and 7C, D, G, H). The mean area of the inner VCs is 400 – 500 µm² (Table 3 and Fig 6C – D), while it is 1000 – 2000 µm² (Table 3 and Fig 6C – D) for the VCs found in the outer cortex of both metapodial bones.

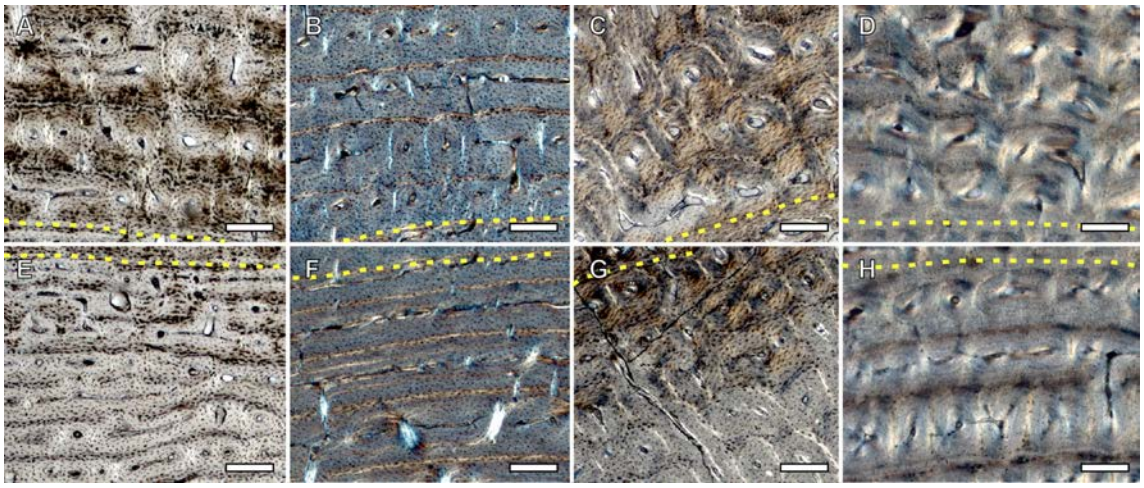

Figure 7. Longitudinal vascular canals (VCs) formed after (A – D) and before (E – F) the presence of the neonatal line (NL) (yellow dotted line) in the different limb bones of *Equus*. **(A)** VCs formed after deposition of the NL in the femur of *E. quagga* IPS92345. **(B)** VCs formed after deposition of the NL in the tibia of *E. hemionus* IPS83153. **(C)** VCs formed after deposition of the NL in the metacarpus of *E. hemionus* IPS83150. **(D)** VCs formed after deposition of the NL in the metatarsus of *E. grevyi* IPS84964. **(E)** VCs formed before deposition of the NL in the femur of *E. quagga* IPS92345. **(F)** VCs formed before deposition of the NL in the tibia of *E. hemionus* IPS83153. **(G)** VCs formed before deposition of the NL in the metacarpus of *E. hemionus* IPS83150. **(H)** VCs formed before deposition of the NL in the metatarsus of *E. grevyi* IPS84964. Scale bars = 200 µm.

	FEMORA				TIBIAE			
	Before the NL		After the NL		Before the NL		After the NL	
	n	Mean ± SD	n	Mean ± SD	n	Mean ± SD	n	Mean ± SD
E. hemionus	137	254.8±95.2	135	372.4±137.6	150	243.5±91.6	169	446.8±177
E. quagga	123	356.6±142.4	114	501.3±246.1	156	497.6±146.4	147	823.3±301.3
E. grevyi	59	177±57.7	70	292.5±137.3	74	270.7±100.6	128	458±170
	METACARPI				**METATARSI**			
	Before the NL		After the NL		Before the NL		After the NL	
	n	Mean ± SD	n	Mean ± SD	n	Mean ± SD	n	Mean ± SD
E. hemionus	449	455.4±191	454	1213.7±660.6	514	499.1±209.2	427	1284.4±655.7
E. quagga	72	508.8±184.5	29	1080.3±276.1	52	525.4±155.9	34	1962.9±656.1
E. grevyi	-	-	-	-	100	426.1±202.4	72	1502.6±873

Table 3. Area of the longitudinal vascular canals (VCs) at both sides of the neonatal line in the limb bones of *Equus*. n = number of observations; SD = standard deviation.

Discussion

Most of the skeletochronological research developed so far focuses on the study of cyclical bone growth marks present in the limb bones of vertebrates (Castanet 2006; Köhler et al. 2012; Woodward et al. 2013). Hitherto, however, little is known about the causes leading to the deposition of non-cyclical features. Non-cyclical BGMs identified in bone cortex are usually classified as cortical drift lines (Woodward et al. 2013), while non-cyclical lines that record periods of physiological stress are less studied (Castanet et al. 1993). The non-cyclical BGM identified in our equid sample is not restricted to a

specific location within the cross-section of the bone, but it can be followed around the whole cortex (Fig 3). Thus, it cannot be considered a resorption line caused by cortical drift (Woodward et al. 2013). Rather, it appears to record a specific biological event: the moment of birth. The NL is well described in dental histology and can be easily found in the enamel and dentine of different mammalian species (Schour 1936; Weber and Eisenmann 1971; Carlson 1990; Smith et al. 2006; Tafforeau et al. 2007). To our knowledge, however, there is no previous reference to the NL in histological studies of any mammalian taxon. With the present study, hence, we provide the first description of a non-cyclical BGM related to the moment of birth in the limb bones of mammals. From foals to adults, we recognized a NL in all species and bones studied, except for the femora of juvenile and adult specimens (Fig 1), where it has been removed during resorption of the medullary cavity (Fig 3). Also, we did not identify a NL in any of the perinatal bones analyzed (Fig 1), probably indicating that the youngest animals of our sample died before or at birth (stillborn). The identification of the NL is essential for histological research performed in the appendicular bones of mammals, and especially in Equidae. For instance, in a previous study on the limb bone histology of *Hipparion concudense*, Martínez-Maza et al. (2014) reported the presence of a non-cyclical BGM that these authors interpreted as a drift line. Based on their descriptions and the images provided by the authors (Martínez-Maza et al. 2014), however, we consider this non-cyclical feature as a NL. Though the identification of the NL does not affect the conclusions of their study, it provides a time anchorage (the moment of birth) for skeletochronological studies. It further facilitates the estimation of the size at birth in extinct species, an important life history trait in mammals (Stearns 1992). Considering that the NL represents the bone circumference at the moment of birth, its dimension can be used to estimate the weight (Anderson et al. 1985) of the newborn foal, a proxy of its body size (Damuth and MacFadden 1990).

Despite the huge amount of studies that describe hatching lines and metamorphosis lines in reptiles and amphibians (Hemelaar 1985; Castanet and Baéz 1991; Esteban et al. 1999; Khonsue et al. 2001; Ento and Matsui 2002; Esteban et al. 2002; Jakob et al. 2002; Olgun et al. 2005; Bruce and Castanet 2006; Chinsamy and Hurum 2006; Hugi and Sánchez-Villagra 2012; Sinsch 2015), only few studies report the presence of non-cyclical BGMs related to life history events in mammalian bones (Morris 1970; Castanet et al. 2004). In their study of *Microcebus murinus*, Castanet et al. (2004) described a weak mark in several long bones of this species that they suggest might be recording the weaning event. Likewise, Morris (1970) identified a line of weaning in the jaws of the hedgehog. In the equid species analyzed here, weaning occurs at 1 – 1.5 years (Asiatic wild ass), around the first year (Plains zebra) and at the eighth month of life (Grevy's zebra) (Churcher 1993; Nowak 1999; Ernest 2003; Tacutu et al. 2013). However, we found the non-cyclical BGM in our specimens at an earlier age (Fig 1), already present only one month after birth in the youngest foal of *E. grevyi* (Fig 2). Thus, our results do not match the weaning event previously described for the prosimian *Microcebus* or the hedgehog (Morris 1970; Castanet et al. 2004). The coincidence between the perimeter of the perinatal individual and that of the non-cyclical BGM identified in other age groups of *E. hemionus* (Table 2 and Fig 4) supports however the idea that this feature is related to the birth of the animal.

In equids, as well as in other groups of mammals, birth is a moment of physiological stress where many organic systems of the foal (respiratory, circulatory, etc.) undergo important changes that adapt them to a life *ex utero* (Fowden et al. 2012). This transition also implies a variation in the concentration values of the most important hormones (Stewart et al. 1993; Messer et al. 1998; Fowden et al. 2012) that regulate bone growth (Buchanan and Preece 1992). At the moment of birth, equid foals present low concentration values of growth and thyroid hormones (Stewart et al. 1993; Messer et al. 1998), endocrine regulators that control several key growth factor signaling pathways to tune and stimulate skeletal growth (Buchanan and Preece 1992; Kim and Mohan 2013). At this moment, neonatal foals also show high levels of cortisol (Fowden et al. 2012), a glucocorticoid that constrains bone growth in stressful conditions (Buchanan and Preece 1992). This hormonal scenario, hence, suggests an arrest of bone growth at the moment of birth, which, in turn, agrees with the presence of a rest line (Francillon-Vieillot et al. 1990; Castanet et al. 1993) such as the NL found in our sample (Fig 1).

We have also identified changes in bone tissue type and in vascularization in the surroundings of the NL (Fig 5). Regarding bone matrix, our study reveals a notable change in the proportion of PFB within the FLC shortly before deposition of the NL in the femora of both zebras and in the tibiae of all *Equus* species analyzed (Fig 5B – F). Previous studies have also reported a change in bone tissue type associated to a non-cyclical BGM that reflect a biological event, such as the hatching line (Chinsamy and Hurum 2006; Hugi and Sánchez-Villagra 2012; Curry Rogers et al. 2016). Contrary to our observations in equids, however, dinosaurs and reptiles show a change from a disorganized bone matrix (woven-fibered bone) before the hatching line to a more organized one (parallel-fibered bone) after this line (Chinsamy and Hurum 2006; Hugi and Sánchez-Villagra 2012; Curry Rogers et al. 2016). The differences between these findings and our results from *Equus* might be related to the higher postnatal growth rates of mammals in comparison with that of reptiles (Case 1978; Peters 1983; Calder 1984). In fact, histological studies on Elephantidae (Curtin et al. 2012) and thoroughbred horses (Stover et al. 1992) agree with our results, as the postnatally deposited FLC in these animals also presents a lower proportion of PFB than the prenatally formed bone tissue (Stover et al. 1992; Curtin et al. 2012). In agreement with these investigations (Stover et al. 1992; Curtin et al. 2012), the reduction in PFB observed in the present study (Fig 5B – F) suggests a higher rate of bone deposition in *Equus* after birth. Nonetheless, the qualitative variation in PFB observed in equids (Fig 5B – F) can also been interpreted as an adaptation to the change in biomechanical loads (Martin et al. 1998; Currey 2002) that these animals experience after birth. In this sense, it has been suggested that the disposition of VCs within the bone tissue might be related to biomechanics (de Margerie 2002; de Margerie et al. 2004). The change in the orientation of the VCs observed in *E. hemionus* just after deposition of the NL (Fig 5A), thus, seems to be associated with the onset of weight-bearing and locomotion just after birth (Nacarino-Meneses et al. 2016a). In our equid sample, we also observe a change in diameter of the longitudinal VCs associated to the deposition of the NL (Fig 5G – I – 7). In all limb bones and species examined, longitudinal VCs identified before this feature are significantly smaller than those found after the mark (Table 3 and Fig 6

and 7). In metapodia, the mean area of the VCs formed after deposition of the NL even doubles the mean area of those VCs formed before the formation of the NL (Table 3 and Fig 6). These results agree with the findings of Stover et al. (1992) of perinatal histological modifications in thoroughbred horses. Although these authors analyzed primary osteons of the third metacarpus instead of VCs, they described that postnatally formed primary osteons are larger than those formed prenatally (Stover et al. 1992). Larger VCs have also been related to higher rates of bone deposition (de Margerie et al. 2002). Thus, the higher area of the VCs identified after deposition of the NL in *Equus* limb bones (Table 3 and Fig 6) also suggests higher rates of postnatal bone formation in equids.

Conclusions

In the present research, we describe for the first time a non-cyclical BGM in the limb bones of mammals that records the moment of birth. During this life history event, physiological levels of cortisol, thyroid hormones, and growth hormones agree with a period of growth arrest in the newborn foal that leads to the deposition of the NL. We identified this NL in femora, tibiae and metapodia of *E. hemionus*, *E. quagga* and *E. grevyi*. While the NL is observable in tibia, metacarpus and metatarsus of foals, yearlings, juveniles and adults, it disappears in juvenile and adult femora due to early resorption of the medullary cavity in this bone. We have also identified several histological changes associated to the presence of the NL. On the one hand, the proportion of PFB within the FLC is reduced after deposition of the NL in the femora of plains and Grevyi's zebra and in the tibiae of all *Equus* species studied. This suggests a higher rate of bone deposition in these bones after birth. In the femora of the Asiatic wild ass, however, we observed a change in orientation of the VCs from a preferentially longitudinal to a circular organization, which is likely related to biomechanical loads. Finally, a difference in size of the longitudinal VCs has been identified in all limb bones and species studied, showing larger VCs after deposition of the NL. Our findings about perinatal bone histology, both the presence of the NL and the histological changes (bone tissue and vascularization) associated to it, are essential for future skeletochronological studies in equids and related mammals.

Acknowledgments

We thank B. Lamglait (currently at Université de Montréal, Canada) and the Réserve Africaine de Sigean (Sigean, France) for donation of aged equid specimens. T. Kaiser and R. Schafberg are acknowledged for loans and permission to cut bones from the collections of the Zoological Institute of Hamburg University (Hamburg, Germany) and the Museum of Domesticated Animals of the Martin-Luther-University Halle-Wittenberg (Halle, Saale, Germany) respectively. We are grateful to M. Fernández, G. Prats-Muñoz and L. Gordon for the preparation of the histological slices for this study. Two anonymous reviewers

are acknowledged for comments and suggestions that improved an earlier version of the manuscript.

References

Amprino R. 1947. La structure du tissu osseux envisagée comme expression de différences dans la vitesse de l'accroissement. Arch. Biol. 58:315–330.

Anderson JF, Hall-Martin A, Russell DA. 1985. Long-bone circumference and weight in mammals, birds and dinosaurs. J. Zool. 207:53–61.

Bruce RC, Castanet J. 2006. Application of skeletochronology in aging larvae of the salamanders *Gyrinophilus porphyriticus* and *Pseudotriton ruber*. J. Herpetol. 40:85–90.

Buchanan CR, Preece MA. 1992. Hormonal control of bone growth. In: Hall BK, editor. Bone, Vol. 6. Boca Raton: CRC Press. p. 53–89.

Calder WAI. 1984. Size, Function and Life History. New York: Dover Publications.

Carlson SJ. 1990. Vertebrate dental structures. In: Carter J, editor. Skeletal Biomineralization: Patterns, Processes and Evolutionary Trends. Vol. 5. New York: Van Nostrand Reinhold. p. 235–260.

Case TJ. 1978. On the evolution and adaptive significance of postnatal growth rates in the terrestrial vertebrates. Quaterly Rev. Biol. 53:243–282.

Castanet J. 2006. Time recording in bone microstructures of endothermic animals; functional relationships. Comptes Rendus - Palevol 5:629–636.

Castanet J, Baéz M. 1991. Adaptation and evolution in *Gallotia* lizards from the Canary Islands: age, growth, maturity and longevity. Amphibia-Reptilia 12:81–102.

Castanet J, Croci S, Aujard F, Perret M, Cubo J, de Margerie E. 2004. Lines of arrested growth in bone and age estimation in a small primate: *Microcebus murinus*. J. Zool. 263:31–39.

Castanet J, Curry Rogers K, Cubo J, Boisard J-J. 2000. Periosteal bone growth rates in extant ratites (ostriche and emu). Implications for assessing growth in dinosaurs. C. R. Acad. Sci. III. 323:543–550.

Castanet J, Francillon-Vieillot H, Meunier F, Ricqlès A. 1993. Bone and individual aging. In: Hall BK, editor. Bone: A Treatise, Vol. 7. Boca Raton: CRC Press. p. 245–283.

Chinsamy-Turan A. 2005. The microstructure of dinosaur bone. Deciphering biology with fine-scale techniques. Baltimore and London: The Johns Hopkins University Press.

Chinsamy A, Hurum JH. 2006. Bone microstructure and growth patterns of early mammals. Acta Palaeontol. Pol. 51:325–338.

Chinsamy A, Valenzuela N. 2008. Skeletochronology of the endangered side-neck turtles *Podocnemis expansa*. S. Afr. J. Sci. 104:311–314.

Churcher C. 1993. *Equus grevyi*. Mamm. Species 453:1–9.

Cubo J, le Roy N, Martinez-Maza C, Montes L. 2012. Paleohistological estimation of bone growth rate in extinct archosaurs. Paleobiology 38:335–349.

Currey JD. 2002. Bones. Structure and mechanics. Princeton: Princeton University Press.

Curry Rogers K, Whitney M, Bagley B. 2016. Precocity in a tiny titanosaur from the Cretaceous of Madagascar. Science 352:450–454.

Curtin AJ, Macdowell AA, Schaible EG, Curtin AJ, Macdowell AA, Schaible EG, Roth VL, Carolina N. 2012. Noninvasive histological comparison of bone growth patterns among fossil and extant neonatal elephantids using synchrotron radiation x-ray microtomography. J. Vertebr. Paleontol. 32:939–955.

Damuth J, MacFadden BJ. 1990. Body size in mammalian Paleobiology. Estimations and biological implications. Cambridge: Cambridge University Press.

Dytham C. 2011. Choosing and Using Statistics: A Biologist's Guide. 3rd ed. Chichester: Wiley-Blackwell.

Ento K, Matsui M. 2002. Estimation of age structure by skeletochronology of a population of *Hynobius nebulosus* in a breeding season (Amphibia, Urodela). Zoolog. Sci. 19:241–247.

Ernest SKM. 2003. Life history characteristics of placental nonvolant mammals. Ecology 84:3402.

Esteban M, García-París M, Buckley D, Castanet J. 1999. Bone growth and age in *Rana saharica*, a water frog living in a desert environment. Finnish Zool. Bot. Publ. Board 36:53–62.

Esteban M, Sánchez-Herráiz MJ, Barbadillo LJ, Castanet J, Márquez R. 2002. Effects of age, size and temperature on the advertisement calls of two Spanish populations of *Pelodytes punctatus*. Amphibia-Reptilia 23:249–258.

Fellows I. 2012. Deducer: A Data Analysis GUI for R. J. Stat. Softw. 49:1–15.

Fowden AL, Forhead AJ, Ousey JC. 2012. Endocrine adaptations in the foal over the perinatal period. Equine Vet. J. 44:130–139.

Francillon-Vieillot H, de Buffrénil V, Castanet J, Géraudie J, Meunier FJ, Sire JY, Zylberberg L, de Ricqlès A. 1990. Microstructure and mineralization of vertebrate skeletal tissues. In: Carter JG, editor. Skeletal biomineralization: patterns, processes and evolutionary trends. New York: Van Nostrand Reinhold. p. 471–530.

Hemelaar A. 1985. An improved method to estimate the number of year rings resorbed in phalanges of *Bufo bufo* (L.) and its application to populations from different latitudes and altitudes. Amphib. Publ. Soc. Eur. Herpetol. 6:323–341.

Hugi J, Sánchez-Villagra MR. 2012. Life history and skeletal adaptations in the galapagos marine iguana (*Amblyrhynchus cristatus*) as reconstructed with bone histological data—A comparative study of iguanines. J. Herpetol. 46:312–324.

Huttenlocker AK, Woodward HN, Hall BK. 2013. The biology of bone. In: Padian K, Lamm E-T, editors. Bone histology of fossil tetrapods: advancing methods, analysis, and interpretation. Berkeley: University of California Press. p. 13–34.

Jakob C, Seitz A, Crivelli A, Miaud C. 2002. Growth cycle of the marbled newt (*Triturus marmoratus*) in the Mediterranean region assessed by skeletochronology. Amphibia-Reptilia 23:407–418.

Jordana X, Marín-Moratalla N, Moncunill-Solé B, Nacarino-Meneses C, Köhler M. 2016. Ontogenetic changes in the histological features of zonal bone tissue of ruminants: A quantitative approach. Comptes Rendus - Palevol 15:255–266.

Kaczensky P, Lkhagvasuren B, Pereladova O, Hemami M, Bouskila A. 2015. *Equus hemionus*. IUCN Red List Threat. Species e.T7951A45.

Khonsue W, Matsui M, Hirai T, Misawa Y. 2001. A comparison of age structures in two populations of a pond frog *Rana nigromaculata* (Amphibia: Anura). Zoolog. Sci. 18:597–603.

Kim H-Y, Mohan S. 2013. Role and mechanisms of actions of thyroid hormone on the skeletal development. Bone Res. 1:146–161.

King SRB, Moehlman PD. 2016. *Equus quagga*. IUCN Red List Threat. Species:e.T41013A45172424.

Köhler M. 2010. Fast or slow? The evolution of life history traits associated with insular dwarfing. In: Pérez-Mellado V, Ramon C, editors. Islands and Evolution. Vol. 19. Maó: Institut Menorquí d'Estudis. Recerca. p. 261–280.

Köhler M, Marín-Moratalla N, Jordana X, Aanes R. 2012. Seasonal bone growth and physiology in endotherms shed light on dinosaur physiology. Nature 487:358–361.

Köhler M, Moyà-Solà S. 2009. Physiological and life history strategies of a fossil large mammal in a resource-limited environment. Proc. Natl. Acad. Sci. U. S. A. 106:20354–20358.

Lamm E-T. 2013. Preparation and sectioning of specimens. In: Padian K, Lamm E-T, editors. Bone histology of fossil tetrapods: advancing methods, analysis, and interpretation. Berkeley: University of California Press. p. 55–160.

Lee AH, Huttenlocker AK, Padian K, Woodward HN. 2013. Analysis of Growth Rates. In: Padian K, Lamm E-T, editors. Bone histology of fossil tetrapods: advancing methods, analysis, and interpretation. Berkeley: University of California Press. p. 217–251.

Lkhagvasuren D, Ansorge H, Samiya R, Schafberg R, Stubbe A, Stubbe M. 2013. Age determination of the Mongolian wild ass (*Equus hemionus* Pallas, 1775) by the dentition patterns and annual lines in the tooth cementum. J. Species Res. 2:85–90.

de Margerie E. 2002. Laminar bone as an adaptation to torsional loads in flapping flight. J. Anat. 201:521–526.

de Margerie E, Cubo J, Castanet J. 2002. Bone typology and growth rate: Testing and quantifying "Amprino's rule" in the mallard (*Anas platyrhynchos*). Comptes Rendus - Biol. 325:221–230.

de Margerie E, Robin J-P, Verrier D, Cubo J, Groscolas R, Castanet J. 2004. Assessing a relationship between bone microstructure and growth rate: a fluorescent labelling study in the king penguin chick (*Aptenodytes patagonicus*). J. Exp. Biol. 207:869–879.

Marín-Moratalla N, Cubo J, Jordana X, Moncunill-Solé B, Köhler M. 2014. Correlation of quantitative bone histology data with life history and climate: A phylogenetic approach. Biol. J. Linn. Soc. 112:678–687.

Marín-Moratalla N, Jordana X, Köhler M. 2013. Bone histology as an approach to providing data on certain key life history traits in mammals: Implications for conservation biology. Mamm. Biol. 78:422–429.

Martin RB, Burr DB, Sharkey NA. 1998. Skeletal tissue mechanics. New York: Springer-Verlag.

Martínez-Maza C, Alberdi MT, Nieto-Diaz M, Prado JL. 2014. Life-history traits of the miocene *Hipparion concudense* (Spain) inferred from bone histological structure. PLoS One 9:e103708.

Messer NT, Riddle WT, Traub-Dargatz JL, Dargatz DA, Refsal KJ, Thompson Jr. DL. 1998. Thyroid hormone levels in thoroughbred mares and their foals at parturition. AAEP Proc. 44:248–251.

Moncunill-Solé B, Orlandi-Oliveras G, Jordana X, Rook L, Köhler M. 2016. First approach of the life history of *Prolagus apricenicus* (Ochotonidae, Lagomorpha) from Terre Rosse sites (Gargano, Italy) using body mass estimation and paleohistological analysis. Comptes Rendus - Palevol 15:227–237.

Morris P. 1970. A method for determining absolute age in the hedgehog. J. Zool. 161:277–281.

Nacarino-Meneses C, Jordana X, Köhler M. 2016a. First approach to bone histology and skeletochronology of *Equus hemionus*. Comptes Rendus - Palevol 15:267–277.

Nacarino-Meneses C, Jordana X, Köhler M. 2016b. Histological variability in the limb bones of the Asiatic wild ass and its significance for life history inferences. PeerJ 4:e2580.

Nacarino-Meneses C, Jordana X, Orlandi-Oliveras G, Köhler M. 2017. Reconstructing molar growth from enamel histology in extant and extinct *Equus*. Sci. Rep. 7:15965.

Nowak RM. 1999. Walker's mammals of the world. Baltimore and London: The Johns Hopkins University Press.

Olgun K, Uzum N, Avci A, Miaud C. 2005. Age, size and growth of the southern *Triturus karelinii* in a population from Turkey. Amphibia-Reptilia 26:223–230.

Orlandi-Oliveras G, Jordana X, Moncunill-Solé B, Köhler M. 2016. Bone histology of the giant fossil dormouse *Hypnomys onicensis* (Gliridae, Rodentia) from Balearic Islands. Comptes Rendus - Palevol 15:238–244.

Padian K, de Ricqlès A, Horner JR. 2001. Dinosaurian growth rates and bird origins. Nature 412:405–408.

Penzhorn BL. 1982. Age determination in cape mountain zebras *Equus zebra zebra* in the Mountain Zebra National Park. Koedoe 25:89–102.

Peters RH. 1983. The ecological implications of body size. Cambridge: Cambridge University Press.

Prondvai E, Stein KHW, de Ricqlès A, Cubo J. 2014. Development-based revision of bone tissue classification: the importance of semantics for science. Biol. J. Linn. Soc. 112:799–816.

Rubenstein D, Low Mackey B, Davidson Z, Kebede F, King SR. 2016. *Equus grevyi*. IUCN Red List Threat. Species:e.T7950A89624491.

Schöpke K, Stubbe A, Stubbe M, Batsaikhan N, Schafberg R. 2012. Morphology and variation of the Asiatic wild ass (*Equus hemionus hemionus*). Erforsch. Biol. Ressourcen der Mongolei 12:77–84.

Schour I. 1936. The neonatal line in the enamel and dentin of the human deciduous teeth and first permanent molar. J. Am. Dent. Assoc. 23:1946–1955.

Silver IA. 1963. The aging of domestic animals. In: Brothwell D, Higgs E, editors. Science in Archaeology: a comprehensive survey of progress and research. New York: Basic Books. p. 250–268.

Sinsch U. 2015. Review: Skeletochronological assessment of demographic life-history traits in amphibians. Herpetol. J. 25:5–13.

Smith TM, Reid DJ, Sirianni JE. 2006. The accuracy of histological assessments of dental development and age at death. J. Anat. 208:125–138.

Smuts GL. 1974. Age determination in Burchell's zebra (*Equus burchelli antiquorum*) from the Kruger National Park. J. South. african Wildl. Manag. Assoc. 4:103–105.

Stearns SC. 1992. The evolution of life histories. New York: Oxford University Press.

Stewart F, Goode JA, Allen WR. 1993. Growth hormone secretion in the horse: Unusual pattern at birth and pulsatile secretion through to maturity. J. Endocrinol. 138:81–89.

Stover SM, Pool RR, Martin RB, Morgan JP. 1992. Histological features of the dorsal cortex of the third metacarpal bone mid-diaphysis during postnatal growth in thoroughbred horses. J. Anat. 181:455–469.

Tacutu R, Craig T, Budovsky A, Wuttke D, Lehmann G, Taranukha D, Costa J, Fraifeld VE, De Magalhães JP. 2013. Human Ageing Genomic Resources: Integrated databases and tools for the biology and genetics of ageing. Nucleic Acids Res. 41:1027–1033.

Tafforeau P, Bentaleb I, Jaeger J-J, Martin C. 2007. Nature of laminations and mineralization in rhinoceros enamel using histology and X-ray synchrotron microtomography: Potential implications for palaeoenvironmental isotopic studies. Palaeogeogr. Palaeoclimatol. Palaeoecol. 246:206–227.

Turner-Walker G, Mays S. 2008. Histological studies on ancient bone. In: Pinhasi R, Mays S, editors. Advances in human paleopathology. Chichester: John Wiley & Sons, Ltd. p. 121–146.

Weber DF, Eisenmann DR. 1971. Microscopy of the neonatal line in developing human enamel. Am. J. Anat. 132:375–392.

Woodward HN, Freedman Fowler EA, Farlow JO, Horner JR. 2015. *Maiasaura*, a model organism for extinct vertebrate population biology: a large sample statistical assessment of growth dynamics and survivorship. Paleobiology 41:503–527.

Woodward HN, Padian K, Lee AH. 2013. Skeletochronology. In: Padian K, Lamm E-T, editors. Bone histology of fossil tetrapods: advancing methods, analysis, and interpretation. Berkeley: University of California Press. p. 195–215.

Zuckerman S. 1952. The breeding seasons of mammals in captivity. J. Zool. 122:827–950.

Supporting Information

S1 Fig. Methodology employed to estimate the area of the longitudinal vascular canals (VCs) in the limb bones of *Equus* at both sides of the NL. (A) Metatarsal cross-section of *E. hemionus* IPS83149. White dashed rectangles indicate areas of image magnification. **(B)** VCs after the presence of the NL in *E. hemionus* IPS83149. **(C)** VCs before the presence of the NL in *E. hemionus* IPS83149. For each VC, we adjusted an ellipse (red circles) and measured its area with ImageJ software. Secondary osteons (white star), canals with no longitudinal orientation and non-circular form (green star) or canals with blurred edges (blue star) were not measured. Yellow dashed line indicates the NL. White scale bar = 200 μm.

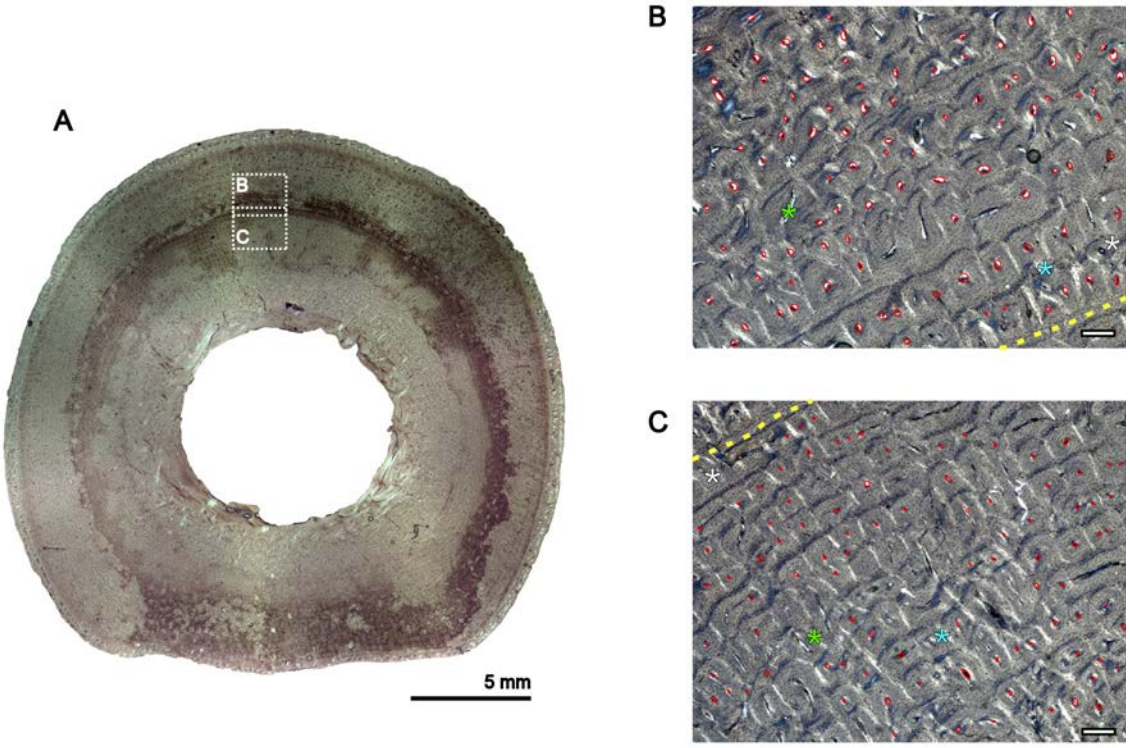

- Chapter 7 -

The life history of European Middle Pleistocene equids: first insights from bone histology

To be submitted

The life history of European Middle Pleistocene equids: first insights from bone histology

Carmen Nacarino-Meneses[1]* & Guillem Orlandi-Oliveras[1]

[1] Institut Català de Paleontologia Miquel Crusafont (ICP), Campus de la Universitat Autònoma de Barcelona, 08193 Bellaterra, Barcelona, Spain.

Correspondence (*): Carmen Nacarino-Meneses, Institut Català de Paleontologia Miquel Crusafont (ICP), C/ de les Columnes s/n, Edifici Z, Campus UAB, 08193 Bellaterra, Barcelona, Spain. Phone number: +34 93 586 86 19. E-mail: carmen.nacarino@icp.cat

Abstract

Body size is one of the most important life history traits of an animal. Thus, evolutionary trends in body size are a central issue of study in Paleontology. In the European evolution of the genus *Equus*, a shift towards a decrease in body size during the Pleistocene and Holocene periods is observed. However, this evolutionary change has never been analyzed under a life history framework. Here, we used bone histology to reconstruct the life history of two large Middle Pleistocene species (*Equus mosbachensis* and *Equus steinheimensis*) and to compare it with that of smaller extant *Equus* (*Equus grevyi* and *Equus hemionus*). We studied bone tissue types, vascularization and bone growth marks in the metapodia of these extinct equids to infer key life history traits that correlate with body size (e.g. size at birth, growth rate, longevity). Our results show that neonatal size of these Middle Pleistocene equids fits the predictions from body mass scaling. We estimate a similar age at skeletal maturity for the metapodia of *E. mosbachensis* and *E. steinheimensis* and that of extant equids. Our findings also reveal that extinct equids grew at higher rates than extant *E. hemionus* and *E. grevyi*. This result conforms to the predictions of life history theory on environments with different levels of resource availability and provides a new framework of study for body size shifts on European Pleistocene equids.

Keywords

Bone histology, body size, life history, growth rate, Pleistocene, *Equus*

Introduction

The family Equidae has been deeply studied due to its relevance for Paleontology and evolution (MacFadden 1992; Janis 2007). The abundance of equid remains in the fossil record has facilitated the tracking of evolutionary changes in the clade (Orlando 2015), positioning Equidae as a classic example of macroevolution (MacFadden 2005; Janis 2007). Along with modifications in dentition and number of digits (Simpson 1953; Azzaroli 1992; MacFadden 1992; Strömberg 2006; Janis 2007; Cantalapiedra et al. 2017; McHorse et al. 2017), this mammalian group experienced significant variations in size during its evolutionary history (Simpson 1953; MacFadden 1986; Eisenmann 1991; Forsten 1991a; MacFadden 1992; Alberdi et al. 1995; Guthrie 2003; Ortiz-Jaureguizar and Alberdi 2003; Shoemaker and Clauset 2014; Cantalapiedra et al. 2017). Generally, a phylogenetical large-scale trend towards ever increasing body size is observed (Cope's law, Stanley (1973)), although several clades of the family experienced size reduction (MacFadden 1986; Forsten 1991a; Forsten 1991b; MacFadden 1992; Alberdi et al. 1995; Alberdi et al. 1998). One of these dwarfing tendencies occurred during the evolution of the genus *Equus* in the Old World (Forsten 1991b; Alberdi et al. 1995), as both the stenonoid and the caballoid lineages progressively reduced their size during the Pleistocene (Alberdi et al. 1995; Alberdi et al. 1998). This size decrease trend continued throughout the Holocene (Forsten 1988; Forsten 1991b), resulting in a smaller body size of extant *Equus* (Ernest 2003) in comparison to their Pleistocene relatives (Alberdi et al. 1995).

Body size is one of the most important characteristics of an animal, as it tightly correlates with its physiology (Kleiber 1932; Peters 1983; McNab 1990), life history (Blueweiss et al. 1978; Western 1979; Calder 1984) and ecology (Damuth 1981; Peters 1983; Eisenberg 1990). Due to the close relationship between body size and the ecological conditions of the ecosystem, the size shift observed in Pleistocene equids has usually been related to the climatic and resources variations occurring during that epoch (Forsten 1991b; Alberdi et al. 1995; Cantalapiedra et al. 2017). Demographic (population density) and behavioral (social structure) characteristics of the species have also been proposed to explain the body size differences observed between European Pleistocene horses (Saarinen et al. 2016). Nevertheless, body size is also a key life history trait that correlates with other biological traits (Peters 1983; Calder 1984; Damuth and MacFadden 1990), but no previous research has investigated the body size variations observed in *Equus* within a life history framework. In fossil mammals, the histological analysis of bones is known to provide valuable insights into their life history strategy (Köhler and Moyà-Solà 2009; Köhler 2010; Marín-Moratalla et al. 2011; Martínez-Maza et al. 2014; Amson et al. 2015; Kolb et al. 2015; Moncunill-Solé et al. 2016; Orlandi-Oliveras et al. 2016). The kind of bone tissue type, its vascularization, and the bone growth marks (BGMs) present within a bone cortex, record the pace of growth and development of the species (Chinsamy-Turan 2005; Huttenlocker et al. 2013; Lee et al. 2013; Woodward et al. 2013). The detailed study of these histological features, hence, allows the inference of key life history traits of the species such as longevity, growth rate or age at maturity in extant and extinct vertebrates (Woodward et al. 2015; Jordana et al. 2016; Nacarino-Meneses et al. 2016a; Nacarino-

Meneses et al. 2016b).

In the present research, we aim to investigate whether the body size shift observed in the *Equus* lineage is related to changes in the life history of the species. We focus our study in the European Middle Pleistocene species *Equus steinheimensis* and *Equus mosbachensis*. Both extinct caballoid horses were described for the first time in Steinheim an der Murr and Mosbach Sands respectively, two classical Middle Pleistocene localities of Germany (Adam 1954; Forsten 1999; Koenigswald et al. 2007; Van Asperen 2013). Previous studies based on measurements of their dental and postcranial remains have reported differences in body size for these extinct equids (Eisenmann 1991; Forsten 1999). While *E. steinheimensis* is considered a medium-sized caballoid horse (Eisenmann 1991; Forsten 1999), *E. mosbachensis* is one of the largest equids that can be found in the Pleistocene fossil record of Europe (Eisenmann 1991; Alberdi et al. 1995). From bone histology, we reconstruct their pace of life and compare it with that of extant *Equus*, as both Middle Pleistocene equids greatly exceeded in size extant representatives of the group (Alberdi et al. 1995; Forsten 1999; Ernest 2003). Thus, we also examine here the bone histology of the extant equid species of Asiatic wild ass (*Equus hemionus*) and Grevyi's zebra (*Equus grevyi*). These two extant taxa dwell in very different habitats and present extreme values of body size and life history traits within extant *Equus* (Churcher 1993; Nowak 1999; Ernest 2003; Kaczensky et al. 2015; Orlando 2015; Rubenstein et al. 2016), which makes them as the most appropriate ones for comparison with our fossil sample.

Material & methods

Species	Code	Collection code	Bone	Site/Habitat	Institution
*E. steinheimensis**	IPS96010	32917/23	Mt	Steinheim an der Murr	SMNS
	IPS96011	32803/61	Mc	Steinheim an der Murr	SMNS
	IPS96012	32803/235	Mt	Steinheim an der Murr	SMNS
	IPS96013	32803/321	Mc	Steinheim an der Murr	SMNS
*E. mosbachensis**	IPS96014	32850/87	Mt	Mosbach Sands	SMNS
	IPS96016	32850/6	Mc	Mosbach Sands	SMNS
	IPS96017	32850/112	Mc	Mosbach Sands	SMNS
E. hemionus	IPS83876	225	Mc, Mt	Gobi Desert	MDA
	IPS83877	381	Mc, Mt	Gobi Desert	MDA
E. grevyi	IPS84963	7111	Mt	Hagenbeck Zoo	ZIHU

Table 1.- Sample studied for bone histology. Mc = metacarpus; Mt = metatarsus; SMNS = Staatliches Museum für Naturkunde Stuttgart (Stuttgart, Germany); MDA = Museum of Domesticated Animals (Halle, Germany); ZIHU = Zoological Institute of Hamburg University (Hamburg, Germany). The star (*) indicates fossil species.

Equid sample

We analyzed postcranial fossil remains of *E. steinheimensis* and *E. mosbachensis* belonging to the collections of the Staatliches Museum für Naturkunde (Stuttgart, Germany) (Table 1). Specifically, metapodial bones (metacarpi and metatarsi) were used for paleohistological analyses, while phalanges and metacarpi were analyzed for body mass estimations. The material of *E. steinheimensis* comes from Steinheim an der Murr site (Steinheim, henceforward), a late Middle Pleistocene locality (Van Asperen 2013) situated in south-west Germany (Fig. 1). Steinheim fossil site presents a mix of glacial and interglacial fauna (Adam 1954) due to a sampling bias during the recovery of the remains and/or to the coexistence of species with flexible adaptations (Pushkina et al. 2014). Although the dating of Steinheim site is, hence, controversial, it is thought to generally correlate with the Holsteinian Interglacial (MIS 11) (Van Asperen 2013). The sample of *E. mosbachensis* belongs to Mosbach Sands, an early Middle Pleistocene site (Koenigswald et al. 2007) located in Wiesbaden (Germany) (Fig. 1). This German classical site is divided into two different stratigraphic ages based on lithological and paleontological criteria (Maul et al. 2000). The *E. mosbachensis* sample analyzed here belongs to the Mosbach 2 fauna, which is known to present interglacial conditions (Koenigswald et al. 2007) and to correlate with the Cromerian Interglacial (MIS 13, 15) (Maul et al. 2000; Kahlke et al. 2011).

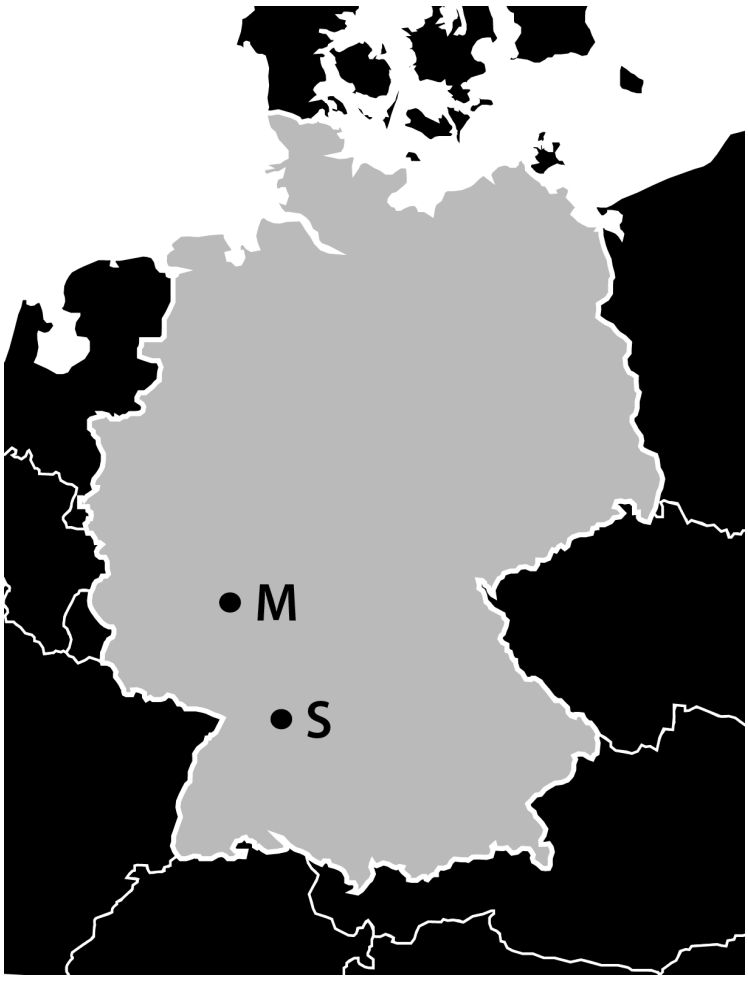

Figure 1. Map of Germany showing the provenance of the fossil sample. M = Mosbach Sands; S = Steinheim an der Murr.

We also studied an adult metapodial sample of extant *E. hemionus* and *E. grevyi* (Table 1) for comparison. Specimens of *E. hemionus* are stored at the Museum of Domesticated Animals (Halle, Germany) and lived wild in the Gobi Desert (Table 1). They were found killed by poachers and collected during the Mongolian-German Biological Expeditions (2001 – 2006) (Schöpke et al. 2012). The *E. grevyi* individual belongs to the collections of the Zoological Institute of Hamburg University (Germany) (Table 1), after living captive in the Hagenbeck Zoo (Hamburg, Germany) (Table 1).

Preparation and analysis of histological thin-sections

We sectioned 12 metapodia of extant and extinct equids: 4 metapodia of *E. steinheimensis*, 3 metapodia of *E. mosbachensis*, 4 metapodia of *E. hemionus* and 1 metatarsus of *E. grevyi* (Table 1). To avoid damaging of the most valuable fossil specimens, only metapodia fragmented at the mid-shaft level were used in the present study. The preparation of the histological thin-sections follows standard procedures in our laboratory (Köhler et al. 2012; Nacarino-Meneses et al. 2016a). In all extant and extinct exemplars, a chunk of 2 – 3 cm was extracted from the mid-diaphysis of each bone and embedded in an epoxy resin (Araldite 2020). Afterwards, this block was cut into two halves with a low speed diamond saw (IsoMet, Buehler). The mid-shaft surface of each block was later polished using a Metaserv®250 (Buehler) or carborundum powder, and fixed to a frosted glass with ultraviolet-curing glue (Loctite 358). Each sample was then cut and grounded with a diamond saw (PetroThin, Buehler) and polished again using the Metaserv®250 (Buehler) or carborundum powder to obtain histological thin-sections of 100 – 120 μm thick. Finally, histological slices obtained from fossil samples were dehydrated in alcohol, bathed in a histological clearing agent (Histo-Clear II) and mounted using DPX mounting medium (Scharlau). Thin-sections prepared from extant specimens were covered, however, with a mix of oils (Lamm 2013) to improve their view under the microscope.

Samples were analyzed under polarized light in a Zeiss Scope.A1 microscope and photographed with the camera incorporated on it (AxioCam ICc5). We also observed the histological thin-sections under polarized light with a ¼λ filter, which helps on the identification and visualization of the bone tissue and the bone growth marks (BGMs) (Turner-Walker and Mays 2008). Histological description of bone tissue types and vascular organization follows classical bibliography (Francillon-Vieillot et al. 1990; de Margerie et al. 2002; Huttenlocker et al. 2013). Regarding BGMs, both cyclical and non-cyclical features were identified in our metapodial equid sample. Cyclical BGMs (CGMs) record annual cycles of growth in response to hormonal and environmental cycles (Castanet et al. 1993; Köhler et al. 2012). From their study, we inferred the minimum longevity of extinct equid species by counting the total number of CGMs within a bone cross-section (Nacarino-Meneses et al. 2016a). A non-cyclical BGM related to birth (Nacarino-Meneses and Köhler accepted) was also recognized in our metapodial sample. We considered this neonatal line (NL) as time zero in growth reconstructions. The perimeter of each BGM, regardless of its cyclicality, was calculated using Image J software and the results were plotted to reconstruct the pattern of metapodial growth (Bybee et al. 2006; Woodward

et al. 2013). From the obtained metapodial growth curves, we estimated the timing of epiphyseal fusion in these bones for each fossil species (Nacarino-Meneses et al. 2016a).

Adult and neonatal body size estimation

We analyzed metacarpi and phalanges of *E. steinheimensis* and *E. mosbachensis* to estimate their adult body mass, a proxy of its body size (Damuth and MacFadden 1990). For each species, we measured the proximal depth on the first phalanx and the distal minimal depth of the lateral condyle on the third metacarpus (Eisenmann et al. 1988), as these linear measurements present the best correlation with body mass in extant equids (Alberdi et al. 1995). Measurements were taken using a digital electronic precision caliper (0.05 mm error). We used the equations provided by Alberdi et al. (1995) to perform body mass estimations. These data were based on allometric models expressed as the power function $y = ax^b$ (Damuth and MacFadden 1990) and logarithmically transformed to obtain a linear relationship ($\ln y = \ln a + b \ln x$) (Peters 1983); where y is body mass, x is the measurement taken on the bone, b is the allometric coefficient and a is a constant (Alberdi et al. 1995).

We also estimated the size at birth of extinct and extant equids from the analysis of the NL found in their metapodia (Nacarino-Meneses and Köhler accepted). Alberdi et al. (1995) did not found a significant correlation between the measurements taken at the mid-diaphysis on the metapodia of extant *Equus* (measures 3 and 4 according to Eisenmann et al. (1988)) and their adult body mass. Because histological slices of the present study were prepared at this level of the diaphysis, we cannot use measurements of the NL to infer body weight at birth. Moreover, equations of Alberdi et al. (1995) are calculated for adult individuals. Thus, they are little useful for estimating body mass at earlier ontogenetic stages (Köhler 2010). We decided, then, to represent size at birth as a linear measurement instead of on terms of body mass, by using the perimeter of the NL as a proxy of the neonatal size.

Results

Bone histology is generally better preserved in Steinheim (Fig. 2A, C; Fig. 3A, B) than in Mosbach samples (Fig. 2B, D; Fig. 3C, D). Although several histological slices from both fossil sites present microtaphonomical alterations (Fig. 2; Fig. 3), it is still possible to recognize the primary bone tissue and the BGMs in all fossil specimens studied.

Primary bone histology

Metapodial bones of *E. steinheimensis* and *E. mosbachensis* are mainly composed of fibrolamellar bone (Fig. 2A–C), the same as in extant equids (Fig. 2E, F). Most of the vascular canals identified in extinct species are oriented longitudinally (Fig. 2A, B). However, both fossil equids also present multiple circular and radial canals that interconnect primary

osteons (Fig. 2A, B). Hence, we found a qualitatively higher proportion of vascular canals in fossil (Fig. 2A, B) than in extant metapodia (Fig. 2E, F).

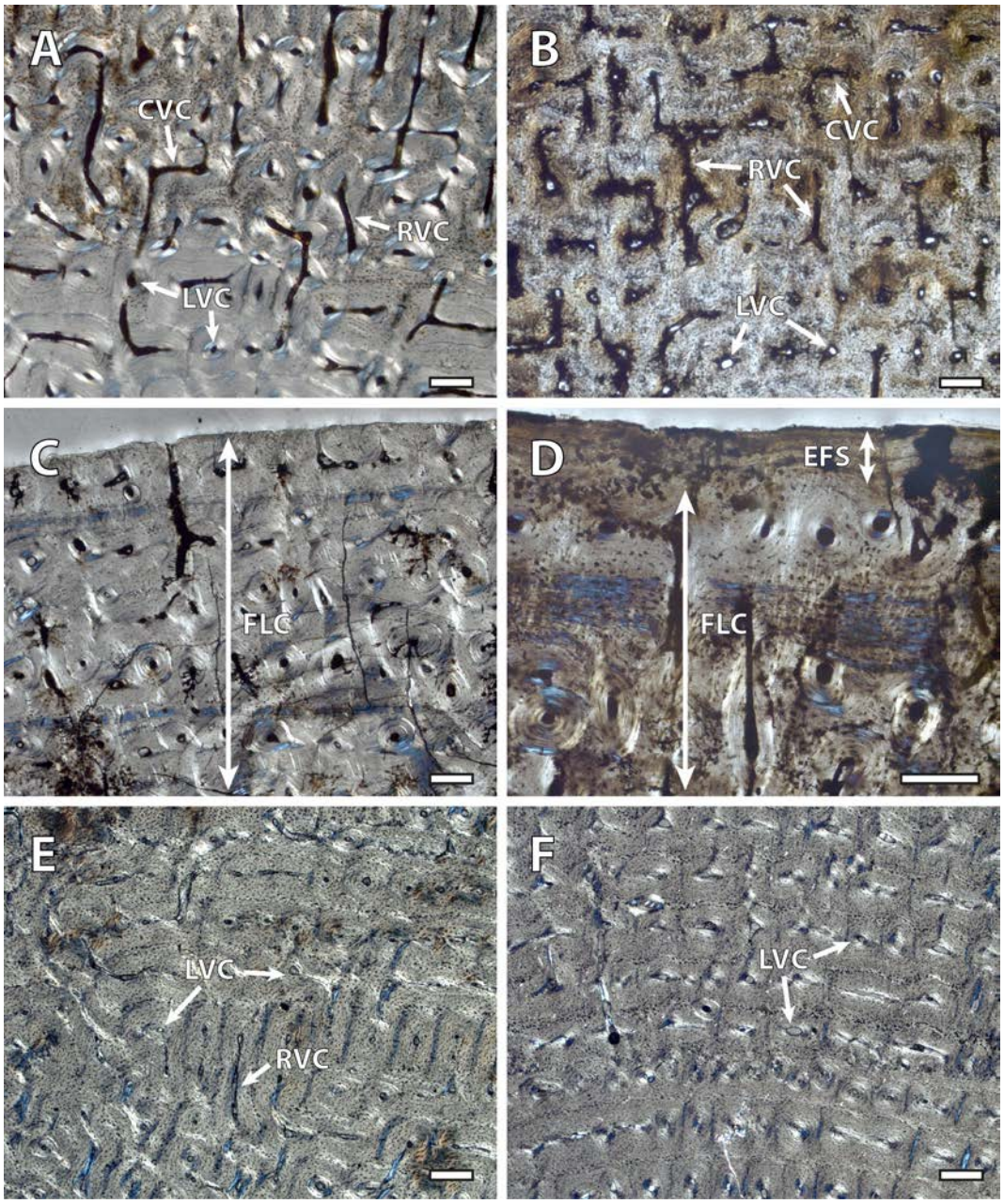

Figure 2. Metapodial bone histology of European Middle Pleistocene (A – D) and extant *Equus* (E, F). (A) Metacarpal bone cortex of *Equus steinheimensis* (IPS96013). **(B)** Metatarsal bone cortex of *Equus mosbachensis* (IPS96014). **(C)** Metacarpal bone cortex of *Equus steinheimensis* (IPS96011). **(D)** Metacarpal bone cortex of *Equus mosbachensis* (IPS96017). **(E)** Metacarpal bone cortex of *Equus hemionus* (IPS83877). **(F)** Metatarsal bone cortex of *Equus grevyi* (IPS84963). CVC = circular vascular canals; EFS = external fundamental system; FLC = fibrolamellar complex; LCV = longitudinal vascular canals; RVC = radial vascular canals. Scale bars = 200 µm.

Metacarpi of *E. steinheimensis* do not show an external fundamental system (EFS) in their outermost cortex (Fig. 2C). This avascular and lamellar bone tissue (Huttenlocker et al. 2013) is recognized, however, in the metatarsi of this species and in metacarpi and metatarsi of *E. mosbachensis* (Fig. 2D).

Skeletochronology

Up to five cyclical BGMs are identified in the metapodia of *E. steinheimensis* (Fig. 3A, B). In *E. mosbachensis*, the highest number of cyclical BGMs is found in the metacarpus IPS96017 (Fig. 3C). This specimen presents six cyclical BGMs within the primary bone tissue (Fig. 3C). Besides, all fossil metapodia show a non-cyclical BGM in the most internal cortex (Fig. 3) that corresponds to the NL observed in extant *Equus* (Nacarino-Meneses and Köhler accepted).

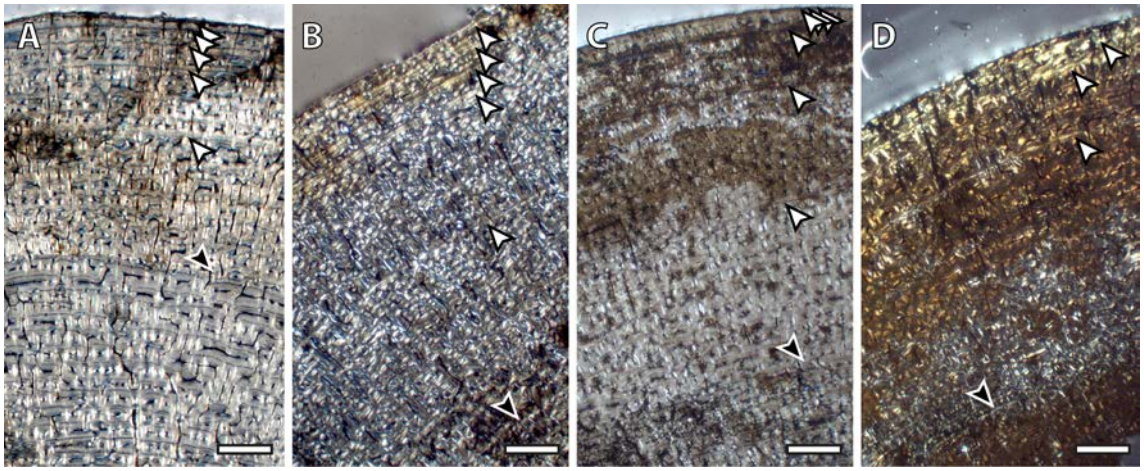

Figure 3. Bone growth marks identified in the metapodia of *Equus steinheimensis* (A, B) and *Equus mosbachensis* (C, D). (A) Metacarpal bone cortex of *Equus steinheimensis* IPS96013. **(B)** Metatarsal bone cortex of *Equus steinheimensis* IPS96010. **(C)** Metacarpal bone cortex of *Equus mosbachensis* IPS96017. **(D)** Metatarsal bone cortex of *Equus mosbachensis* IPS96014. White arrows = cyclical bone growth marks; black arrows = non-cyclical bone growth marks (neonatal line - NL). Scale bars = 1 mm.

From the study of cyclical and non-cyclical BGMs, we reconstruct the metapodial growth pattern of *E. steinheimensis* and *E. mosbachensis* (Fig. 4). As Figure 4 shows, metacarpus (Fig. 4A) and metatarsus (Fig. 4B) of extinct equids follow the same growth pattern as the metapodia of extant *E. hemionus* and *E. grevyi* (Fig. 4). In both fossil and extant species, it is observed a decrease in growth rate at the second year of life (Fig. 4). Growth reconstruction also shows, however, a steeper slope in fossil than in extant samples (Fig. 4), both during the phase of highest growth rate and during residual growth (Fig. 4). These differences in growth rate are unlikely related to sex differences, as equid bones from males and females are known to grow similarly (Nacarino-Meneses et al. 2016a).

Adult and neonatal body size

Species	Locality	Metacarpus		Phalanx		Mean±SD (N)
		N	Mean±SD	N	Mean±SD	
E. steinheimensis	Steinheim an der Murr	18	478.7±63.1	36	464.7±131.2	469.3±112.6 (54)
E. mosbachensis	Mosbach Sands	7	595.6±82	9	616.54±275.2	607.4±207.8 (16)

Table 2. Adult body weight estimation (kg) in extinct *Equus*.

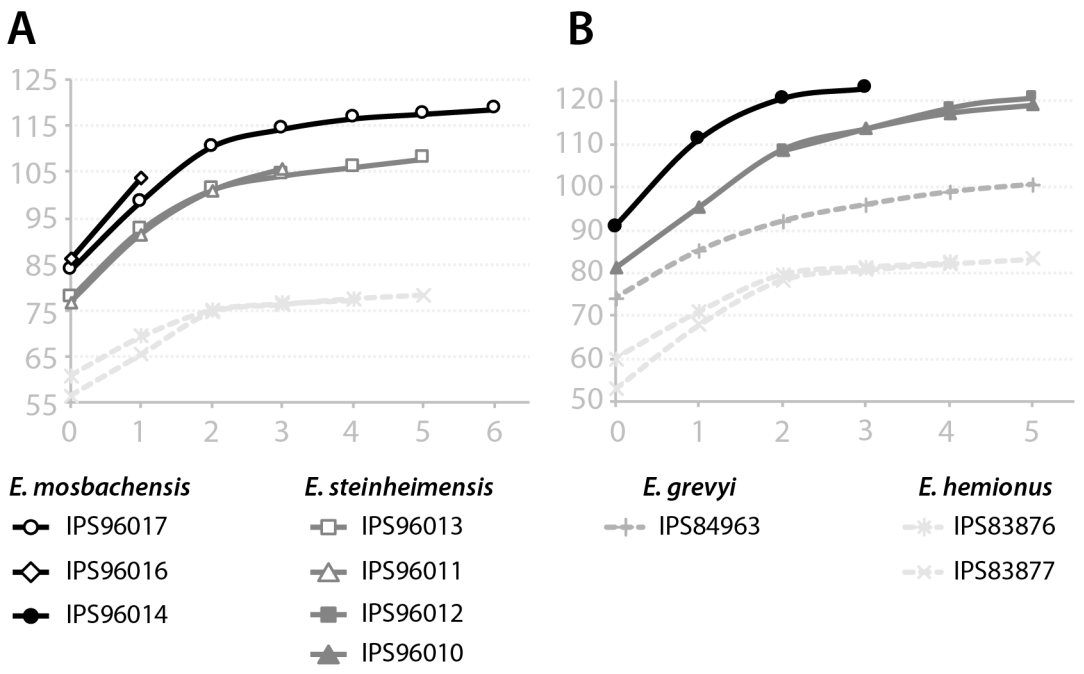

Figure 4. Metapodial growth of European Middle Pleistocene (continuous lines) and extant (dashed lines) *Equus*. Bone perimeter (mm, ordinate axis) is plotted against estimated age (years, abscissa axis) to obtain growth curves. **(A)** Growth curves obtained from the metacarpus. **(B)** Growth curves obtained from the metatarsus. Legend is shown at the bottom of the figure.

We estimated the adult weight of fossil equid species from measurements on metacarpi and phalanges (Table 2). A mean adult body mass of 469.3 kg is obtained for *E. steinheimensis*, while adult *E. mosbachensis* is predicted to weight around 607.4 kg (Table 2; Fig. 5).

The perimeter of the NL is used here to provide a rough estimation of the size at the birth for the Pleistocene species studied (Table 3, Fig. 4). As Table 3 shows, extinct equids present a larger size at birth than extant *E. hemionus* and *E. grevyi*. The mid-shaft perimeter of the metacarpi and metatarsi of a neonate *E. mosbachensis* measures between 83.65 and 90.86 mm (Table 3, Fig. 4), while that of *E. steinheimensis* does around 80 mm (Table 3, Fig. 4). Perimeters of neonate metapodia in extant species are considerably smaller, as they vary between 50 – 60 mm in *E. hemionus* and around 75 mm in *E. grevyi* (Table 3, Fig. 4).

Species	Code	Perimeter of the NL (mm)	
		Metacarpi	Metatarsi
*E. steinheimensis**	IPS96010	-	81.26
	IPS96011	76.55	-
	IPS96013	77.59	-
*E. mosbachensis**	IPS96014	-	90.86
	IPS96016	86.02	-
	IPS96017	83.65	-
E. hemionus	IPS83876	60.77	60.04
	IPS83877	56.29	53.09
E. grevyi	IPS84963	-	74.15

Table 3. Size at birth in extant and extinct *Equus*. The perimeter of the neonatal line (NL), considered as a proxy of the size at birth, is shown. The star (*) indicates fossil species.

Discussion

Evolutionary trends in body size of European extinct *Equus* are widely studied (Eisenmann 1991; Forsten 1991b; Alberdi et al. 1995; Cantalapiedra et al. 2017). A size shift towards a smaller body size is described for the first monodactyl horses (stenonoid horses) (Alberdi et al. 1995; Alberdi et al. 1998) that arrived in Eurasia between 3.0 – 2.5 M.y. ago (Lindsay et al. 1980; Azzaroli 1983). A second migratory event (1 – 0.8 M.y. ago) introduced the equid caballine forms in Europe (Alberdi and Bonadonna 1988), which also experienced size reduction during their Pleistocene and Holocene evolution in this continent (Forsten 1991b; Alberdi et al. 1995). To date, these dwarfing trends have been usually explained as an adaptation to the environmental changes that occur during the European Pleistocene (Forsten 1991b; Alberdi et al. 1995; Cantalapiedra et al. 2017), and no previous study has investigated its relationship with the life history of the species. In the present research, we reconstruct for the first time we reconstruct for the first time several life history traits of the extinct caballoid horses *E. steinheimensis* and *E. mosbachensis*, providing a unique life history framework for the analysis of the size shifts observed in European Pleistocene equids.

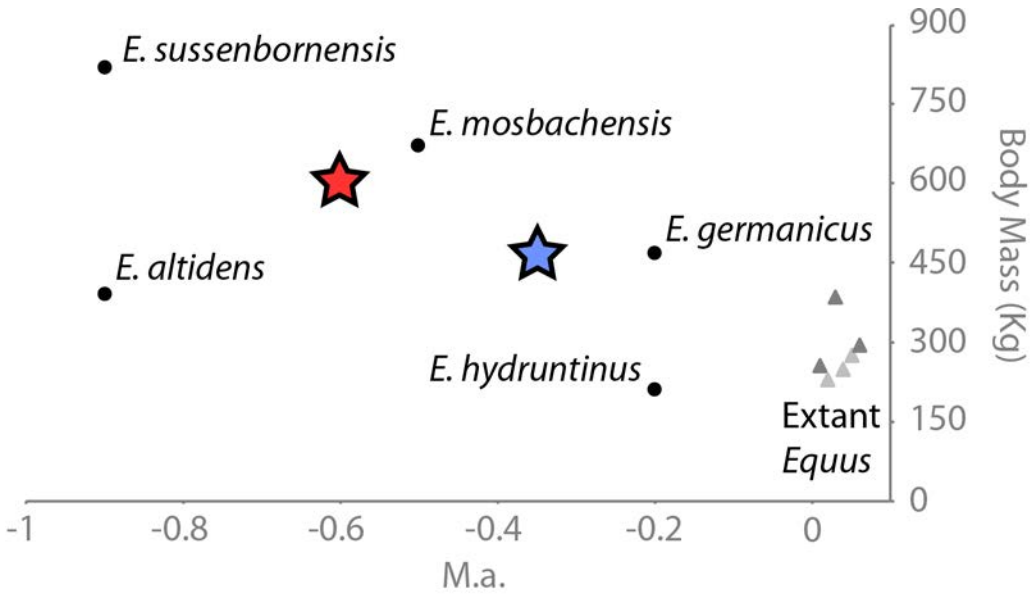

Figure 5. Estimated body mass of *Equus mosbachensis* (red star) and *Equus steinheimensis* (blue star) in comparison with Pleistocene (circles; Alberdi et al. 1995) and extant (triangles; Ernest 2003) Equus. 75% grey triangles = zebras; 25% grey triangles = asses.

Body size of European Middle Pleistocene *Equus*

Body size is usually represented by body mass (i.e. the weight of an individual), as this measure does not consider the shape of the organisms (Saarinen et al. 2016). The exhaustive study of Alberdi et al. (1995) reported adult body mass estimations for the most important Plio-Pleistocene *Equus* species of Europe, Africa and America. Here, we expand their database by calculating the body weight of *E. steinheimensis*. Our results show that its

mean body mass is around 470 kg (Table 2), which is similar to that reported for the Late Pleistocene species *Equus germanicus* (Fig. 5) (Alberdi et al. 1995). This finding agrees with a previous study by Forsten (1999), where she indicated similarities in metapodial size between *E. steinheimensis* and latter caballine equids such as *E. germanicus*. Our adult body mass estimations for this equid also matches previously published data about the weight of Steinheim horses (Saarinen et al. 2016). We further estimate body mass of *E. mosbachensis* from measurements on its metacarpi and phalanges (Table 2). We obtained a mean body weight of 607 kg for this early Middle Pleistocene species (Table 2), a result that match previous body mass estimations of 671.15 kg for it (Fig. 5) (Alberdi et al. 1995).

Size at birth is one of the most important life history traits of mammals (Stearns 1992). In the present study, we obtained an estimation of this attribute for the Middle Pleistocene equids of the analysis (Table 3) based on the perimeter of the NL identified in their metapodia (Fig. 3) (Nacarino-Meneses and Köhler accepted). Our findings reveal that *E. mosbachensis* presents the largest size at birth within the equids studied, followed by *E. steinheimensis*, *E. grevyi* and *E. hemionus* (Table 3, Fig. 4). *E. mosbachensis* is also the largest *Equus* of the study (Table 2, Fig. 5), while the Asiatic wild ass is the smallest (230 kg, Ernest 2003). *E. steinheimensis* (Table 2, Fig. 5) and *E. grevyi* (384 kg, Ernest 2003) present intermediate adult weights between *E. mosbachensis* and *E. hemionus*. Therefore, our results on neonatal body size of extinct equids (Table 3) are the expected by scaling, as they agree with the known correlation between size at birth and adult body size (Blueweiss et al. 1978; Calder 1984).

Growth rate of European Middle Pleistocene *Equus*

Some of the most important life history traits that correlate with body size can be inferred from bone histology (Köhler 2010). Thus, the number of studies that histologically examine bone remains in extinct taxa to estimate their growth rate (Padian et al. 2001; Köhler and Moyà-Solà 2009; Cubo et al. 2012; Amson et al. 2015; Orlandi-Oliveras et al. 2016), longevity (Köhler 2010; Marín-Moratalla et al. 2011; Martínez-Maza et al. 2014; Moncunill-Solé et al. 2016) or age at maturity (Horner et al. 2000; Köhler and Moyà-Solà 2009; Marín-Moratalla et al. 2011; Martínez-Maza et al. 2014) has considerably increased over the last years. Growth rate inferences are usually based on the combined analysis of the bone matrix and its vascularization (Amprino 1947; de Margerie et al. 2002; Chinsamy-Turan 2005; Huttenlocker et al. 2013; Lee et al. 2013). Our histological study of *E. steinheimensis* and *E. mosbachensis* has not revealed differences in bone tissue type and/or vascularization between both extinct species (Fig. 2A – D), which indicates similar rates of bone formation in these Pleistocene equids (de Margerie et al. 2002; Lee et al. 2013). We have observed, however, a higher proportion of vascular canals in their metapodia (Fig. 2A, B) than in extant *Equus* (Fig. 2E, F). According to de Margerie et al. (2002), this suggests a higher rate of bone deposition in the Pleistocene equids analyzed, which could be generally interpreted as a higher growth rate. Radial canals, as those identified in the metapodia of *E. steinheimensis* and *E. mosbachensis* (Fig. 2A, B), have also been related to higher rates of bone deposition (de Margerie et al. 2004). Growth curves have also been

commonly used to report differences in growth rate between sexes (Marín-Moratalla et al. 2013), taxa (Erickson et al. 2001; Erickson 2005) and even between animals under different ecological regimes (Marín-Moratalla et al. 2013; Nacarino-Meneses et al. 2016a). The slope of the metapodial growth curves obtained here for extinct equids is steeper than that of *E. hemionus* and *E. grevyi* (Fig. 4), suggesting higher rates of growth for *E. steinheimensis* and *E. mosbachensis* in comparison with these extant species. Therefore, our metapodial growth reconstruction (Fig. 4) supports our histological inference (Fig. 2A, B) of higher growth rates in *E. steinheimensis* and *E. mosbachensis*.

Age at maturity and longevity of European Middle Pleistocene *Equus*

Estimates about the age at maturity in fossil taxa use to rely on the identification of the lamellar and avascular bone tissue that is deposited in the outer cortex of bones: the external fundamental system (EFS) (Köhler et al. 2012; Marín-Moratalla et al. 2013). The timing of deposition of this tissue in equid and ruminant femora is known to correlate with the age at first reproduction of the species (Jordana et al. 2016; Nacarino-Meneses et al. 2016a), as it is supposed to record the life history trade-off between growth and reproduction (Stearns 1992). The significance of deposition of the EFS in other bones, however, is poorly known. Although several authors have suggested a relationship between the presence of EFS and the skeletal maturity of the species (Martínez-Maza et al. 2014), the appearance of this bone tissue in metapodial bones is likely related with the cessation of periosteal/radial bone growth (Nacarino-Meneses et al. 2016a). Therefore, the lack of EFS in metacarpi of *E. steinheimensis* (Fig. 2C) might just indicates a prolonged periosteal bone growth in this Pleistocene species. Alternatively, inferences on skeletal maturity can be made from growth reconstructions, as growth curves provide reliable information about the cessation of longitudinal bone growth (Nacarino-Meneses et al. 2016a). The decrease in growth rate observed at the second year of life in metapodia of Pleistocene and extant species (Fig. 4) suggests a similar age of epiphyseal fusion in these bones for both groups of equids (Nacarino-Meneses et al. 2016a). As metapodia fuse their epiphyses very early in ontogeny (Silver 1963), we cannot use this finding to infer an absolute age at skeletal maturity for *E. mosbachensis* and *E. steinheimensis*. Future histological studies on other long bones that finish later their growth, such as the femur or the tibia (Silver 1963), will be necessary to obtain information about this biological trait in the extinct taxa studied. These forthcoming studies would also shed light on the onset of sexual maturity in these Middle Pleistocene species, by analyzing the timing of deposition of the EFS in their femora (Nacarino-Meneses et al. 2016a).

The total number of CGMs within a bone cortex is known to broadly match the age at death of an individual (Castanet et al. 1993). Hence, several studies have analyzed these histological features on ancient bones to estimate longevity on extinct mammals (Köhler and Moyà-Solà 2009; Marín-Moratalla et al. 2011; Moncunill-Solé et al. 2016; Orlandi-Oliveras et al. 2016). Because mammals present asymptotic growth (Lee et al. 2013) and the identification of CGMs within the EFS is sometimes a challenging issue (Woodward et al. 2013), this methodology always yields a minimum longevity in this

group of vertebrates (Castanet et al. 2004; Castanet 2006). Moreover, femur is the most valuable bone for skeletochronological studies (Horner et al. 1999; García-Martínez et al. 2011; Nacarino-Meneses et al. 2016a), although metapodia is known to yield accurate individual age estimations in equids (Martínez-Maza et al. 2014; Nacarino-Meneses et al. 2016a). In our Pleistocene equid sample, we have identified a maximum of 5 and 6 CGMs in the metapodial cortex of *E. steinheimensis* and *E. mosbachensis* respectively (Fig. 3). These results suggest that the minimum longevity of *E. steinheimensis* is 5 years, while it is of 6 years in *E. mosbachensis*. Although the number of CGMs identified in the metapodial cortex of these extinct equids is similar to that found in the limb bones of *E. hemionus* (Nacarino-Meneses et al. 2016a), the small sample size of the present research limit us to perform a comparison with enough confidence between the longevity of extinct species (*E. steinheimensis* and *E. mosbachensis*) and that of extant equids. Further studies with a larger sample size are necessary, hence, to estimate the longevity of these Middle Pleistocene species.

Size variation in Old World *Equus*: environment and life history

Our life history reconstruction of *E. mosbachensis* and *E. steinheimensis* indicates that these Middle Pleistocene species grew at higher rates than extant horses (Fig. 2 and 4). As resource availability is the main selection pressure acting on individual growth rate (Palkovacs 2003), the difference in adult body size between extant and Middle Pleistocene equids would likely be influenced by the resource availability of each habitat. On the one hand, paleoenvironmental reconstructions on Mosbach (Cromerian interglacial (MIS 13, 15); Kahlke et al. 2011) suggest open steppe landscapes interrupted by warm and humid episodes with extended forests to be the main habitats at this fossil site (Maul et al. 2000; Kahlke et al. 2011). Steinheim horse sample, on the other hand, is thought to be originated in the Holsteinian interglacial (MIS11) (Van Asperen 2013), which is characterized by temperate, humid and forested environments (Nitychoruk et al. 2005). Specifically, Steinheim site during this interglacial is thought to present a temperate humid habitat of woodland and shrubland (Pushkina et al. 2014). Extant Grevy's zebra also occurs in grasslands and shrublands, but its habitat is considered as arid or semiarid (Rubenstein et al. 2016) with a negative mean annual climatic water balance (Schulz and Kaiser 2013). Thus, the habitat of *E. grevyi* can be considered as poor-resourced in comparison with that of *E. steinheimensis* or *E. mosbachensis*. The drier habitat of the Grevy's zebra probably forces it to grow at lower rates than extinct *Equus* (Fig. 2 and 4) following the model of Palkovacs (2003), which finally results in a smaller adult body size for *E. grevyi* than for Middle Pleistocene taxa. A similar reasoning applies to *E. hemionus*, which also grows at lower rates than *E. steinheimensis* and *E. mosbachensis* (Fig. 2 and 4). The Asiatic wild ass is endemic of the Gobi desert, one of the most arid habitats of the world (Kaczensky et al. 2015). This poor-resourced environment also limits the growth rate of *E. hemionus* and, hence, its final body size.

Along with modifications in growth rate, the life history model proposed by Palkovacs (2003) postulates that age at maturity also influences adult body size. However,

and as previously mentioned, we could not obtain information about this LH trait from our histological analysis due to the characteristic of the sample studied (e.g. lack of femora). Following this model (Palkovacs 2003), we would expect that the fast-growing Middle Pleistocene equids present an advance in their age at maturity in comparison with extant taxa, although future histological studies on femora (Nacarino-Meneses et al. 2016a) must be done to confirm this preliminary hypothesis. Interestingly, the hypothesis of an earlier maturation in the Middle Pleistocene species *E. mosbachensis* and *E. steinheimensis* conforms to the predictions of life history theory in environments where there is a high extrinsic mortality pressure (i.e. predation) (Roff 1992; Stearns 1992; Roff 2002). In these circumstances, theory predicts that organisms mature early to reduce the time of exposure to juvenile mortality (Stearns 2000). Paleontological and ecological data indeed suggest differences in levels of extrinsic mortality between Middle Pleistocene equids and extant species. Thus, while important potential predators for equids such as felids (*Lynx issiodorensis*, *Panthera gombaszoegensis*, *Panthera leo fossilis*, *Panthera pardusi*, *Acinonyx pardinensis*, *Homotherium*), canids (*Canis lupus mosbachensis*, *Cuon alpinus priscus*, *Cuon dubius stehlini*) and hyaenids (*Pliocrocuta perrieri*, *Crocuta spelaea*) have been found in Mosbach or Steinheim sites (Adam 1954; Kahlke 1961; Kahlke 1975), the extant *E. grevyi* and *E. hemionus* are threatened by a few number of carnivore species (Churcher 1993; Feh et al. 2001).

Conclusions

Our study infers, for the first time, several life history traits of European Middle Pleistocene *Equus* from the histological analysis of their metapodia. Bone histology and growth reconstruction performed in these bones indicate higher growth rates for the extinct *E. mosbachensis* and *E. steinheimensis* in comparison with extant representatives of the group (*E. hemionus* and *E. grevyi*). Their occurrence in temperate and humid habitats during European interglacials explains the higher growth rates found in these extinct equids, as they dwelt in resource-richer environments than those inhabited today by the extant Asiatic wild ass and the Grevyi's zebra. The resource levels of each habitat seems to be, thus, one of the main selection pressures acting upon individual growth rate and finally determining body size in *Equus*. The influence of other key life history traits, such as age at maturity, in determining the adult body size of these mammals could not be assessed in the present research, although some hypotheses are proposed. Our first approach to the skeletochronology of these Middle Pleistocene equids suggests a similar age at epiphyseal fusion for the metapodia in *E. mosbachensis* and *E. steinheimensis* and extant *Equus*, and yields a minimum age at death for these extinct species. In the present study, we also provide estimates of the adult (in terms of body mass) and the neonatal body size (considering the perimeter of the NL as a proxy of this size) of *E. mosbachensis* and *E. steinheimensis*. Our results match previous adult weight estimations for these extinct equids and show that their size at birth is the expected from allometric scaling.

Acknowledgments

We thank Reinhard Ziegler for access to the collections of the Staatliches Museum für Naturkunde (Stuttgart, Germany) and for permission to cut the metapodia of *E. steinheimensis* and *E. mosbachensis*. We are also grateful to Renate Schafberg and Thomas Kaiser for loans and permission to cut bones from the collections of the Museum of Domesticated Animals of the Martin-Luther-University Halle-Wittenberg (Halle, Saale, Germany) and the Zoological Institute of Hamburg University (Hamburg, Germany) respectively. Manuel Fernández and Gemma Prats-Muñoz are acknowledged for the preparation of the histological thin-sections of the study. We are also in debt to Meike Köhler for discussion on this paper and revision of earlier versions of the manuscript. This work was supported by the Spanish Ministry of Economy and Competitiveness (CGL-2015-63777) and the Government of Catalonia (2014-SGR-1207; CERCA Programme). C.N.-M. holded a FPI grant from the Spanish Ministry of Economy and Competitiveness (BES-2013-066335) and was awarded with a fellowship for a short-term stay at the Staatliches Museum für Naturkunde (Stuttgart, Germany) from the same Ministry (EEBB-I-16-10546). G.O.-O. is supported by a FI-DGR 2016 grant from the Government of Catalonia AGAUR (2016FI_B00202).

References

Adam KD. 1954. Die mittelpleistozänen Faunen von Steinheim an der Murr (Württemberg). Quaternaria 1:131–144.

Alberdi MT, Bonadonna FP. 1988. Equidae (Perissodactyla, Mammalia): extinctions subsequent to the climatic changes. Rev. Española Paleontol. 3:39–43.

Alberdi MT, Ortiz-Jaureguizar E, Prado JL. 1998. A quantitative review of European stenonoid horses. J. Paleontol. 72:371–387.

Alberdi MT, Prado JL, Ortiz-Jaureguizar E. 1995. Patterns of body size changes in fossil and living Equini (Perissodactyla). Biol. J. Linn. Soc. 54:349–370.

Amprino R. 1947. La structure du tissu osseux envisagée comme expression de différences dans la vitesse de l'accroissement. Arch. Biol. 58:315–330.

Amson E, Kolb C, Scheyer TM, Sánchez-Villagra MR. 2015. Growth and life history of Middle Miocene deer (Mammalia, Cervidae) based on bone histology. Comptes Rendus - Palevol 14:637–645.

Van Asperen EN. 2013. Position of the Steinheim interglacial sequence within the marine oxygen isotope record based on mammal biostratigraphy. Quat. Int. 292:33–42.

Azzaroli A. 1983. Quaternary mammals and the "end-Villafranchian" dispersal event - A turning point in the history of Eurasia. Palaeogeogr. Palaeoclimatol. Palaeoecol. 44:117–139.

Azzaroli A. 1992. Ascent and decline of monodactyl equids: a case for prehistoric overkill. Ann. Zool. Fennici 28:151–163.

Blueweiss L, Fox H, Kudzma V, Nakashima D, Peters R, Sams S. 1978. Relationships between body size and some life history parameters. Oecologia 37:257–272.

Bybee PJ, Lee AH, Lamm E-T. 2006. Sizing the Jurassic theropod dinosaur *Allosaurus*: assessing growth strategy and evolution of ontogenetic scaling of limbs. J. Morphol. 267:347–359.

Calder WA III. 1984. Size, Function and Life History. New York: Dover Publications.

Cantalapiedra JL, Prado JL, Hernández Fernández M, Alberdi MT. 2017. Decoupled ecomorphological evolution and diversification in Neogene-Quaternary horses. Science 355:627–630.

Castanet J. 2006. Time recording in bone microstructures of endothermic animals; functional relationships. Comptes Rendus - Palevol 5:629–636.

Castanet J, Croci S, Aujard F, Perret M, Cubo J, de Margerie E. 2004. Lines of arrested growth in bone and age estimation in a small primate: *Microcebus murinus*. J. Zool. 263:31–39.

Castanet J, Francillon-Vieillot H, Meunier F, de Ricqlès A. 1993. Bone and individual aging. In: Hall BK, editor. Bone: A Treatise, Vol. 7. Boca Raton: CRC Press. p. 245–283.

Chinsamy-Turan A. 2005. The microstructure of dinosaur bone. Deciphering biology with fine-scale techniques. Baltimore and London: The Johns Hopkins University Press.

Churcher C. 1993. *Equus grevyi*. Mamm. Species 453:1–9.

Cubo J, le Roy N, Martinez-Maza C, Montes L. 2012. Paleohistological estimation of bone growth rate in extinct archosaurs. Paleobiology 38:335–349.

Damuth J. 1981. Population density and body size in mammals. Nature 290:699–700.

Damuth J, MacFadden BJ. 1990. Body size in mammalian Paleobiology. Estimations and biological implications. Cambridge: Cambridge University Press.

Eisenberg JF. 1990. The behavioral/ecological significance of body size in the Mammalia. In: Damuth J, MacFadden BJ, editors. Body size in mammalian Paleobiology. Estimations and biological implications. Cambridge: Cambridge University Press. p. 25–37.

Eisenmann V. 1991. Les chevaux quaternaires européens (Mammalia, Perissodactyla). Taille, typologie, biostratigraphie et taxonomie. Geobios 24:747–759.

Eisenmann V, Alberdi MT, de Giuli C, Staesche U. 1988. Studying fossil horses. Collected papers after the "New York International Hipparion Conference, 1981". Volume I: Methodology. Woodburne M, Sondaar P, editors. Leiden: E.J. Brill.

Erickson GM. 2005. Assessing dinosaur growth patterns: A microscopic revolution. Trends Ecol. Evol. 20:677–684.

Erickson GM, Rogers KC, Yerby SA. 2001. Dinosaurian growth patterns and rapid avian growth rates. Nature 412:429–433.

Ernest SKM. 2003. Life history characteristics of placental nonvolant mammals. Ecology 84:3402.

Feh C, Munkhtuya B, Enkhbold S, Sukhbaatar T. 2001. Ecology and social structure of the Gobi khulan *Equus hemionus* subsp. in the Gobi B National Park, Mongolia. Biol. Conserv. 101:51–61.

Forsten A. 1988. The small caballoid horse of the upper Pleistocene and Holocene. J. Anim. Breed. Genet. 105:161–176.

Forsten A. 1991a. Size trends in Holarctic anchitherines (Mammalia, Equidae). J. Paleontol. 65:147–159.

Forsten A. 1991b. Size decrease in Pleistocene-Holocene true or caballoid horses of Europe. Mammalia 55:407–420.

Forsten A. 1999. The horses (genus *Equus*) from the Middle Pleistocene of Steinheim, Germany. In: Haynes G, Klimowicz J, Reumer JWF, editors. Mammoths and the Mammoth Fauna: Studies of an Extinct Ecosystem. Deinsea 6. p. 147–154.

Francillon-Vieillot H, de Buffrénil V, Castanet J, Géraudie J, Meunier FJ, Sire JY, Zylberberg L, de Ricqlès A. 1990. Microstructure and mineralization of vertebrate skeletal tissues. In: Carter JG, editor. Skeletal biomineralization: patterns, processes and evolutionary trends. New York: Van Nostrand Reinhold. p. 471–530.

García-Martínez R, Marín-Moratalla N, Jordana X, Köhler M. 2011. The ontogeny of bone growth in two species of dormice: reconstructing life history traits. Comptes Rendus - Palevol 10:489–498.

Guthrie RD. 2003. Rapid body size decline in Alaskan Pleistocene horses before extinction. Nature 426:169–171.

Horner JR, de Ricqlès A, Padian K. 1999. Variation in dinosaur skeletochronology indicators: implications for age assessment and physiology. Paleobiology 25:295–304.

Horner JR, De Ricqlès A, Padian K. 2000. Long bone histology of the hadrosaurid dinosaur *Maiasaura peeblesorum*: growth dynamics and physiology based on an ontogenetic series of skeletal elements. J. Vertebr. Paleontol. 20:115–129.

Huttenlocker AK, Woodward HN, Hall BK. 2013. The biology of bone. In: Padian K, Lamm E-T, editors. Bone histology of fossil tetrapods: advancing methods, analysis, and interpretation. Berkeley: University of California Press. p. 13–34.

Janis C. 2007. The Horse Series. In: Regal B, editor. Icons of Evolution. Westport: Greenwood Press. p. 251–280.

Jordana X, Marín-Moratalla N, Moncunill-Solé B, Nacarino-Meneses C, Köhler M. 2016. Ontogenetic changes in the histological features of zonal bone tissue of ruminants: a quantitative approach. Comptes Rendus - Palevol 15:255–266.

Kaczensky P, Lkhagvasuren B, Pereladova O, Hemami M, Bouskila A. 2015. *Equus hemionus*. IUCN Red List Threat. Species e.T7951A45.

Kahlke HD. 1975. The Macro-faunas of Continental Europe during the Middle Pleistocene: Stratigraphic sequence and problems of intercorrelation. In: Butzer KW, Isaac GL, editors. After the Australopithecines. Stratigraphy, Ecology, and Culture Change in the Middle Pleistocene. The Hague: Mouton Publishers. p. 309–374.

Kahlke RD, García N, Kostopoulos DS, Lacombat F, Lister AM, Mazza PPA, Spassov N, Titov V V. 2011. Western Palaearctic palaeoenvironmental conditions during the Early and early Middle Pleistocene inferred from large mammal communities, and implications for hominin dispersal in Europe. Quat. Sci. Rev. 30:1368–1395.

Kahlke VH-D. 1961. Revision der Säugetierfaunen der klassischen deutschen Pleistozän-Fundstellen von Süßenborn, Mosbach und Taubach. Geologie 10:493–532.

Kleiber M. 1932. Body size and metabolism. Hilgardia 6:315–353.

Koenigswald W V, Smith BH, Keller T. 2007. Supernumerary teeth in a subadult rhino mandible (*Stephanorhinus hundsheirnensis*) from the middle Pleistocene of Mosbach in Wiesbaden (Germany). Paläontologische Zeitschrift 81:416–428.

Köhler M. 2010. Fast or slow? The evolution of life history traits associated with insular dwarfing. In: Pérez-Mellado V, Ramon C, editors. Islands and Evolution. Vol. 19. Maó: Institut Menorquí d'Estudis. Recerca. p. 261–280.

Köhler M, Marín-Moratalla N, Jordana X, Aanes R. 2012. Seasonal bone growth and physiology in endotherms shed light on dinosaur physiology. Nature 487:358–361.

Köhler M, Moyà-Solà S. 2009. Physiological and life history strategies of a fossil large mammal in a resource-limited environment. Proc. Natl. Acad. Sci. U. S. A. 106:20354–20358.

Kolb C, Scheyer TM, Veischegger K, Van den Hoek Ostende LW, Hayashi S, Sánchez-Villagra MR. 2015. Mammalian bone palaeohistology: a survey and new data with emphasis on island forms. PeerJ 3:e1358.

Lamm E-T. 2013. Preparation and sectioning of specimens. In: Padian K, Lamm E-T, editors. Bone histology of fossil tetrapods: advancing methods, analysis, and interpretation. Berkeley: University of California Press. p. 55–160.

Lee AH, Huttenlocker AK, Padian K, Woodward HN. 2013. Analysis of growth rates. In: Padian K, Lamm E-T, editors. Bone histology of fossil tetrapods: advancing methods, analysis, and interpretation. Berkeley: University of California Press. p. 217–251.

Lindsay EH, Opdyke ND, Johnson NM. 1980. Pliocene dispersal of the horse *Equus* and late Cenozoic mammalian dispersal events. Nature 287:135–138.

MacFadden BJ. 1986. Fossil horses from "Eohippus" (*Hyracotherium*) to *Equus*: scaling, Cope's Law, and the evolution of body size. Paleobiology 12:355–369.

MacFadden BJ. 1992. Fossil horses. Systematics, Paleobiology, and Evolution of the Family Equidae. Cambridge: Cambridge University Press.

MacFadden BJ. 2005. Fossil Horses - Evidence for Evolution. Science 307:1728–1730.

de Margerie E, Cubo J, Castanet J. 2002. Bone typology and growth rate: Testing and quantifying "Amprino's rule" in the mallard (*Anas platyrhynchos*). Comptes Rendus - Biol. 325:221–230.

de Margerie E, Robin J-P, Verrier D, Cubo J, Groscolas R, Castanet J. 2004. Assessing a relationship between bone microstructure and growth rate: a fluorescent labelling study in the king penguin chick (*Aptenodytes patagonicus*). J. Exp. Biol. 207:869–879.

Marín-Moratalla N, Jordana X, García-Martínez R, Köhler M. 2011. Tracing the evolution of fitness components in fossil bovids under different selective regimes. Comptes Rendus - Palevol 10:469–478.

Marín-Moratalla N, Jordana X, Köhler M. 2013. Bone histology as an approach to providing data on certain key life history traits in mammals: implications for conservation biology. Mamm. Biol. 78:422–429.

Martínez-Maza C, Alberdi MT, Nieto-Diaz M, Prado JL. 2014. Life-history traits of the miocene *Hipparion concudense* (Spain) inferred from bone histological structure. PLoS One 9:e103708.

Maul LC, Rekovets L, Heinrich W-D, Keller T, Storch G. 2000. *Arvicola mosbachensis* (Schmidtgen 1991) of Mosbach 2: a basic sample for the early evolution of the genus and a reference for further biostratigraphical studies. Senckenbergiana lethaea 80:129–147.

McHorse BK, Biewener AA, Pierce SE. 2017. Mechanics of evolutionary digit reduction in fossil horses (Equidae). Proc. R. Soc. B Biol. Sci. 284:20171174.

McNab BK. 1990. The physiological significance of body size. In: Damuth J, MacFadden BJ, editors. Body size in mammalian Paleobiology. Estimations and biological implications. Cambridge: Cambridge University Press. p. 11–23.

Moehlman PD, Rubenstein DI, Kebede F. 2013. *Equus grevyi*. IUCN Red List Threat. Species:e. T7950A21070406.

Moncunill-Solé B, Orlandi-Oliveras G, Jordana X, Rook L, Köhler M. 2016. First approach of the life history of *Prolagus apricenicus* (Ochotonidae, Lagomorpha) from Terre Rosse sites (Gargano, Italy) using body mass estimation and paleohistological analysis. Comptes Rendus - Palevol 15:227–237.

Nacarino-Meneses C, Jordana X, Köhler M. 2016a. Histological variability in the limb bones of the Asiatic wild ass and its significance for life history inferences. PeerJ 4:e2580.

Nacarino-Meneses C, Jordana X, Köhler M. 2016b. First approach to bone histology and skeletochronology of *Equus hemionus*. Comptes Rendus - Palevol 15:267–277.

Nacarino-Meneses C, Köhler M. Accepted. Limb bone histology records birth in mammals. PLoS ONE

Nitychoruk J, Bińka K, Hoefs J, Ruppert H, Schneider J. 2005. Climate reconstruction for the Holsteinian Interglacial in eastern Poland and its comparison with isotopic data from Marine Isotope Stage 11. Quat. Sci. Rev. 24:631–644.

Nowak RM. 1999. Walker's mammals of the world. Baltimore and London: The Johns Hopkins University Press.

Orlandi-Oliveras G, Jordana X, Moncunill-Solé B, Köhler M. 2016. Bone histology of the giant fossil dormouse *Hypnomys onicensis* (Gliridae, Rodentia) from Balearic Islands. Comptes Rendus - Palevol 15:238–244.

Orlando L. 2015. Equids. Curr. Biol.:R973–R978.

Ortiz-Jaureguizar E, Alberdi MT. 2003. The pattern of body mass changes in the Hipparionini (Perissodactyla, Equidae) of the Iberian Peninsula during the Upper Miocene-Upper Pliocene. Coloquios Paleontol. 1:499–509.

Padian K, de Ricqlès A, Horner JR. 2001. Dinosaurian growth rates and bird origins. Nature 412:405–408.

Palkovacs EP. 2003. Explaining adaptive shifts in body size on islands: a life history approach. Oikos 103:37–44.

Peters RH. 1983. The ecological implications of body size. Cambridge: Cambridge University Press.

Pushkina D, Bocherens H, Ziegler R. 2014. Unexpected palaeoecological features of the Middle and Late Pleistocene large herbivores in southwestern Germany revealed by stable isotopic abundances in tooth enamel. Quat. Int. 339–340:164–178.

Roff DA. 1992. The evolution of life histories. Theory and analysis. New York: Chapman and Hall.

Roff DA. 2002. Life history evolution. Sunderland: Sinauer Associates.

Rubenstein D, Low Mackey B, Davidson Z, Kebede F, King SR. 2016. *Equus grevyi*. IUCN Red List Threat. Species:e.T7950A89624491.

Saarinen J, Eronen J, Fortelius M, Seppä H, Lister AM. 2016. Patterns of diet and body mass of large ungulates from the Pleistocene of Western Europe, and their relation to vegetation. Palaeontol. Electron. 19:1–58.

Schöpke K, Stubbe A, Stubbe M, Batsaikhan N, Schafberg R. 2012. Morphology and variation of the Asiatic wild ass (*Equus hemionus hemionus*). Erforsch. Biol. Ressourcen der Mongolei 12:77–84.

Schulz E, Kaiser TM. 2013. Historical distribution, habitat requirements and feeding ecology of the genus *Equus* (Perissodactyla). Mamm. Rev. 43:111–123.

Shoemaker L, Clauset A. 2014. Body mass evolution and diversification within horses (family Equidae). Ecol. Lett. 17:211–220.

Silver IA. 1963. The aging of domestic animals. In: Brothwell D, Higgs E, editors. Science in Archaeology: a comprehensive survey of progress and research. New York: Basic Books. p. 250–268.

Simpson GG. 1953. The major features of evolution. New York: Columbia University Press.

Stanley SM. 1973. An explanation for Cope's rule. Evolution 27:1–26.

Stearns SC. 1992. The evolution of life histories. New York: Oxford University Press.

Stearns SC. 2000. Life history evolution: successes, limitations, and prospects. 87:476–486.

Strömberg CAE. 2006. Evolution of hypsodonty in equids: testing a hypothesis of adaptation. Paleobiology 32:236–258.

Turner-Walker G, Mays S. 2008. Histological studies on ancient bone. In: Pinhasi R, Mays S, editors. Advances in human paleopathology. Chichester: John Wiley & Sons, Ltd. p. 121–146.

Western D. 1979. Size, life history and ecology in mammals. Afr. J. Ecol. 17:185–204.

Woodward HN, Freedman Fowler EA, Farlow JO, Horner JR. 2015. *Maiasaura*, a model organism for extinct vertebrate population biology: a large sample statistical assessment of growth dynamics and survivorship. Paleobiology 41:503–527.

Woodward HN, Padian K, Lee AH. 2013. Skeletochronology. In: Padian K, Lamm E-T, editors. Bone histology of fossil tetrapods: advancing methods, analysis, and interpretation. Berkeley: University of California Press. p. 195–215.

- Chapter 8 -

Reconstructing molar growth from enamel histology in extant and extinct *Equus*

Reproduced from:

Nacarino-Meneses C., Jordana X., Orlandi-Oliveras G. & Köhler M. (2017)
Scientific Reports 7: 15965. DOI: 10.1038/s41598-017-16227-2

www.nature.com/scientificreports

SCIENTIFIC REPORTS

OPEN

Reconstructing molar growth from enamel histology in extant and extinct *Equus*

Received: 12 June 2017
Accepted: 9 November 2017
Published online: 21 November 2017

Carmen Nacarino-Meneses[1], Xavier Jordana[2], Guillem Orlandi-Oliveras[1] & Meike Köhler[1,3]

The way teeth grow is recorded in dental enamel as incremental marks. Detailed analysis of tooth growth is known to provide valuable insights into the growth and the pace of life of vertebrates. Here, we study the growth pattern of the first lower molar in several extant and extinct species of *Equus* and explore its relationship with life history events. Our histological analysis shows that enamel extends beyond the molar's cervix in these mammals. We identified three different crown developmental stages (CDS) in the first lower molars of equids characterised by different growth rates and likely to be related to structural and ontogenetic modifications of the tooth. Enamel extension rate, which ranges from ≈400 μm/d at the beginning of crown development to rates of ≈30 μm/d near the root, and daily secretion rate (≈17 μm/d) have been shown to be very conservative within the genus. From our results, we also inferred data of molar wear rate for these equids that suggest higher wear rates at early ontogenetic stages (13 mm/y) than commonly assumed. The results obtained here provide a basis for future studies of equid dentition in different scientific areas, involving isotope, demographic and dietary studies.

The reconstruction of tooth growth is essential to understanding the biology and palaeobiology of mammals[1,2], as dental development is closely related with a species' life history[2–6]. For instance, the eruption of the first permanent molar correlates well with weaning[4,7]. Similarly, the emergence of the third molar correlates with skeletal maturity[2]. Thus, the estimation of rate and duration of molar growth in extant and extinct vertebrates yields key information about their pace of life[1–3,8–11]. Furthermore, an understanding of tooth growth is crucial for palaeoecological and palaeobiological studies that involve the analysis of stable isotopes[12,13]. Tooth crowns preserve a temporal record of isotopic variation that can be related to changes in climatic conditions and/or modifications of an animal's behaviour[14–18]. Therefore, the rate and duration of tooth growth must be precisely known to accurately develop isotopic sampling methods[19] and correctly interpret the isotopic data obtained in this type of investigation[12,13].

The pace of growth and development of teeth is recorded, among others, in dental enamel[20]. From the cusp to the root, enamel is rhythmically deposited by enamel-forming cells called ameloblasts in the amelogenesis process, which involves a first stage of enamel secretion followed by a second phase of enamel maturation[21,22]. As a result, the histological microstructure of dental tissue registers the pattern of enamel growth in the form of incremental markings[20,23]. Incremental features have traditionally been classified as short- or long-period marks[24]. The first ones include cross-striations and laminations and represent a circadian rate of enamel formation[23,25,26]. Retzius lines, on the other hand, are long-period lines that indicate the successive positions of the developing enamel front[20,23]. Counts and measurements of incremental markings in enamel provide the basis for quantifying tooth growth, estimating various dental growth parameters such as daily secretion rate or extension rate, and for calculating crown formation time[1].

In large herbivorous mammals, studies aimed at reconstructing tooth growth through the analysis of enamel incremental markings have increased considerably in number over the last years[3,8–11,19,27–29]. However, an analysis of life history parameters from the enamel microstructure in key groups of evolution such as equids[30] is still lacking. Only the work of Hoppe *et al.*[13] provided some data about the periodicity and disposition of incremental lines in the enamel of the domestic horse, but recently their results have been questioned by other authors[28,31].

[1]Institut Català de Paleontologia Miquel Crusafont (ICP), Campus de la Universitat Autònoma de Barcelona, 08193 Bellaterra, Barcelona, Spain. [2]Unitat d'Antropologia Biològica, BABVE department, Universitat Autònoma de Barcelona (UAB), 08193 Bellaterra, Barcelona, Spain. [3]ICREA, Pg. Lluís Companys 23, 08010, Barcelona, Spain. Correspondence and requests for materials should be addressed to C.N.-M. (email: carmen.nacarino@icp.cat)

Indeed, the development of equid teeth has hitherto been determined from radiographic observations[13,32–34] or by measurements of the crown height[12,35], but it has not yet been studied using dental histology.

In the present study, we aim to analyse the enamel microstructure of several wild equid species to provide information about the dental growth pattern and development in this mammalian group. Nowadays, the genus *Equus* comprises the wild extant species of zebras (*E. zebra*, *E. grevyi*, *E. quagga*), asses (*E. africanus*, *E. kiang*, *E. hemionus*) and horses (*E. ferus*) that dwell in different areas of Africa and Asia[36,37]. Here, we quantified incremental markings and enamel growth parameters in the Asiatic wild ass (*E. hemionus*), plains zebra (*E. quagga*) and Grevy's zebra (*E. grevyi*). These three taxa are the most appropriate ones to infer the dental growth pattern of the clade, as they cover most of the range of habitat, body mass and life history traits observed in extant wild equids[38–42]. To apply our results to the equid fossil record, we examined the dental enamel of Pleistocene fossil specimens of *E. ferus* and *E. hydruntinus* to infer their pattern of molar growth. These two different-sized equids are frequent in European Late Pleistocene mammal assemblages[43]. Because body size is a fundamental life history trait that tightly correlates with other biological traits such as growth rate[44–46], we calculated their molar growth rate as a proxy of their overall growth rate to understand whether the differences in body size resulted from changes in life history.

Results

Dental histology of extant *Equus*. Enamel, dentine and cementum are the three dental tissues that conform the molar crown in all extant *Equus* (Figs 1a,b; 2b). A thin layer of enamel is also observable in the region that is macroscopically considered as the root[13,32,47] (Fig. 2). Therefore, the molar crown, understood as the part of the tooth composed of enamel[22], extends further than macroscopically considered[47,48] (Fig. 2). To avoid confusion between the morphological and histological distinction of tooth root in *Equus* first molars, the term root will be used here to designate the most apical area of the tooth which is enamel-free[49] (Fig. 2b).

Laminations are fine incremental markings running parallel to the enamel formation front[20] and are the most common incremental features identified in the enamel of our equid sample (Fig. 1c). Considering that laminations follow the one-day periodicity previously described in other herbivorous mammals[3,8,26–28], we calculated the crown formation time (CFT) of unworn teeth. As it is shown in Table 1, CFT estimations are a reasonable match for the age of the specimen previously determined by classical methods, confirming the daily periodicity of laminations in equids.

Long-termed Retzius lines, prominent lines formed at an oblique angle to the enamel prisms[23], are also observed in the enamel of extant equids (Fig. 1d), mainly in cervical enamel. The periodicity of these features in our equid sample range from 5 to 7 days in *E. hemionus* and 5 to 6 days in both zebra species (*E. grevyi* and *E. quagga*) (RI, Table 2).

A mean daily secretion rate of ≈17–18 μm/d was calculated in the enamel of extant equids (DSR, Table 2) regardless of the part of the crown (occlusal, cervical) or the enamel zone (inner, outer) analysed (Kruskal-Wallis, p-value > 0.05, Supplementary Table S1, S2). The Asiatic wild ass shows the slowest daily secretion rate within the extant species, while Grevy's zebra presents the fastest rate (Table 2, Fig. 3). However, no significant differences have been observed among the species analysed (Kruskal-Wallis, p-value > 0.05, Supplementary Table S3) (Fig. 3).

The pace of growth of the first lower molars of extant equids (crown height against crown formation time) is plotted in Fig. 4a and b. As equid teeth start to wear before the crown is completely formed[32,49], crown development is reconstructed from the cusp tip in unworn teeth (Fig. 4a) and from the root in worn molars (Fig. 4b). Differences in growth between species have only been identified in the most cervical enamel (Fig. 4b), concretely, at the beginning of the morphological root[13,32,47] (Fig. 2a). As Fig. 4b shows, *E. hemionus* deposits enamel in that part of the tooth for a longer period than both zebras. In all studied species, unworn teeth without roots experienced fast linear growth (Fig. 4a) while growth curves of worn molars fit to a polynomial of quadratic order (Fig. 4b). These results indicate that teeth experience different types and rates of growth during formation. Furthermore, the inflection point of the polynomial growth curve (Fig. 4b) is related to macroscopic anatomical changes in the tooth, as it matches the crown divergence that results in the formation of the morphological roots (Fig. 2a). Enamel, then, is still being deposited after the morphological roots are formed, but at much lower rates (Fig. 4b,e).

Three different crown developmental stages (CDS) that significantly differ in enamel extension rate (Kruskal-Wallis, p-value < 0.05, Supplementary Table S4) could be established based on the different growth patterns (Fig. 4). During a first stage of fast linear growth (Fig. 4a) enamel extends at a mean rate of 350–400 μm/d (Fig. 4c, Table 2). At the second stage of development, which corresponds to the fastest period of polynomial growth (Fig. 4b), enamel extension progressively decreases up to rates of ≈130 μm/d (Fig. 4d, Table 2). At the third stage, enamel extension rate (EER) decreases quickly to ≈30 μm/d (Fig. 4e, Table 2), representing the slowest period of polynomial growth (Fig. 4b). The decrease in the rate of enamel extension observed throughout tooth formation is mainly due to changes in the enamel formation front angle (EFFa), which presents a range of values that vary from ≈1° on the tooth cusp to ≈11° near the root (Table 2). The EFFa reflects the number of ameloblasts that are secreting matrix at the same time, with smaller angles indicating higher EERs because more ameloblasts are activated along the EEF[3,50]. Thus, the number of activated ameloblasts in the first lower molars of extant equids is progressively reduced during the development of their crowns.

No significant differences have been found in the rate of enamel extension between the different species of extant *Equus* analysed within each CDS (Kruskal-Wallis, p-value > 0.05, Supplementary Table S5). This suggests that EER is conservative and characteristic for each developmental stage in extant *Equus*. On that basis, we reconstructed the complete growth of the crown for the first lower molars of the Asiatic wild ass (Fig. 5a), establishing the overlap area between unworn and worn teeth where similarities in EER were found (Fig. 5b). The timing of several ontogenetic and structural changes of the first molar, such as the time of emergence, eruption and crown

www.nature.com/scientificreports/

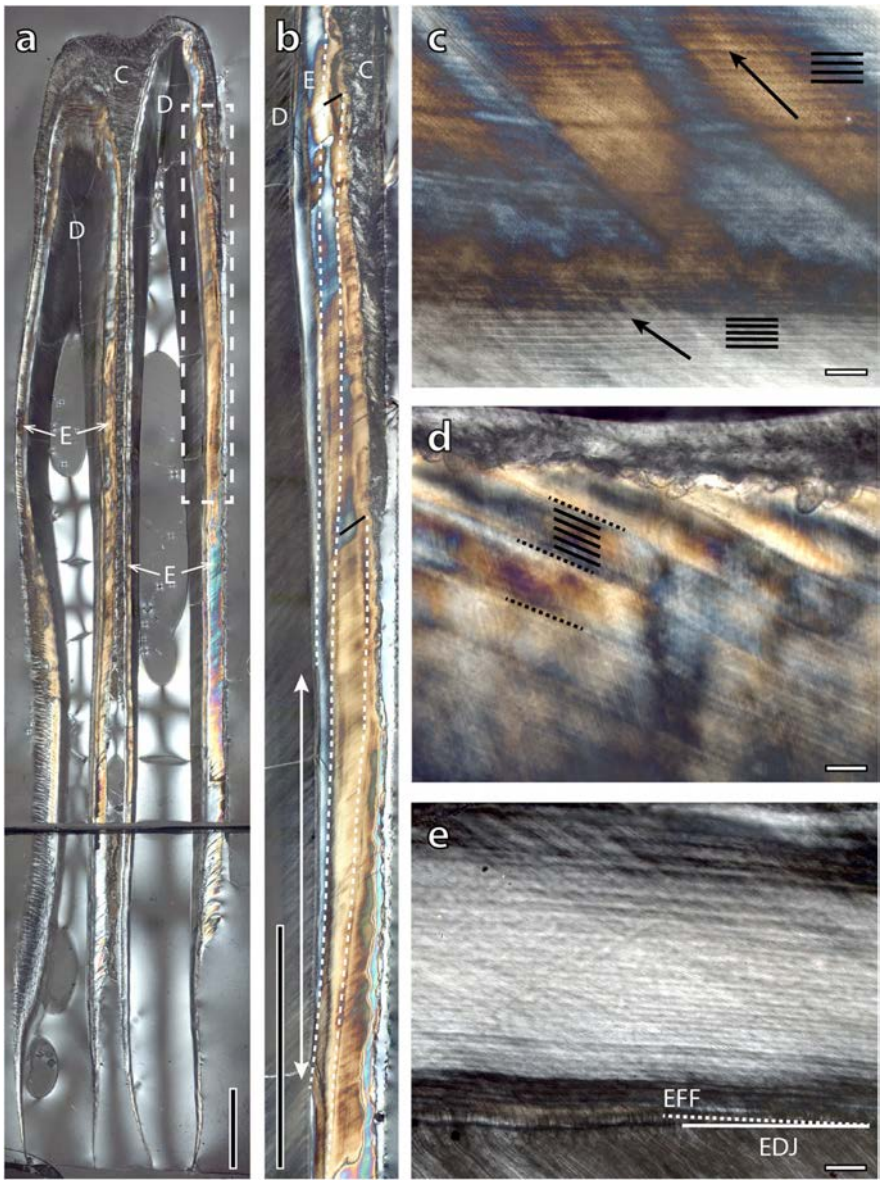

Figure 1. Dental histology of *Equus* and methodologies used to analyse the pattern of enamel growth. (**a**) Longitudinal section of *Equus hemionus*' first lower molar (IPS83151) mounted on two different slides. White dashed rectangle indicates the magnified area in b. (**b**) Methodology employed to calculate the crown formation time (CFT; IPS83151). The distance between incremental lines (white dashed lines) is measured following the course of enamel prisms (black lines) and divided by the daily secretion rate to determine the time required to form a specific portion of the enamel dentine junction (EDJ; white doubled arrow). (**c**) Laminations (black lines) and enamel prisms (black arrows) identified in the enamel of *E. hemionus* (IPS92347). (**d**) Laminations (black lines) between consecutive Retzius lines (black dashed lines) in the outer enamel of *E. grevyi* (IPS84963). (**e**) Angle between the enamel dentine junction (EDJ; white line) and the enamel formation front (EFF; white dashed line) in *E. quagga* (IPS92346). C = cementum; D = dentine; E = enamel. Black scale bars: 5 mm; white scale bars = 50 μm.

divergence obtained from dental histology (Fig. 5a), agrees well with data in the literature on timing of occurrence of these events in equid's first molars[32,51,52]. This confirms the validity of the growth reconstruction based on EER for this species and indicates that the complete crown of the first lower molar of *E. hemionus* takes about three years to be formed. Changes in curve's slope coinciding with teeth eruption and crown divergence indicate the start of the different CDS (Fig. 5a).

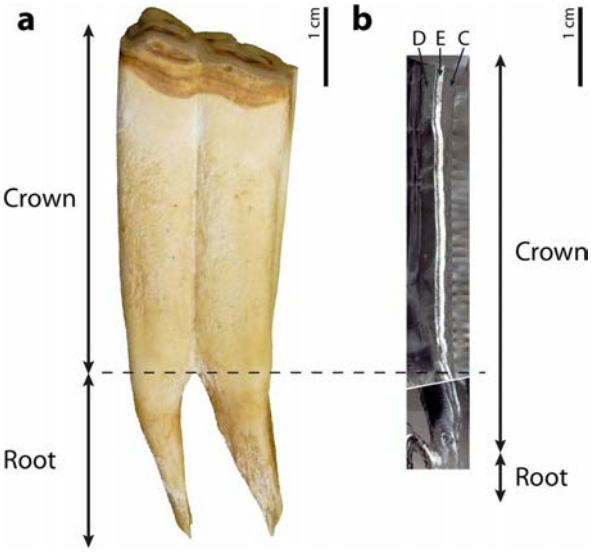

Figure 2. Macroscopic (**a**) *versus* histological (**b**) distinction of tooth crown and root. Figure shows that dental enamel extends beyond the limit of the macroscopic crown (black dashed line). (**a**) First lower molar of *E. quagga* (IPS92346) in buccal view. (**b**) Histological section of the buccal cusp in IPS92346. C = cementum; D = dentine; E = enamel.

Species	Code	CFT (days)	CFT (months)	Estimated age (months)
E. hemionus	IPS83153	137	5	0 – 6
	IPS83151	184	6	6 – 12
E. quagga	IPS92345	134	4	0 – 3
	IPS92342	160	5	3 – 6
E. grevyi	IPS84964	117	4	0 – 6

Table 1. Age and crown formation time (CFT) estimates in unworn teeth of extant species.

We performed superimposition of teeth considering similarities in EER to infer data about wear rate in the species. As shown in Fig. 5b, the cervical portion of a recently erupted tooth from a one-year old individual (IPS83155) presents similar extension rates as the occlusal part of the crown of a seven-year-old tooth (IPS92347), while EER values at the mid-crown of IPS92347 match those estimated on the occlusal enamel of a thirteen-year-old individual (IPS92339). Superimposition of teeth indicates that approximately 110 mm of tooth crown has been worn down in 12 years: almost 80 mm during the first six years of life and around 30 mm during the next six (Fig. 5). Thus, a wear rate of around 13 mm/y is estimated for the first six-year period, while this is 5 mm/y for the second one. These results indicate that most of the crown formed during the first year of life (IPS83155, Fig. 5b) is worn away by when the individual is seven years old (IPS92347, Fig. 5b).

Dental histology of fossil *Equus*. As in extant *Equus*, both laminations and Retzius lines are identified in the enamel of the Pleistocene fossils studied. Long-termed Retzius lines present a periodicity of 5 to 7 days in *E. ferus*, while they are deposited every 4 to 6 days in *E. hydruntinus* (Table 2).

The fossil species analysed (*E. ferus* and *E. hydruntinus*) secrete enamel at similar rates (Kruskal-Wallis, p-value > 0.05, Supplementary Table S3) (Fig. 3, Table 2). When compared with extant species, however, differences in daily secretion rate have been found between *E. hydruntinus*, *E. quagga* and *E. hemionus* (Fig. 3) (Kruskal-Wallis, p-value < 0.05, Supplementary Table S3). The small extinct species *E. hydruntinus* secretes enamel a mean rate of ≈19 μm/d, while the Plains zebra and the Asiatic wild ass do at ≈17 μm/d (Fig. 3, Table 2).

We analysed the rate of enamel extension of each fossil tooth based on its macroscopic appearance and the CDS established for extant equids (Fig. 6). The EER of IPS87523 (*E. hydruntinus* Stage I, Table 2) matches the first stage of crown development (Kruskal-Wallis, p-value > 0.05, Supplementary Table S6) (Fig. 6) and its macroscopic appearance (slight wear and no presence of morphological roots, Table 3) is also that expected for this developmental stage. The rate of enamel extension of IPS87540, IPS87497 and IPS87509 (*E. hydruntinus* and *E. ferus* Stage II, Table 2) corresponds to that estimated for the second phase of crown formation (Kruskal-Wallis, p-value > 0.05, Supplementary Table S3). As these teeth show moderate wear and macroscopic roots (Table 3), a stage II of development was expected for their crowns too. These results on EER of fossil *Equus* confirm that this dental growth parameter is very conservative within the genus.

Species	BM (kg)[42,58]	HI[58]	DSR (μm/d)		RI (days)	
			N	Mean ± SD	N	Min. — Max.
E. hemionus	230	4.76	45	16.92 ± 2.3	18	5 — 7
E. quagga	257	4.44	45	16.98 ± 1.64	12	5 — 6
E. grevyi	384	5.19	37	17.74 ± 1.6	13	5 — 6
*E. ferus**	350	3.8	28	17.8 ± 2.48	21	5 — 7
*E. hydruntinus**	215	3.54	28	18.87 ± 2.01	22	4 — 6
Species	EER (μm/d)					
	CDS I		CDS II		CDS III	
	N	Mean ± SD	N	Mean ± SD	N	Mean ± SD
E. hemionus	28	349.28 ± 118.7	23	123.46 ± 76.32	48	31.38 ± 11.58
E. quagga	14	427.08 ± 129.58	12	140 ± 65.56	17	28.21 ± 9.25
E. grevyi	7	358.39 ± 101.33	13	153.37 ± 81.26	17	36.83 ± 12.58
*E. ferus**	—	—	26	138.04 ± 52.74	—	—
*E. hydruntinus**	12	256.82 ± 122.64	21	97.40 ± 45.01	—	—
Species	EFFa (degrees)					
	CDS I		CDS II		CDS III	
	N	Mean ± SD	N	Mean ± SD	N	Mean ± SD
E. hemionus	25	1.25 ± 0.54	17	3.35 ± 0.87	17	10.63 ± 3.4
E. quagga	14	1.49 ± 0.63	9	3.34 ± 0.76	16	11.13 ± 3.85
E. grevyi	8	1.21 ± 0.3	7	2.9 ± 0.87	15	11.73 ± 3.37
*E. ferus**	—	—	39	3.47 ± 1.46	—	—
*E. hydruntinus**	17	2.33 ± 1.16	20	4.34 ± 2.27	—	—

Table 2. Body mass, hypsodonty index and values of the different enamel growth parameters inferred in extant and extinct equids. BM = body mass; HI = hypsodonty index; DSR = daily secretion rate; RI = repeat interval; EER = enamel extension rate; EFFa = enamel formation front angle; N = number of observations; SD = standard deviation; Min = minimum; Max = maximum. The star (*) indicates fossil specimens.

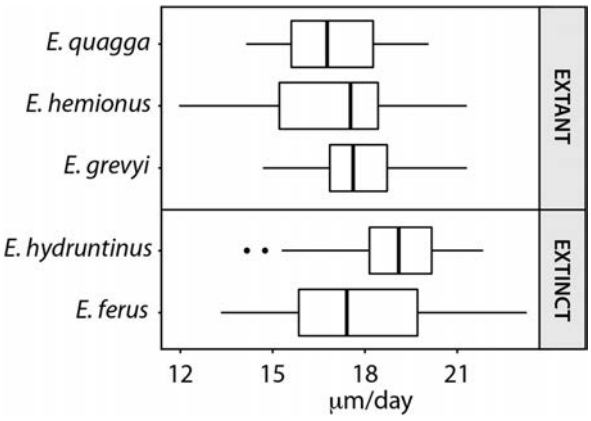

Figure 3. Boxplot of the daily secretion rate (DSR) of the enamel in the extant and extinct species of *Equus* analysed.

Discussion

The aim of the present research was to reconstruct, for the first time, the pace of growth and development of the first lower molars in *Equus* based on the analysis of enamel microstructure. Until now, most of the research concerning enamel histology has been limited to low-crowned, brachydont teeth of different primate species[1] and only a few studies have focused on hypsodont mammals[3,8,28,53]. Our findings in three species of extant (*E. hemionus*, *E. quagga* and *E. grevyi*) and two Pleistocene (*E. ferus* and *E. hydruntinus*) equids contribute to the knowledge of enamel microstructure in high-crowned vertebrates and provide the basis for future research in Perissodactyls. However, the results obtained here are not only relevant for histological research but also for isotopic studies on fossil and archaeological vertebrates. *Equus*' teeth, concretely equid enamel, are widely used in palaeobiological and palaeoecological isotopic studies[15,17,18] because their extremely high crowns record several years of the individual's life[13]. A thorough understanding of the timing, geometry and rate of enamel maturation is key to interpretation of isotopic results[54]. Although enamel incremental marks do not provide relevant information about the timing[26] and/or the pattern[54] of enamel mineralization because they only register the secretory

www.nature.com/scientificreports/

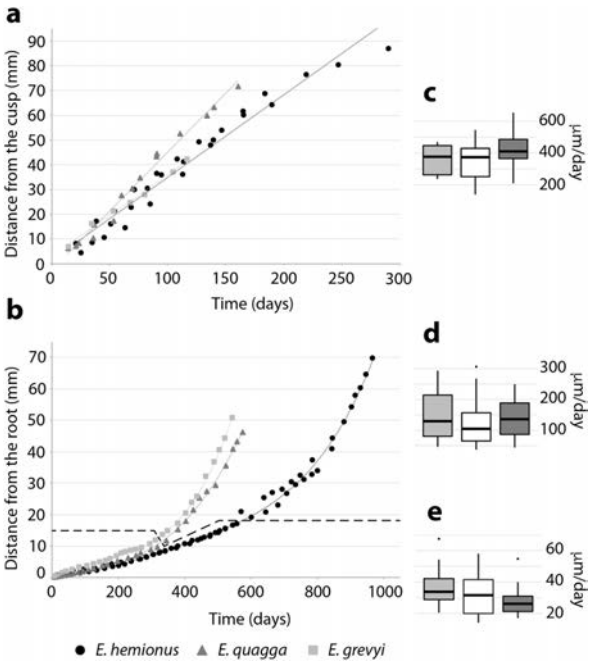

Figure 4. Crown formation time (CFT) related to crown height (**a**,**b**) and enamel extension rates (EER) (**c**,**d**,**e**) in the extant *Equus* species studied. (**a**) CFT related to crown height in unworn teeth. (**b**) CFT related to crown height in worn teeth. Dashed line separates measures obtained for the enamel that is deposited before (upward) and after (downward) the crown divergence. (**c**) EER of unworn teeth studied. (**d**) EER in macroscopic crowns of worn teeth. (**e**) EER of the enamel deposited beyond the limit of the macroscopic crown. Legend for scatter plots is shown at the bottom of the figure. 75% grey boxplot = *E. quagga*; 25% grey boxplot = *E. grevyi*; white boxplot = *E. hemionus*.

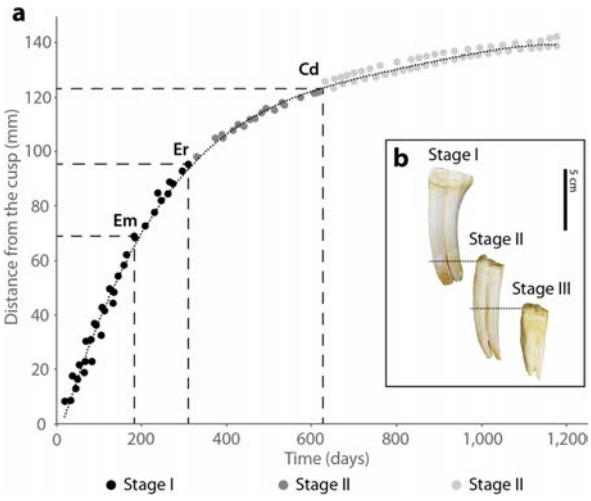

Figure 5. Reconstruction of growth of the first molar crown in *Equus hemionus* based on similarities in EER. (**a**) Crown formation time against crown height. Three different crown developmental stages (CDS) are identified from the slope of the curve. (**b**) Teeth of *E. hemionus* that differ on degree of wear and root development showing the correspondences of EER (black dashed lines) that enabled growth reconstruction (Stage I = IPS83155; Stage II = IPS92347; Stage III = IPS92339). Em = emergence; Er = eruption; Cd = crown divergence. Colour legend is shown at the bottom of the figure.

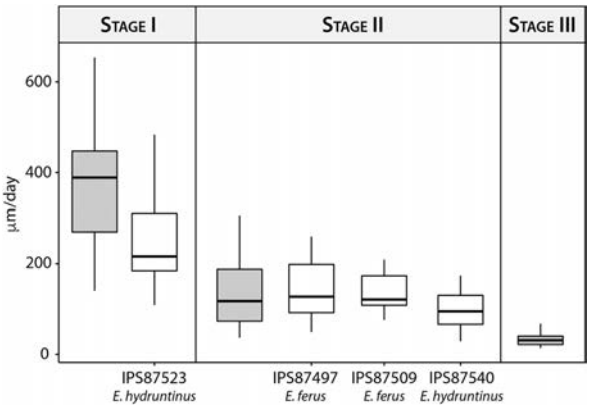

Figure 6. Enamel extension rate of Pleistocene *Equus* specimens compared with the mean enamel extension rate of the three crown developmental stages established for extant species (grey boxplots).

Species	Code	Eruption stage	Wear degree	Estimated age	Site	Collection
E. hemionus	IPS83153	NE	Unworn	0 – 6 mo.	Hagenbeck Zoo	ZIHU
	IPS83151	E	Unworn	6 – 12 mo.	Hagenbeck Zoo	ZIHU
	IPS83155	E	Slight	1 – 2 y.	Hagenbeck Zoo	ZIHU
	IPS92347	E	Moderate	7 y.	Hagenbeck Zoo	ZIHU
	IPS92339	E	Advanced	13 y.	Hagenbeck Zoo	ZIHU
E. quagga	IPS92345	NE	Unworn	0 – 3 mo.	Hagenbeck Zoo	ZIHU
	IPS92342	E	Unworn	3 – 6 mo.	Hagenbeck Zoo	ZIHU
	IPS92346	E	Moderate	5 y.	Hagenbeck Zoo	ZIHU
E. grevyi	IPS84964	NE	Unworn	0 – 6 mo.	Hagenbeck Zoo	ZIHU
	IPS84963	E	Moderate	5 y.	Hagenbeck Zoo	ZIHU
*E. ferus**	IPS87509	E	Moderate	Adult	La Carihuela	ICP
	IPS87497	E	Moderate	Adult	La Carihuela	ICP
*E. hydruntinus**	IPS97523	E	Moderate	Adult	La Carihuela	ICP
	IPS87540	E	Slight	Subadult	La Carihuela	ICP

Table 3. Sample studied. E: erupted; NE: no erupted; mo.: months; y: years; ZIHU: Zoological Institute of Hamburg University (Hamburg, Germany); ICP: Catalan Institute of Paleontology (Barcelona, Spain). The star (*) indicates fossil species.

stage of amelogenesis[20], these features are known to yield accurate estimations on tooth growth rates[19]. Indeed, our results on enamel extension rates (≈130 µm/d or ≈48 mm/y for the second CDS, Table 2) are similar to the maturation rates reported for equids (40–60 mm/y)[55]. Thus, rates of enamel extension seem to be a good proxy of rates of enamel maturation in *Equus*. This finding, along with the detailed description of the growth and development of the equid crown presented here, will help in the understanding of the isotopic microsamples extracted from this mammalian group[12,13].

Crown height and formation time. To date, the timing and pace of crown formation in equid teeth has been assessed by measuring crown height[12,35] and by identification of dental roots in radiographic images[13,32–34]. In agreement with previous studies[47,48], our results indicate that the external division of teeth into crown and root does not match the histological definition of these structures (Fig. 2), as dental enamel extends over the limit of what is usually considered the macroscopic crown of the tooth[47] (Fig. 2b). As enamel is characteristic of a tooth's crown[22], we suggest that this portion of the tooth should be considered part of the crown and not part of root; this view is in contrast to a previous study by Kirkland *et al.*[32]. Apart from this terminological issue, it is worth noting that the presence of enamel beyond the crown divergence might affect results of previous studies which considered this anatomical point to be the crown's end. Thus, reconstructions of crown growth that exclude its final portion[12,13] may underestimate total crown formation time, as this cervical enamel takes up to one or two years to be formed in zebras and *E. hemionus*, respectively (Fig. 4b), due to low rates of enamel extension (Fig. 4e, Table 2). On the other hand, the discrepancy between macro- and microanatomical tooth structure (Fig. 2) may lead to a miscalculation of dental indexes that involve measurements of the complete crown. For instance, the hypsodonty index usually used in palaeoecological studies[47,56] requires the identification of the crown end to measure the crown height[57]. Consequently, difficulty in differentiating the exact point where enamel ends from tooth macroanatomy[47] (Fig. 2) makes the estimation of the degree of hypsodonty in *Equus* a challenging issue. Thus,

hypsodonty values previously reported for this genus[57–59] should be viewed with caution because the crown-root transition might be not homologous when measuring crown height. Furthermore, the enamel identified in the morphological roots represents up to 1–1.5 cm of tooth height (Fig. 4b). Failure to consider this area when measuring crown height leads to underestimation of the hypsodonty index.

An alternative approach to estimating hypsodonty in equids can be made from enamel histology. Our results indicate a longer period of crown formation in *E. hemionus* than in both African zebra species (Fig. 4b), suggesting a higher hypsodonty in the former species. However, previous studies described similar hypsodonty values for these three equids[57–59]. The increase in crown height that characterises hypsodont teeth has usually been explained as an adaptation which extends the durability of the teeth in animals feeding on an abrasive diet[56,57]. Like all extant equids, *E. hemionus*, *E. quagga* and *E. grevyi* are classified as grazers[38–41,60] with similar abrasive diets[60]. However, they dwell in different habitats, which also influence tooth wear[61]. While the Asiatic wild ass is endemic on the steppe and desert plains of central Asia[38,40], *E. quagga* and *E. grevyi* usually occur in different types of African grasslands[38,41]. Our findings of an extended deposition of enamel in the Asiatic wild ass (Fig. 4b) is congruent with previous research that correlates hypsodonty and mean annual precipitation[60,61], as this species dwells in a more arid habitat. Furthermore, hypsodonty has been explained to occur in response to an increase in lifespan of the species[56,62–64]. A higher degree of hypsodonty in *E. hemionus* (Fig. 4b) is consistent with this hypothesis, as the maximum longevity reported for this species in the wild is 29 years[65], while it is 18 and 21 years for Grevy's zebra[66] and plains zebra[51], respectively. Theory suggests that in a resource-limited environment with low extrinsic mortality, natural selection favours a shift in energy allocation from reproduction to growth and maintenance[67], and that triggers extended longevity[62,64,68,69]. The Asiatic wild Ass inhabits a resource-poor environment (steppes and deserts of Asia[40]) and faces low rates of predation (grey wolves are its only known non-human predators[70]). Thus, the increase in crown height observed in *E. hemionus* can alternatively be explained as an increase in durability of its teeth to extend life span. The extended deposition of enamel in the Asiatic wild Ass has been identified after the crown divergence, at the beginning of the macroscopic root (Fig. 4b). Although, as far as we know, there are no descriptions of equid molars which are worn below the crown bifurcation, teeth with such exceptional degree of wear could still be functional. In very old horses, teeth are known to present minimal reserve crowns and very elongated roots that allow stable alveolar attachment[49]. Thus, a hypothetical equid molar worn below the crown divergence would be viable. This also supports the hypothesis of a prolonged enamel deposition in *E. hemionus* related to the extended longevity of the species, as the presence of enamel beyond the crown bifurcation increases the durability of the tooth in animals of advanced ontogenetic stages.

Crown developmental stages (CDS). Our results indicate that the rate of crown formation exponentially decreases throughout tooth development (Figs 4a,b; 5), as already suggested by Bendrey *et al.*[12]. The EER decreases from values of ≈350–400 μm/d at the beginning of crown development to rates of ≈30 μm/d at the end of crown formation (Fig. 4c–e, Table 2). A reduction on EER during crown development has also been observed in other mammalian species[1,8,10,28,31]. Based on such variation of EER along the tooth's crown, we determined three different developmental stages of the crown (CDS) in the first lower molars of extant *Equus* (Fig. 4, Table 2). During a first phase of crown formation, dental enamel grows fast and linearly (Fig. 4a,c, Table 2). The next stages of enamel development, however, follow polynomial growth (Fig. 4b). Thus, the second CDS, which presents extension rates values of around ≈130 μm/d (Fig. 4d, Table 2), corresponds to the fastest period of this polynomial growth (Fig. 4b), while CDS III represents the slowest period (Fig. 4b) with very low rates of enamel extension (Fig. 4e, Table 2). The limit between the different CDS seems to correlate with both structural and ontogenetic changes in the tooth in *E. hemionus* (Fig. 5a). Therefore, the transition from stage I to stage II matches the first molar's eruption time[52], while the beginning of stage III correlates well with the macroscopic appearance of the tooth roots in related *Equus* species[32] (Fig. 5a). Correspondence between the beginning of CDS III and the divergence of the crown has also been detected in *E. quagga* and *E. grevyi* (Fig. 4b). Our results also show that the rate of enamel extension is very conservative within the genus *Equus* and, as previously mentioned, characteristic for each CDS (Figs 4c–e; 6). This result is especially relevant for palaeodemographic studies, as EER estimations of a fragmentary fossil/archaeological equid tooth allow researchers to assigned it to a CDS and, hence, to an age category. Studies aimed to infer the life history strategy of extinct species, however, require combined analysis of the macroscopic appearance of the tooth and the microscopic examination of its EER. Thus, in the case of the estimated CDS of a fossil tooth failing to match the degree of dental wear and/or root development expected for this stage, differences in growth and, thus, in life history might be deduced for the species.

Estimation of wear rates. Superimposition of teeth of *E. hemionus* based on similarities of EER (Fig. 5) also yield data on wear rates in *Equus*. A wear rate of around 13 mm/y has been estimated for the first six years of life, a value far above the 3–5 mm/y previously reported in extant[49,71] and in extinct equids[72]. However, the latter published wear rates agree with the estimated wear rate of 5 mm/y obtained for the next six-year period. Therefore, our results suggest that (i) first lower molars of the Asiatic wild ass wear down at an exponentially decreasing rate and that (ii) wear rates are much higher at the beginning of the animal's life, as already proposed by Levine[35]. This is explained by the eruption sequence of the species. As the first molar is the first permanent tooth to erupt, and complete permanent dentition is not visible until almost the fifth year of life[52], it seems reasonable that higher wear rates in the first molar would be found at early ontogenetic stages. Due to these greater wear rates, the crown formed during the first year of life is almost worn down in a seven-year-old tooth (Fig. 5b). This observation is of special interest for the correct interpretation of isotopic values obtained from enamel microsampling in equids.

Daily Secretion Rate (DSR). The DSR of enamel in equids has recently been a matter of discussion[28,31]. The results obtained here suggest that extant equid species secrete enamel at a mean rate of ≈17–18 μm/d (Fig. 3, Table 2). These values agree well with rates of enamel apposition reported for other hypsodont mammals[3,8,27,28],

but they differ from previously published estimates of only 5 μm/d for the domestic horse[13]. Kierdorf *et al.*[29,31] considered that these lower values of enamel apposition rates reported in horses might be due to a misidentification of sub-daily incremental marks as daily marks. The daily periodicity of laminations is well-established in several mammalian taxa using experimental labelling[23,28,31], but this type of study has never been conducted in equids. Therefore, we compared the estimated age of the youngest individuals with the time of formation of their first molar crown (Table 1), in order to validate and corroborate the periodicity of these features in *Equus*. As the formation of the first permanent molar in equids starts around the time of birth[13,33], the CFT of the still-developing, unworn tooth must be equivalent to the previously calculated age of the individual. Our results show that both methodologies provide similar times for crown formation (Table 1). These results confirm the hypothesis of Kierdorf *et al.*[29,31] that previous studies misidentified incremental lines in equid enamel[13].

First insights into enamel histology of fossil equids. Finally, the enamel microstructure of the Late Pleistocene species, *E. ferus* and *E. hydruntinus*, was analysed in a first attempt to infer their pattern of molar growth. Both fossil equids present similar values for enamel secretion and extension rate but differ in the periodicity of Retzius lines, namely the repeat interval (RI) (Table 2). As is shown in Table 2, RI in *E. hydruntinus* comprises 4–6 days, while RI in *E. ferus* consists of 5–7 days. In agreement with previous research on primates and proboscideans[73], these results suggest that equid repeat interval is related to body mass, as *E. hydruntinus* presents the lowest body mass as well as the lowest RI within the equid species investigated. The EER of all fossil teeth studied was as expected due to their macroscopic appearance (degree of wear and root development) (Fig. 6), which suggests that the time of crown formation and eruption in both extinct species was similar to that reported for extant equids. When comparing extant and extinct *Equus*, our results show that the daily secretion rate of enamel in *E. hydruntinus* significantly differs from that of *E. quagga* and *E. hemionus* (Fig. 3, Table 2). According to Dirks *et al.*[10], "the daily secretion rate of enamel is likely to be dependent on a complex interaction of tooth size, morphology and life history". A full assessment of the factors responsible for the higher rates of enamel apposition detected in *E. hydruntinus* requires a more detailed analysis involving a larger sample size, beyond the scope of the present study. However, some hypotheses can be drawn from our results. On the one hand, our findings do not match expected DSR values for this species based on body size (life history factor) or hypsodonty (tooth size factor). As *E. hydruntinus* is the smallest and less hypsodont equid analysed here (Table 2), an enamel secretion rate comparable to that of *E. quagga* would be expected. The unexpected elevation in daily secretion rates in this extinct equid species might be related to tooth morphology. Although genetically related to the extant Asiatic wild ass, *E. hydruntinus* is a singular extinct species that shares morphological features with extant asses, zebras and the Pliocene equid, *E. stenonis*[74–76]. Specifically, the lower molar enamel of *E. hydruntinus* presents a primitive pattern that appears to be similar to that of *E. stenonis*[75]. Future histological studies of the enamel in this early Pliocene species might shed light on the factors that lead to the daily secretion rates found in *E. hydruntinus*.

In conclusion, our histological analysis of enamel in the first lower molars of several extant and extinct *Equus* species allowed the estimation of dental growth parameters and the reconstruction of the enamel growth pattern in the clade. Our results provide further evidence of the already known discrepancy between dental macro- and microanatomy that might hamper growth inferences using external measurements of the crown. This finding calls for a revision of commonly used palaeontological and palaeoecological indexes, requiring a correct identification of the crown-root transition, such as the hypsodonty index. We identified three crown developmental stages (CDS) based on different growth patterns during the formation of the first molar. The beginning of each CDS is related to ontogenetic and morphological changes of the tooth. EER is very conservative within the genus and characteristic for each of the three CDS, thus showing a high potential for use in palaeodemographic and/or life history studies. We estimated a daily secretion rate for enamel of ≈17–18 μm/d in the three extant *Equus* species, suggesting that previously reported values of DSR in *E. caballus* are erroneous. Superimposition of different-aged teeth of *E. hemionus* reveals a high wear rate during the first six years of the animal's life. This information should be considered in isotopic studies of tooth enamel to correctly interpret isotopic microsamples. Our results show that there are no differences in extension rate or daily secretion rate in the enamel of *E. hemionus*, *E. quagga* and *E. grevyi*. However, the Asiatic wild ass shows a longer period of crown formation in comparison with plains zebra and Grevy's zebra, which indicates a higher hypsodonty in the ass. Such increase in tooth height is likely to be an adaptation of the Asiatic wild ass to counterbalance tooth wear resulting from both the more arid habitat and the extended longevity of the species. Finally, enamel histology of the Pleistocene species (*E. ferus* and *E. hydruntinus*) reveals that the smallest fossil species secreted enamel at higher rates than extant equids of the same size, *E. quagga* for example. We suggest that this might be related to the tooth morphology of *E. hydruntinus* rather than its tooth size or life history. Further studies with a larger sample size and related taxa are needed to corroborate these results.

Methods

Material. In the present study, we analysed 14 first lower molars from three extant and two Pleistocene species of *Equus* (Table 3). A total of 10 teeth representing different eruption stages and degrees of wear were studied in specimens from three extant species (*E. hemionus*, *E. grevyi* and *E. quagga*) from the Hagenbeck Zoo (Hamburg, Germany). Each extant specimen was aged by the eruption and wear patterns described for the different *Equus* species[51,52,77,78]. In view of this methodology becoming less reliable when all permanent teeth are erupted, the age of adult individuals was confirmed by counting annual growth marks present in the cementum of the first lower incisors[51,52]. In addition to the extant samples, four teeth of the Pleistocene species, *E. ferus* and *E. hydruntinus*, were examined. Each fossil tooth was assigned to an age category (sub-adult or adult) based on the degree of wear and root development[32]. The fossil material came from La Carihuela, a Late Pleistocene cave located in Piñar (Granada, Spain) and dated between 82,500 and 11,200 years BP[79–81]. Fossil samples were housed at the

Catalan Institute of Palaeontology (Barcelona, Spain), while extant specimens belonged to the collections of the Zoological Institute of Hamburg University (Hamburg, Germany).

Preparation of histological thin-sections. Histological sections of teeth were prepared in our laboratory following standard procedures[8]. In the case of extant species, teeth were firstly extracted from the mandible and dehydrated using different concentrations of alcohol for a total period of 72 hours (70, 96 and 100%; 24 h in each). With both extant and fossil samples, each tooth was then embedded in epoxy resin (Araldite 2020) and longitudinally sectioned at the level of the protoconid in the bucco-lingual plane using a low-speed diamond saw (IsoMet, Buehler). The cut surface was later polished using a Metaserv®250 (Buehler) and fixed to a frosted glass with ultraviolet-curing adhesive (Loctite 358). Each sample was then cut and ground with a diamond saw (PetroThin, Buehler) up to a thickness of 150 μm and polished again to obtain a final thickness of approximately 120 μm. Finally, the thin sections obtained were dehydrated again in increasing concentrations of alcohol, immersed in a histological clearing agent (Histo-Clear II) and mounted using DPX medium (Scharlau) to improve visualisation of the dental microscopic features. Due to the high height of equids' crowns, most of the samples had to be mounted on two separate slides[10]. The identification of incremental markings enabled confirmation of both slides being cut from the same plane (Fig. 1a).

Analysis of thin histological sections. Thin sections were examined using a polarised light microscope (Zeiss Scope.A1 microscope) and images were captured with a digital camera mounted on the microscope (AxioCam ICc5). Enamel tissue was examined in detail and different types of incremental markings were identified. Counts and measures of daily periodic laminations (Fig. 1c) along the buccal cusp were performed using ImageJ software, allowing estimates of several histological parameters that reflect the growth rate of the enamel. Firstly, the daily secretion rate (DSR) was calculated in different areas of the crown by measuring the distance between adjacent daily lines following the course of enamel prisms[8] (Fig. 1c). Secondly, the repeat interval (RI), representing the periodicity of long-period lines, was quantified by counting the number of laminations between Retzius lines[1] (Fig. 1d). In those areas where laminations were not well-preserved, this parameter was estimated by dividing the distance between consecutive Retzius lines by the DSR[1]. Thirdly, the course of incremental marks was used to reconstruct the crown formation time (CFT) of each tooth, following the method of Jordana & Köhler[8]. As indicated in Fig. 1b, the path of the incremental lines was traced from the enamel-dentine junction (EDJ) to the enamel surface. The distance between these lines was then measured following the course of the enamel prism; this value was divided by the DSR to determine the time required to form a specific portion of EDJ. The sum of all times along the EDJ results in the CFT. In unworn teeth of extant species, in which the crown development has not been completed, the CFT was compared with the estimated age of each specimen[51,52] to validate and calibrate the daily periodicity of laminations in *Equus*. Fourthly, the enamel extension rate (EER) was calculated as the quotient between a determinate length of the EDJ and the number of days that it takes to be formed, as this parameter represents the growth of teeth along the EDJ[1]. The angle between the enamel formation front (EEF) and the EDJ was also quantified (Fig. 1e) because it is directly related to the EER[3,21].

Statistics. Statistical analyses were carried out with Java Gui for R© version 1.7-16[82]. Kruskal-Wallis and Mann-Whitney U tests were performed to analyse differences between groups. A value of $p < 0.05$ was considered to be statistically significant after applying the Bonferroni correction.

Data availability. All data generated or analysed during this study are included in this published article (and its Supplementary Information files).

References

1. Smith, T. M. Incremental dental development: Methods and applications in hominoid evolutionary studies. *J. Hum. Evol.* **54**, 205–224 (2008).
2. Dean, M. C. Tooth microstructure tracks the pace of human life-history evolution. *Proc. R. Soc. B Biol. Sci.* **273**, 2799–2808 (2006).
3. Jordana, X., Marín-Moratalla, N., Moncunill-Solé, B. & Köhler, M. Ecological and life-history correlates of enamel growth in ruminants (Artiodactyla). *Biol. J. Linn. Soc.* **112**, 657–667 (2014).
4. Smith, B. H. Dental development and the evolution of life history in Hominidae. *Am. J. Phys. Anthropol.* **86**, 157–174 (1991).
5. Smith, B. H. In Development, Function and Evolution of teeth (eds. Teaford, M. F., Smith, M. M. & Ferguson, M.) 212–227 (Cambridge University Press, 2000).
6. Smith, B. H. Dental development as a measure of life history in primates. *Evolution.* **43**, 683–688 (1989).
7. Dirks, W. & Bowman, J. E. Life history theory and dental development in four species of catarrhine primates. *J. Hum. Evol.* **53**, 309–320 (2007).
8. Jordana, X. & Köhler, M. Enamel microstructure in the fossil bovid *Myotragus balearicus* (Majorca, Spain): Implications for life-history evolution of dwarf mammals in insular ecosystems. *Palaeogeogr. Palaeoclimatol. Palaeoecol.* **300**, 59–66 (2011).
9. Dirks, W., Anemone, R. L., Holroyd, P. A., Reid, D. J. & Walton, P. In *Comparative Dental Morphology* (eds. Koppe, T., Meyer, G. & Alt, K. W.) **13**, 3–8 (Karger, 2009).
10. Dirks, W., Bromage, T. G. & Agenbroad, L. D. The duration and rate of molar plate formation in *Palaeoloxodon cypriotes* and *Mammuthus columbi* from dental histology. *Quat. Int.* **255**, 79–85 (2012).
11. Macho, G. A. & Williamson, D. K. The effects of ecology on life history strategies and metabolic disturbances during development: an example from the African bovids. *Biol. J. Linn. Soc.* **75**, 271–279 (2002).
12. Bendrey, R., Vella, D., Zazzo, A., Balasse, M. & Lepetz, S. Exponentially decreasing tooth growth rate in horse teeth: Implications for isotopic analyses. *Archaeometry* **57**, 1104–1124 (2015).
13. Hoppe, K. A., Stover, S. M., Pascoe, J. R. & Amundson, R. Tooth enamel biomineralization in extant horses: Implications for isotopic microsampling. *Palaeogeogr. Palaeoclimatol. Palaeoecol.* **206**, 355–365 (2004).
14. Bryant, J. D., Froelich, P. N., Showers, W. J. & Genna, B. J. Biologic and climatic signals in the oxygen isotopic composition of Eocene-Oligocene equid enamel phosphate. *Palaeogeogr. Palaeoclimatol. Palaeoecol.* **126**, 75–89 (1996).
15. Bryant, J. D., Froelich, P. N., Showers, W. J. & Genna, B. J. A tale of two quarries: Biologic and taphonomic signatures in the oxygen isotope composition of tooth enamel phosphate from modern and Miocene equids. *Palaios* **11**, 397–408 (1996).

16. D'Ambrosia, A. R., Clyde, W. C., Fricke, H. C. & Chew, A. E. Stable isotope patterns found in early Eocene equid tooth rows of North America: Implications for reproductive behavior and paleoclimate. *Palaeogeogr. Palaeoclimatol. Palaeoecol.* **414**, 310–319 (2014).
17. Wang, Y., Cerling, T. E. & MacFadden, B. J. Fossil horses and carbon isotopes: new evidence for Cenozoic dietary, habitat, and ecosystem changes in North America. *Palaeogeogr. Palaeoclimatol. Palaeoecol.* **107**, 269–279 (1994).
18. MacFadden, B. J. Cenozoic Mammalian Herbivores from the Americas: Reconstructing Ancient Diets and Terrestrial Communities. *Annu. Rev. Ecol. Syst.* **31**, 33–59 (2000).
19. Metcalfe, J. Z. & Longstaffe, F. J. Mammoth tooth enamel growth rates inferred from stable isotope analysis and histology. *Quat. Res.* **77**, 424–432 (2012).
20. Smith, T. M. & Tafforeau, P. New visions of dental tissue research: Tooth development, chemistry, and structure. *Evol. Anthropol.* **17**, 213–226 (2008).
21. Boyde, A. The structure and development of mammalian enamel. (1964).
22. Hillson, S. *Teeth*. (Cambridge University Press, 2005).
23. Smith, T. M. Experimental determination of the periodicity of incremental features in enamel. *J. Anat.* **208**, 99–113 (2006).
24. Fitzgerald, C. M. & Rose, J. C. In Biological Anthropology of the Human Skeleton (eds. Katzenberg, M. A. & Saunders, S. R.) 237–263 (John Wiley & Sons, Inc, 2008).
25. Bromage, T. G. Enamel incremental periodicity in the pig-tailed macaque: A polychrome fluorescent labeling study of dental hard tissues. *Am. J. Phys. Anthropol.* **86**, 205–214 (1991).
26. Tafforeau, P., Bentaleb, I., Jaeger, J.-J. & Martin, C. Nature of laminations and mineralization in rhinoceros enamel using histology and X-ray synchrotron microtomography: Potential implications for palaeoenvironmental isotopic studies. *Palaeogeogr. Palaeoclimatol. Palaeoecol.* **246**, 206–227 (2007).
27. Iinuma, Y. M. *et al*. Dental incremental lines in sika deer (*Cervus nippon*); polarized light and fluorescence microscopy of ground sections. *J. Vet. Med. Sci.* **66**, 665–669 (2004).
28. Kierdorf, H., Kierdorf, U., Frölich, K. & Witzel, C. Lines of Evidence-Incremental Markings in Molar Enamel of Soay Sheep as Revealed by a Fluorochrome Labeling and Backscattered Electron Imaging Study. *PLoS One* **8**, e74597 (2013).
29. Mao, F.-Y., Wang, Y.-Q., Meng, J. & Jin, X. Tooth crown formation time in three Asian coryphodontids, and its implications for identifying living analogues. *Vertebr. Palasiat.* **52**, 153–170 (2014).
30. MacFadden, B. J. Fossil Horses - Evidence for Evolution. *Science.* **307**, 1728–1730 (2005).
31. Kierdorf, H., Breuer, F., Richards, A. & Kierdorf, U. Characterization of enamel incremental markings and crown growth parameters in minipig molars. *Anat. Rec.* **297**, 1935–1949 (2014).
32. Kirkland, K. D., Baker, G. J., Marretta, S. M., Eurell, J. A. C. & Losonsky, J. M. Effects of aging on the endodontic system, reserve crown, and roots of equine mandibular cheek teeth. *Am. J. Vet. Res.* **57**, 31–38 (1996).
33. Soana, S., Gnudi, G. & Bertoni, G. The Teeth of the Horse: Evolution and Anatomo-Morphological and Radiographic Study of Their Development in the Foetus. *Anat. Histol. Embryol.* **28**, 273–280 (1999).
34. Dixon, P. M. & Copeland, A. N. The radiological appearance of mandibular cheek teeth in ponies of different ages. *Equine Vet. Educ.* **5**, 317–323 (1993).
35. Levine, M. A. In *Ageing and Sexing Animal Bones from Archaeological* Sites (eds. Wilson, B., Grigson, C. & Payne, S.) **109**, 223–250 (B.A.R., 1982).
36. Orlando, L. Equids. *Curr. Biol.* R973–R978 (2015).
37. IUCN. *The IUCN Red List of Threatened Species*. Version2016-3. www.iucnredlist.org (2016).
38. Nowak, R. M. *Walker's Mammals of the World*. (The Johns Hopkins University Press, 1999).
39. King, S. R. B. & Moehlman, P. D. *Equus quagga*. *IUCN Red List Threat. Species*, e.T41013A45172424; 10.2305/IUCN.UK.2016-2.RLTS.T41013A45172424.en (2016).
40. Kaczensky, P., Lkhagvasuren, B., Pereladova, O., Hemami, M. & Bouskila, A. *Equus hemionus*. *IUCN Red List Threat. Species*, e.T7951A45**;** 10.2305/IUCN.UK.2015-4.RLTS.T7951A45171204.en (2015).
41. Rubenstein, D., Low Mackey, B., Davidson, Z. D., Kebede, F. & King, S. R. B. *Equus grevyi*. *IUCN Red List Threat. Species*, e.T7950A89624491; 10.2305/IUCN.UK.2016-3.RLTS.T7950A89624491.en (2016).
42. Ernest, S. K. M. Life history characteristics of placental nonvolant mammals. *Ecology* **84**, 3402 (2003).
43. Palombo, M. R. Deconstructing mammal dispersals and faunal dynamics in SW Europe during the Quaternary. *Quat. Sci. Rev.* **96**, 50–71 (2014).
44. Calder, W. A. III. *Size, Function and Life History*. (Dover Publications, 1984).
45. Peters, R. H. *The ecological implications of body size*. (Cambridge University Press, 1983).
46. Damuth, J. & MacFadden, B. J. *Body Size in Mammalian Paleobiology: Estimations and Biological Implications*. (Cambridge University Press, 1990).
47. Strömberg, C. A. E. Evolution of hypsodonty in equids: testing a hypothesis of adaptation. *Paleobiology* **32**, 236–258 (2006).
48. Sisson, S. *The anatomy of domestic animals*. (W. B. Saunders company, 1914).
49. Dixon, P. M. & du Toit, N. In *Equine Dentistry* (eds. Easley, J., Dixon, P. M. & Schumacher, J.) 51–76 (Elsevier Ltd, 2011).
50. Hogg, R. T. & Walker, R. S. Life-history correlates of enamel microstructure in Cebidae (Platyrrhini, Primates). *Anat. Rec.* **294**, 2193–2206 (2011).
51. Smuts, G. L. Age determination in Burchell's zebra (*Equus burchelli antiquorum*) from the Kruger National Park. *J. South. african Wildl. Manag. Assoc.* **4**, 103–105 (1974).
52. Lkhagvasuren, D. *et al*. Age determination of the Mongolian wild ass (*Equus hemionus* Pallas, 1775) by the dentition patterns and annual lines in the tooth cementum. *J. Species Res.* **2**, 85–90 (2013).
53. Kierdorf, H., Witzel, C., Upex, B., Dobney, K. & Kierdorf, U. Enamel hypoplasia in molars of sheep and goats, and its relationship to the pattern of tooth crown growth. *J. Anat.* **220**, 484–495 (2012).
54. Trayler, R. B. & Kohn, M. J. Tooth enamel maturation reequilibrates oxygen isotope compositions and supports simple sampling methods. *Geochim. Cosmochim. Acta* **198**, 32–47 (2017).
55. Kohn, M. J. Comment: Tooth enamel mineralization in ungulates: Implications for recovering a primary isotopic time-series, by B. H. Passey and T. E. Cerling (2002). *Geochim. Cosmochim. Acta* **68**, 403–405 (2004).
56. Damuth, J. & Janis, C. M. On the relationship between hypsodonty and feeding ecology in ungulate mammals, and its utility in palaeoecology. *Biol. Rev.* **86**, 733–758 (2011).
57. Janis, C. M. In *Teeth revisited*: P*roceedings of the 7th International Symposium on Dental Morphology, 20-24 May, 1986* (eds. Russell, D. E., Santoro, J. P. & Sigogneau-Russel, D.) 367–387 (Muséum National D'Histoire Naturelle, 1988).
58. Cantalapiedra, J. L., Prado, J. L., Hernández Fernández, M. & Alberdi, M. T. Decoupled ecomorphological evolution and diversification in Neogene-Quaternary horses. *Science.* **355**, 627–630 (2017).
59. Mendoza, M. & Palmqvist, P. Hypsodonty in ungulates: An adaptation for grass consumption or for foraging in open habitat? *J. Zool.* **274**, 134–142 (2008).
60. Schulz, E. & Kaiser, T. M. Historical distribution, habitat requirements and feeding ecology of the genus *Equus* (Perissodactyla). *Mamm. Rev.* **43**, 111–123 (2013).
61. Kaiser, T. M. *et al*. Hypsodonty and tooth facet development in relation to diet and habitat in herbivorous ungulates: implications for understanding tooth wear. *Mamm. Rev.* **43**, 34–46 (2013).
62. Köhler, M. In *Islands and Evolution* (eds. Pérez-Mellado, V. & Ramon, C.) **19**, 261–280 (Institut Menorquí d'Estudis. Recerca, 2010).

63. Ozaki, M. *et al*. The relationship between food habits, molar wear and life expectancy in wild sika deer populations. *J. Zool.* **280**, 202–212 (2010).
64. Jordana, X. & Marín-Moratalla, N. de Miguel, D., Kaiser, T. M. & Köhler, M. Evidence of correlated evolution of hypsodonty and exceptional longevity in endemic insular mammals. *Proc. R. Soc. B Biol. Sci.* **279**, 3339–3346 (2012).
65. Lkhagvasuren, D. Some Population Characteristics of the Asiatic Wild Ass (Equus hemionus Pallas, 1775) in Mongolia. (2015).
66. Churcher, C. *Equus grevyi*. *Mamm. Species* **453**, 1–9 (1993).
67. Stearns, S. C. *The evolution of life histories*. (Oxford University Press, 1992).
68. Köhler, M. & Moyà-Solà, S. Physiological and life history strategies of a fossil large mammal in a resource-limited environment. *Proc. Natl. Acad. Sci. USA* **106**, 20354–20358 (2009).
69. Köhler, M. The evolution of life history traits associated to dwarfing in insular large mammals: a paleontological approach. *J. Vertebr. Paleontol.* **29**, Suppl. 128A (2009).
70. Feh, C., Munkhtuya, B., Enkhbold, S. & Sukhbaatar, T. Ecology and social structure of the Gobi khulan *Equus hemionus* subsp. in the Gobi B National Park, Mongolia. *Biol. Conserv.* **101**, 51–61 (2001).
71. Spinage, C. A. Age estimation of zebra. *Afr. J. Ecol.* **10**, 273–277 (1972).
72. Hulbert, R. C. J. Population Dynamics of the Three-Toed Horse *Neohipparion* from the Late Miocene of Florida. *Paleobiology* **8**, 159–167 (1982).
73. Bromage, T. G. *et al*. Lamellar bone is an incremental tissue reconciling enamel rhythms, body size, and organismal life history. *Calcif. Tissue Int.* **84**, 388–404 (2009).
74. Orlando, L. *et al*. Geographic distribution of an extinct equid (*Equus hydruntinus*: Mammalia, Equidae) revealed by morphological and genetical analyses of fossils. *Mol. Ecol.* **15**, 2083–2093 (2006).
75. Burke, A., Eisenmann, V. & Ambler, G. K. The systematic position of *Equus hydruntinus*, an extinct species of Pleistocene equid. *Quat. Res.* **59**, 459–469 (2003).
76. Geigl, E. M. & Grange, T. Eurasian wild asses in time and space: Morphological versus genetic diversity. *Ann. Anat.* **194**, 88–102 (2012).
77. Silver, I. A. In Science in Archaeology: a comprehensive survey of progress and research (eds. Brothwell, D. & Higgs, E.) 250–268 (Basic Books, 1963).
78. Penzhorn, B. L. Age determination in cape mountain zebras *Equus zebra zebra* in the Mountain Zebra National Park. *Koedoe* **25**, 89–102 (1982).
79. Fernández, S. *et al*. The Holocene and Upper Pleistocene pollen sequence of Carihuela Cave, southern Spain. *Geobios* **40**, 75–90 (2007).
80. Samper Carro, S. C. In Cidaris, número 30, *VIII Encuentro de Jóvenes Investigadores en Paleontología* (eds. Moreno-Azanza, M. et al.) 283–291 (2010).
81. Carrión, J. S. Late quaternary pollen sequence from Carihuela Cave, southern Spain. *Rev. Palaeobot. Palynol.* **71**, 37–77 (1992).
82. Fellows, I. Deducer: A Data Analysis GUI for R. *J. Stat. Softw.* **49**, 1–15 (2012).

Acknowledgements

We thank T. Kaiser for permission to cut the teeth of the extant species. We are grateful to J. Madurell-Malapeira for his help in identifying the fossil species from La Carihuela. G. Prats-Muñoz and M. Fernández are acknowledged for the preparation of histological slices. We would also like to thank Jin Meng as editor of Scientific Reports, Tim Bromage and one anonymous reviewer for their valuable comments and suggestions. This work is supported by the Spanish Ministry of Economy and Competitiveness (CGL-2015-63777, PI: MK) and the Government of Catalonia (2014-SGR-1207, PI: MK; CERCA Programme, MK). C. Nacarino-Meneses holds a FPI grant from the Spanish Ministry of Economy and Competitiveness (BES-2013-066335) and G. Orlandi-Oliveras is supported by a FI-DGR 2016 grant from the Government of Catalonia AGAUR (2016FI_B00202).

Author Contributions

C.N.-M., X.J. and M.K. conceived and designed the experiments. C.N.-M. wrote the paper and prepared figures and tables. All authors analysed the data and reviewed drafts of the paper.

Additional Information

Supplementary information accompanies this paper at https://doi.org/10.1038/s41598-017-16227-2.

Competing Interests: The authors declare that they have no competing interests.

Publisher's note: Springer Nature remains neutral with regard to jurisdictional claims in published maps and institutional affiliations.

Supplementary Tables for

Reconstructing molar growth from enamel histology in extant and extinct *Equus*

Carmen Nacarino-Meneses, Xavier Jordana, Guillem Orlandi-Oliveras & Meike Köhler

Supplementary Table S1. Daily secretion rate in different parts of the crown (occlusal, middle, cervical) and enamel zones (inner, middle, outer) in the extant *Equus* studied.

Part of the crown

	Occlusal		Middle		Cervical	
	N	**Mean±SD**	**N**	**Mean±SD**	**N**	**Mean±SD**
E. hemionus	30	17.53±1.68	6	17.42±3.04	6	15.62±1.96
E. quagga	26	17.31 ±1.56	12	16.04±1.13	7	17.39±2.18
E. grevyi	19	18.12±1.82	12	17.52±1.24	6	17.02±1.33

Enamel zone

	Inner		Middle		Outer	
	N	**Mean±SD**	**N**	**Mean±SD**	**N**	**Mean±SD**
E. hemionus	17	16.18±2.6	15	17.58±2.03	13	17.11±2.06
E. quagga	14	16.98±1.82	15	16.42±1.39	16	17.5±1.6
E. grevyi	15	17.43±1.3	14	17.89±1.86	8	18.08±1.70

Supplementary Table S2. Results of Kruskal-Wallis test on differences of daily secretion rate (DSR) between enamel zones (inner, middle, outer) and between parts of the crown (occlusal, middle, cervical). P-value adjustment method: Bonferroni. α = 0.05.

	Chi-squared	**p-value**
Enamel zones	2.0576	0.3574
Part of the crown	3.8434	0.1463

Supplementary Table S3. Results of Kruskal-Wallis test on differences of daily secretion rate (DSR) between *Equus* species. Pairwise comparisons were calculated using Mann-Whitney U test. P-value adjustment method: Bonferroni. α = 0.05.

	Chi-squared	p-value
DSR	18.83402	< 0.001

	E. ferus	*E. grevyi*	*E. hemionus*	*E. hydruntinus*
E. grevyi	1	-	-	-
E. hemionus	1	1	-	-
E. hydruntinus	0.86813	0.05080	0.00265	-
E. quagga	1	0.52253	1	< 0.001

Supplementary Table S4. Results of Kruskal-Wallis test on differences of enamel extension rate (EER) between crown developmental stages (CDS) in the different extant *Equus* species analysed. Pairwise comparisons were calculated using Mann-Whitney U test. P-value adjustment method: Bonferroni. $\alpha = 0.05$.

	Chi-squared	p-value
E. hemionus	78.0673	< 0.001
E. quagga	36.5513	< 0.001
E. grevyi	28.8870	< 0.001

E. hemionus

	CDSI	CDSII
CDSII	< 0.001	-
CDSIII	< 0.001	< 0.001

E. quagga

	CDSI	CDSII
CDSII	< 0.001	-
CDSIII	< 0.001	< 0.001

E. grevyi

	CDSI	CDSII
CDSII	0.0015	-
CDSIII	< 0.001	< 0.001

Supplementary Table S5. Results of Kruskal-Wallis test on differences of enamel extension rate (EER) between species within each crown developmental stage (CDS). $\alpha = 0.05$.

	Chi-squared	**p-value**
CDS I	2.5601	0.2780
CDS II	2.0468	0.3593
CDS III	4.3409	0.1141

Supplementary Table S6. Results of Kruskal-Wallis test on differences of enamel extension rate (EER) between Pleistocene *Equus* specimens and crown developmental stages (CDS) established for extant equids. Pairwise comparisons were calculated using Mann-Whitney U test. P-value adjustment method: Bonferroni. $\alpha = 0.05$.

	Chi-squared	**p-value**
EER	191.3405	< 0.001

	CDS I	CDS II	CDS III	IPS87497	IPS87509	IPS87523
CDS II	< 0.001	-	-	-	-	-
CDS III	< 0.001	< 0.001	-	-	-	-
IPS87497	< 0.001	1	< 0.001	-	-	-
IPS87509	< 0.001	1	< 0.001	1	-	-
IPS87523	0.15828	0.01037	< 0.001	0.30434	0.04284	-
IPS87540	< 0.001	1	< 0.001	1	0.71513	< 0.001

- Chapter 9 -

Discussion

Discussion

The central aim of the present PhD dissertation is to reconstruct the life history (LH) strategies of extant and extinct *Equus* from the histological analysis of their bones and teeth. To achieve this goal, limb bones and first lower molars have been histologically analyzed in the extant species *E. hemionus*, *E. quagga* and *E. grevyi* (Chapters 4 to 6 and 8). The results have provided novel findings about the growth and development of these biological structures that not only contribute to our knowledge of mammalian bone and dental histology but also set a well-founded basis for the study of fossil species. The information obtained from living equids has subsequently been applied to European extinct *Equus* species, providing a first insight into their pace of life. Specifically, bone histology of the Middle Pleistocene equids *E. steinheimensis* and *E. mosbachensis* (Chapter 7) and enamel tissue of the Late Pleistocene species *E. ferus* and *E. hydruntinus* (Chapter 8) have been studied. In the present chapter, the main results of this dissertation are discussed following the order of the objectives detailed in Chapter 2. In a first section (9.1), the most significant findings obtained from the histological analysis of skeletal and dental elements in extant *Equus* are reviewed, highlighting their relevance for the inference of LH characteristics. In a second section (9.2), several LH traits of European Pleistocene equids are inferred from the study of bone and enamel microstructure. Their LH strategy is analyzed within the framework of Palkovacs' (2003) LH model in order to better understand the evolution of body size from this novel point of view (9.2).

9.1. Bone and dental histology of extant *Equus*: Setting the basis for life history inferences

9.1.1. Bone histology of extant *Equus*

Over the last decades, the number of studies that investigate mammalian bone tissue under a LH perspective has increased importantly (see a review in Kolb et al. 2015a). However, and despite several authors claimed that research in living taxa is crucial to decipher how organismal biology is recorded in bone microstructure (Martínez-Maza et al. 2014; Woodward et al. 2014; Cambra-Moo et al. 2015; Kolb et al. 2015a; Jordana et al. 2016), most investigations have focused on fossil organisms (Chinsamy and Hurum 2006; Sander and Andrássy 2006; Köhler and Moyà-Solà 2009; Marín-Moratalla et al. 2011; Martínez-Maza et al. 2014; Amson et al. 2015; Kolb et al. 2015b; Moncunill-Solé et al. 2016). In extant species, studies aimed at inferring LH traits from bone histology

are limited to primates (Castanet et al. 2004), ruminants (Köhler et al. 2012; Marín-Moratalla et al. 2013; Marín-Moratalla et al. 2014) and rodents (García-Martínez et al. 2011). The present dissertation partially fills this gap by providing new and unique results about the bone microanatomy in the genus *Equus*. Specifically, this PhD thesis presents the first comprehensive histological description of the femur, the tibia and the metapodial bones for complete ontogenetic series (from perinates to adults) of the extant species *E. hemionus* (Asiatic wild ass) (Nacarino-Meneses et al. 2016a; Nacarino-Meneses et al. 2016b; Chapters 4 and 5). According to Forstén (1992), the Asiatic wild ass is ecologically and morphologically similar to fossil stenonoid equids, which makes *E. hemionus* one of the most appropriate extant taxa for comparison with extinct equids. Furthermore, *E. hemionus* is near threatened in the wild (Kaczensky et al. 2015; IUCN 2018) and the LH information obtained from the histological analysis of its bones may aid the development of new conservation strategies for the species, as has been suggested for a few other taxa (Chinsamy and Valenzuela 2008; García-Martínez et al. 2011; Marín-Moratalla et al. 2013). Therefore, the Asiatic wild ass has been used in this thesis as a test-case taxon to exemplify the histological development of bones in the genus *Equus*. Nonetheless, bone microstructure has also been thoroughly analyzed in the extant species of plains and Grevy's zebra, shedding light on the relationship between non-cyclical BGMs of physiological origin and key LH events in equids in particular and in mammals in general (Nacarino-Meneses and Köhler accepted; Chapter 6).

9.1.1.1. The bone tissue of extant Equus*: ontogenetic changes in bone matrix and vascularization*

The exhaustive analysis of limb bone histology performed in *E. hemionus* along Chapters 4 and 5 of the present dissertation (Nacarino-Meneses et al. 2016a; Nacarino-Meneses et al. 2016b) has revealed important changes in bone tissue types and vascularization along growth and development. Early in ontogeny, all limb bones of the Asiatic wild ass are composed of well-vascularized fibrolamellar complex (FLC) interrupted by bone growth marks (BGMs) (Fig. 2 and 5 in Chapter 4; Fig. 1 to 6 in Chapter 5). This primary bone tissue is progressively replaced by secondary osteons (Haversian systems) (Fig. 5 in Chapter 4; Fig. 1 and 2 in Chapter 5), which usually concentrate in those cortical areas that suffer higher biomechanical stress (e.g. tendon attachment sites). Besides, closely-packaged laminar bone with BGMs was identified in the outermost cortex of adult femora and metapodia (Fig. 5I in Chapter 4; Fig. 2D in Chapter 5), forming the external fundamental system (EFS; Cormack 1987). Differences between limb bones are restricted to the arrangement of the vascular canals (VCs): while femoral and tibial cortices are mainly composed of laminar bone (circular VCs) (Fig. 5C in Chapter 4; Fig. 1A and 2A in Chapter 5), metapodia present longitudinal primary osteons (POs) oriented in circular rows (Fig. 2A in Chapter 5). These observations agree with previous histological descriptions reported for the limb bones of extant and extinct Equidae (Enlow and Brown 1958; Stover et al. 1992; Sander and Andrássy 2006; Cuijpers and Lauwerier 2008; Martínez-Maza et al. 2014). As the pattern of vascularization is intimately related to biomechanics (de Margerie 2002), differences in VC arrangement between appendicular

bones are likely reflecting the different weight-bearing forces acting upon each of them.

In femora of *E. hemionus*, differences in bone matrix components have been identified between areas of the same cross-section (Chapter 4; Nacarino-Meneses et al. 2016a). At all ontogenetic stages, the lateral regions of the cortex present a higher proportion of parallel-fibered bone (PFB) than woven-fibered bone (WFB) within the FLC matrix (Fig. 5F in Chapter 4). Even in the juvenile individual (IPS83155), a PFB matrix is identified in this specific area of the bone cortex (Fig. 5G in Chapter 4). As bone tissue types differ in their rate of deposition (Amprino 1947; de Margerie et al. 2002), these findings suggest different rates of growth for the different cross-section regions. This is likely a consequence of bone drift, an ontogenetic process that adjusts diaphyses of long bones during growth to their final adult size and shape (Martin et al. 1998; Currey 2002; Chinsamy-Turan 2005).

Especially remarkable are the changes in bone tissue and vascularization that take place in the limb bones of *Equus* at a specific moment in ontogeny: the time of birth (Chapters 4 to 6; Nacarino-Meneses et al. 2016a; Nacarino-Meneses et al. 2016b; Nacarino-Meneses and Köhler accepted). Our analysis has revealed the presence of a non-cyclical BGM that records this LH event in the bone microstructure of extant equid species (Chapter 6; see also section 9.1.1.2.). Associated to this feature, we have identified differences in the components of the FLC matrix and in vascular canal size and arrangement. On the one hand, results of the present dissertation showed that prenatally formed FLC in the tibiae of all *Equus* species and in the femora of both zebras presents a higher proportion of PFB than postnatally formed tissue (Fig. 5C in Chapter 4; Fig. 1A in Chapter 5; Fig. 5B–F in Chapter 6), suggesting higher rates of bone formation (de Margerie 2002) after birth. This finding agrees with previous histological studies in Elephantidae (Curtin et al. 2012) and *E. caballus* (Stover et al. 1992), which described lower proportions of PFB in the limb bones of these animals in postnatally formed tissue (Stover et al. 1992; Curtin et al. 2012). Our results, however, contrast with studies in reptiles and dinosaurs, which reported a more organized bone matrix composed of PFB in these taxa after hatching (Chinsamy and Hurum 2006; Hugi and Sánchez-Villagra 2012; Curry Rogers et al. 2016). Differences on postnatal bone tissue between equids and reptiles or dinosaurs are probably related to the higher postnatal growth rates described for mammals in comparison with these egg-laying vertebrates (Case 1978; Peters 1983; Calder 1984). Results of the present dissertation also reveal changes in bone vascularity associated to the moment of birth. VCs in the femora of *E. hemionus*, for instance, change from a longitudinal to a mainly circular arrangement after this LH event (Fig. 5C in Chapter 4; Fig. 5A in Chapter 6). As previously stated, VC pattern is generally associated with biomechanics (de Margerie 2002) and laminar bone (FLC mainly composed of circular VCs (Francillon-Vieillot et al. 1990)), specifically, has been suggested to be adapted to support torsional loads (de Margerie 2002). These stresses, along with bending loads, are the main forces affecting the limb bones of horses during locomotion (Gross et al. 1992). Therefore, the change in VC orientation identified in femora of *E. hemionus* is probably related with the onset of locomotion just after birth. Not only differences in VC arrangement but also in VC size have been identified in *Equus* associated to the moment of birth. In all limb bones of the

equid species studied (*E. hemionus*, *E. quagga* and *E. grevyi*), VCs formed postnatally are larger than those formed prenatally (Fig. 5G–I, Fig. 6, Fig. 7 and Table 3 in Chapter 6). This finding agrees with results on PO size reported by Stover et al. (1992), who described bigger POs in bone tissue deposited after birth. Larger VCs have also been associated with higher rates of bone formation (de Margerie 2002). Thus, the larger area of the VCs formed after birth suggests higher rates of postnatal bone formation in equids, as already inferred from bone matrix changes (Fig. 1A in Chapter 5; Fig. 5B–F in Chapter 6).

9.1.1.2. Non-cyclical and cyclical BGMs: bone skeletochronology and the inference of biological and LH traits in extant Equus

Bone growth marks (BGMs) are classified as cyclical (CGMs) and non-cyclical features in relation to their periodicity (Castanet et al. 1993; Woodward et al. 2013). The first ones appear in bone cortices due to endogenous physiological rhythms linked to seasonality (Köhler et al. 2012), registering annual cycles of growth (Castanet et al. 1993; Woodward et al. 2013). Causes of deposition of non-cyclical BGMs, however, are little studied. In amphibians and reptiles, these features have been suggested to record key LH events such as metamorphosis or hatching respectively (Hemelaar 1985; Castanet and Baéz 1991; Esteban et al. 1999; Khonsue et al. 2001; Ento and Matsui 2002; Esteban et al. 2002; Jakob et al. 2002; Olgun et al. 2005; Chinsamy and Hurum 2006; Hugi and Sánchez-Villagra 2012; Sinsch 2015). Nonetheless, non-cyclical BGMs in mammalian cross-sections are commonly related to bone drift (Woodward et al. 2013; Martínez-Maza et al. 2014) and only a few authors have proposed a relationship between these and mammalian LHs (Morris 1970; Castanet et al. 2004; Castanet 2006). In the present dissertation, we identified a non-cyclical BGM (LAG) in the limb bones of the Asiatic wild ass, the plains zebra and the Grevy's zebra (Chapter 6) that does not result from cortical bone drift but from the physiological changes that occur in the organism during a biological stressful event (Nacarino-Meneses and Köhler accepted). Specifically, this mark was identified in the tibiae and the metapodia of all *Equus* specimens studied (Fig. 1 in Chapter 6), from foal to adult stage. It was also recognized in femoral cortices, but only in that of foals and yearlings (Fig. 1 in Chapter 6). Later in ontogeny, this non-cyclical BGM is lost in the femur due to expansion of the medullary cavity (Fig. 3 in Chapter 6). Superimposition (Woodward et al. 2013) performed in the Asiatic wild ass indicated a coincidence between the perimeter of perinatal bones and that of the non-cyclical BGM identified at later ontogenetic stages (Fig. 4 and Table 2 in Chapter 6), suggesting that this mark records the birth of the animal. Consequently, and in analogy to the neonatal line described in enamel and dentine tissues (Schour 1936; Weber and Eisenmann 1971; Carlson 1990; Smith et al. 2006; Tafforeau et al. 2007), we refer to it as neonatal line (NL). NLs have never been described before in mammalian bone tissue. Hitherto, previous reports on non-cyclical BGMs of physiological origin in mammals have always been related to the weaning event (Morris 1970; de Margerie et al. 2004; Castanet 2006). However, weaning occurs much later in all equid species studied (12 – 18 months in *E. hemionus* (Nowak 1999); 7 – 11 months in *E. quagga* (Nowak 1999); 9 months in *E. grevyi* (Churcher 1993); see also Table 1.1 in Chapter 1) than the appearance of the non-cyclical BGM in their limb bones

(before the first month of life in the femur and the tibia and before the fourth month in the metapodia; Fig. 1 and Fig. 2 in Chapter 6). Furthermore, low physiological levels of thyroid and growth hormones (Stewart et al. 1993; Messer et al. 1998) and high concentration values of cortisol (Fowden et al. 2012) in equids during birth are consistent with an arrest or reduction in the rate of bone formation (Buchanan and Preece 1992) that likely leads to the deposition of a NL. The description of a NL in the bone tissue of equids offers new and interesting possibilities for the reconstruction of LHs in this and in related groups of mammals. Considering that this feature records the bone circumference of newborn foals, its measurement can be used, for instance, to obtain estimations of the weight at birth (Anderson et al. 1985) in extant and fossil species. Body weight is commonly used as a proxy of body size (Damuth and MacFadden 1990). Therefore, weight estimates obtained from dimensions of the NL can be used as a proxy of the size at birth, which is one of the most important LH traits of mammals (Stearns 1992). The accurate identification of the NL further provides a "time zero" that may be crucial for skeletochronological research and growth reconstructions.

Bone skeletochronology constitutes the basis for the estimation of key LH characteristics in mammals (e.g. age at death, age at maturity) from the counting of CGMs (Castanet et al. 1993; Castanet 2006; Marín-Moratalla et al. 2013; Woodward et al. 2013). The correspondence of CGMs with annual growth cycles has been tested in several mammalian groups including ruminants, primates and rodents (Castanet et al. 2004; García-Martínez et al. 2011; Köhler et al. 2012), but not in equids. In the present dissertation, we checked for the first time the reliability of skeletochronology in the genus *Equus* by comparing the number of CGMs in several femora of *E. hemionus* with the estimated age of the specimens (Chapter 4; Nacarino-Meneses et al. 2016a). In this preliminary study, all BGMs within a bone cortex were considered as cyclical features, as they are the most common growth marks in the bone cortices of vertebrates (Castanet et al. 1993). Results showed a general agreement between the number of CGMs in femoral bone cortices and the age assessed for each individual from the eruption sequence (Chapter 4; Nacarino-Meneses et al. 2016a), validating the application of skeletochronology in this group of mammals. Reliability of bone skeletochronology was also tested in tibiae and metapodia of the Asiatic wild ass in order to determine which limb bone provides the most accurate LH estimations in equids (Chapter 5; Nacarino-Meneses et al. 2016b). Generally, our results show that tibiae record a lower number of CGMs than femora and/or metapodia (Table 2 in Chapter 5). Also, Haversian systems appear very early in ontogeny in tibial cortices (Fig. 1B in Chapter 5), which increases the probability that BGMs are erased earlier than in other long bones. Furthermore, estimations of the age at maturity based on the appearance of an EFS (Chinsamy-Turan 2005; Marín-Moratalla et al. 2013; Jordana et al. 2016) cannot be performed in this bone, as this tissue type was not identified in the adult tibia of *E. hemionus* (Fig. 1C in Chapter 5). For all these reasons, and contrasting with previous studies in dinosaurs (Horner et al. 1999), we consider that tibiae are not suitable for skeletochronological studies in Equidae. Metacarpi and metatarsi, on the other hand, register a similar total number of CGMs as femora, but fewer CGMs are located within the FLC (Table 2 in Chapter 5). This underlines the relevance of metapodia

for the estimation of individual age (Castanet et al. 2004), which is especially interesting for fossil species as these bones are the most common equid skeletal elements found at paleontological sites. Metapodia, however, do not provide reliable inferences about the age at maturity due to the lower number of CGMs before deposition of the EFS (Chinsamy-Turan 2005; Marín-Moratalla et al. 2013; Jordana et al. 2016), which likely results from the advanced attainment of adult size and shape of metapodia in comparison with other long bones. This contrasts with a previous study of Martínez-Maza et al. (2014), who analyzed cross-sections of *Hipparion concudense* metapodia to infer age at maturity of the species. Actually, our findings agree with investigations in mammals (García-Martínez et al. 2011) and dinosaurs (Horner et al. 1999) that suggest the femur as the best limb bone for performing skeletochronological studies. In equids, the femur does not only register the highest total number of CGMs of all limb bones analyzed, but also the highest number of these features within the FLC (Table 2 in Chapter 5). Furthermore, and as previously stated, the number of CGMs in this bone fairly matches the estimated age of each specimen (Chapter 4). Hence, femora provide the best results for the estimation of both the age at death and the age at maturity in extant and extinct equids.

Age at reproductive maturity is one of the most important LH traits of mammals (Stearns 1992). Based on the energetic trade-off between growth and reproduction postulated by the life history theory (LHT) (Stearns 1992), several authors have proposed that this LH characteristic is registered in mammalian bone microstructure as the timing of deposition of the EFS (Marín-Moratalla et al. 2013; Jordana et al. 2016). Due to the close relationship between bone tissue types and their rate of deposition (Amprino 1947; de Margerie et al. 2002; Huttenlocker et al. 2013), however, other authors argued that the occurrence of this tissue is related to the attainment of skeletal maturity (Cormack 1987; Woodward et al. 2013; Martínez-Maza et al. 2014; Amson et al. 2015; Kolb et al. 2015b). In all limb bones of *E. hemionus*, the EFS is deposited after the time of epiphyseal fusion (Fig. 7 and Table 3 in Chapter 5), indicating that it does not record skeletal maturity in equid bones (Nacarino-Meneses et al. 2016b). The timing of deposition of the EFS in the femora of the Asiatic wild ass, however, matches the age at first breeding (see Kaczensky et al. (2015) for the age at first breeding of *E. hemionus*) of the species, in both the female and the male specimen analyzed (Fig. 7 and Table 3 in Chapter 5). Our findings thus support previous studies that consider the presence of EFS in the femora as an indicator of the onset of reproductive maturity (Marín-Moratalla et al. 2013; Jordana et al. 2016). The occurrence of an EFS in metacarpi and metatarsi does not seem to correlate, however, with any LH or biological trait (e.g. epiphyseal fusion) (Chapter 5; Nacarino-Meneses et al. 2016b). In these bones, deposition of this tissue type simply indicates the end of radial bone growth (Huttenlocker et al. 2013). Valuable insights into the timing of sexual and skeletal maturity can also be obtained from growth reconstructions (Sander 2000; Lee et al. 2013). In Chapter 5 of the present dissertation, we obtained growth curves for the different limb bones of *E. hemionus* by measuring the perimeters of the BGMs (Fig. 7 in Chapter 5). Interestingly, we observed that the decrease in periosteal growth rate, which is represented by the inflection point in the growth curve, agrees with the age of epiphyseal fusion (see Silver (1963) for the age of epiphyseal fusion in *E. caballus*) in

almost every bone analyzed (Fig. 7 and Table 3 in Chapter 5). This result suggests the change in the rate of radial growth to be a good indicator of the end of longitudinal bone growth. Bone growth curves do not provide information, however, about the sexual or the reproductive maturity of equid species. Regardless of the limb bone analyzed, reduction in periosteal growth rate occurs at the same time in *E. hemionus*' male and female (Fig. 7 in Chapter 5), though mares of Asiatic wild ass attain sexual and reproductive maturity earlier than stallions (Nowak 1999; Kaczensky et al. 2015; see also Table 1.1 in Chapter 1). Changes in the rate of radial bone growth are therefore unlike to be related to the onset of physiological/reproductive maturity in *Equus*.

Growth plots are also commonly used to analyze differences in growth rate between individuals and species (Marín-Moratalla et al. 2013; Padian and Stein 2013; Woodward et al. 2014). The growth curves obtained in Chapters 4 and 5 for femur, tibia and metapodia of *E. hemionus* reveal differences in growth rate between captive and wild specimens (Nacarino-Meneses et al. 2016a; Nacarino-Meneses et al. 2016b). Specifically, captive individuals grow at higher rates than wild individuals (Fig. 4 in Chapter 4; Fig. 7 in Chapter 5), probably due to the continuous food supply and care to which captive animals have access during their lifetime (Asa 2010). Growth rate differences between habitats have also been observed in alligators (Woodward et al. 2014) and ruminants (Marín-Moratalla et al. 2013), pointing out the influence of the environment on the life history of the species.

9.1.2. Enamel histology of extant *Equus*

Along with bones, mammalian teeth are frequently analyzed at their histological level to obtain LH information (Bromage et al. 2002; Dean 2006; Dirks et al. 2009; Jordana and Köhler 2011; Dirks et al. 2012). Specifically, daily and supra-daily incremental markings of dental enamel are usually examined to reconstruct rate and timing of tooth formation (Smith 2008). In mammals, dental development is tightly linked with key LH events such as weaning or age at maturity (Smith 1989; Smith 2000; Dean 2006). Thus, enamel formation time is usually considered a good proxy of their overall LH. Nevertheless, most of the research developed so far has focused on brachydont teeth (see a review in Smith 2008) and hypsodont species still remain poorly studied. Hitherto, dental enamel has only been extensively studied in some bovids and cervids (Macho and Williamson 2002; Iinuma et al. 2004a; Jordana and Köhler 2011; Kierdorf et al. 2013; Jordana et al. 2014; Jordana et al. 2015). In this thesis, enamel microstructure of the first lower molar has been thoroughly analyzed in the extant species *E. quagga*, *E. hemionus* and *E. grevyi* (Chapter 8; Nacarino-Meneses et al. 2017), increasing our knowledge on the histological growth and development of high-crowned teeth. Moreover, equid enamel is frequently examined in isotopic studies aimed at reconstructing the paleobiology and paleoecology of these vertebrates (Wang et al. 1994; Bryant et al. 1996; MacFadden 2000). The results obtained in the present dissertation, hence, may also help to correctly interpret the isotopic microsamples obtained from these mammals (Hoppe et al. 2004; Bendrey et al. 2015).

9.1.2.1. Daily incremental markings in the enamel of extant Equus*: the assessment of enamel secretion rate in equids*

The microscopic study of equid enamel has previously been addressed by Hoppe at al. (2004) in the extant domestic horse. These authors described the presence of incremental markings of daily periodicity in the enamel of premolars and third molars of *E. caballus*, and calculated an average rate of enamel secretion of 5 μm/day for this species (Hoppe et al. 2004). Strikingly, related hypsodont taxa such as bovids (Jordana and Köhler 2011; Kierdorf et al. 2013; Jordana et al. 2014) or cervids (Iinuma et al. 2004a; Jordana et al. 2014), secrete enamel at much more higher rates: between 10 μm/day and 17 μm/day. These discrepancies in daily secretion rate (DSR) between high-crowned mammals led certain authors to suggest that published observations in equid enamel might be incorrect, possibly as a consequence of a misidentification of sub-daily and daily incremental features (Kierdorf et al. 2013; Kierdorf et al. 2014). In the present dissertation, we tested the daily periodicity of enamel laminations in *Equus* by comparing the crown formation time (CFT) of still-developing unworn molars (calculated from histology) with the age of the individual estimated from the eruption pattern (see section 3.2.2.3 in Chapter 3 for further information). We postulate that both methodologies should provide equivalent results because equid first molars start their formation around birth (Soana et al. 1999; Hoppe et al. 2004). Our findings show indeed a high coincidence between the values of CFT estimated from enamel histology and the age of the individual to which they belong (Table 1 in Chapter 8), which corroborates both the daily periodicity of enamel laminations in *Equus* and the error in the classification of enamel incremental markings in previous studies, as suggested by Kierdorf et al. (2013, 2014). Actually, estimations of DSR obtained in this thesis and based on the counting of enamel laminations indicate that this biological tissue is secreted at a mean rate of ≈17 – 18 μm/day in extant *Equus* (Fig. 3 and Table 1 in Chapter 8). This finding agrees with the DSR values reported for other hypsodont vertebrates (Iinuma et al. 2004a; Jordana and Köhler 2011; Kierdorf et al. 2013; Jordana et al. 2014) and underlines the importance of a correct identification of enamel incremental markings when assessing enamel growth parameters.

9.1.2.2. Growth and ontogeny of equid molar crowns: histological findings and LH implications

Rates and patterns of equid molar crown formation have traditionally been studied from radiographic images (Dixon and Copeland 1993; Kirkland et al. 1996; Soana et al. 1999; Hoppe et al. 2004) or from measurements of the crown height (Levine 1982; Bendrey et al. 2015). In this PhD thesis, however, growth and development of equid first lower molars were reconstructed from the histological study of dental enamel for the first time (Chapter 8; Nacarino-Meneses et al. 2017). Our results suggest that equid molar crowns grow at an exponentially decreasing rate (Fig. 4 and Fig. 5 in Chapter 8), in agreement with previous investigations (Bendrey et al. 2015) that reported this pace of growth for equid enamel maturation. From the tooth cusp to the root, rates of enamel extension vary from ≈350 – 400 μm/day to ≈30 μm/day (Fig. 4C – E and Table 2 in Chapter 8), recording

a reduction in the rate of enamel formation along tooth development that has previously been reported in other mammalian clades (Smith 2008; Jordana and Köhler 2011; Dirks et al. 2012; Kierdorf et al. 2013; Kierdorf et al. 2014). Our histological analysis further shows that equid first lower molars experience different growth patterns during crown formation. Specifically, enamel grows linearly at the beginning of crown development (Fig. 4A in Chapter 8) but follows polynomial growth at later stages of crown formation (Fig. 4B in Chapter 8). Based on these different growth patterns, we established three developmental stages (CDS) for the crowns of extant *Equus*, each of them characterized by a specific enamel extension rate (EER) value (Fig. 4 and Table 2 in Chapter 8). Thus, CDSI corresponds to the first phase of crown formation in which enamel extends at very fast rates (≈350 – 400 μm/day) following linear growth (Fig. 4A, C and Table 2 in Chapter 8). The second phase of crown development (CDSII) registers the fastest period of polynomial growth and presents EER values of ≈130 μm/day (Fig. 4B, D and Table 2 in Chapter 8). Finally, rates of enamel extension are of ≈30 μm/day during CDSIII, which corresponds to the slowest phase of polynomial growth (Fig. 4B, E and Table 2 in Chapter 8). Our results do not revealed differences between species in the rate of enamel extension within each CDS (Fig. 4C – E and Supplementary Table S5 in Chapter 8), which suggests EER to be a very conservative enamel growth parameter and, as previously mentioned, characteristic of each CDS. This finding highlights the potential of EER for both paleodemographic and LH studies. On the one hand, estimations of this parameter on fragmentary teeth allows its assignment to a specific age category that broadly corresponds to one of the CDS already described. On the other hand, EER must be analyzed along with the macroscopic appearance of the tooth to obtain LH information from equid enamel. Differences in growth rate and, therefore, in LH will only be found if the estimated CDS of a tooth do not match the degree of macroscopic root development and/or dental wear expected for this ontogenetic stage.

Using *E. hemionus* as a test-case of study, we reconstructed the complete pace of growth of the equid first lower molar and we found evidence that the onset of each CDS is related to ontogenetic and structural modifications of the tooth (Fig. 5 in Chapter 8). The beginning of CDSII, for instance, correlates well with the time of eruption of this tooth in the Asiatic wild ass (see Lkhagvasuren et al. (2013) for dental eruption time in *E. hemionus*). In mammals, this ontogenetic event is closely related with the age at weaning (Smith 1989; Dirks and Bowman 2007), an important LH trait in these vertebrates (Stearns 1992). Therefore, reconstruction of dental growth in equids provides useful information about this LH characteristic by identifying the transition from CDSI to CDSII. The beginning of CDSIII, on the other hand, matches the start of structural tooth root formation (or crown divergence) in all species under study (see Kirkland et al. (1996) for timing of appearance of structural roots in *E. caballus*) (Fig. 4B and Fig. 5A in Chapter 8). In agreement with previous studies (Sisson 1914; Strömberg 2006), the analysis of equid enamel performed in the present dissertation reveals that this biological tissue extends over the limit of what is generally considered the crown of the tooth (Fig. 2 in Chapter 8), indicating a discrepancy between the histological definition of the crown (part of the tooth composed of enamel; Hillson (2005)) and the macroscopic division of the equid tooth in crown and

root. This inconsistency between the macro- and microanatomy of equid teeth challenges previous studies that considered crown divergence as the crown's end in these mammals. This includes, for instance, estimations of the hypsodonty index (Janis 1988; Mendoza and Palmqvist 2008; Cantalapiedra et al. 2017) or the reconstruction of dental growth from external observations of the tooth crown (Hoppe et al. 2004; Bendrey et al. 2015), as both kinds of research involve measurements of the crown height (Janis 1988; Bendrey et al. 2015). As dental enamel covering the structural tooth roots makes up almost 1 – 1.5 cm of the crown and takes between 1 and 2 years to be formed (Fig. 4B in Chapter 8), failure to consider this area of the tooth in the previously mentioned studies leads to underestimates of the hypsodonty index or the crown formation time (CFT).

In equids, more reliable estimates of both dental parameters (hypsodonty index and CFT) can be obtained from enamel histology. The results of this PhD thesis show that the first lower molar crown requires almost twice the time to be formed in the Asiatic wild ass than in the Grevy's and plains zebra (Fig. 4B in Chapter 8). This suggests that *E. hemionus* is more hypsodont in comparison with the African zebras, which contrasts with previous studies that reported comparable hypsodonty indexes for these three equids (Janis 1988; Mendoza and Palmqvist 2008; Cantalapiedra et al. 2017). High-crowned (hypsodont) molars have usually been related to very abrasive diets (Janis 1988; Damuth and Janis 2011) such as in living equids, which mainly feed on grass (Nowak 1999). Although the extant *Equus* species analyzed here present a similar degree of abrasiveness in their diets (Schulz and Kaiser 2013), a higher degree of hypsodonty is expected in the Asiatic wild ass because it dwells in a much more arid habitat (Nowak 1999; Kaczensky et al. 2015), which also influences the rate of tooth wear (Kaiser et al. 2013). Nevertheless, the higher crown heights here inferred for *E. hemionus* can also be explained as an adaptation of the species to an extended longevity (Veiberg et al. 2007; Köhler 2010; Ozaki et al. 2010; Damuth and Janis 2011; Jordana et al. 2012; Pérez-Barbería et al. 2015). According to LHT, organisms inhabiting resource-limited environments and facing low rates of predation invest more energy in growth and maintenance than in reproduction (Stearns 1992), which triggers extended longevity (Palkovacs 2003; Köhler 2009; Köhler and Moyà-Solà 2009; Köhler 2010; Jordana et al. 2012). *E. hemionus* lives in a very poor habitat (the Gobi Desert) and it is only predated by grey wolves (Feh et al. 2001; Kaczensky et al. 2015). Therefore, an increase in life span would be expected for this species. Actually, this animal lives up to 29 years in the wild (Lkhagvasuren et al. 2018), while the maximum longevity reported for *E. quagga* and *E. grevyi* is only of 21 and 18 years respectively (Smuts 1974; Churcher 1993; see also Table 1.1. in Chapter 1). Thus, a higher degree of hypsodonty in *E. hemionus* likely increases the durability of its teeth over a longer life span in response to the low resource levels in its habitat.

The exhaustive analysis of equid enamel performed in the present dissertation has not only revealed information about rates and patterns of tooth formation in *Equus* but also about rates of tooth wear in this group (Fig. 5B in Chapter 8). Superimposition of *E. hemionus*' teeth based on correspondences of EER indicated wear rates of ≈13 mm/year for the first six years of life and of ≈5 mm/year for the next six-year period. The

estimation obtained for the first time lapse contrasts importantly with published wear rates in extant and extinct Equidae of 3 – 5 mm/year (Spinage 1972; Hulbert 1982; Dixon and du Toit 2011), while the published estimations fairly match the values for the second ontogenetic period. Overall, our findings are consistent with the eruption pattern of the Asiatic wild Ass. In this animal, the first lower molar is the first permanent tooth to erupt (Lkhagvasuren et al. 2013). Also, complete permanent dentition, which distributes grinding and, hence, the amount of wear over a larger surface, is not present until the fifth year of life (Lkhagvasuren et al. 2013). Therefore, higher rates of wear such as those inferred in the present dissertation (Chapter 8) are expected at earlier ontogenetic stages. These greater wear rates early in ontogeny make that the crown formed during the first year of life is almost completely worn down in a seven-year-old tooth (Fig. 5B in Chapter 8). This should be taken into account in isotopic studies performed on equid enamel to correctly interpret the results obtained.

9.2. The life history of extinct *Equus*: Insights from bone and dental histology

The histological analysis of bone and enamel tissue is an important tool to reconstruct the LH strategy of fossil mammals (e.g. Bromage et al. 2002; Köhler and Moyà-Solà 2009; Köhler 2010; Jordana and Köhler 2011; Marín-Moratalla et al. 2011; Amson et al. 2015; Kolb et al. 2015b; Moncunill-Solé et al. 2016; Orlandi-Oliveras et al. 2016). Because LH strategies are shaped by environmental selective pressures (Stearns 1992; Roff 2002; Ricklefs 2008), they are indicative of the prevailing ecological conditions. LHs of fossil taxa, hence, provide both information about past environments and key data for the interpretation of evolutionary trends in body size (Bromage et al. 2002; Palkovacs 2003; Raia et al. 2003; Raia and Meiri 2006; Köhler and Moyà-Solà 2009; Köhler 2010; Jordana and Köhler 2011; Marín-Moratalla et al. 2011; Moncunill-Solé et al. 2016; Orlandi-Oliveras et al. 2016), as predicted from allometric scaling rules between LH traits and body mass (Peters 1983; Calder 1984). The trend in size-reduction observed in Old World *Equus* is one of the most remarkable features that characterize the evolution of the genus (Eisenmann 1991; Forsten 1991; Alberdi et al. 1995; Cantalapiedra et al. 2017). Both the stenonoid and the caballoid lineages of equids experienced size reduction during their Pleistocene and Holocene evolution in Africa and Eurasia (Forsten 1988; Forsten 1991; Alberdi et al. 1995; Alberdi et al. 1998), which finally resulted in the smaller body size of extant horses (Ernest 2003) in comparison with most of their Pleistocene relatives (Alberdi et al. 1995). Paleontological studies have traditionally proposed changes in resources, habitat and climate during the Pleistocene to be the main selective forces determining body size in *Equus* and therefore the main drivers of the size variation observed in this group (Forsten 1991; Alberdi et al. 1995; Cantalapiedra et al. 2017). LHT provides an alternative framework of analysis in which size shifts are the result of LH adaptations to different environments (Palkovacs 2003), which has been poorly explored for fossil forms. An exception is the dwarfing of elephants in Mediterranean islands, which has been claimed to result from selection for

enhanced reproduction (*r*) (Bromage et al. 2002; Raia et al. 2003; Raia and Meiri 2006). However, evolutionary changes in body size described for *Equus* have never been studied under this perspective.

In the present dissertation, we used bone and dental histology for the first time to obtain data on key LH traits such as age at maturity and growth rate of several Middle and Late Pleistocene European equid species (Chapter 7 and 8). From these data, we obtained preliminary results about the LH strategy of these extinct mammals that allowed us to investigate the body size variations described for the *Equus* lineage within the framework of the LHT.

9.2.1. The LH of Middle Pleistocene Equus*: inferences from bone histology*

In Chapter 7 of the present dissertation, several metapodia of the Middle Pleistocene species *E. steinheimensis* and *E. mosbachensis* were histologically analyzed to estimate certain LH traits. Specifically, we inferred their growth rate, their age at maturity and their age at death from the study of bone tissue types and BGMs (de Margerie et al. 2002; Huttenlocker et al. 2013; Woodward et al. 2013; Nacarino-Meneses et al. 2016b). These latter histological features, specifically non-cyclical BGMs, also allowed the estimation of the size at birth (Chapter 6, see also section 9.1.1.2) in these Middle Pleistocene species.

Growth rate of extinct Middle Pleistocene species was qualitatively assessed from the analysis of bone vascularization (de Margerie et al. 2002; Lee et al. 2013) and from bone growth plots (Marín-Moratalla et al. 2013; Nacarino-Meneses et al. 2016b). Results of this thesis show that metapodia of both fossil equids are composed of a FLC with multiple VCs (Fig. 2A – D in Chapter 7). Most of them are oriented longitudinally, although circular and radial VCs are also present in the metapodial bone cortices of Middle Pleistocene horses (Fig. 2A – D in Chapter 7). No qualitative differences in bone microstructure or vascularization have been observed between *E. steinheimensis* and *E. mosbachensis*, suggesting similar rates of bone deposition (de Margerie et al. 2002; Lee et al. 2013), and thus of growth rate, for both Middle Pleistocene equids. When comparing their bone microanatomy with that of the extant *E. grevyi* and *E. hemionus* (Fig. 2E, F in Chapter 7), however, a higher proportion of VCs, and specifically of radial VCs, was identified in the metapodia of the extinct species (Fig. 2A, B in Chapter 7). This suggests higher rates of bone deposition (de Margerie et al. 2002; de Margerie et al. 2004) and, therefore, higher growth rates for the Middle Pleistocene taxa in comparison with the extant Asiatic wild ass and the Grevy's zebra. Results obtained from growth reconstructions (Fig. 4 in Chapter 7) agree with the information inferred from bone histology (Fig. 2 in Chapter 7). Metapodial growth curves evince higher growth rates in Middle Pleistocene equids in comparison with living representatives of the group, as metacarpi and metatarsi of *E. steinheimensis* and *E. mosbachensis* grow at higher rates than metapodia of the Asiatic wild ass and/or the Grevy's zebra (Fig. 4 in Chapter 7).

Bone growth curves also yielded information about the skeletal maturity of Middle Pleistocene equids (Chapter 7). According to our results, metapodial growth rate decreases at the second year of life in *E. steinheimensis* and *E. mosbachensis*, the same as in extant species (Fig. 4 in Chapter 7). This finding suggests that metapodia fuse their epiphyses at a similar age in both groups of equids (Nacarino-Meneses et al. 2016b; see also section 9.1.1.2). From this result, however, we cannot infer an absolute age at skeletal maturity for the extinct *E. mosbachensis* and *E. steinheimensis*, as metapodia are among those long bone of equids that finish their growth earliest (Silver 1963). Future histological studies of other long bones that fuse their epiphyses later in ontogeny, such as femora (Silver 1963), are necessary to obtain information about this biological trait in Middle Pleistocene horses. The histological analysis of the femur is also essential to determine the age at reproductive maturity in these Middle Pleistocene species, as the femur is the only long bone in which the presence of the EFS marks the attainment of this LH trait in equids (Nacarino-Meneses et al. 2016b; see also section 9.1.1.2). The presence of EFS in the metapodia of equids is not related with this LH trait (Nacarino-Meneses et al. 2016b; see also section 9.1.1.2), so we could not provide an assessment of the age at reproductive maturity from metapodial bone histology for the extinct Middle Pleistocene species studied in this dissertation.

Age at death estimates for *E. steinheimensis* and *E. mosbachensis* were obtained from the counting of CGMs. As previously demonstrated in this thesis, metapodia provide accurate individual age estimations in equids (Chapter 5, Nacarino-Meneses et al. 2016b; see also section 9.1.1.2). These age inferences, however, should always be considered as minimum ages (Castanet et al. 2004). Considering this limitation, we inferred a minimum age at death of 6 years for *E. mosbachensis* and of 5 years for *E. steinheimensis*, as a maximum of 6 and 5 CGMs were identified in their metapodial bone cortices respectively (Fig. 3 in Chapter 7). The number of CGMs registered in the metapodia of both Middle Pleistocene species is comparable to that of the Asiatic wild ass (Nacarino-Meneses et al. 2016b). However, the small fossil sample size of this thesis limits reliable comparisons between the longevity of *E. steinheimensis* and *E. mosbachensis* and that of extant equids. Future research on a larger sample size is necessary to assess longevity of these extinct equids with more confidence.

Size at birth of Middle Pleistocene equids was inferred from the analysis of the NL (Chapter 6; Nacarino-Meneses and Köhler accepted) found in metapodial bones (Fig. 3 in Chapter 7). Results indicate that neonate foals were bigger in the larger *E. mosbachensis* than in the smaller *E. steinheimensis*, as the perimeter of their NL is 80 – 90 mm and 75 – 80 mm respectively (Fig. 4 and Table 3 in Chapter 7). The smallest extant *E. hemionus* and *E. grevyi* are also considerably smaller at the time of birth than Middle Pleisocene taxa, with perimeters of the NL of only 50 – 60 mm in the Asiatic wild ass and around 75 mm in Grevy's zebra (Fig. 4 and Table 3 in Chapter 7). Interestingly, *E. mosbachensis* is also the largest species of the sample with a mean adult body weight of 607 kg (Fig. 5 and Table 2 in Chapter 7). It is followed by *E. steinheimensis*, whose adult body mass is around 470 kg (Fig. 5 and Table 2 in Chapter 7). Adult individuals of Asiatic wild ass and Grevy's zebra, however, are much lighter than Middle Pleistocene equids, with a mean adult body mass

of 230 kg and 384 kg respectively (Ernest 2003). Thus, results obtained for neonatal body size of Middle Pleistocene *Equus* conform to the allometric predictions from LHT for the relation between size at birth and adult body size in vertebrates (Blueweiss et al. 1978; Calder 1984), as bigger species give rise to bigger neonate foals and vice versa (Tables 2 and 3 in Chapter 7).

9.2.2. The LH of Late Pleistocene Equus*: inferences from enamel histology*

Dental enamel of the first lower molar was histologically analyzed in the Late Pleistocene species *E. ferus* and *E. hydruntinus* to reconstruct their pattern and rate of molar growth (Chapter 8; Nacarino-Meneses et al. 2017). Enamel growth parameters such as repeat interval (RI), daily secretion rate (DSR) and enamel extension rate (EER) were calculated in these extinct *Equus* species to infer rates of tooth development (Smith 2008). In a first attempt to infer LH information for these extinct taxa, these parameters were considered as a proxy of the overall growth rate of the organism. Unfortunately, crown formation times (CFT) could not be calculated in any of the Late Pleistocene species studied because of the characteristics of the sample. All fossil teeth presented some degree of wear (Table 3 in Chapter 8) that hampered the reconstruction of the complete pattern of crown formation.

It has been suggested that the periodicity of deposition of Retzius lines in mammalian enamel, also known as repeat interval (RI), correlates with a specific LH characteristic: the body mass (Bromage et al. 2009; Bromage et al. 2012). Results of this dissertation (Table 2 in Chapter 8) support these previous studies, which described a relationship between RI and body mass in proboscideans and primates (Bromage et al. 2009). RI in *E. hydruntinus* consists of 4 – 6 days, while it comprises 5 – 7 or 5 – 6 days in the fossil *E. ferus* and in the extant equids studied (*E. hemionus*, *E. quagga*, *E. grevyi*) (Table 2 in Chapter 8). *E. hydruntinus* is the smallest equid of the analysis (Table 2 in Chapter 8), suggesting that this enamel growth parameter is also related to body mass in equids.

E. hydruntinus also differs significantly in DSR from *E. quagga* and *E. hemionus* (Fig. 3, Table 2 and Supplementary Table S3 in Chapter 8). Specifically, the mean rate of enamel secretion in this extinct species is ≈19 μm/day, while the Asiatic wild ass and the plains zebra secrete enamel at ≈17 μm/day. This result was totally unexpected, as *E. hydruntinus* presents the lowest weight and the lowest hypsodonty index among extant and extinct *Equus* species studied (Table 2 in Chapter 8). Because DSRs have been related to tooth size (Jordana et al. 2014) and LH (Dirks et al. 2012), values comparable to that of *E. quagga* (the smallest and less hypsodont living species of the analysis, see Table 2 in Chapter 8) were expected for *E. hydruntinus*. DSR, however, is also strongly linked to tooth morphology (e.g. enamel thickness) (Dirks et al. 2012). Therefore, the higher rates of enamel secretion found in the Late Pleistocene species *E. hydruntinus* may be related to dental morphology. This extinct equid shares several morphological characteristics with both extant and extinct *Equus* (Burke et al. 2003; Orlando et al. 2006; Geigl and Grange 2012), among which the primitive enamel pattern of the lower molars is noteworthy

because it resembles that of *E. stenonis* (Burke et al. 2003). A histological analysis of the enamel in this early Pliocene species, as well as future studies on *E. hydruntinus* involving a larger sample, might help uncovering the main factors affecting DSR in this particular Late Pleistocene taxon.

Among enamel growth parameters, EER is known to provide key information about the LH of the species (Jordana et al. 2014). Indeed, results obtained in the present dissertation reveal that the combined analysis of EER and the macroscopic appearance of the tooth (degree of root development and wear) yields valuable information about the pace of life of equids (Chapter 8; see also section 9.1.2.2.). Specifically, differences in LH should be expected if both features do not match when comparing *Equus* species. Values of EER obtained for the fossil teeth of *E. hydruntinus* and *E. ferus* were the expected from their degree of wear and root development (Fig. 6 and Supplementary Table S6 in Chapter 8), which suggests a similar time of crown formation and eruption for the first lower molar of Late Pleistocene species and extant equids.

9.2.3. Evolutionary changes in body size of the genus Equus*: preliminary analysis from a LH perspective*

Although size trends are traditionally believed to result from selective pressures acting directly on body size (Foster 1964; Lomolino 1985), several researchers have suggested that size variation can instead result from the direct action of selective pressures on key LH traits to which adult body size is sensitive (Stearns 1992; Palkovacs 2003). Based on this latter assumption, Palkovacs (2003) proposed a predictive model that explains the changes in body size experienced by insular mammals in relation to their mainland relatives (the island rule, Van Valen (1973)). Following LHT (Stearns 1992; Roff 2002), he stated that resource levels and predation pressure (extrinsic mortality) are the key mechanisms (selection pressures) acting on growth rate and age at maturity (LH traits) to determine the LH strategy that maximizes reproductive success (Palkovacs 2003). According to this model, body size variation can be a by-product of natural selection. The theoretical framework of Palkovacs (2003) has successfully been tested in insular environments (Köhler 2010; Jordana and Köhler 2011; Marín-Moratalla et al. 2011; Moncunill-Solé et al. 2016; Orlandi-Oliveras et al. 2016), but it has never been applied before to exploring body size tendencies that occur on continent, such as those observed in *Equus* during their evolution in Europe (Forsten 1991; Alberdi et al. 1995; Alberdi et al. 1998). Here we use Palkovacs' (2003) LH model to analyze the size-trend reduction observed in the *Equus* lineage by comparing continental environments that differ in resource levels and in the degree of predation pressure (extrinsic mortality).

The histological analysis of bones and teeth performed in the present dissertation has yielded preliminary data about one of the most important LH features, i.e. the growth rate, in Middle and Late Pleistocene *Equus* species (Chapters 7 and 8; see also sections 9.2.1 and 9.2.2). Specifically, our preliminary findings reveal higher rates of growth in the larger Middle Pleistocene *Equus* species than in the smaller extant taxa (Chapter 7; see

also section 9.2.1), but comparable growth rates between similar-sized Late Pleistocene and living equids (Chapter 8; see also section 9.2.1). These results suggest that larger Middle Pleistocene taxa grew at higher rates than smaller species, a finding that agrees with previous observations in fossil artiodactyls (Köhler 2010; Amson et al. 2015) and conforms to allometric predictions (Calder 1984). According to Palkovacs (2003), resource availability is the main selection pressure acting on individual growth rate, which, in turn, influences final body size. In resource-poor environments, for instance, growth rate is reduced because individuals expend more energy in acquiring resources (Palkovacs 2003). The higher growth rates inferred for the larger Middle Pleistocene equids (*E. mosbachensis* and *E. steinheimensis*) suggests, hence, that these equids dwelt in more resource-rich environments in comparison to Late Pleistocene (*E. ferus* and *E. hydruntinus*) or extant species (*E. quagga*, *E. hemionus*, *E. grevyi*). This hypothesis is supported by the paleoecological conditions described for each habitat and species (Table 9.1). Mosbach and Steinheim sites, on the one hand, are Middle Pleistocene localities dated as Cromerian (MIS 13, 15) and Holsteinian (MIS11) interglacials, respectively (Kahlke et al. 2011; Van

Species	BM (kg)	Chronology	Extrinsic mortality	Habitat
E. mosbachensis	600	Middle Pleistocene	*Lynx issiodorensis, Panthera gombaszoegensis, Panthera leo fossilis, Panthera pardusi, Acinonyx pardinensis, Homotherium, Canis lupus mosbachensis, Cuon alpinus priscus, Cuon dubius stehlini, Pliocrocuta perrieri, Crocuta spelaea*	Open steppes interrupted by warm and humid episodes with extended forests
E. steinheimensis	470		*Canis lupus, Panthera* cf. *leo, Homotherium*	Temperate, humid woodland and shrubland
E. ferus	350	Late Pleistocene	*Canis, Panthera, Crocuta*	Cold and dry climate conditions in grasslands and open pine forests
E. hydruntinus	215			
E. hemionus	230	Extant	*Canis lupus*	Desert and semi-desert plains
E. quagga	257		*Panthera leo, Crocuta crocuta, Acinonyx jubatus, Lycaon pictus*	Open savanna or open woodland
E. grevyi	384		*Panthera leo, Crocuta crocuta, Lycaon pictus, Panthera pardus*	Arid and semi-arid grasslands and shrublands

Table 9.1. Environmental conditions of extinct and extant *Equus*. Data on body mass (BM) was calculated from bone measurements for the species *E. mosbachensis* and *E. steinheimensis* (Chapter 7) and compiled from Cantalapiedra et al. (2017) for *E. ferus* and *E. hydruntinus*, and Ernest (2003) for *E. hemionus*, *E. quagga* and *E. grevyi*. Information of extrinsic mortality compiled from Kahlke (1961) and Kahlke (1975) for *E. mosbachensis*, Adam (1954) and Kahlke (1975) for *E. steinheimensis*, Carrión (1992) and Fernández et al. (2007) for *E. ferus* and *E. hydruntinus*, Feh et al. (2001) for *E. hemionus*, Grubb (1981) for *E. quagga*, Churcher (1993) for *E. grevyi*. Habitat information compiled from Maul et al. (2000) and Kahlke et al. (2011) for *E. mosbachensis*, Pushkina et al. (2014) for *E. steinheimensis*, Carrión (1992) and Fernández et al. (2007) for *E. ferus* and *E. hydruntinus*, Kaczensky et al. (2015) for *E. hemionus*, King and Moehlman (2016) for *E. quagga*, Rubenstein et al. (2016) for *E. grevyi*.

Asperen 2013). While the Mosbach site is characterized by open steppes and extended forests (Maul et al. 2000; Kahlke et al. 2011), the Steinheim site is thought to present a habitat composed of woodland and shrubland (Pushkina et al. 2014). Both Middle Pleistocene localities are described as dominated by temperate and humid climates (Maul et al. 2000; Kahlke et al. 2011; Pushkina et al. 2014). Paleoenvironmental reconstructions of La Carihuela site (Late Pleistocene), on the other hand, evoke cold and dry habitats of grasslands and open forests for the period when *E. hydruntinus* and *E. ferus* inhabited this area (Carrión 1992; Fernández et al. 2007). This suggests low resource levels in the habitats of Late Pleistocene species in comparison to those of Middle Pleistocene *Equus*, which agrees with the reduction in growth rate observed in the more recent taxa. Actually, extant equids also dwell in more resource-limited environments than Middle Pleistocene species, particularly the Grevy's zebra and the Asiatic wild ass (Kaczensky et al. 2015; Rubenstein et al. 2016). *E. grevyi*, specifically, dwells in arid or semiarid grasslands and shrublands (Rubenstein et al. 2016) characterized by a negative mean annual climatic water balance (Schulz and Kaiser 2013). The Asiatic wild ass, on the other hand, is endemic of the desert plains of Asia (Kaczensky et al. 2015). The low resource levels of these environments likely conditioned the growth rate of these equids, thus affecting their final body size (Palkovacs 2003).

According to Palkovacs (2003), adult body size is also determined by the age at maturity. Unfortunately, the characteristics of the fossil sample analyzed in this dissertation did not allow the estimation of this LH trait in the extinct Middle or Late Pleistocene *Equus*. For instance, due to the lack of femora, which is the most reliable bone for calculating age at maturity (Nacarino-Meneses et al. 2016b; see also section 9.1.1.2), we could not assess an absolute timing of physiological or reproductive maturity for the extinct *E. mosbachensis* and *E. steinheimensis*. Following the LH model proposed by Palkovacs (2003), we would expect, however, that the slow-growing Late Pleistocene and extant *Equus* delayed their maturity in comparison to Middle Pleistocene taxa. Nevertheless, future histological studies are necessary to corroborate this hypothesis. The advance or delay in the age at maturity is generally determined by the degree of extrinsic mortality (i.e. predation) (Roff 1992; Stearns 1992). Under conditions of low extrinsic mortality, organisms mature later to increase fecundity and to produce higher-quality offspring (Stearns 2000). In contrast, organisms advance their age at maturity when facing high extrinsic mortality, as it reduces the time of exposure to juvenile mortality (Stearns 2000). The hypothesis of delayed maturity in Late Pleistocene and extant species would be the result, hence, of experiencing lower rates of extrinsic mortality. Paleontological data support this hypothesis which, as already mentioned, should be tested in future investigations. As Table 9.1. shows, a higher number of potential predators has been found in Middle Pleistocene localities (mainly in Mosbach Sands) than in Late Pleistocene or extant environments. Thus, while *E. mosbachensis* was potentially threatened by many different species of felids, canids and hyaenids (Kahlke 1961; Kahlke 1975), the number of potential predators of Late Pleistocene or of extant equids was/is much lower (Grubb 1981; Carrión 1992; Churcher 1993; Feh et al. 2001; Fernández et al. 2007). It is worth noting that human remains have been found in some of the paleontological sites analyzed in the present dissertation, such as Steinheim an der

Murr (Street et al. 2006) and La Carihuela (Fernández et al. 2007). As hunting affects the LH strategy of mammals (Fisher 2009) and influences their habitat selection (Djagoun et al. 2014), these humans also may have influenced the degree of extrinsic mortality experienced by extinct equids. This issue, however, is actually beyond the aims and scope of the present dissertation, and future demographic studies would be necessary to address this question using bone and dental histology.

From the preliminary histological analysis performed in this PhD dissertation, hence, we obtained evidence that growth rate is a key LH trait in determining adult body size of extant and extinct *Equus*. This represents a first step towards the understanding of size trends observed in European Pleistocene equids from the angle of LH theory. The use of Palkovacs' (2003) LH model also permits to formulate new hypotheses regarding modifications in other LH traits (i.e. age at maturity) which will be tested through future research.

- Chapter 10 -

Conclusions

Conclusions

I. Bone tissue types in equid limb bones vary through ontogeny, recording individual growth and development. At early ontogenetic stages, femur, tibia and metapodia of the Asiatic wild ass are composed of a fibrolamellar complex (FLC) with multiple vascular canals (VCs). These mainly present a circular orientation in the femur and the tibia, but a longitudinal arrangement forming circular rows in metapodia, probably reflecting different biomechanical stresses that each limb bone suffers. The FLC is gradually replaced by Haversian systems, beginning in young individuals within the innermost cortex and expanding towards the outer cortex with increasing age. They, thus, make up most of the bone cortex in older individuals. Adult specimens further present a poorly-vascularized laminar bone, namely the external fundamental system (EFS), in the most external femoral and metapodial cortices. Bone tissue types and components of the FLC matrix also vary within femoral cross-sections in *E. hemionus*, related with the bone drift process.

II. Certain changes in bone matrix and vascularity occur in the limb bones of equids at the time of birth. In the tibiae of all *Equus* species and in the femora of *E. quagga* and *E. grevyi*, the FLC deposited before birth shows a higher proportion of parallel-fibered bone (PFB) than the FLC formed after this life history (LH) event. This suggests higher rates of postnatal bone formation in equids. Perinatal variation in VC size also supports this inference, as VCs formed postnatally are larger than those formed prenatally in all species and limb bones studied. Furthermore, VCs change from longitudinal to mainly circular orientation in the femora of *E. hemionus* just after birth, probably associated with the onset of locomotion in these equids.

III. Birth is also recorded in the limb bones of equids in the form of a non-cyclical bone growth mark (BGM) (LAG). The deposition of this feature matches a period of growth decline/arrest in newborn foals regulated by cortisol, growth and thyroid hormones. This neonatal line (NL), which is analogous to the NL described in mammalian dental tissues, was identified in the tibiae and metapodia of all *Equus* species studied, from foals to adults. The NL also appears in the femur of foals and yearlings, but it was not recognized in juvenile and adult femora due to resorption of the medullary cavity.

IV. Cyclical BGMs (CGMs) in individuals of Asiatic wild ass of known age reveal that femora provide the most accurate age and LH estimations, as this bone registers the highest number of CGMs both within the FLC and within the whole bone

cortex. The total number of CGMs in femoral cortices further matches the age at death of the specimen, confirming for the first time the annual deposition of these features in equids. Metapodia yield good individual age estimations, as they record a similar number of CGMs as femora. Tibiae, however, do not provide reliable skeletochronological results in equids, due to the great number of secondary osteons at early ontogenetic stages and to the lack of EFSs in adult specimens.

V. Key LH and biological traits can be inferred from bone histology in equids. Thus, deposition of the EFS in the femora of *E. hemionus* marks the attainment of reproductive maturity. Inferences about skeletal maturity can be obtained, however, from bone growth plots, as the abrupt reduction in the rate of bone formation matches the timing of epiphyseal fusion in femora and metapodia of the Asiatic wild ass. Bone growth curves also revealed differences in growth rate between captive and wild individuals, which likely result from the different environments that these animals inhabited.

VI. The histological analysis of first lower equid molars showed that enamel laminations are deposited daily in these mammals. This evinces the misidentification of enamel incremental markings in previous studies performed in *Equus* and invalidates already published rates of enamel secretion for the group. Actually, our findings revealed enamel secretion rates of around 17 – 18 μm/day for extant equids, which are almost 4 times higher than previously reported.

VII. Three different crown developmental stages (CDS) can be established for the first lower molars of *Equus* based on the different rates and growth patterns that this tooth experiences during formation. CDSI is characterized by very high rates of enamel extension (EER) and linear growth, while CDSII and CDSIII present intermediate and very low values of EER, respectively, following polynomial growth. The beginning of each CDS corresponds to ontogenetic and structural modifications of the tooth, such as the eruption time (transition from CDSI to CDSII) or the appearance of the structural tooth roots (transition from CDSII to CDSIII). These CDSs are a powerful tool for age determination and demographic studies, as well as for LH research.

VIII. Dental enamel extends beyond the molar cervix in equids, evidencing the already known discrepancy between dental macro- and microanatomy and highlighting the need to correctly measure crown height from the external appearance of the teeth in these mammals. Previous studies on the estimation of the hypsodonty index or on the calculation of crown formation time in *Equus* should therefore be reviewed, as they likely underestimated data as a consequence of an erroneous identification of the point of crown divergence (beginning of structural roots) as the crown's end.

IX. Estimates of crown formation time for the first lower molar obtained from enamel histology revealed a longer period of crown growth in the Asiatic wild ass than in

the Grevy's and plains zebras. This suggests an increase in tooth height (hypsodonty) in *E. hemionus* in comparison to both African taxa, which likely results from an adaptation of the Asiatic wild ass to a more arid habitat and from its extended longevity.

X. We inferred very high rates of wear for *E. hemionus*' first lower molars during the earlier stages of ontogeny (≈13 mm/year). These rates decrease up to 3 – 5 mm/year later in ontogeny, when the permanent dentition has completely erupted and wear is distributed over a larger surface.

XI. Several LH traits were estimated in the Middle Pleistocene species *E. steinheimensis* and *E. mosbachensis* from the histological analysis of their metapodia. From the counting of CGMs, we inferred a minimum longevity of 5 and 6 years for each fossil species respectively. Our results also indicated higher growth rates in these extinct equids than in extant *E. hemionus* and *E. grevyi*, but a similar timing of skeletal maturity for the metapodia in Middle Pleistocene species and extant *Equus*. Size at birth was also estimated in *E. steinheimensis* and *E. mosbachensis*. The results conform to allometric predictions for this LH trait from adult body size.

XII. Enamel histology was analyzed in the first lower molars of the Late Pleistocene species *E. ferus* and *E. hydruntinus*. Results showed that *E. hydruntinus* secreted enamel at significantly lower rates than similar-sized extant species such as *E. hemionus* and/or *E. quagga*. These differences, however, are likely related to tooth morphology rather than to LH or tooth size (hypsodonty). Nevertheless, Late Pleistocene and extant *Equus* presented similar values of EER, which suggests similar times of formation and eruption for the first lower molar in both groups of equids.

XIII. The trend in size-decrease that characterizes the evolution of Old World *Equus* is analyzed within a LH framework here for the first time. Our first results indicate that growth rate is an important LH trait that influences adult body size in *Equus*, and that shifts in this trait are triggered by changes in the key selection pressure resource availability. Following the LH model proposed by Palkovacs (2003), we hypothesize that changes in growth rate were probably coupled with changes in age at maturity. Future studies on a larger and more suitable fossil sample are necessary, however, to corroborate this suggestion.

- Chapter 11 -

References

References

Adam KD. 1954. Die mittelpleistozänen Faunen von Steinheim an der Murr (Württemberg). *Quaternaria* 1:131–144.

Alberdi MT., Bonadonna FP. 1988. Equidae (Perissodactyla, Mammalia): extinctions subsequent to the climatic changes. *Revista Española de Paleontologia* 3:39–43.

Alberdi MT., Cerdeño E. 2003. Sistemática y distribución de los perisodáctilos del Neógeno y Cuaternario. In: Jiménez Fuentes E, Civis Llovera J eds. *Los vertebrados fósiles en la historia de la vida. Excavación, estudio y patrimonio*. Salamanca: Aquilafuente, Ediciones Universidad de Salamanca, 237–279.

Alberdi MT., Ortiz-Jaureguizar E., Prado JL. 1998. A quantitative review of European stenonoid horses. *Journal of Paleontology* 72:371–387.

Alberdi MT., Prado JL., Ortiz-Jaureguizar E. 1995. Patterns of body size changes in fossil and living Equini (Perissodactyla). *Biological Journal of the Linnean Society* 54:349–370.

Amprino R. 1947. La structure du tissu osseux envisagée comme expression de différences dans la vitesse de l'accroissement. *Archives of Biology* 58:315–330.

Amson E., Kolb C., Scheyer TM., Sánchez-Villagra MR. 2015. Growth and life history of Middle Miocene deer (Mammalia, Cervidae) based on bone histology. *Comptes Rendus - Palevol* 14:637–645.

Anderson JF., Hall-Martin A., Russell DA. 1985. Long-bone circumference and weight in mammals, birds and dinosaurs. *Journal of Zoology* 207:53–61.

Asa CS. 2010. Reproductive physiology. In: Kleiman DG, Thompson K V., Kirk Baer C eds. *Wild Mammals in Captivity*. Chicago: The University of Chicago Press, 411–428.

Azorit C., Muñoz-Cobo J., Hervás J., Analla M. 2004. Aging through growth marks in teeth of Spanish red deer. *Wildlife Society Bulletin* 32:702–710.

Azzaroli A. 1983. Quaternary mammals and the "end-Villafranchian" dispersal event - A turning point in the history of Eurasia. *Palaeogeography, Palaeoclimatology, Palaeoecology* 44:117–139.

Azzaroli A. 1990. The genus *Equus* in Europe. In: Lindsay EH, Fahlbusch V, Mein P eds. *European Neogene Mammal Chronology*. Ney York: Plenum Press, 239–256.

Azzaroli A. 1992. Ascent and decline of monodactyl equids: a case for prehistoric overkill. *Annales Zoologici Fennici* 28:151–163.

Barnosky AD., Lindsey EL. 2010. Timing of Quaternary megafaunal extinction in South America in relation to human arrival and climate change. *Quaternary International* 217:10–29.

Begon M., Townsend CR., Harper JL. 2006. *Ecology: from individuals to ecosystems*. Malden: Blackwell Publishing Ltd.

Bendrey R., Vella D., Zazzo A., Balasse M., Lepetz S. 2015. Exponentially decreasing tooth growth rate in horse teeth: Implications for isotopic analyses. *Archaeometry* 57:1104–1124.

Blueweiss L., Fox H., Kudzma V., Nakashima D., Peters R., Sams S. 1978. Relationships between body size and some life history parameters. *Oecologia* 37:257–272.

Botha-Brink J., Angielczyk KD. 2010. Do extraordinarily high growth rates in Permo-Triassic dicynodonts (Therapsida, Anomodontia) explain their success before and after the end-Permian extinction? *Zoological Journal of the Linnean Society* 160:341–365.

Botha-Brink J., Codron D., Huttenlocker AK., Angielczyk KD., Ruta M. 2016. Breeding young as a survival strategy during Earth's greatest mass extinction. *Scientific Reports* 6:1–9.

Botha J., Chinsamy A. 2000. Growth patterns deduced from the bone histology of the cynodonts *Diademodon* and *Cynognathus*. *Journal of Vertebrate Paleontology* 20:705–711.

Botha J., Chinsamy A. 2005. Growth patterns of *Thrinaxodon liorhinus*, a non-mammalian cynodont from the Lower Triassic of South Africa. *Palaeontology* 48:385–394.

Boyde A. 1964. The structure and development of mammalian enamel. PhD thesis.

Braendle C., Heyland A., Flatt T. 2011. Integrating mechanistic and evolutionary analysis of life history variation. In: Flatt T, Heyland A eds. *Mechanisms of Life History Evolution. The Genetics and Physiology of Life History Traits and Trade-Offs*. Oxford: Oxford University Press, 3–10.

Bromage TG. 1991. Enamel incremental periodicity in the pig-tailed macaque: a polychrome fluorescent labeling study of dental hard tissues. *American Journal of Physical Anthropology* 86:205–214.

Bromage TG., Dean MC. 1985. Re-evaluation of the age at death of immature fossil hominids. *Nature* 317:525–527.

Bromage TG., Dirks W., Erdjument-Bromage H., Huck M., Kullmer O., Öner R., Sandrock O., Schrenk F. 2002. A life history and climate change solution to the evolution and extinction of insular dwarfs: a Cypriot experience. In: Waldren WH, Ensenyat JA eds. *World Islands in Prehistory: International Insular Investigations, V Deia International Conference of Prehistory*. Oxford: Archaeopress, 420–427.

Bromage TG., Goldman HM., McFarlin SC., Warshaw J., Boyde A., Riggs CM. 2003. Circularly polarized light standards for investigations of collagen fiber orientation in bone. *Anatomical Record - Part B New Anatomist* 274B:157–168.

Bromage TG., Hogg RT., Lacruz RS., Hou C. 2012. Primate enamel evinces long period biological timing and regulation of life history. *Journal of Theoretical Biology* 305:131–144.

Bromage TG., Lacruz RS., Hogg R., Goldman HM., McFarlin SC., Warshaw

J., Dirks W., Perez-Ochoa A., Smolyar I., Enlow DH., Boyde A. 2009. Lamellar bone is an incremental tissue reconciling enamel rhythms, body size, and organismal life history. *Calcified Tissue International* 84:388–404.

Bromage TG., Werning S. 2013. Image standardization in paleohistology. In: Padian K, Lamm ET eds. *Bone histology of fossil tetrapods: advancing methods, analysis, and interpretation*. Berkeley: University of California Press, 161–176.

Bruce RC., Castanet J. 2006. Application of skeletochronology in aging larvae of the salamanders *Gyrinophilus porphyriticus* and *Pseudotriton ruber*. *Journal of Herpetology* 40:85–90.

Bryant JD., Froelich PN., Showers WJ., Genna BJ. 1996. A tale of two quarries: Biologic and taphonomic signatures in the oxygen isotope composition of tooth enamel phosphate from modern and Miocene equids. *Palaios* 11:397–408.

Buchanan CR., Preece MA. 1992. Hormonal control of bone growth. In: Hall BK ed. *Bone, Vol. 6*. Boca Raton: CRC Press, 53–89.

Burke A., Castanet J. 1995. Histological observations of cementum growth in horse teeth and their application to archaeology. *Journal of Archaeological Science* 22:479–493.

Burke A., Eisenmann V., Ambler GK. 2003. The systematic position of *Equus hydruntinus*, an extinct species of Pleistocene equid. *Quaternary Research* 59:459–469.

Bybee PJ., Lee AH., Lamm E-T. 2006. Sizing the Jurassic theropod dinosaur *Allosaurus*: assessing growth strategy and evolution of ontogenetic scaling of limbs. *Journal of Morphology* 267:347–359.

Calder WA III. 1984. *Size, Function and Life History*. New York: Dover Publications.

Cambra-Moo O., Nacarino-Meneses C., Díaz-Güemes I., Enciso S., García Gil O., Llorente Rodríguez L., Rodríguez Barbero MA., de Aza AH., González Martín A. 2015. Multidisciplinary characterization of the long-bone cortex growth patterns through sheep's ontogeny. *Journal of Structural Biology* 191:1–9.

Cantalapiedra JL., Prado JL., Hernández Fernández M., Alberdi MT. 2017. Decoupled ecomorphological evolution and diversification in Neogene-Quaternary horses. *Science* 355:627–630.

Carlson SJ. 1990. Vertebrate dental structures. In: Carter J ed. *Skeletal Biomineralization: Patterns, Processes and Evolutionary Trends*. New York: Van Nostrand Reinhold, 235–260.

Carrión JS. 1992. Late quaternary pollen sequence from Carihuela Cave, southern Spain. *Review of Palaeobotany and Palynology* 71:37–77.

Case TJ. 1978. On the evolution and adaptive significance of postnatal growth rates in the terrestrial vertebrates. *The Quaterly Review of Biology* 53:243–282.

Castanet J. 2006. Time recording in bone microstructures of endothermic animals; functional relationships. *Comptes Rendus - Palevol* 5:629–636.

Castanet J., Baéz M. 1991. Adaptation and evolution in *Gallotia* lizards from the Canary Islands: age, growth, maturity and longevity. *Amphibia-Reptilia* 12:81–102.

Castanet J., Croci S., Aujard F., Perret M., Cubo J., de Margerie E. 2004. Lines of arrested growth in bone and age estimation in a small primate: *Microcebus murinus*. *Journal of Zoology* 263:31–39.

Castanet J., Francillon-Vieillot H., Meunier F., De Ricqlès A. 1993. Bone and individual aging. In: Hall BK ed. *Bone: A Treatise, Vol. 7*. Boca Raton: CRC Press, 245–283.

Charlesworth B. 1980. *Evolution in age-structured populations*. Cambridge: Cambridge University Press.

Chinsamy-Turan A. 2005. *The microstructure of dinosaur bone. Deciphering biology with fine-scale techniques*. Baltimore and London: The Johns Hopkins University Press.

Chinsamy-Turan A. 2012. *Forerunners of mammals: radiation, histology, biology*. Bloomington: Indiana University Press.

Chinsamy A., Chiappe LM., Dodson P. 1994. Growth rings in Mesozoic birds. *Nature* 368:196–197.

Chinsamy A., Hurum JH. 2006. Bone microstructure and growth patterns of early mammals. *Acta Palaeontologica Polonica* 51:325–338.

Chinsamy A., Raath MA. 1992. Preparation of fossil bone for histological examination. *Palaeontologia Africana* 29:39–44.

Chinsamy A., Valenzuela N. 2008. Skeletochronology of the endangered side-neck turtles *Podocnemis expansa*. *South African Journal of Science* 104:311–314.

Churcher C. 1993. *Equus grevyi*. *Mammalian Species* 453:1–9.

Cody ML. 1966. A general theory of clutch size. *Evolution* 20:174–184.

Cole LC. 1954. The population consequences of life history phenomena. *The Quarterly Review of Biology* 29:103–137.

Cormack DH. 1987. *Ham's Histology*. Philadelphia: JB Lippincott.

Cubo J., le Roy N., Martinez-Maza C., Montes L. 2012. Paleohistological estimation of bone growth rate in extinct archosaurs. *Paleobiology* 38:335–349.

Cucchi T., Mohaseb A., Peigné S., Debue K., Orlando L., Mashkour M. 2017. Detecting taxonomic and phylogenetic signals in equid cheek teeth: towards new palaeontological and archaeological proxies. *Royal Society Open Science* 4:160997.

Cuijpers S., Lauwerier RCGM. 2008. Differentiating between bone fragments from horses and cattle: a histological identification method for archaeology. *Environmental Archaeology* 13:165–179.

Currey JD. 2002. *Bones. Structure and mechanics*. Princeton: Princeton University Press.

Curry Rogers K., Whitney M., Bagley B. 2016. Precocity in a tiny titanosaur from the Cretaceous of Madagascar. *Science* 352:450–454.

Curtin AJ., Macdowell AA., Schaible EG., Curtin AJ., Macdowell AA., Schaible EG., Roth VL., Carolina N. 2012. Noninvasive histological comparison of bone growth patterns among fossil and extant neonatal elephantids using synchrotron radiation x-ray microtomography. *Journal of Vertebrate*

Paleontology 32:939–955.

Damuth J., Janis CM. 2011. On the relationship between hypsodonty and feeding ecology in ungulate mammals, and its utility in palaeoecology. *Biological Reviews* 86:733–758.

Damuth J., MacFadden BJ. 1990. *Body size in mammalian Paleobiology. Estimations and biological implications*. Cambridge: Cambridge University Press.

Dean MC. 1987. Growth layers and incremental markings in hard tissues; a review of the literature and some preliminary observations about enamel structure in *Paranthropus boisei*. *Journal of Human Evolution* 16:157–172.

Dean MC. 2000. Incremental markings in enamel and dentine: what they can tell us about the way teeth grow. In: Teaford M, Smith M, Ferguson M eds. *Development, Function and Evolution of teeth*. Cambridge: Cambridge University Press, 119–130.

Dean MC. 2006. Tooth microstructure tracks the pace of human life-history evolution. *Proceedings of the Royal Society B: Biological Sciences* 273:2799–2808.

Dean MC., Leakey MG. 2004. Enamel and dentine development and the life history profile of Victoriapithecus macinnesi from Maboko Island, Kenya. *Annals of Anatomy* 186:405–412.

Dean C., Leakey MG., Reid D., Schrenk F., Schwartz GT., Stringer C., Walker A. 2001. Growth processes in teeth distinguish modern humans from *Homo erectus* and earlier hominins. *Nature* 414:628–631.

Dean MC., Scandrett AE. 1996. The relation between long-period incremental markings in dentine and daily cross-striations in enamel in human teeth. *Archives of Oral Biology* 41:233–241.

Dirks W. 1998. Histological reconstruction of dental development and age at death in juvenile gibbon (*Hylobates lar*). *Journal of Human Evolution* 35:411–425.

Dirks W., Anemone RL., Holroyd PA., Reid DJ., Walton P. 2009. Phylogeny, life history and the timing of molar crown formation in two archaic ungulates, *Meniscotherium* and *Phenacodus* (Mammalia, "Condylarthra"). In: Koppe T, Meyer G, Alt KW eds. *Comparative Dental Morphology*. Basel: Karger, 3–8.

Dirks W., Bowman JE. 2007. Life history theory and dental development in four species of catarrhine primates. *Journal of Human Evolution* 53:309–320.

Dirks W., Bromage TG., Agenbroad LD. 2012. The duration and rate of molar plate formation in *Palaeoloxodon cypriotes* and *Mammuthus columbi* from dental histology. *Quaternary International* 255:79–85.

Dirks W., Reid DJ., Jolly CJ., Phillips-Conroy JE., Brett FL. 2002. Out of the mouths of baboons: stress, life history, and dental development in the Awash National Park hybrid zone, Ethiopia. *American Journal of Physical Anthropology* 118:239–252.

Dixon PM., Copeland AN. 1993. The radiological appearance of mandibular cheek teeth in ponies of different ages. *Equine Veterinary Education* 5:317–323.

Dixon PM., du Toit N. 2011. Dental anatomy. In: Easley J, Dixon PM, Schumacher J eds. *Equine Dentistry*. Elsevier Ltd, 51–76.

Djagoun CAMS., Kassa B., Djossa BA., Coulson T., Mensah GA., Sinsin B. 2014.

Hunting affects dry season habitat selection by several bovid species in northern Benin. *Wildlife Biology* 20:83–90.

Eisenmann V. 1991. Les chevaux quaternaires européens (Mammalia, Perissodactyla). Taille, typologie, biostratigraphie et taxonomie. *Geobios* 24:747–759.

Eisenmann V. 1992. Origins, dispersals, and migrations of *Equus* (Mammalia, Perissodactyla). *Courier Forschungsinstitut Senckenberg*:161–170.

Eisenmann V. 1993. L'evolution des équidés. *Arvicola* 5:3–9.

Eisenmann V., Alberdi MT., de Giuli C., Staesche U. 1988. *Studying fossil horses. Collected papers after the "New York International Hipparion Conference, 1981". Volume I: Methodology*. Leiden: E.J. Brill.

Eisenmann V., Howe J., Pichardo M. 2008. Old world hemiones and new world slender species (Mammalia, Equidae). *Paleovertebrata* 36:159–233.

Enlow DH., Brown SO. 1956. A comparative histological study of fossil and recent bone tissues. Part I. *The Texas Journal of Science* 8:405–412.

Enlow DH., Brown SO. 1957. A comparative histological study of fossil and recent bone tissues. Part II. *The Texas Journal of Science* 9:186–214.

Enlow DH., Brown SO. 1958. A comparative histological study of fossil and recent bone tissues. Part III. *The Texas Journal of Science* 10:187–230.

Ento K., Matsui M. 2002. Estimation of age structure by skeletochronology of a population of *Hynobius nebulosus* in a breeding season (Amphibia, Urodela). *Zoological Science* 19:241–247.

Erickson GM. 1996. Incremental lines of von Ebner in dinosaurs and the assessment of tooth replacement rates using growth line counts. *Proceedings of the National Academy of Sciences of the United States of America* 93:14623–14627.

Erickson GM., Zelenitsky DK., Kay DI., Norell MA. 2017. Dinosaur incubation periods directly determined from growth-line counts in embryonic teeth show reptilian-grade development. *Proceedings of the National Academy of Sciences of the United States of America* 114:540–545.

Ernest SKM. 2003. Life history characteristics of placental nonvolant mammals. *Ecology* 84:3402.

Esteban M., García-París M., Buckley D., Castanet J. 1999. Bone growth and age in *Rana saharica*, a water frog living in a desert environment. *Finnish Zoological and Botanical Publishing Board* 36:53–62.

Esteban M., Sánchez-Herráiz MJ., Barbadillo LJ., Castanet J., Márquez R. 2002. Effects of age, size and temperature on the advertisement calls of two Spanish populations of *Pelodytes punctatus*. *Amphibia-Reptilia* 23:249–258.

Fancy SG. 1980. Preparation of mammalian teeth for age determination by cementum layers: a review. *Wildlife Society Bulletin* 8:242–248.

Feh C., Munkhtuya B., Enkhbold S., Sukhbaatar T. 2001. Ecology and social structure of the Gobi khulan *Equus hemionus* subsp. in the Gobi B National Park, Mongolia. *Biological Conservation* 101:51–61.

Fellows I. 2012. Deducer: A Data Analysis GUI for R. *Journal of Statistical Software*

49:1–15.

Fernández S., Fuentes N., Carrión JS., González-Sampériz P., Montoya E., Gil G., Vega-Toscano G., Riquelme JA. 2007. The Holocene and Upper Pleistocene pollen sequence of Carihuela Cave, southern Spain. *Geobios* 40:75–90.

Fisher DC. 2009. Paleobiology and extinction of proboscideans in the Great Lakes region of North America. In: Haynes G ed. *American Megafaunal Extinctions at the End of the Pleistocene. Vertebrate Paleobiology and Paleoanthropology*. Dordrecht: Springer, 55–75.

FitzGerald CM. 1998. Do enamel microstructures have regular time dependency? Conclusions from the literature and a large-scale study. *Journal of Human Evolution* 35:371–386.

FitzGerald CM., Rose JC. 2008. Reading between the lines: dental development and subadult age assessment using the microstructural growth markers of teeth. In: Katzenberg MA, Saunders SR eds. *Biological Anthropology of the Human Skeleton*. New Jersey: John Wiley & Sons, Inc, 237–263.

Forsten A. 1988. Middle Pleistocene replacement of stenonid horses by caballoid horses - Ecological implications. *Palaeogeography, Palaeoclimatology, Palaeoecology* 65:23–33.

Forsten A. 1989. Horse diversity through the ages. *Biological Reviews* 64:279–304.

Forsten A. 1991. Size decrease in Pleistocene-Holocene true or caballoid horses of Europe. *Mammalia* 55:407–420.

Forstén A. 1992. Mitochondrial-DNA time-table and the evolution of *Equus*: comparison of molecular and paleontological evidence. *Annales Zoologici Fennici* 28:301–309.

Foster JB. 1964. Evolution of mammals on islands. *Nature* 202:234–235.

Foster BL. 2017. On the discovery of cementum. *Journal of Periodontal Research* 52:666–685.

Fowden AL., Forhead AJ., Ousey JC. 2012. Endocrine adaptations in the foal over the perinatal period. *Equine Veterinary Journal* 44:130–139.

Francillon-Vieillot H., de Buffrénil V., Castanet J., Géraudie J., Meunier FJ., Sire JY., Zylberberg L., de Ricqlès A. 1990. Microstructure and mineralization of vertebrate skeletal tissues. In: Carter JG ed. *Skeletal biomineralization: patterns, processes and evolutionary trends*. New York: Van Nostrand Reinhold, 471–530.

Froehlich DJ. 2002. Quo vadis eohippus? The systematics and taxonomy of the early Eocene equids (Perissodactyla). *Zoological Journal of the Linnean Society* 134:141–256.

Gadgil M., Bossert WH. 1970. Life historical consequences of natural selection. *The American Naturalist* 104:1–24.

García-Martínez R., Marín-Moratalla N., Jordana X., Köhler M. 2011. The ontogeny of bone growth in two species of dormice: reconstructing life history traits. *Comptes Rendus - Palevol* 10:489–498.

Garrido G. 2008. Generalidades sobre los perisodáctilos y los proboscídeos del Villafranquiense Superior en relación con el registro fósil de Fonelas P-1. In: Arribas

A ed. *Vertebrados del Plioceno superior terminal en el suroeste de Europa: Fonelas P-1 y el proyecto Fonelas*. Madrid: Instituto Geológico y Minero de España. Cuadernos del Museo Geominero, 517–551.

Geigl EM., Grange T. 2012. Eurasian wild asses in time and space: Morphological versus genetic diversity. *Annals of Anatomy* 194:88–102.

George M., Ryder OA. 1986. Mitochondrial DNA evolution in the genus *Equus*. *Molecular Biology and Evolution* 3:535–546.

González-Suárez M., Revilla E. 2013. Variability in life-history and ecological traits is a buffer against extinction in mammals. *Ecology Letters* 16:242–251.

Grinder MI., Krausman PR., Hoffmann RS. 2006. *Equus asinus*. *Mammalian Species* 794:1–9.

Gross TS., McLeod KJ., Rubin CT. 1992. Characterizing bone strain distributions in vivo using three triple rosette strain gages. *Journal of Biomechanics* 25:1081–1087.

Grubb P. 1981. *Equus burchelli*. *Mammalian Species* 157:1–9.

Guthrie RD. 2003. Rapid body size decline in Alaskan Pleistocene horses before extinction. *Nature* 426:169–171.

Hall BK. 2005. *Bones and Cartilage: Developmental and Evolutionary Skeletal Biology*. San Diego: Elsevier Ltd.

Heintzman PD., Zazula GD., MacPhee RDE., Scott E., Cahill JA., McHorse BK., Kapp JD., Stiller M., Wooller MJ., Orlando L., Southon J., Froese DG., Shapiro B. 2017. A new genus of horse from Pleistocene North America. *eLife* 6:1–43.

Hemelaar A. 1985. An improved method to estimate the number of year rings resorbed in phalanges of *Bufo bufo* (L.) and its application to populations from different latitudes and altitudes. *Amphibia-Reptilia* 6:323–341.

Hillson S. 2005. *Teeth*. Cambridge: Cambridge University Press.

Hogg RT., Walker RS. 2011. Life-history correlates of enamel microstructure in Cebidae (Platyrrhini, Primates). *Anatomical Record* 294:2193–2206.

Hoppe KA., Stover SM., Pascoe JR., Amundson R. 2004. Tooth enamel biomineralization in extant horses: Implications for isotopic microsampling. *Palaeogeography, Palaeoclimatology, Palaeoecology* 206:355–365.

Hopwood AT. 1936. The former distribution of caballine and zebrine horses in Europe and Asia. *Proceedings of the Zoological Society of London* 106:897–912.

Horner JR., De Ricqlès A., Padian K. 1999. Variation in dinosaur skeletochronology indicators: implications for age assessment and physiology. *Paleobiology* 25:295–304.

Horner JR., De Ricqlès A., Padian K. 2000. Long bone histology of the hadrosaurid dinosaur *Maiasaura peeblesorum*: growth dynamics and physiology based on an ontogenetic series of skeletal elements. *Journal of Vertebrate Paleontology* 20:115–129.

Hugi J., Sánchez-Villagra MR. 2012. Life history and skeletal adaptations in the galapagos marine iguana (*Amblyrhynchus cristatus*) as reconstructed with bone histological data—A comparative study of iguanines. *Journal of Herpetology* 46:312–

324.

Hulbert RCJ. 1982. Population dynamics of the three-toed horse *Neohipparion* from the late Miocene of Florida. *Paleobiology* 8:159–167.

Hurum JH., Chinsamy-Turan A. 2012. The radiation, bone histology and biology of early mammals. In: Chinsamy-Turan A ed. *Forerunners of mammals: Radiation, histology, biology*. Bloomington: Indiana University Press, 249–270.

Huttenlocker AK., Woodward HN., Hall BK. 2013. The biology of bone. In: Padian K, Lamm E-T eds. *Bone histology of fossil tetrapods: advancing methods, analysis, and interpretation*. Berkeley: University of California Press, 13–34.

Iinuma YM., Tanaka S., Kawasaki K., Kuwajima T., Nomura H., Suzuki M., Ohtaishi N. 2004a. Dental incremental lines in sika deer (*Cervus nippon*); polarized light and fluorescence microscopy of ground sections. *Journal of Veterinary Medical Science* 66:665–669.

Iinuma YM., Suzuki M., Matsura Y., Asano M., Onuma M., Ohtaishi N. 2004b. Identification and morphological characteristics of dental neonatal line in sika deer (*Cervus nippon*). *Japanese Journal of Veterinary Research* 51:161–166.

IUCN. 2018. The IUCN Red List of Threatened Species. Version 2017-3. <www.iucnredlist.org>

Jakob C., Seitz A., Crivelli A., Miaud C. 2002. Growth cycle of the marbled newt (*Triturus marmoratus*) in the Mediterranean region assessed by skeletochronology. *Amphibia-Reptilia* 23:407–418.

Janis CM. 1988. An estimation of tooth volume and hypsodonty indices in ungulate mammals. In: Russell DE, Santoro JP, Sigogneau-Russel D eds. *Teeth revisited: Proceedings of the 7th International Symposium on Dental Morphology, 20-24 May, 1986*. Paris: Muséum National D'Histoire Naturelle, 367–387.

Janis C. 1976. The evolutionary strategy of the Equidae and the origins of rumen and cecal digestion. *Evolution* 30:757–774.

Janis C. 2007. The Horse Series. In: Regal B ed. *Icons of Evolution*. Westport: Greenwood Press, 251–280.

Jónsson H., Schubert M., Seguin-Orlando A., Ginolhac A., Petersen L., Fumagalli M., Albrechtsen A., Petersen B., Korneliussen TS., Vilstrup JT., Lear T., Myka JL., Lundquist J., Miller DC., Alfarhan AH., Alquraishi SA., Al-Rasheid KAS., Stagegaard J., Strauss G., Bertelsen MF., Sicheritz-Ponten T., Antczak DF., Bailey E., Nielsen R., Willerslev E., Orlando L. 2014. Speciation with gene flow in equids despite extensive chromosomal plasticity. *Proceedings of the National Academy of Sciences of the United States of America* 111:18655–18660.

Jordana X., Köhler M. 2011. Enamel microstructure in the fossil bovid *Myotragus balearicus* (Majorca, Spain): implications for life-history evolution of dwarf mammals in insular ecosystems. *Palaeogeography, Palaeoclimatology, Palaeoecology* 300:59–66.

Jordana X., Marín-Moratalla N., de Miguel D., Kaiser TM., Köhler M. 2012. Evidence of correlated evolution of hypsodonty and exceptional longevity in

endemic insular mammals. *Proceedings of the Royal Society B: Biological Sciences* 279:3339–3346.

Jordana X., Marín-Moratalla N., Moncunill-Solé B., Köhler M. 2014. Ecological and life-history correlates of enamel growth in ruminants (Artiodactyla). *Biological Journal of the Linnean Society* 112:657–667.

Jordana X., Marín-Moratalla N., Moncunill-Solé B., Nacarino-Meneses C., Köhler M. 2016. Ontogenetic changes in the histological features of zonal bone tissue of ruminants: a quantitative approach. *Comptes Rendus - Palevol* 15:255–266.

Jordana X., de Miguel D., Köhler M. 2015. On the relationship between hypsodonty and longevity in *Myotragus balearicus* - A comment on van der Geer (2014). *Integrative Zoology* 10:227–229.

Kaczensky P., Lkhagvasuren B., Pereladova O., Hemami M., Bouskila A. 2015. *Equus hemionus*. *The IUCN Red List of Threatened Species*: e.T7951A45.

Kahle P., Witzel C., Kierdorf U., Frölich K., Kierdorf H. 2018. Mineral apposition rates in coronal dentine of mandibular first molars in soay sheep: results of a fluorochrome labeling study. *The Anatomical Record* 301:902-912.

Kahlke VH-D. 1961. Revision der Säugetierfaunen der klassischen deutschen Pleistozän-Fundstellen von Süßenborn, Mosbach und Taubach. *Geologie* 10:493–532.

Kahlke HD. 1975. The Macro-faunas of Continental Europe during the Middle Pleistocene: Stratigraphic sequence and problems of intercorrelation. In: Butzer KW, Isaac GL eds. *After the Australopithecines. Stratigraphy, Ecology, and Culture Change in the Middle Pleistocene*. The Hague: Mouton Publishers, 309–374.

Kahlke RD., García N., Kostopoulos DS., Lacombat F., Lister AM., Mazza PPA., Spassov N., Titov VV. 2011. Western Palaearctic palaeoenvironmental conditions during the Early and early Middle Pleistocene inferred from large mammal communities, and implications for hominin dispersal in Europe. *Quaternary Science Reviews* 30:1368–1395.

Kaiser TM., Müller DWH., Fortelius M., Schulz E., Codron D., Clauss M. 2013. Hypsodonty and tooth facet development in relation to diet and habitat in herbivorous ungulates: implications for understanding tooth wear. *Mammal Review* 43:34–46.

Khonsue W., Matsui M., Hirai T., Misawa Y. 2001. A comparison of age structures in two populations of a pond frog *Rana nigromaculata* (Amphibia: Anura). *Zoological Science* 18:597–603.

Kierdorf H., Breuer F., Richards A., Kierdorf U. 2014. Characterization of enamel incremental markings and crown growth parameters in minipig molars. The *Anatomical Record* 297:1935–1949.

Kierdorf H., Kierdorf U., Frölich K., Witzel C. 2013. Lines of evidence - Incremental markings in molar enamel of soay sheep as revealed by a fluorochrome labeling and backscattered electron imaging study. *PLoS ONE* 8:e74597.

Kierdorf H., Witzel C., Upex B., Dobney K., Kierdorf U. 2012. Enamel hypoplasia in molars of sheep and goats, and its relationship to the pattern of tooth crown growth. *Journal of Anatomy* 220:484–495.

King SRB., Boyd L., Zimmermann W., Kendall BE. 2015. *Equus ferus*. *The IUCN Red List of Threatened Species*: e.T41763A97204950.

King SRB., Moehlman PD. 2016. *Equus quagga*. *The IUCN Red List of Threatened Species*: e.T41013A45172424.

Kirkland KD., Baker GJ., Marretta SM., Eurell JAC., Losonsky JM. 1996. Effects of aging on the endodontic system, reserve crown, and roots of equine mandibular cheek teeth. *American Journal of Veterinary Research* 57:31–38.

Klevezal GA. 1996. *Recording structures of mammals: Determination of age and reconstruction of life history*. Rotterdam: AA Balkema.

Klingel H. 1974. A comparison of the social behaviour of the Equidae. In: Geist V, Walther F eds. *The behaviour of Ungulates and its relation to management*. IUCN Publications, 124–132.

Klingel H. 1998. Observations on social organization and behaviour of African and Asiatic Wild Asses (*Equus africanus* and *Equus hemionus*). *Applied Animal Behaviour Science* 60:103–113.

Koenigswald W V., Smith BH., Keller T. 2007. Supernumerary teeth in a subadult rhino mandible (*Stephanorhinus hundsheirnensis*) from the middle Pleistocene of Mosbach in Wiesbaden (Germany). *Paläontologische Zeitschrift* 81:416–428.

Köhler M. 2009. The evolution of life history traits associated to dwarfing in insular large mammals: a paleontological approach. *Journal of Vertebrate Paleontology* 29:Suppl. 128A.

Köhler M. 2010. Fast or slow? The evolution of life history traits associated with insular dwarfing. In: Pérez-Mellado V, Ramon C eds. *Islands and Evolution*. Maó: Institut Menorquí d'Estudis. Recerca, 261–280.

Köhler M., Marín-Moratalla N., Jordana X., Aanes R. 2012. Seasonal bone growth and physiology in endotherms shed light on dinosaur physiology. *Nature* 487:358–361.

Köhler M., Moyà-Solà S. 2009. Physiological and life history strategies of a fossil large mammal in a resource-limited environment. *Proceedings of the National Academy of Sciences of the United States of America* 106:20354–20358.

Kolb C., Scheyer TM., Veitschegger K., Forasiepi AM., Amson E., Van der Geer AAE., Van den Hoek Ostende LW., Hayashi S., Sánchez-Villagra MR. 2015a. Mammalian bone palaeohistology: a survey and new data with emphasis on island forms. *PeerJ* 3:e1358.

Kolb C., Scheyer TM., Lister AM., Azorit C., de Vos J., Schlingemann M., Rössner GE., Monaghan NT., Sánchez-Villagra MR. 2015b. Growth in fossil and extant deer and implications for body size and life history evolution. *BMC Evolutionary Biology* 15:19.

Lack D. 1954. *The natural regulation of animal numbers*. Oxford: Clarendon Press.

Lacruz RS., Habelitz S., Wright JT., Paine ML. 2017. Dental enamel formation and implications for oral health and disease. *Physiological Reviews* 97:939–993.

Lacruz RS., Hacia JG., Bromage TG., Boyde A., Lei Y., Xu Y., Miller JD., Paine ML., Snead ML. 2012. The circadian clock modulates enamel development. *Journal*

of Biological Rhythms 27:237–245.

Lamm E-T. 2013. Preparation and sectioning of specimens. In: Padian K, Lamm E-T eds. *Bone histology of fossil tetrapods: advancing methods, analysis, and interpretation*. Berkeley: University of California Press, 55–160.

Lee AH., Huttenlocker AK., Padian K., Woodward HN. 2013. Analysis of Growth Rates. In: Padian K, Lamm E-T eds. *Bone histology of fossil tetrapods: advancing methods, analysis, and interpretation*. Berkeley: University of California Press, 217–251.

Levine MA. 1982. The use of crown height measurements and eruption-wear sequences to age horse teeth. In: Wilson B, Grigson C, Payne S eds. *Ageing and Sexing Animal Bones from Archaeological Sites*. Oxford: B.A.R., 223–250.

Lieberman DE. 1993. Life history variables preserved in dental cementum microstructure. *Science* 261:1162–1164.

Lindsay EH., Opdyke ND., Johnson NM. 1980. Pliocene dispersal of the horse *Equus* and late Cenozoic mammalian dispersal events. *Nature* 287:135–138.

Lkhagvasuren D., Ansorge H., Samiya R., Schafberg R., Stubbe A., Stubbe M. 2013. Age determination of the Mongolian wild ass (*Equus hemionus* Pallas, 1775) by the dentition patterns and annual lines in the tooth cementum. *Journal of Species Research* 2:85–90.

Lkhagvasuren D., Batsaikhan N., Fagan WF., Ghandakly EC., Kaczensky P., Müller T., Samiya R., Schafberg R., Stubbe A., Stubbe M., Ansorge H. 2018. First assessment of the population structure of the Asiatic wild ass in Mongolia. *European Journal of Wildlife Research* 64:4–9.

Lomolino M V. 1985. Body size of mammals on islands: the Island Rule reexamined. *The American naturalist* 125:310–316.

Lorenzen ED., Nogués-Bravo D., Orlando L., Weinstock J., Binladen J., Marske KA., Ugan A., Borregaard MK., Gilbert MTP., Nielsen R., Ho SYW., Goebel T., Graf KE., Byers D., Stenderup JT., Rasmussen M., Campos PF., Leonard JA., Koepfli KP., Froese D., Zazula G., Stafford TW., Aaris-Sørensen K., Batra P., Haywood AM., Singarayer JS., Valdes PJ., Boeskorov G., Burns JA., Davydov SP., Haile J., Jenkins DL., Kosintsev P., Kuznetsova T., Lai X., Martin LD., McDonald HG., Mol D., Meldgaard M., Munch K., Stephan E., Sablin M., Sommer RS., Sipko T., Scott E., Suchard MA., Tikhonov A., Willerslev R., Wayne RK., Cooper A., Hofreiter M., Sher A., Shapiro B., Rahbek C., Willerslev E. 2011. Species-specific responses of Late Quaternary megafauna to climate and humans. *Nature* 479:359–364.

MacArthur R., Wilson E. 1967. *The theory of island biogeography*. Princeton: Princeton University Press.

MacFadden BJ. 1992. *Fossil horses. Systematics, Paleobiology, and Evolution of the Family Equidae*. Cambridge: Cambridge University Press.

MacFadden BJ. 2000. Cenozoic mammalian hervibores from the Americas : Reconstructing ancient diets and terrestrial communities. *Annual Review of Ecology and Systematics* 31:33–59.

MacFadden BJ. 2005. Fossil Horses - Evidence for Evolution. *Science* 307:1728–1730.

MacFadden BJ. 2013. Dispersal of Pleistocene *Equus* (Family Equidae) into South America and calibration of GABI 3 based on evidence from Tarija, Bolivia. *PLoS ONE* 8:e59277.

Macho GA., Williamson DK. 2002. The effects of ecology on life history strategies and metabolic disturbances during development: an example from the African bovids. *Biological Journal of the Linnean Society* 75:271–279.

de Margerie E. 2002. Laminar bone as an adaptation to torsional loads in flapping flight. *Journal of Anatomy* 201:521–526.

de Margerie E., Cubo J., Castanet J. 2002. Bone typology and growth rate: Testing and quantifying "Amprino's rule" in the mallard (*Anas platyrhynchos*). *Comptes Rendus - Biologies* 325:221–230.

de Margerie E., Robin J-P., Verrier D., Cubo J., Groscolas R., Castanet J. 2004. Assessing a relationship between bone microstructure and growth rate: a fluorescent labelling study in the king penguin chick (*Aptenodytes patagonicus*). *Journal of Experimental Biology* 207:869–879.

Marín-Moratalla N., Cubo J., Jordana X., Moncunill-Solé B., Köhler M. 2014. Correlation of quantitative bone histology data with life history and climate: A phylogenetic approach. *Biological Journal of the Linnean Society* 112:678–687.

Marín-Moratalla N., Jordana X., García-Martínez R., Köhler M. 2011. Tracing the evolution of fitness components in fossil bovids under different selective regimes. *Comptes Rendus - Palevol* 10:469–478.

Marín-Moratalla N., Jordana X., Köhler M. 2013. Bone histology as an approach to providing data on certain key life history traits in mammals: implications for conservation biology. *Mammalian Biology* 78:422–429.

Martin RB., Burr DB., Sharkey NA. 1998. *Skeletal tissue mechanics*. New York: Springer-Verlag.

Martínez-Maza C., Alberdi MT., Nieto-Diaz M., Prado JL. 2014. Life-history traits of the miocene *Hipparion concudense* (Spain) inferred from bone histological structure. *PLoS ONE* 9:e103708.

Maul LC., Rekovets L., Heinrich W-D., Keller T., Storch G. 2000. *Arvicola mosbachensis* (Schmidtgen 1991) of Mosbach 2: a basic sample for the early evolution of the genus and a reference for further biostratigraphical studies. *Senckenbergiana lethaea* 80:129–147.

McKinney ML. 1997. Extinction vulnerability and selectivity: combining ecological and paleontological views. *Annual Review of Ecology and Systematics* 28:495–516.

Mendoza M., Palmqvist P. 2008. Hypsodonty in ungulates: An adaptation for grass consumption or for foraging in open habitat? *Journal of Zoology* 274:134–142.

Messer NT., Riddle WT., Traub-Dargatz JL., Dargatz DA., Refsal KJ., Thompson Jr. DL. 1998. Thyroid hormone levels in thoroughbred mares and their foals at parturition. *AAEP Proceedings* 44:248–251.

Metcalfe JZ., Longstaffe FJ. 2012. Mammoth tooth enamel growth rates inferred from stable isotope analysis and histology. *Quaternary Research* 77:424–432.

Mimura T. 1939. The periodicity of growth lines seen in enamel. *Kobyo-shi* 13:45455.

Moehlman PD. 2002. *Equids: Zebras, Asses and Horses. Status Survey and Conservation Action Plan*. Gand, Switzerland and Cambridge: IUCN/ SSC Equid Specialist Group.

Moehlman PD., Kebede F., Yohannes H. 2015. *Equus africanus. The IUCN Red List of Threatened Species*: e.T7949A45170994.

Moncunill-Solé B., Orlandi-Oliveras G., Jordana X., Rook L., Köhler M. 2016. First approach of the life history of *Prolagus apricenicus* (Ochotonidae, Lagomorpha) from Terre Rosse sites (Gargano, Italy) using body mass estimation and paleohistological analysis. *Comptes Rendus - Palevol* 15:227–237.

Monfort SL., Arthur NP., Wildt DE. 1994. Reproduction in the Przewalski's horse. In: Boyde L, Houpt KA eds. *Przewalski's horse. The history and biology of an endangered species*. Albany: State University of New York Press, 173–194.

Montoya-Sanhueza G., Chinsamy A. 2017. Long bone histology of the subterranean rodent *Bathyergus suillus* (Bathyergidae): ontogenetic pattern of cortical bone thickening. *Journal of Anatomy* 230:203–233.

Morris P. 1970. A method for determining absolute age in the hedgehog. *Journal of Zoology* 161:277–281.

Morris P. 1972. A review of mammalian age determination methods. *Mammal Review* 2:69–104.

Nacarino-Meneses C., Jordana X., Köhler M. 2016a. First approach to bone histology and skeletochronology of *Equus hemionus*. *Comptes Rendus - Palevol* 15:267–277.

Nacarino-Meneses C., Jordana X., Köhler M. 2016b. Histological variability in the limb bones of the Asiatic wild ass and its significance for life history inferences. *PeerJ* 4:e2580.

Nacarino-Meneses C., Jordana X., Orlandi-Oliveras G., Köhler M. 2017. Reconstructing molar growth from enamel histology in extant and extinct *Equus*. *Scientific Reports* 7:15965.

Nacarino-Meneses C, Köhler M. Accepted. Limb bone histology records birth in mammals. *PLoS ONE.*

van Noordwijk AJ., de Jong G. 1986. Acquisition and allocation of resources: their Influence on variation in life history tactics. *The American Naturalist* 128:137–142.

Novellie P. 2008. *Equus zebra. The IUCN Red List of Threatened Species*: e.T7960A12876787.

Nowak RM. 1999. *Walker's mammals of the world*. Baltimore and London: The Johns Hopkins University Press.

Odadi WO., Jain M., Van Wieren SE., Prins HHT., Rubenstein DI. 2011. Facilitation between bovids and equids on an African savanna. *Evolutionary Ecology Research* 13:237–252.

Okada M. 1943. Hard tissues of animal body. *The Shanghai Evening Post* Especial edition:15–31.

Olgun K., Uzum N., Avci A., Miaud C. 2005. Age, size and growth of the southern *Triturus karelinii* in a population from Turkey. *Amphibia-Reptilia* 26:223–230.

Orlandi-Oliveras G., Jordana X., Moncunill-Solé B., Köhler M. 2016. Bone histology of the giant fossil dormouse *Hypnomys onicensis* (Gliridae, Rodentia) from Balearic Islands. *Comptes Rendus - Palevol* 15:238–244.

Orlando L. 2015. Equids. *Current Biology*:R973–R978.

Orlando L., Ginolhac A., Zhang G., Froese D., Albrechtsen A., Stiller M., Schubert M., Cappellini E., Petersen B., Moltke I., Johnson PLF., Fumagalli M., Vilstrup JT., Raghavan M., Korneliussen T., Malaspinas AS., Vogt J., Szklarczyk D., Kelstrup CD., Vinther J., Dolocan A., Stenderup J., Velazquez AMV., Cahill J., Rasmussen M., Wang X., Min J., Zazula GD., Seguin-Orlando A., Mortensen C., Magnussen K., Thompson JF., Weinstock J., Gregersen K., Røed KH., Eisenmann V., Rubin CJ., Miller DC., Antczak DF., Bertelsen MF., Brunak S., Al-Rasheid KAS., Ryder O., Andersson L., Mundy J., Krogh A., Gilbert MTP., Kjær K., Sicheritz-Ponten T., Jensen LJ., Olsen J V., Hofreiter M., Nielsen R., Shapiro B., Wang J., Willerslev E. 2013. Recalibrating *Equus* evolution using the genome sequence of an early Middle Pleistocene horse. *Nature* 499:74–78.

Orlando L., Mashkour M., Burke A., Douady CJ., Eisenmann V., Hänni C. 2006. Geographic distribution of an extinct equid (Equus hydruntinus: Mammalia, Equidae) revealed by morphological and genetical analyses of fossils. *Molecular Ecology* 15:2083–2093.

Ozaki M., Kaji K., Matsuda N., Ochiai K., Asada M., Ohba T., Hosoi E., Tado H., Koizumi T., Suwa G., Takatsuki S. 2010. The relationship between food habits, molar wear and life expectancy in wild sika deer populations. *Journal of Zoology* 280:202–212.

Padian K. 2011. Vertebrate palaeohistology then and now: A retrospective in the light of the contributions of Armand de Ricqlès. *Comptes Rendus - Palevol* 10:303–309.

Padian K. 2013. Why study the bone microstructure of fossil tetrapods? In: Padian K, Lamm E-T eds. *Bone histology of fossil tetrapods: advancing methods, analysis, and interpretation*. Berkeley: University of California Press, 1–11.

Padian K., Horner JR., De Ricqlès A. 2004. Growth in small dinosaurs and pterosaurs: the evolution of archosaurian growth strategies. *Journal of Vertebrate Paleontology* 24:555–571.

Padian K., de Ricqlès A., Horner JR. 2001. Dinosaurian growth rates and bird origins. *Nature* 412:405–408.

Palkovacs EP. 2003. Explaining adaptive shifts in body size on islands: a life history approach. *Oikos* 103:37–44.

Penzhorn BL. 1982. Age determination in cape mountain zebras *Equus zebra zebra* in the Mountain Zebra National Park. *Koedoe* 25:89–102.

Penzhorn BL. 1988. *Equus zebra*. *Mammalian Species* 314:1–7.

Pérez-Barbería FJ., Carranza J., Sánchez-Prieto C. 2015. Wear fast, die young: More worn teeth and shorter lives in Iberian compared to Scottish red deer. *PLoS ONE* 10:e0134788.

Peters RH. 1983. *The ecological implications of body size*. Cambridge: Cambridge

University Press.

Pianka ER. 1970. On *r*- and *K*-selection. *The American Naturalist* 104:592–597.

Pianka ER. 2000. *Evolutionary Ecology*. San Francisco: Benjamin Cumins.

Prado JL., Alberdi MT. 1996. A cladistic analysis of the tribe Equini. *Palaeontology* 39:663–680.

Prado JL., Alberdi MT. 2017. *Fossil Horses of South America. Phylogeny, Systematics and Ecology*. Cham: Springer, The Latin American Studies Book Series.

Promislow DEL., Harvey PH. 1990. Living fast and dying young: A comparative analysis of life-history variation among mammals. *Journal of Zoology* 220:417–437.

Prondvai E., Stein KHW., de Ricqlès A., Cubo J. 2014. Development-based revision of bone tissue classification: the importance of semantics for science. *Biological Journal of the Linnean Society* 112:799–816.

Prothero DR. 2009. Evolutionary transitions in the fossil record of terrestrial hoofed mammals. *Evolution: Education and Outreach* 2:289–302.

Purvis A., Gittleman JL., Cowlishaw G., Mace GM. 2000. Predicting extinction risk in declining species. *Proceedings of the Royal Society B: Biological Sciences* 267:1947–1952.

Pushkina D., Bocherens H., Ziegler R. 2014. Unexpected palaeoecological features of the Middle and Late Pleistocene large herbivores in southwestern Germany revealed by stable isotopic abundances in tooth enamel. *Quaternary International* 339–340:164–178.

Raia P., Barbera C., Conte M. 2003. The fast life of a dwarfed giant. *Evolutionary Ecology* 17:293–312.

Raia P., Meiri S. 2006. The Island Rule in large mammals: Paleontology meets Ecology. *Evolution* 60:1731–1742.

Ray S., Botha J., Chinsamy A. 2004. Bone histology and growth patterns of some nonmammalian therapsids. *Journal of Vertebrate Paleontology* 24:634–648.

Read AF., Harvey PH. 1989. Life history differences among the eutherian radiations. *Journal of Zoology* 219:329–353.

Reznick D., Bryant MJ., Bashey F. 2002. r- and K-selection revisited: the role of population regulation in life-history evolution. *Ecology* 83:1509–1520.

Ricklefs RE. 2008. *The Economy of Nature*. New York: W. H. Freeman and Company.

Ricklefs RE., Wilkelski M. 2002. The physiology/life history nexus. *Trends in Ecology and Evolution* 17:462–469.

de Ricqlès A. 1975. Recherches paléohistologiques sur les os longs des tétrapodes VII. — Sur la classification, la signification fonctionnelle et l'histoire des tissus osseux des tétrapodes. Première partie, structures. *Annales de Paléontologie (Vertébrés)* 61:51–129.

de Ricqlès AJ. 2007. Fifty years after Enlow and Brown's Comparative histological study of fossil and recent bone tissues (1956-1958): a review of Professor Donald H. Enlow's contribution to palaeohistology and comparative histology of bone.

Comptes Rendus - Palevol 6:591–601.

de Ricqlès AJ. 2011. Vertebrate palaeohistology: Past and future. *Comptes Rendus - Palevol* 10:509–515.

Roff DA. 1992. *The evolution of life histories. Theory and analysis*. New York: Chapman and Hall.

Roff DA. 2002. *Life history evolution*. Sunderland: Sinauer Associates.

Rosenbom S., Costa V., Chen S., Khalatbari L., Yusefi GH., Abdukadir A., Yangzom C., Kebede F., Teclai R., Yohannes H., Hagos F., Moehlman PD., Beja-Pereira A. 2015. Reassessing the evolutionary history of ass-like equids: Insights from patterns of genetic variation in contemporary extant populations. *Molecular Phylogenetics and Evolution* 85:88–96.

Rubenstein D., Low Mackey B., Davidson Z., Kebede F., King SR. 2016. *Equus grevyi*. *The IUCN Red List of Threatened Species*: e.T7950A89624491.

Ruiz Bustos A., García Sánchez M. 1977. Las condiciones ecológicas del Musteriense en las depresiones granadinas. La fauna de micromamíferos de la Cueva de la Carigüela (Piñar, Granada). *Cuadernos de Prehistoria de la Universidad de Granada*:7–17.

Samper Carro SC. 2010. Systematic description of the equids remains from La Carihuela (Piñar, Grenade). In: Moreno-Azanza M, Díaz-Martínez I, Gasca JM, Melero-Rubio M, Rabal-Garcés R, Sauqué V eds. *Cidaris, número 30, VIII Encuentro de Jóvenes Investigadores en Paleontología*, 283–291.

Saltz D. 2002. The dynamics of equid populations. In: Moehlman PD ed. *Equids: Zebras, Asses and Horses*. Gland: IUCN/ SSC Equid Specialist Group, 118–123.

Sander PM. 2000. Longbone histology of the Tendaguru sauropods: implications for growth and biology. *Paleobiology* 26:466–488.

Sander PM., Andrássy P. 2006. Lines of arrested growth and long bone histology in Pleistocene large mammals from Germany: What do they tell us about dinosaur physiology? *Paleontographica Abteilung A2* 277:143–159.

Sander PM., Mateus O., Laven T., Knötschke N. 2006. Bone histology indicates insular dwarfism in a new Late Jurassic sauropod dinosaur. *Nature* 441:739–741.

Der Sarkissian C., Vilstrup JT., Schubert M., Seguin-Orlando A., Eme D., Weinstock J., Alberdi MT., Martin F., Lopez PM., Prado JL., Prieto A., Douady CJ., Stafford TW., Willerslev E., Orlando L. 2015. Mitochondrial genomes reveal the extinct *Hippidion* as an outgroup to all living equids. *Biology letters* 11:20141058.

Schaffer WM. 1974. Selection for optimal life histories: The effects of age structure. *Ecology* 55:291–303.

Schöpke K., Stubbe A., Stubbe M., Batsaikhan N., Schafberg R. 2012. Morphology and variation of the Asiatic wild ass (*Equus hemionus hemionus*). *Erforschung biologischer Ressourcen der Mongolei* 12:77–84.

Schour I. 1936. The neonatal line in the enamel and dentin of the human deciduous teeth and first permanent molar. *The Journal of the American Dental Association* 23:1946–1955.

Schour I., Hoffman MM. 1939a. Studies in tooth development: I. The 16 microns calcification rhythm in the enamel and dentin from fish to man. *Journal of Dental Research* 18:91–102.

Schour I., Hoffman MM. 1939b. Studies in tooth development: II. The rate of apposition of enamel and dentin in man and other mammals. *Journal of Dental Research* 18:161–175.

Schour I., Massler M. 1940. Studies in tooth development: the growth pattern of human teeth. Part II. *The Journal of the American Dental Association* 27:1918–1931.

Schulz E., Kaiser TM. 2013. Historical distribution, habitat requirements and feeding ecology of the genus *Equus* (Perissodactyla). *Mammal Review* 43:111–123.

Shah N., St. Louis A., Qureshi Q. 2015. *Equus kiang. The IUCN Red List of Threatened Species*: e.T7953A45171635.

Silver IA. 1963. The aging of domestic animals. In: Brothwell D, Higgs E eds. *Science in Archaeology: a comprehensive survey of progress and research*. New York: Basic Books, 250–268.

Simpson GG. 1953. *The major features of evolution*. New York: Columbia University Press.

Sinsch U. 2015. Review: Skeletochronological assessment of demographic life-history traits in amphibians. *Herpetological Journal* 25:5–13.

Sisson S. 1914. *The anatomy of domestic animals*. Philadelphia & London: W. B. Saunders company.

Smith BH. 1989. Dental development as a measure of life history in primates. *Evolution* 43:683–688.

Smith CE. 1998. Cellular and chemical events during enamel maturation. *Critical Reviews in Oral Biology & Medicine* 9:128–161.

Smith BH. 2000. "Schultz's Rule" and the evolution of tooth emergence and replacement patterns in primates and ungulates. In: Teaford MF, Smith MM, Ferguson M eds. *Development, Function and Evolution of teeth*. New York: Cambridge University Press, 212–227.

Smith TM. 2004. Incremental Development of Primate Dental Enamel. PhD thesis.

Smith TM. 2006. Experimental determination of the periodicity of incremental features in enamel. *Journal of Anatomy* 208:99–113.

Smith TM. 2008. Incremental dental development: methods and applications in hominoid evolutionary studies. *Journal of Human Evolution* 54:205–224.

Smith TM., Reid DJ., Sirianni JE. 2006. The accuracy of histological assessments of dental development and age at death. *Journal of Anatomy* 208:125–138.

Smith TM., Tafforeau P. 2008. New visions of dental tissue research: tooth development, chemistry, and structure. *Evolutionary Anthropology* 17:213–226.

Smuts GL. 1974. Age determination in Burchell's zebra (*Equus burchelli antiquorum*) from the Kruger National Park. *Journal of the Southern African Wildlife Management Association* 4:103–105.

Soana S., Gnudi G., Bertoni G. 1999. The teeth of the horse: Evolution and anatomo-

morphological and radiographic study of their development in the foetus. *Anatomia, Histologia, Embryologia* 28:273–280.

Spinage CA. 1972. Age estimation of zebra. *African Journal of Ecology* 10:273–277.

Spinage CA. 1973. A review of the age determination of mammals by means of teeth, with especial reference to Africa. *African Journal of Ecology* 11:165–187.

St-Louis A., Côté SD. 2009. *Equus kiang* (Perissodactyla: Equidae). *Mammalian Species* 835:1–11.

Stearns SC. 1976. Life-history tactics: a review of the ideas. *The Quaterly Review of Biology* 51:3–47.

Stearns SC. 1977. The evolution of life history traits: a critique of the theory and a review of the data. *Annual Review of Ecology and Systematics* 8:145–171.

Stearns SC. 1983. The influence of size and phylogeny on patterns of cavariation among life-history traits in the mammals. *Oikos* 41:173–187.

Stearns SC. 1989. Trade-offs in life-history evolution. *Functional Ecology* 3:259–268.

Stearns SC. 1992. *The evolution of life histories*. New York: Oxford University Press.

Stearns SC. 2000. Life history evolution: successes, limitations, and prospects. 87:476–486.

Stearns SC., Koella JC. 1986. The evolution of phenotypic plasticity in life-history traits: predictions of reaction norms for age and size at maturity. *Evolution* 40:893–913.

Steiner CC., Mitelberg A., Tursi R., Ryder OA. 2012. Molecular phylogeny of extant equids and effects of ancestral polymorphism in resolving species-level phylogenies. *Molecular Phylogenetics and Evolution* 65:573–581.

Steiner CC., Ryder OA. 2011. Molecular phylogeny and evolution of the Perissodactyla. *Zoological Journal of the Linnean Society* 163:1289–1303.

Stewart F., Goode JA., Allen WR. 1993. Growth hormone secretion in the horse: Unusual pattern at birth and pulsatile secretion through to maturity. *Journal of Endocrinology* 138:81–89.

Stover SM., Pool RR., Martin RB., Morgan JP. 1992. Histological features of the dorsal cortex of the third metacarpal bone mid-diaphysis during postnatal growth in thoroughbred horses. *Journal of anatomy* 181:455–469.

Street M., Terberger T., Orschiedt J. 2006. A critical review of the German Paleolithic hominin record. *Journal of Human Evolution* 51:551–579.

Strömberg CAE. 2006. Evolution of hypsodonty in equids: testing a hypothesis of adaptation. *Paleobiology* 32:236–258.

Tacutu R., Craig T., Budovsky A., Wuttke D., Lehmann G., Taranukha D., Costa J., Fraifeld VE., De Magalhães JP. 2013. Human Ageing Genomic Resources: Integrated databases and tools for the biology and genetics of ageing. *Nucleic Acids Research* 41:1027–1033.

Tafforeau P., Bentaleb I., Jaeger J-J., Martin C. 2007. Nature of laminations and mineralization in rhinoceros enamel using histology and X-ray synchrotron

microtomography: potential implications for palaeoenvironmental isotopic studies. *Palaeogeography, Palaeoclimatology, Palaeoecology* 246:206–227.

Turner-Walker G., Mays S. 2008. Histological studies on ancient bone. In: Pinhasi R, Mays S eds. *Advances in human paleopathology*. Chichester: John Wiley & Sons, Ltd, 121–146.

Ungar PS. 2010. *Mammal teeth: origin, evolution and diversity*. Baltimore: The Johns Hopkins University Press.

Van Asperen EN. 2013. Position of the Steinheim interglacial sequence within the marine oxygen isotope record based on mammal biostratigraphy. *Quaternary International* 292:33–42.

Vanpé C., Gaillard J-M., Morellet N., Kjellander P., Liberg O., Delorme D., Hewison AJM. 2009. Age-specific variation in male breeding success of a territorial ungulate species, the European roe deer. *Journal of Mammalogy* 90:661–665.

Van Valen L. 1973. A new evolutionary law. *Evolutionary Theory* 1:1–33.

Veiberg V., Mysterud A., Gaillard J-M., Delorme D., Laere G Van., Klein F. 2007. Bigger teeth for longer life? Longevity and molar height in two roe deer populations. *Biology Letters* 3:268–270.

Vilstrup JT., Seguin-Orlando A., Stiller M., Ginolhac A., Raghavan M., Nielsen SCA., Weinstock J., Froese D., Vasiliev SK., Ovodov ND., Clary J., Helgen KM., Fleischer RC., Cooper A., Shapiro B., Orlando L. 2013. Mitochondrial phylogenomics of modern and ancient equids. *PLoS ONE* 8:e55950.

Wang Y., Cerling TE., MacFadden BJ. 1994. Fossil horses and carbon isotopes: new evidence for Cenozoic dietary, habitat, and ecosystem changes in North America. *Palaeogeography, Palaeoclimatology, Palaeoecology* 107:269–279.

Weber DF., Eisenmann DR. 1971. Microscopy of the neonatal line in developing human enamel. *The American journal of Anatomy* 132:375–392.

Weinstock J., Willerslev E., Sher A., Tong W., Ho SYW., Rubenstein D., Storer J., Burns J., Martin L., Bravi C., Prieto A., Froese D., Scott E., Xulong L., Cooper A. 2005. Evolution, systematics, and phylogeography of Pleistocene horses in the new world: A molecular perspective. *PLoS Biology* 3:e241.

Woodward HN., Horner JR., Farlow JO. 2014. Quantification of intraskeletal histovariability in *Alligator mississippiensis* and implications for vertebrate osteohistology. *PeerJ* 2:e422.

Woodward HN., Padian K., Lee AH. 2013. Skeletochronology. In: Padian K, Lamm E-T eds. *Bone histology of fossil tetrapods: advancing methods, analysis, and interpretation*. Berkeley: University of California Press, 195–215.

Zawojska A., Siudek T. 2016. Bioeconomics as an interdisciplinary discipline. In: *Proceedings of the International Conference "Economic science for rural development."* Jelgava, 274–281.

- Chapter 12 -

Acknowledgements

Acknowledgements

Esta tesis doctoral ha sido realizada gracias a la "Ayuda para contratos predoctorales para la formación de doctores 2013" (FPI, BES-2013-066335, Ministerio de Economía y Competitividad). Además, ha sido financiada por los proyectos de investigación "*The evolution of mammalian life histories in energy-limited environments: a paleobiological focus*" (Ministerio de Economía y Competitividad, CGL2012-34459) y "*Evolution of mammalian life history in continental Iberian ecosystems from the Miocene to Pleistocene: correlation with climatic changes*" (Ministerio de Economía y Competitividad, CGL2015-63777), y por el grupo de investigación "Paleoecologia i ecologia evolutiva, PEE" (Generalitat de Catalunya, 2014-SGR-1207). La estancia en el *Staatliches Museum für Naturkunde* (Stuttgart, Alemania) ha sido subvencionada, por su parte, mediante la "Ayuda a la movilidad predoctoral para la realización de estancias breves en centros de I+D españoles y extranjeros 2015" (EEBB-I-16-10546; Ministerio de Economía y Competitividad). Por último, el proceso de redacción el texto en inglés ha sido supervisado por Judith Wickham, profesora de idiomas de la Universitat Autònoma de Barcelona, mediante la "Ayuda para la redacción de tesis doctorales en inglés" de la Universidad Autònoma de Barcelona (2017).

En primer lugar, quiero dar las gracias a mis directores, la Dra. Meike Köhler y el Dr. Xavier Jordana, por su ayuda y su dedicación a lo largo de estos años. A la Dr. Meike Köhler le agradezco, especialmente, el haberme dado la oportunidad de unirme al departamento de Paleobiología Evolutiva del Institut Català de Paleontología Miquel Crusafont cuando yo era, tan solo, una completa desconocida buscando becas desde Madrid. Muchas gracias por introducirme en el mundo de la *life history* y por enseñarme su aplicación en paleontología a través de la paleohistología. Gracias, también, por ofrecerme trabajar en un grupo tan interesante como los équidos ¡Nunca pensé que aprendería y disfrutaría tanto cuando acepté la tesis! Al Dr. Xavier Jordana, por su parte, le agradezco de manera especial el haberme enseñado todo lo posible sobre histología dental. Gracias por no desistir en comprender conmigo la histología dental de los caballos, ¡a pesar de los quebraderos de cabeza que nos dieron los primeros resultados! A los dos os quiero dar las gracias, además, por acompañarme y aconsejarme en estos primeros años de mi carrera investigadora y por el tiempo y el trabajo que habéis invertido en esta tesis.

A la Dra. Meike Köhler y al Dr. Xavier Jordana les agradezco también, junto a Guillem Orlandi-Oliveras, su labor como coautores de los artículos y/o manuscritos que conforman esta tesis. Gracias a vuestras correcciones, recomendaciones y críticas he conseguido publicaciones que cuando empecé ni siquiera imaginaba. Gracias, igualmente, a los revisores (Dra. Clara Stefen, Dr. Jorge Cubo, Dr. Tim Bromage, y revisores anónimos) y a los editores de dichos artículos (Dr. William Jungers, Dr. Jin Meng, Dr. Jorge Cubo y Dr. Rinaldo Florencio-Silva), así como al Dr. Jorge Cubo y al Dr. Michel Laurin por permitirme participar en la edición especial de la revista Comptes Rendus Palevol dedicada a toda una generación de paleohistólogos franceses. A nivel científico, quiero dar también las

gracias a la Dra. Anusuya Chinsamy-Turan y al Dr. Tim Bromage por elaborar un informe externo sobre la calidad científica de esta tesis y, así, permitirme optar a la Mención de Doctorado Internacional. Quiero agradecer, igualmente, al Dr. Joan Madurell-Malapeira su ayuda con la identificación de las distintas especies de caballos fósiles del yacimiento de la Carihuela, y su disposición a resolver mis dudas sobre équidos fósiles y sobre el Pleistoceno a lo largo de estos años.

Me gustaría dar también las gracias a los investigadores de las distintas instituciones que no solo han cedido el material necesario para la realización de esta tesis, si no que también han permitido su uso en estudios paleohistológicos: Dr. Thomas Kaiser del Zoological Institut of Hamburg University (Hamburgo, Alemania), Dra. Renate Schafberg del Museum of Domesticated Animals de la Martin-Luther-University Halle-Wittenberg (Halle, Saale, Alemania), Dr. Benjamin Lamglait de la Universidad de Montréal (Montreal, Canadá) y, previamente, de la Réserve Africaine de Sigean (Sigean, France), Dr. Reinhard Ziegler del Staatliches Museum für Naturkunde (Stuttgart, Alemania), Dr. Salvador Moyà-Solà y Dr. David Alba del Institut Català de Paleontologia Miquel Crusafont (Barcelona, España). Al Dr. Reinhard Ziegler le estoy especialmente agradecida, además, por recibirme y acogerme en su museo durante tres meses, y por toda la ayuda recibida mientras revisaba las colecciones. Finalmente, a Manuel Fernández, Gemma Prats-Muñoz y Luis Gordón, les agradezco enormemente la preparación de las láminas delgadas que conforman el material de estudio de esta tesis.

A nivel docente, quiero agradecer al profesorado de la Unitat d'Antropologia Biològica del Departament de Biologia Animal, Biologia Vegetal i Ecologia de la Universitat Autònoma de Barcelona el haberme permitido participar en sus clases durante mis años como doctoranda. En especial, quiero dar las gracias a la Dra. Assumpció Malgosa, la Dra. Gemma Armengol, la Dra. Eulàlia Subirà, la Dra. Dominika Nociarová, la Dra. Cristina Santos y el Dr. Xavier Jordana, por haberme permitido conocer un poco más de cerca como es el mundo de la enseñanza universitaria. Gracias también a los técnicos y laborantes de este departamento, en especial a Núria Sánchez, por ayudarme con la preparación del material necesario para las clases. Gracias, igualmente, al Dr. Salvador Moyà-Solà, al Dr. Raef Minwer-Barakat, al Dr. Jacint Ventura y al Dr. Manel López Béjar, por su papel en las comisiones anuales de seguimiento del programa de doctorado, y a la Dra. Assumpció Malgosa por resolver mis múltiples dudas sobre todo el papeleo relacionado con la tesis.

Quiero hacer, también, una mención especial al Laboratorio de Poblaciones del Pasado (LAPP) de la Universidad Autónoma de Madrid, puesto que fue allí donde tuve el primer contacto con el mundo de la investigación. Siempre os estaré agradecida, Dr. Armando González Martín y Dr. Oscar Cambra-Moo, por haberme dado la primera oportunidad de conocer de cerca este mundo entre cajas y cajas de San Nicolás cuando aún era una estudiante de Biología. Gracias, igualmente, al Dr. Miguel Ángel Rodríguez y al Dr. Antonio de Aza, ambos del Instituto de Cerámica y Vidrio (CSIC), por sus consejos esos primeros años y por enseñarme tanto sobre un campo tan desconocido para mí como es la ciencia de los materiales.

Quiero dar también las gracias a toda la gente con la que he compartido mi día a día durante estos cuatro años "y pico" de tesis: mis compañeros del Institut Català de Paleontologia Miquel Crusafont. Gracias a todos por hacer que el tiempo y el trabajo sean lo más entretenidos posible en un edificio que a veces lo pone todo en nuestra contra. De

entre todos mis compañeros, quiero destacar de manera especial a María y a Blanca, ya que en ellas he encontrado dos verdaderas amigas. Gracias por acogerme con tanto cariño desde el primer día, por buscar siempre el lado positivo de las cosas y por todo vuestro apoyo, en especial en esta etapa final de la tesis. Gracias también a "Los Guillems" (Guillem 1 y Guillem 2, Guillem y Guillom, o como queráis que os distingamos) por este tiempo juntos, en especial por los viajes en ferrocarrils a Guillem 1 y por sacarme (un poco) de quicio en el metro de Nueva York a Guillem 2 (ya cada uno de vosotros sabréis quién es quién). A Álex, por los días en Budapest. A Raef, Joan, Judit, Arnau, Isaac, Vinuesa y tantos otros, con los que he compartido muy buenos momentos en los desayunos y las comidas a lo largo de estos años. A Teresa, Silvia, Alessandro y demás predocs y allegados, por las cenas internacionales. A Miriam y Nekane, por las rondas de zumitos al inicio de la tesis. A Manu, ¡por esa estupenda calçotada de Paleobio! Y a tantos otros que seguramente esté olvidando mencionar, por siempre tener unas palabras amables durante mi estancia en el ICP. Por último, gracias al Dr. Salvador Moyà-Solà y al Dr. David Alba por su labor como directores del ICP.

Gracias, también, a toda la gente que he conocido a lo largo de estos años en Barcelona y que han llenado mis fines de semana y ratos libres con actividades que, generalmente, nada tienen que ver con la Ciencia. Gracias Jordi, Alan, Eli, Delia, Guillem y María, por seguirme en la locura de las danzas irlandesas, por las cenas en la Feni y las cervezas en el Petit Café, las noches en Bóveda o las salidas a esquiar o buscar setas. De hecho, ¡gracias María por prestarme tus amigos! Gracias a Jessica, por las comidas en el bar de Ciencias (en este caso, tengo que agradecer a Blanca que me prestara a su amiga). Gracias Carlos, Mafer, y ahora también el pequeño Fernando, por ser como familia, por las madrugadas en el Sants Beer, por las paellas en la playa y por enseñarnos a querer Venezuela sin haberla pisado (todavía). Gracias también a Damián y a "las chicas de baile" (María, Sonia, Jessica, Leti) por preguntar siempre un "¿cómo llevas lo tuyo?" antes de cada clase y conseguir, después, que me olvide de todo mientras hacemos (reconozcámoslo, regular) piruetas, pliés, tendús y demás técnicas de nombre impronunciable.

Gracias, igualmente, a todos aquellos que, aunque no habéis estado cerca este tiempo, siempre os habéis preocupado por saber cómo iba todo. A mis amig@s de siempre, Paula, Paula, Marta, Marta, Belén, Darko y Fabio, por intentar entender mi trabajo y por descubrir, al cabo de algo más de tres años, que de caballos nada, ¡que eran cebras y burros! A mis amigos de Biología, en especial a Blanca, Sergio, Laura y Lucas, por nunca decir que no a unas cervezas por el centro de Madrid. Y a Marta, Oro, Julia y Susana, por aquel aquelarre en Barcelona cuando no llevaba aquí ni seis meses. A Marta, además, le agradezco el haber coincidido estos poquitos meses en Barcelona y, así, haber podido hacer planes juntas después tantos años viviendo separadas.

Gracias a mi familia, por su apoyo y su comprensión durante todo este tiempo. Muchísimas gracias, papá y mamá, por animarme a cumplir siempre mis sueños y por enseñarme que hay que estudiar y trabajar en aquello que te gusta, aunque no siempre sea fácil y te obligue, incluso, a cambiarte de ciudad. Gracias también a mi hermana, María, por demostrarme que esos sueños hay que perseguirlos. Gracias a mis abuelos, en especial a mi abuela Carmen, por ser la persona más fuerte y luchadora que he conocido y conoceré nunca. Ojalá haya heredado de ti algo más que tu nombre. Y gracias a Kira, por tumbarse a mis pies mientras escribía esta tesis y por obligarme a salir a la calle varias veces al día, aunque sus motivos fueran totalmente egoístas. Gracias también mis amigos-

familia, mi familia mexicana. Sadot, Lourdes, Daniela y Mariana, gracias por cuidarme y por haberme cuidado siempre. Y gracias a Alejandro, por las cenas de Nochebuena. Gracias, también, a mi familia política. A Laura, por leerse cada uno de mis artículos. A Maria José y a Francisco, a Leyre y a Javi, y a Aitor, por estar siempre pendientes de cómo iba avanzando la tesis y por quererme como a una más.

Y, por último, gracias a la persona que ha estado a mi lado durante todo este tiempo. Gracias, Íñigo, por no dudar ni un momento en acompañarme a cualquier lugar del mundo, por creer en mí, por hacerme reír con tus (bastante malos) juegos de palabras y por ser mi psicólogo particular en la etapa final de la tesis. En definitiva, gracias por estar ahí siempre.